THE EFFECTS OF THE ABORTIFACIENT PARASITE, *NEOSPORA CANINUM* ON BOVINE FOETUSES IN EARLY AND LATE GESTATION

Thesis submitted in accordance with the requirements of the University of Liverpool for the degree of Doctor in Philosophy

by

Patrick Sylvester Craig

July 2014

AUTHORS'S DECLARATION

Apart from the help and advice acknowledged, this thesis represents the unaided work of the author

……

Patrick Sylvester Craig

July 2014

This research was carried out in the Department of Infection Biology and School of Veterinary Science, University of Liverpool

TABLE OF CONTENTS

DEDICATION

I want to dedicate this thesis to my mother who has struggled with me from my very first day on the planet. She has managed to overcome a terrible sickness while I was in the middle of my PhD fieldwork in Jamaica and that was very traumatic for all of us. She deserves this more than anyone else and I dedicate it all to her.

To Alice with love

ACKNOWLEDGEMENTS

Though only my name appears on the cover of this dissertation, a great many people have contributed to its production. I owe my gratitude to all those people who have made this dissertation possible and because of whom my graduate experience has been one that I will cherish forever. First and foremost, I would like to thank my supervisors Professor Anja Kipar, Professor Diana Williams, Dr Udo Hetzel and Dr Lorenzo Ressel who have all demanded a very high quality of work. Additionally, I would like to thank my PhD advisors, Professor James Stewart and Dr Jane Hodgkinson for their support and interest in my work. Special thanks to the Commonwealth Scholarship Commission for financially supporting my studentship and the Ministry of Finance in Jamaica for selecting me following a rigorous interview process. This work would not have been possible without the help of these organisations and for that I extend all my gratitude.

I am indebted to staff of the Histology Laboratories in the School of Veterinary Science who have put up with me for almost 4 years. Mrs Catherine Hartley from the Department of Infection Biology has been there with me in the labs since my very first day and she was there even on my last day. This work would not have been the same without Catherine's help and for that I say thank you. Thanks to Ms Marion Pope, Electron Microscopy Unit, for processing my samples for TEM. I also would like to thank José María Mateos, Center for Microscopy and Image Analysis, and Lisbeth Nufer, Electron Microscopy Unit, IVPZ, University of Zurich, Switzerland for the preparation of the FIB-SEM Nanotomography specimens.

Thanks to Dr Sophie Ragan from the Department of Molecular and Clinical Pharmacology for her practical and scientific knowledge on primary hepatocyte isolation. Ms Rowena Eakins taught me quite a lot about *in vitro* cultivation of hepatocytes and this was a vital part of this thesis. For that I must give special thanks. Special thanks also to Dr Diane Munday who has taught me a lot about immunoblots and also for allowing me to use her lab equipment.

I would like to thank Dr Michael Motta for his help is acquiring the permission to sample the dairy farms in Jamaica and for helping with the actual sampling over the period on all three farms. The fieldwork would not have been possible without his help and dedication.

I am grateful to my family, friends and colleagues who have helped me to stay sane and focused throughout these very difficult years. Their support and care have helped me overcome setbacks and stay focused on my graduate study. I greatly value their friendship, help and support and I deeply appreciate their belief in me.

ABSTRACT

The effects of the abortifacient parasite, *Neospora caninum* on bovine foetuses in early and late gestation

Patrick Sylvester Craig

Neospora caninum is an obligate intracellular protozoan parasite, which is the most frequently diagnosed abortifacient in dairy cattle in the UK and is a leading cause of abortion worldwide. *Neospora caninum* infection in early gestation is associated with foetal death whereas in late gestation, infection can result in the birth of asymptomatic, but persistently infected animals. How the parasite kills the foetus is not fully understood, but it has been suggested that more mature foetuses are better able to mount a stronger immune response to control parasite multiplication and dissemination. The ability of the bovine foetus to respond to various antigens develops in a sequential fashion during the gestation period and foetal immunocompetence starts to develop at approximately 100 days gestation age (dg), but can only fully recognise antigens during mid-gestation at around 150 dg.

Chapter 2 assessed the pathological effects of *N. caninum* on bovine foetuses in early and late gestation (70 and 210 days gestation, respectively) and also in foetuses from naturally infected dams after recrudescence of *N. caninum* in mid to late gestation. Based on results of an initial histological screen of 35 bovine foetuses and 2 new-born calves, a total of 12 foetuses and calves were selected and subjected to more detailed histological examination. Both haemolymphatic and non-haemolymphatic tissues were used. The distribution of *N. caninum* antigen, CD3-positive T cells, PAX5-positive B cells, monocytes/macrophages and neutrophils (myeloid/histiocyte antigen/calprotectin-positive), antigen presenting cells (MHCII), interferon gamma (IFN-γ) expressing cells, PCNA-positive proliferating cells and apoptotic cells (cleaved caspase 3-positive) was analysed by immunohistology. In uninfected, control foetuses in early gestation (90 days gestation), haemolymphatic tissues were moderately developed and exhibited normal morphological features with low lymphocyte turn over and no evidence of IFN-γ production. Uninfected foetuses in late gestation had fully developed haemolymphatic tissues with high lymphocyte turnover, indicative of a mature immune system. In the infected foetuses in early gestation, extensive apoptosis of lymphocytes was observed in the thymus and spleen compared to controls ($p<0.001$, student's *t*-test). No histological changes were observed in the haemolymphatic tissues of infected foetuses in late gestation. In non-haemolymphatic tissues, infected foetuses in early gestation exhibited extensive hepatocellular necrosis and apoptosis, glial cell necrosis and apoptosis in the CNS and high parasite loads in the liver, CNS and myocardium. There was no evidence of cell death in the heart despite the high parasite loads. In late gestation, histological lesions were restricted mainly to the CNS where non-suppurative inflammation and low parasite loads were observed. Other non-haemolymphatic tissues exhibited only mild mononuclear inflammatory infiltrates. The results suggest that in early gestation, tachyzoites replicate preferentially in foetal liver, brain and myocardium in the absence of an inflammatory response and cause extensive necrosis in the liver and brain. Unlike foetuses in early gestation, those in late gestation exhibited a mild to moderate mononuclear inflammatory infiltrate in various tissues dominated mainly by lymphocytes, plasma cells and smaller numbers of macrophages.

In Chapter 3, the observation that *N. caninum* appeared to induce cellular degeneration in hepatocytes but not in the myocardium was investigated in more

depth. An *in vitro* tissue culture system using the human HepG2 hepatoma cell line and the murine HL-1 cardiomyocyte cell line was used to establish the mechanism of cell death following *N. caninum* infection. The activation of the initiator and effector caspases (caspases 3, 8 and 9) was measured and the mitochondrial organisation in cells following *N. caninum* infection evaluated. Quantitative (caspase 3) and semi-quantitative (caspase 8 and 9) analyses were used to assess differences in *N. caninum*-infected and uninfected HepG2 and HL-1 cells. A significant difference was observed in the numbers of cleaved caspase 3-positive HepG2 cells at 20-36 hours post infection (p=0.029, Mann-Whitney U test) in infected cultures compared to controls. No significant difference was observed for caspase 8 and 9 expression. In HL-1 cultures, no significant difference was observed in the number of caspase 3, 8 and 9-positive cells between infected and control cultures. This suggests that *N. caninum* infection is not associated with activation of the caspase cascade in cardiomyocytes. *Neospora caninum* tachyzoites were detected within intact HepG2 and HL-1 cells with normal cellular morphology and which were not labelled with the caspase antibodies; whereas uninfected surrounding cells were caspase 3, 8 and 9-positive, indicating that the parasites are involved in the inhibition of the caspase pathways (intrinsic and extrinsic). The mitochondrial organisation in *N. caninum*-infected and uninfected cells was assessed in both cell lines using double immunofluorescence, which involved staining with a *N. caninum* specific polyclonal antibody and COX 1 mitochondrial marker. In the control cultures of both HepG2 and HL-1 cells, mitochondrial clumping with large aggregates of mitochondria exhibiting a punctate pattern was observed in high numbers of cells, mainly in the perinuclear region and this is suggestive of mitochondrial fragmentation, which is associated with apoptosis. Other cells within the control cultures revealed an unaltered reticular pattern of mitochondria that is consistent with the normal cellular morphology. In the infected cultures, there was mitochondrial clumping with aggregates of mitochondria detected surrounding parasitophorous vacuoles; while in neighbouring uninfected cells, large aggregates of mitochondria, exhibiting a punctate pattern were present, suggesting mitochondrial clumping and fragmentation associated with cytochrome c release and apoptosis. Other uninfected HepG2 and HL-1 cells exhibited a diffuse, homogenous distribution of mitochondria, often with an unaltered reticular pattern as was observed in the control cultures and is consistent with the normal cellular morphology. The results indicate that *N. caninum* inhibits apoptosis in infected cells and is associated with increased apoptosis in infected HepG2 cultures, while not having any effects on HL-1 cardiomyocytes.

Chapter 4 investigated the seroprevalence of *N. caninum* infection in Jamaican dairy herds. Serum samples were analysed from 499 Holstein-Friesian and Holstein Friesian crossbreed dairy cattle from three different farms in Jamaica. A seroprevalence of approximately 26% was found with the majority of seropositive animals aged 0-2 years old (25%), while the lowest seroprevalence was recorded in animals over 13 years old (13.3%). Pregnancy status was shown to influence the seroprevalence of cows, but no significant relation of seropositivity to age was found, suggesting that vertical transmission is the principal route of transmission in Jamaica.

LIST OF FIGURES

LIST OF TABLES

LIST OF ABBREVIATIONS

%	Percent
°C	Degree Celsius
µg	Microgram
µl	Microlitre
µm	Micrometre
1-DE	One-dimensional gel electrophoresis
3D-EM	3-dimensional electron microscopy
ABC	Avidin biotin complex
APC	Antigen presenting cell
APS	Ammonium persulphate
AR	Antigen retrieval
ATP	Adenosine triphosphate
BALT	Bronchus associated lymphoid tissue
Bcl2	B cell lymphoma 2
BME	β-mercaptoethanol
BSA	Bovine serum antigen
BVDV	Bovine viral diarrhoea virus
CASPASE	Cysteinyl aspartate-specific proteases
CD	Cluster of differentiation
CMI	Cell mediated immunity
CNS	Central nervous system
DAB	Diaminobencidin-tetrahydrochloride
DAPI	Dulbecco's modified eagle medium
ddH_2O	Double distilled water
dg	Days of gestation
dH_2O	Distilled water
DNA	Deoxyribonucleic acid
DPX	Distyrene plasticizer and xylene
ECL	Enhanced chemi-luminescence
EDTA	Ethylenediaminetetraacetic acid
EGTA	Ethylene glycol tetraacetic acid
ELISA	Enzyme-linked immunosorbent assay
ER	Endoplasmic reticulum
FADD	Fas-Associated protein with Death Domain
FBS	Foetal bovine serum
FIB-SEM	Focused ion beam scanning electron microscopy
g	Gram
GALT	Gut-associated lymphoid tissue
h	Hour
HCl	Hydrochloric acid
HE	Haematoxylin and eosin

HLA	Human leucocyte antigen
HMGB1	High mobility group box 1
HPF	High power field
hpi	Hours post infection
HRP	Horseradish peroxidase
IB	Immunoblotting
IF	Immunofluorescence
IFAT	Immunofluorescence antibody test
IFN-γ	Interferon gamma
Ig	Immunoglobulin
IL	Interleukin
IMM	Inner mitochondrial membrane
IP	Immunoperoxidase
iv	Intravenous
KDa	Kilodalton
kV	Kilovolt
L	Litre
mAb	Monoclonal antibody
mg	Milligram
MHC	Major histocompatibility complex
min	Minute
ml	Millilitre
mM	Millimole
mmol/L	Millimole per litre
MOI	Multiplicity of infection
mRNA	Messenger ribonucleic acid
NaCl	Sodium chloride
NaOH	Sodium hydroxide
Nc	*Neospora caninum*
NcGRA	*Neospora caninum* dense granule protein
NcSAG	*Neospora caninum* surface antigen
NcSRS	*Neospora caninum* surface antigen related sequence
NF-κB	Nuclear factor kappa beta
OD	Optical density
OMM	Outer mitochondrial membrane
pAb	Polyclonal antibody
PALS	Periarteriolar lymphoid sheath
PAP	Peroxidase anti-peroxidase
PBS	Phosphate buffered saline
PCNA	Proliferating cell nuclear antigen
PCR	Polymerase chain reaction
PDCD5	Programmed cell death 5
PFA	Paraformaldehyde
pH	Percent hydrogen

PLP	Perforin-like parasite protein
PP	Percent positivity
PV	Parasitophorous vacuole
PVDF	Poly-vinylidine fluoride
PVM	Parasitophorous membrane
RT	Room temperature
SDS-PAGE	Sodium-dodecyl sulphate polyacrylamide gel electrophoresis
SNP	Sodium nitroprusside
TBST	Tris-buffered sulphate tween
TEM	Transmission electron microscope
TEMED	Tetramethylethylenediamine
Tg	*Toxoplasma gondii*
TGF-β	Transforming growth factor beta
Th	T helper cell
TMB	Tetramethylbenzidine
TNFR	Tumour necrosis factor receptor
TNF-α	Tumour necrosis factor alpha
TRADD	TNF receptor type 1-associated DEATH domain protein
TUNEL	Terminal deoxynucleotidyl transferase dUTP nick end labelling
v/v	Volume/volume
w/v	Weight/volume

CHAPTER ONE: INTRODUCTION

1.1 *Neospora caninum*

Neospora caninum is a protozoan cyst forming apicomplexan parasite that causes neosporosis, notably in cattle (*Bos taurus*) and domestic dogs (*Canis familiaris*) (Bjerkas et al., 1984; Dubey and Lindsay, 1996). It is closely related to *Toxoplasma gondii* and has emerged as a major cause of reproductive failure in cattle world-wide (Dubey and Lindsay, 1996). It has been indicated by the point estimate of the population aetiology fraction for *N. caninum* that approximately 12 percent of abortions in cattle in England and Wales may be attributable to neosporosis which represents a major economic loss to the dairy industry (Davison et al., 1999b). Seroprevalence to *N. caninum* varies from approximately 6% in England and Wales (Davison et al., 1999b), 22% in Danish dairy cattle (Jensen et al., 1999), to 24% in beef cattle in the USA (Sanderson et al., 2000).

Neospora caninum has been isolated from a variety of animal host species, such as the dog [Nc1; (Dubey et al., 1988b) and Nc-Liverpool (Barber et al., 1993)], cattle [BPA1 and BPA2 (Conrad et al., 1993)], sheep [NC-Sheep (Koyama et al., 2001)] and water buffalo [NCBrbuf-1,2,3,4,5 (Rodrigues et al., 2004)]. Dogs (*Canis familiaris*) were the first to be identified as a definitive host for *N. caninum* (McAllister et al., 1998); however, dogs do not always seroconvert or excrete oocysts when exposed to *N. caninum* infected tissues (Larson and Hardin, 2003). Apart from the dog, other canids have also been considered as potential definitive hosts of *N. caninum* (McAllister, 1999). Some of these in which antibodies were found included the North American coyotes (*Canis latrans*) and Australian dingoes (*Canis familiaris dingo*) (Lindsay et al., 1996; Barber et al., 1997; Buxton et al., 1997). To date, coyotes (Gondim et al., 2004b), wolves (*Canis lupus*) (Dubey et al., 2011) and dingoes (King et al., 2010) have also been named as definitive hosts because they have been shown to shed oocysts after being fed infected tissues, while many other domestic and wild mammal species have been identified as intermediate hosts (Dubey et al., 2007; Dubey and Schares, 2011). Antibodies to *N. caninum* have also been identified in the captive sika deer (Cerus Nippon), mouflon (Ovis musimon), fallow deer (*Dama dama*), moose (*Alces alces*), European bison (*Bison bonasus bonasus* L.), wild rabbits (*Oryctolagus cuniculus*), brown hares (*Lepus europeus*) and dolphin (*Tursiops truncatus*) (reviewed by Dubey et al. (2007). A recent study in the

UK has reported DNA detection of *N. caninum* in mustelid species (Bartley et al., 2013b). Finally, *N. caninum* antibodies have been detected in wild birds such as crows (*Corvus corax*) (Molina-López et al., 2012), and *N. caninum* DNA has been detected in the magpie (*Pica pica*) (Darwich et al., 2012). These findings could have significant implications for both domestic and sylvatic cycles as the latter can affect the seroprevalence of *N. caninum* in cattle in a given area especially if these animals could serve as a reservoir host for wild dogs (Almería and López-Gatius, 2013).

Horses are an intermediate hosts of *Neospora hughesi* (Marsh et al., 1998), which was identified in an aborted equine foetus (Dubey and Porterfield, 1990). The parasite was later isolated from an 11-year old horse and described as a new species, with molecular differences to *N. caninum* (Marsh et al., 1998). The internal transcribed spacer 1 (ITS1) of *N. hughesi* differs in seven nucleotides from that of *N. caninum;* however, no structural or molecular differences were found between different *Neospora* isolates from dogs and cattle (Dubey, 1999). Tissues cysts for *N. hughesi* are generally smaller with thinner cyst walls than that of *N. caninum,* and bradyzoites are also smaller (Marsh et al., 1998). Recently, *Neospora* antibodies were detected in 100 adult horses in Northwest Iran (Yagoob, 2012), but it was unclear which species had actually infected these animals. High levels of antibodies to *N. hughesi* were also detected in presuckling colostral sera of naturally exposed foals from three mares in California (Pusterla et al., 2011). It is still unknown whether *N. hughesi* is the sole species of *Neospora* that infects horses or if *N. caninum* also plays a part in infection as both species can cross react serologically with each other (Gondim et al., 2009).

1.2 History and economic impact of *N. caninum*

Neospora caninum was first described in a dog with encephalomyelitis and myositis (Bjerkas et al., 1984). Neosporosis was later described in calves with myeloencephalitis (O'Toole and Jeffrey, 1987; Parish et al., 1987). The parasite was first isolated from dogs (NC-1) and named into a new genus and species (Dubey et al., 1988a). *Neospora caninum* (BPA1) was later isolated for the first time from an aborted bovine foetus in the United States (Conrad et al., 1993). In addition, *N. caninum* has also been implicated in causing sporadic disease in other livestock species including sheep (Dubey et al., 1990a), goats (Barr et al., 1992), horses (Marsh et al., 1996), deer (Woods et al., 1994), foxes (Buxton et al., 1997), and other

carnivores (Barber et al., 1997). Retrospective studies carried out in California confirmed that *N. caninum* has been endemic in the region since at least 1984; the infection was also identified retrospectively in a stillborn calf in Australia (Dubey and Lindsay, 1996). The latter was a full term animal that was born dead (Hartley and Bridge, 1975). Toxoplasmosis was excluded because the aborting cow had no *T. gondii* antibodies and furthermore, *T. gondii* is not an abortifacient in cattle (Dubey and Lindsay, 1996). Diagnosis was confirmed when *N. caninum* specific antiserum became available and parasites in bovine tissues were found to react with *N. caninum* antibodies (Lindsay and Dubey, 1989a).

Neospora caninum is regarded as one of the most important infectious causes of abortion in cattle worldwide, yet there are no definitive studies that quantify losses due to neosporosis to the cattle industry; however, losses are estimated to be in the millions of dollars per year (Dubey, 2003; Reichel et al., 2013). The major economic loss due to neosporosis is as a result of reproductive failure in cattle in many countries worldwide (Dubey et al., 2007). The economic costs attributed to *N. caninum* infection are the product of estimations of the damage cause by the infection and their effect on the economy (Trees et al., 1999). Diagnosing *Neospora*-associated abortion in cattle can be difficult and expensive (Dubey and Schares, 2006). There are numerous other indirect costs associated with losses due to neosporosis and include possible loss of milk yield (seropositive cows in California were found to produce approximately one kilogramme less milk per day than their seronegative herd mates), rebreeding, replacement cost if cows are culled (Thurmond and Hietala, 1997a, b), and losses from the potential value of infected animals, which could be considerable (Trees et al., 1999). Early culling could, perhaps, account for a large proportion of the losses associated with neosporosis. In a retrospective study of a 2,000-cow dairy herd that had a history of *N. caninum*-associated abortion, *Neospora*-seropositive cows were culled on average six months earlier than seronegative animals (Dubey et al., 2007).

Since reproductive efficiency, which is a measure of the percentage of cows exposed to bulls that weaned a calf, will be decreased in herds with more abortions, income will therefore be reduced in these herds with poorer reproductive performance (Larson et al., 2004). The cost of replacement heifers will increase and income from selling fewer heifers will be less (Larson et al., 2004). Presently, only a little is known about the causes of abortion in beef cattle probably because of the

difficulty in monitoring expulsion of small foetuses in the first trimester; therefore, accurate assessments of *Neospora*-induced losses in beef cattle is lacking (Dubey et al., 2007).

1.3 Life cycle of *N. caninum*

Neospora caninum is a coccidian parasite which has a heteroxenous life cycle (Dubey et al., 2006). The parasite has three asexual infectious development stages, i.e. tachyzoites, bradyzoites and sporozoites (Dubey, 1999). The sexual stages of *Neospora* have not been described, but it is likely that the schizont (asexual) and gamont (sexual) stages also exist in the gut epithelium of the definitive hosts as was shown for *T. gondii* when kittens were fed *Toxoplasma* cysts since these two parasites are closed related (Frenkel et al., 1970). The asexual development occurs in the intermediate hosts, whereas sexual reproduction occurs within the definitive hosts (Dubey, 1999). The tachyzoites are the rapidly dividing stage that can infect various cells types including neurons, hepatocytes, skeletal muscle cells, cardiomyocytes, tubular epithelial cells, alveolar macrophages, and placental trophoblasts (Barr et al., 1991; Dubey et al., 2002; Macaldowie et al., 2004; Gibney et al., 2008). Tachyzoites were also found it the amniotic fluid of pregnant cows (King et al., 2011). In one publication it was assumed, but not proven, that tachyzoites can differentiate into bradyzoites in neurons, following the onset of a strong immune response resulting in the formation of tissue cysts (Peters et al., 2001).

Bradyzoites are the slowly replicating encysted stages of *N. caninum* (Dubey et al., 2006). They remain within tissue cysts until reactivation (recrudescence), possibly due to changes in the immune system of the intermediate hosts as a consequence of pregnancy or infectious diseases, such as bovine viral diarrhoea (Björkman et al., 2000; Guy et al., 2001). Tissue cysts vary considerably in size depending on the number of bradyzoites they contain (Dubey et al., 2006).

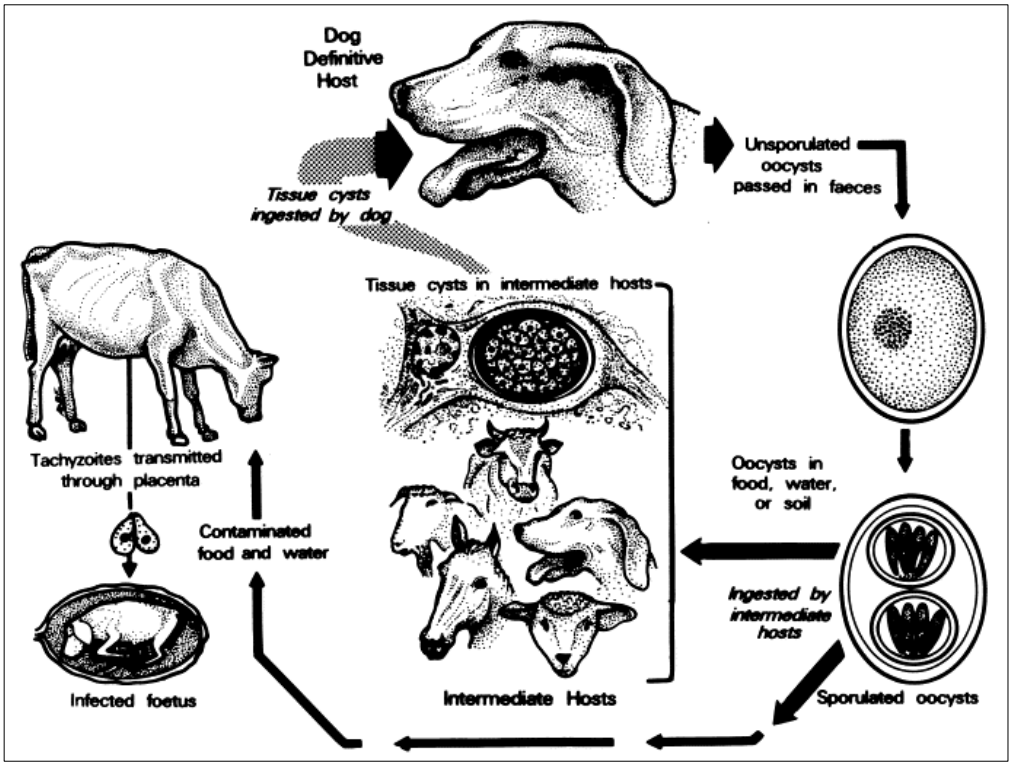

Figure 1.1. Life cycle of *Neospora caninum*. The diagram shows the ingestion of tissue cysts by the definitive host (dog), which then pass out unsporulated oocysts in the faeces. The oocysts will later sporulate and can contaminate food and water, which will then be picked up by the intermediate host (in this case, cattle). The sporulated oocysts form tachyzoites, which may be transmitted transplacentally to the foetus (vertical transmission). Adopted from (Dubey, 1999).

The environmentally resistant oocysts are excreted in the faeces of the definitive hosts (Fig.1.1) after consumption of infected materials such as foetal membranes (McAllister et al., 1998). Following ingestion of the oocysts, sporozoites (an oocyst contains two sporocysts with four sporozoites each) are released into the intestinal tract of the intermediate host, differentiate into tachyzoites and probably spread via the mononuclear phagocyte system (macrophages, monocytes) to the uterus in pregnant animals where they ultimately cross the placenta and infect the foetus (Williams et al., 2009).

1.4 Structure and biology of *N. caninum*

Tachyzoites and bradyzoites are the stages which occur in tissues of infected intermediate and definitive hosts, whereas sporozoites are present within sporocysts inside the oocysts which are excreted in the faeces of the definitive hosts (Dubey et al., 2006). Tachyzoites and bradyzoites of *N. caninum* have an ultrastructural morphology similar to that of *T. gondii* and contain two apical rings, a conoid, a pellicle which consists of a plasmalemma and an inner membrane complex, 22

subpellicular microtubules, micronemes, rhoptries, a mitochondrium, a nucleolus within the nucleus, Golgi complex, plastid, ribosomes, polysomes, dense granules, amylopectin granules, lipid bodies, vesicles, endoplasmic reticulum, micropores and a posterior pore (Speer et al., 1999).

Tachyzoites (Figure 1.2) are usually present in the host cells within a parasitophorous vacuole (PV) that contains a well-developed tubulo-vesicular membrane network; a few host cell mitochondria are usually observed in close association with the PV (Speer et al., 1999). The tachyzoites of *N. caninum* are ovoid, lunate or globular and measure approximately 3-7 x 1-5 µm depending on the stage of division (Dubey et al., 2002). Each tachyzoite contains an average of 6-16 rhoptries, which are homogenously electron-dense. Some rhoptries are located posterior to the centrally located zoite nucleus(Speer et al., 1999). Micronemes are numerous in *N. caninum* tachyzoites, with perpendicular orientation to the zoite pellicle as opposed to the haphazard orientation in *T. gondii* tachyzoites; in contrast, dense granules are scattered throughout the cytoplasm of the parasite, but tend to be more numerous at the posterior end in *N. caninum* and the anterior end in *T. gondii* (Speer et al., 1999).

Bradyzoites are the slowly replicating, encysted stages of *N. caninum* and cysts may vary in size up to approximately 100µm in diameter depending on the number of parasites it contains (Dubey et al., 2006). Tissues cysts are mainly found in the brain and spinal cord of congenitally infected calves, but a few thin-walled tissue cysts have been reported in skeletal muscles of two naturally infected 2-day-old calves (Dubey et al., 1989). Bradyzoites are slender and measure 8 x 2 µm, contain fewer rhoptries (6-12) with electron-dense contents, amylopectin granules and terminally located nucleus (Dubey et al., 2006; Ortega-Mora et al., 2006).

Neospora caninum oocysts are approximately 10 x 12 µm and are excreted in the faeces of the definitive hosts in the unsporulated form, after which sporulation occurs so that each oocyst contains two sporocysts, each containing four sporozoites (Lindsay et al., 1999). The oocysts are spherical to subspherical with smooth colourless walls of approximately 0.6 x 0.8 µm thickness (Lindsay et al., 1999). The sporocysts are ellipsoidal and measure approximately 8 x 6 µm in diameter with a sporocyst wall measuring 0.5 x 0.6 µm thickness. Sporozoites are elongated, sometimes flattened on one side and measure approximately 6 x 2 µm; they contain a central or slightly posterior nucleus (Lindsay et al., 1999). The schizogonic and

gametogenic stages, that have been speculated to precede the formation of oocysts in the intestines of dogs, are yet to be observed (Dubey et al., 2004).

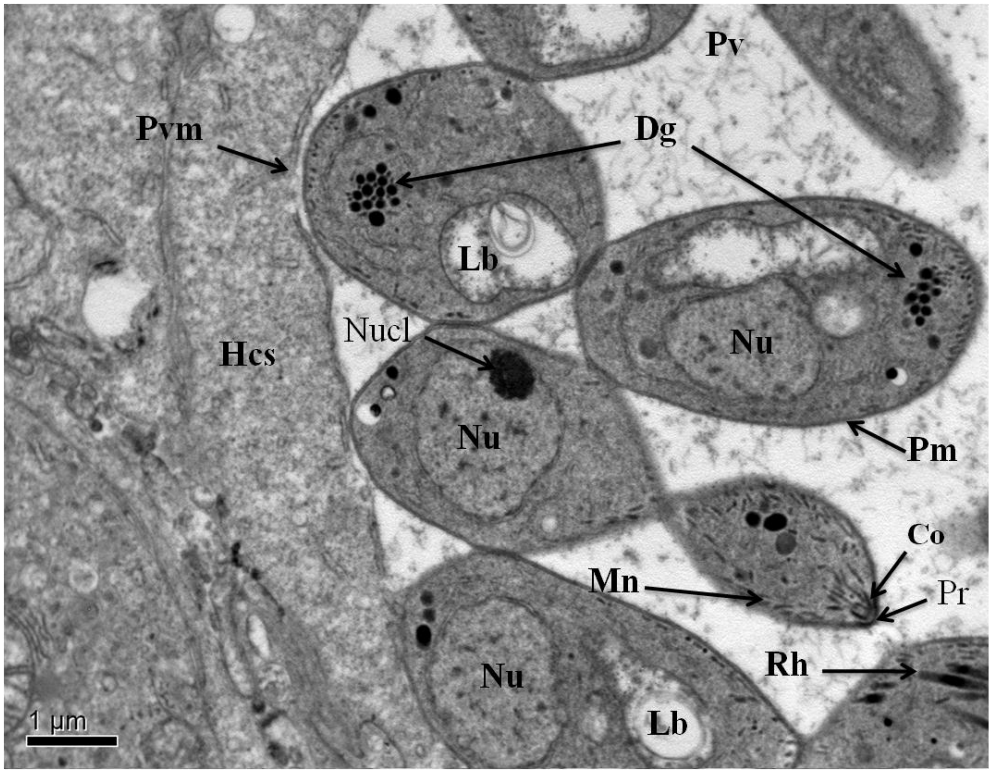

Figure 1.2. *N. caninum* (NC-Liverpool strain) infected cultured human hepatocyte (for method, see chapter 3 section 3.4.11). Transmission electron micrograph. Hepatocyte containing several tachyzoites. Co: conoid; Dg: dense granules; Hcs: host cell cytoplasm; Lb: lipid body; Mn: microneme; Nu: nucleus of tachyzoite; Nucl: nucleolus of tachyzoite; Pm: plasmalemma; Pr: polar ring; Pvm: parasitophorous vacuole membrane; Pv: parasitophorous vacuole; Rh: rhoptry. TEM. X8900

1.5 Epidemiology of neosporosis and *N. caninum* infection

The serological prevalence of *N. caninum* in cattle worldwide has been summarised and it showed considerable differences among and within countries, regions and between beef and dairy cattle (Dubey et al., 2007; Dubey and Schares, 2011). There are also indications that differences exist in seropositivity among different breeds of cattle (Duong et al., 2008; Munhoz et al., 2009), but it is argued that the production system used for the different breeds might have been a major cause for these differences rather than a breed susceptibility (Dubey and Schares, 2011). The prevalence differences of neosporosis are related to various risk and protective factors, which affect the risk of both infection and abortion (Goodswen et al., 2013). Some of the factors listed as affecting the risk of individual cattle or herds becoming infected with *N. caninum* were age of animals (Rinaldi et al., 2005), increasing

gestation number (Jensen et al., 1999), presence and number of farm dogs (Von Blumröder et al., 2006), stocking density and large herds (Barling et al., 2000; Schares et al., 2004), rearing of own heifers rather than acquiring from external sources (Barling et al., 2001) and the effect of climatic changes on sporulation or oocyst survival (Rinaldi et al., 2005). Additional factors influencing the risk of *N. caninum*-associated abortion in individual cattle or herds are the number of ingested oocysts by animals and the stage of gestation (Gondim et al., 2004a), immune status of the dam (Dubey et al., 2007) and seropositivity, as seropositive cows are more likely to abort than seronegative animals (Weston et al., 2005; Corbellini et al., 2006).

Neospora caninum-associated abortion in cattle herds may have a sporadic, epidemic or endemic pattern (Moen et al., 1998; McAllister et al., 2000). Sporadic abortion occurs occasionally within a herd, while an epidemic is defined as a temporary outbreak or exposure to a single source of infection and is defined as a 10% of at-risk cows aborting over a 3 month period (McAllister et al., 2000; Schares et al., 2002). In endemic abortions, the pattern of infection is characterised by chronic, long term persistence of the infection as a point source exposure and abortion problems can persist for several months to years (Davison et al., 1999a; Dijkstra et al., 2002).

Oocysts are the key in the epidemiology of bovine neosporosis and little is known about the biology of this stage of the *N. caninum* life cycle (Dubey et al., 2007). Models of neosporosis depend on the environmental contamination by oocysts, so the larger the number of oocysts shed by the definitive hosts, the greater the chances or rates of horizontal transmission to hosts (Goodswen et al., 2013). Following experimental infection of 3 puppies with *N. caninum*-infected tissues, an average of 166,400 oocysts were observed and it continued for approximately 24 days; coproscopic examination in many large dog population in Germany over a 3 year period found evidence of oocyst shedding in 0.2% of dogs (McAllister et al., 1998; Gondim et al., 2002; Schares et al., 2005). The number of oocysts required to establish an infection in cattle and induce abortion has not yet been determined; however, a few studies have experimented with varying doses of oocysts and revealed a low abortion rate (Trees et al., 2002; McCann et al., 2007). The maintenance of infection in cattle herds might not be entirely dependent on

transplacental transmission alone, but may be augmented by horizontal transmission from the environment (French et al., 1999).

1.6 Transmission of *N. caninum* in cattle

The two major routes of *N. caninum* transmission are horizontal, where cattle ingest sporulated *N. caninum* oocysts and vertical transmission, which includes transmission of the agent to the foetus during pregnancy either following reactivation of bradyzoites in the infected dam or *de novo* infection of the dam during pregnancy (Trees and Williams, 2005). Both routes play an important role and are vital for the survival of the parasite (Dubey et al., 2006; Dubey et al., 2007). The transplacental transmission of *N. caninum* is very efficient in cattle. Consequently, vertical transmission contributes significantly to the persistence of *N. caninum* in a herd by propagating the infection to successive generations (Björkman et al., 1996; Anderson et al., 1997; Schares et al., 1998; Wouda et al., 1998). Cows may remain infected for life (Trees et al., 1999) and may transmit the parasite to offspring either in several consecutive pregnancies (Hietala and Thurmond, 1999) or intermittently (Boulton et al., 1995; Wouda et al., 1998).

The prevalence of congenital infection varies (Dubey et al., 2006), with reported infection rates ranging from approximately 40% to 95% (Davison et al., 1999a; Bergeron et al., 2000; Björkman et al., 2003; Romero and Frankena, 2003; Pan et al., 2004). In one Dutch study involving foetuses of 500 infected dams, infection was found in 80% of calves from heifers, 71% of calves from second parity cows, 67% of calves from third parity cows and 66% of calves from fourth parity and older cows (Dijkstra et al., 2003). Despite the efficiency of vertical transmission, it is evident from theoretical modelling that infection with *N. caninum* cannot be sustained in cattle herds without horizontal transmission (French et al., 1999). So far, the ingestion of sporulated *N. caninum* oocysts from the environment is the only demonstrated natural mode of infection in cattle after birth (Dubey et al., 2007). Despite investigations of neosporosis outbreaks in cattle herds, which suggest an external source of infection, oral infection with oocysts from the environment or infection via contact with infected tissues and/or faeces, have not been demonstrated conclusively (Yaeger et al., 1994; McAllister et al., 1996).

Shedding of oocysts by infected canids in cattle-feeding areas is a likely cause of horizontal transmission that could play an important role in infected herds, where

a lack of association between the seropositivity of dams and daughters is seen (Thurmond et al., 1997; Waldner et al., 1999; Dyer et al., 2000; Dijkstra et al., 2001). However, it was shown that ingestion of oocysts can lead to transplacental infection, as inoculation of cows with oocysts via an oesophageal tube led to abortion in one animal, and the foetus exhibited typical lesions consistent with neosporosis in which *N. caninum* was demonstrated by immunohistology and polymerase chain reaction (PCR). From the 19 cows infected, 17 seroconverted, while the control animals remained seronegative (Gondim et al., 2004a). In a later study in which 18 cows were challenged orally, only one abortion was definitively associated with *N. caninum* as in the previous study (McCann et al., 2007). It is believed that the oocysts excyst in the small intestine, each releasing eight sporozoites, which then parasitise the intestinal epithelium, transform into tachyzoites and undergo a phase of multiplication, possibly in the mesenteric lymph nodes (Dubey et al., 2006). The parasites are then released into the blood causing a parasitaemia, which leads to dissemination of *N. caninum* throughout the body, including the gravid uterus (Dubey et al., 2006). *Neospora caninum* DNA has been demonstrated in the leukocyte fraction of blood from naturally infected cattle in mid gestation (Okeoma et al., 2004) and after experimental infection, tachyzoites have been identified in leukocytes within placental maternal blood vessels (Gibney et al., 2008). These findings support the hypothesis that tachyzoites cross the placenta in the maternal circulation (Williams et al., 2000).

Cow-to-cow transmission has not been observed to date, but many authors have looked at the possibility of infection via contaminated semen from infected bulls (Ortega-Mora et al., 2003; Canada et al., 2006; Serrano-Martínez et al., 2007; Jozani et al., 2012). However, artificial insemination of cows with semen *in vitro* contaminated with *N. caninum* tachyzoites (6.5×10^7 and 1.8×10^7 on day one and two, respectively) failed to induce infection (Canada et al., 2006). One animal developed a low antibody titre of 1:80 in the direct agglutination test at day ten after insemination, but was negative at day 45, which shows that the parasites were able to stimulate the immune system of this animal without causing infection (Uggla et al., 1998; Davison et al., 2001; Canada et al., 2006).

Bradyzoite reactivation and differentiation into tachyzoites, leading to transplacental transmission of *N. caninum* in naturally infected animals, is thought to be triggered by the down regulation of cell mediated immunity that occurs around

mid-gestation; at this time, a Th2 cytokine environment at the materno-foetal interface would favour parasite invasion of the placenta and infection of the foetus. This process is probably due to down-regulation of interferon gamma (IFN-γ), a Th1 type cytokine produced by a range of cell types including NK cells and CD4-positive T cells, which is able to limit multiplication of intracellular parasites (Innes et al., 2001; Almeria et al., 2003; Innes et al., 2005; Rosbottom et al., 2008; Almería et al., 2011, 2012).

1.7 Pathogenesis of *N. caninum* infection in cattle

The pathogenesis of *N. caninum* induced abortion in cattle is yet to be fully elucidated. *N. caninum* infection in cows is mainly manifested in the placenta and foetal tissues following a maternal parasitaemia (reviewed in Dubey et al., 2006). Experimental studies have shown that infection of pregnant cows in early gestation leads to foetal death, which could be due to both extensive placental necrosis and necrosis in foetal tissues, such as the liver and brain (Williams et al., 2000; Macaldowie et al., 2004; Maley et al., 2006; Rosbottom et al., 2007; Gibney et al., 2008; Rosbottom et al., 2008; Rosbottom et al., 2011).

The occurrence of cellular damage in tissues of foetuses infected in early gestation has been reported by many authors and this destruction was attributed to the lack of ability of the foetuses to defend themselves from the effects of the parasites due to insufficient or lack of a mature immune defence mechanism (Williams et al., 2000; Gibney et al., 2008; Bartley et al., 2012; Caspe et al., 2012). Similarly, studies have also been conducted looking at foetal damage and immune response following infection at mid to late gestation, when the foetal immune system would have started to develop or is fully capable of recognising pathogens (Williams et al., 2000; Maley et al., 2003; Gibney et al., 2008; Almería et al., 2010; Bartley et al., 2013a). Others have focused on the detection of a *N. caninum* specific cell mediated immune (CMI) response, because CMI mechanisms can play an essential role in reducing parasite replication in the host, hence reducing parasitaemia and tissues damage (Almeria et al., 2003; Bartley et al., 2004; Bartley et al., 2012; Bartley et al., 2013a). In addition, foetal lymphocytes from foetuses in early gestation stimulated *in vitro* with *N. caninum* tachyzoite lysate failed to produce any detectable IFN-γ, while those harvested from foetal spleen and lymph nodes in mid to late gestation showed a *N. caninum* specific cytokine response, indicating that the

immune cells in older foetuses are mature and functional and would be better able to protect the foetus from parasite-induced pathological changes (Bartley et al., 2004; Bartley et al., 2012; Bartley et al., 2013a). The virulence of different strains of *N. caninum* must also be taken into consideration when interpreting the data available on foetal infection and pathological changes following infection. It is now clear that the more virulent strains result in greater damage to foetal tissues leading to foetal death, whereas parasites of low virulent strains induce only mild pathological changes, and foetal death was not recorded in one study where a low virulent Nc-Spain 1H isolate was used in an experimental infection (Rojo-Montejo et al., 2009).

Pathological changes in the placenta is often more severe during experimental infection and this is probably due to the parasite loads used and the time of infection. Lesions were evident in the placenta of dams infected at 70 days gestation age (dg) starting as early as 14 days post infection (dpi) (Macaldowie et al., 2004). Foetal death was recorded at approximately 21 dpi of the dams with a high virulent strain of *N. caninum* (Gibney et al., 2008), which signifies that pathological changes are induced in the placenta before parasite replication in foetal tissues and it is also likely that parasites reinvade the placenta after multiplying in the foetus and cause further damage. Foetal abortion is therefore likely due to the direct damage of the placenta (necrosis and inflammation), damage to vital foetal organs or a combination of both. There is a need to further elucidate the pathogenesis of *N. caninum* to fully understand how the parasites kill the foetus and the role of the foetal immune response in protecting itself from parasite-induced lesions.

1.8 Host cell invasion and parasite replication

Bovine neosporosis is a disease that is manifested during pregnancy. It is mainly a disease of the placenta and foetus following maternal parasitaemia, triggered either by an exogenous infection or by parasite recrudescence in chronically infected dams (Dubey et al., 2006). *Neospora caninum* is capable of actively invading a range of target cells, a process that has been investigated using different types of *in vitro* culture systems (Hemphill et al., 1996; Weiss et al., 1999; Naguleswaran et al., 2003; Hemphill et al., 2004; Vonlaufen et al., 2004; Lv et al., 2010).

The first step in the physical encounter between the parasites and their host cells is the establishment of a low-affinity contact, mediated by *N. caninum* surface antigen 1 (NcSAG1) and *N. caninum* SAG1-related sequence 2 (NcSRS2), between

the tachyzoites and host cell membrane; this is followed by the actual adhesion process (Hemphill et al., 1996). Prior to, during and after invasion of the host cells, *N. caninum* tachyzoites sequentially discharge micronemes, rhoptries and dense granules, respectively (Hemphill et al., 2004). Adhesion to and invasion of the parasite into the host cell is an active process, which requires metabolic energy on the part of the parasite only, whereas the host cell is only passively involved (Hemphill et al., 2004). As shown for *T. gondii*, during invasion, the parasite orientates itself perpendicularly to the host cell surface membrane and enters the cytoplasm by first advancing the anterior end until it is located within the cell enclosed by a PV (Dobrowolski and Sibley, 1996; Dobrowolski et al., 1997a; Dobrowolski et al., 1997b; Meissner et al., 2002). It is likely that penetration of the host cell membrane by *N. caninum* is also dependent on and powered by the parasite actin/myosin system as in *T. gondii* (Hemphill et al., 2004). The organelles secreted by *N. caninum* tachyzoites at the onset of adhesion are the micronemes, and proteins within these organelles are also thought to be secreted as the parasites egress from host cells (Naguleswaran et al., 2001; Keller et al., 2002; Hemphill et al., 2004). Once inside the host cell, *N. caninum* resides in the PV, surrounded by a parasitophorous vacuole membrane (PVM), which is derived from the host cell plasma membrane (Hemphill and Gottstein, 2006). The PV is usually located in the vicinity of the host cell nucleus in associated with the mitochondria and endoplasmic reticulum (Hemphill et al., 1996; Sinai et al., 1997). This was shown for *T. gondii*, but limited information is available regarding *N. caninum*. The secretory products from the rhoptries are probably involved in modulating the host cell plasma membrane and triggering the formation of the PV (Hemphill et al., 2004; Hemphill and Gottstein, 2006).

Neospora caninum tachyzoites start to divide by endodyogeny soon after invasion; the first division was observed at approximately 6 h post-invasion, and the number of parasites increased steadily with time (Hemphill et al., 1999; Hemphill et al., 2004). Following parasite multiplication, which continued for up to 72-80 h in the PV, host cell lysis occurs and tachyzoites egressed to infect neighbouring cells (Hemphill, 1999). Under normal circumstances, *T. gondii* egression takes place between 24 and 48 h after invasion (Caldas et al., 2010). *Neospora caninum* tachyzoites (Nc-1 isolate) were first observed egressing from infected bovine aortal endothelial cells in an *in vitro* model from 60–72 hours post infection (hpi)

(Hemphill et al., 1996). Parasite egress was considered to be passive due to cell lysis as a consequence of the high parasite loads, however there are reports providing evidence of an ordered and active egress of apicomplexan parasites from host cells (Kafsack et al., 2009; Caldas et al., 2010; Graewe et al., 2012). It is thought that the invasion and egress of protozoan parasites are dependent upon parasite motility and appear to be directed by fluctuations in intracellular calcium (Ca^{2+}) levels (Black et al., 2000).

1.9 Host immune response to *N. caninum*

The mammalian immune system is highly complex and has evolved to protect the host against many forms of diseases (Entrican, 2002). *Neospora caninum* is an obligate intracellular pathogen, which means that CMI responses are likely to play a pivotal role in protective immunity, by reducing the multiplication of parasites within the host, hence reducing parasitaemia (Innes et al., 2005; Almeria et al., 2011). Protective immunity to intracellular pathogens is associated with type 1 T helper cells (Th1 cells), which secrete pro-inflammatory cytokines, such as interferon gamma (IFN-γ), tumour necrosis factor alpha (TNF-α) and interleukin (IL)12 (Baszler et al., 1999b). These cytokines were shown to be upregulated during *T. gondii* infection in mice (Gazzinelli et al., 1994). Since both parasites are closely related and exhibit a similar biology, it has been predicted that the immune response to *N. caninum* will resemble that of *T. gondii* (Williams et al., 2000). It has been suggested that in sufficient quantity, the pro-inflammatory cytokines may be harmful during pregnancy due to IFN-γ production in response to the presence of the parasites in the placenta and it is believed this may play a role in compromising foetal survival (Innes et al., 2002), though there is limited evidence supporting this hypothesis. The pro-inflammatory cytokines, especially IFN-γ, are effective at limiting the multiplication of *N. caninum* and this was shown in an *in vitro* model using recombinant ovine IFN-γ in *N. caninum*-infected fibroblast cultures (Innes et al., 1995). During pregnancy, there appears to be a bias towards a Th2 type cytokine (anti-inflammatory) response, away from the Th1 type, which was found to be protective in protozoan infection (Almeria et al., 2011). It has been suggested that the switch from a Th1 to a Th2 bias can result in the pregnant host being unable to control the protozoan infection (Long and Baszler, 2000). Progesterone is also known to bias a T cell response towards a Th2 phenotype and can induce IL-4

production in established Th1 type T cell clones (Piccinni et al., 1995). The presence of prostaglandin E_2 can also cause dendritic cells to produce IL-10, which biases the priming of naive T cells towards a Th2 phenotype (Kaliński et al., 1997).

It has been suggested that the Th2 type (anti-inflammatory) cytokines, namely IL-4, and regulatory cytokines which includes IL-10 and transforming growth factor beta (TGF-β) are produced at the foeto-maternal interface in the placenta and can counteract the effect of the pro-inflammatory cytokines (Entrican, 2002). The Th2 cytokines are associated with implantation of the foetus and maintenance of early pregnancy by suppression of local inflammatory responses (Wegmann et al., 1993; Chaouat et al., 2002). Foetal trophoblast cells produce IL-10, which floods the maternal immune system, creating a local Th2 cytokine environment at the foeto-maternal interface (Wegmann et al., 1993). IL-10 can down-regulate the production of IFN-γ, which might facilitate the multiplication of *N. caninum* during pregnancy and alter the host-parasite balance in favour of the parasite (Entrican, 2002).

Rosbottom et al. (2008) have shown that there was a significant increase in the cytokine response at the foeto-maternal interface in cattle when foetuses died after experimental infection at 70 dg, as opposed to a modest increase observed in cattle infected at 210 dg when the foetuses survived. The pro-inflammatory cytokines were upregulated, but the levels of the anti-inflammatory Th2 cytokines including IL-4, IL-10 and TGF-β1 were also increased in the placenta (Rosbottom et al., 2008). These results are consistent with other findings in naturally infected cows where Th1 cytokines were up-regulated in the placenta, but were balanced by a significant increase in IL-4 and IL-10, which suggested that the response in the placenta was not polarised towards either a Th1 or Th2 phenotype (Rosbottom et al., 2011). Foetal derived Th1 type cytokines may play an important role in determining if foetuses survive during infection in early gestation, while the Th2 type cytokines are pivotal in reducing the harmful effects of the Th1 type maternal immune response and facilitating transplacental transmission of the parasite (Rosbottom et al., 2008; Gibney et al., 2008).

1.10 *In vitro* cultivation of *N. caninum*

One of the most important biological features shared between the invasive stages of *N. caninum* and *T. gondii* is their low degree of host cell specificity *in vitro* (Hemphill et al., 2004). Different cell types have been used for the *in vitro*

cultivation of *N. caninum*. The parasite was first isolated from dogs and cultured in bovine monocytes and cardio-pulmonary arterial endothelial cells (CPAE) (Lindsay and Dubey, 1989b). Since that time, *N. caninum* has been grown in several other cell types including Madin-Derby bovine kidney cells, human foreskin fibroblasts, human breast carcinoma cell 7 (MCF-7), African green monkey kidney cells (COS-1), monkey kidney cells (MARC-145), bovine endothelial cells, CPAE (ATCC-CCL209), different established and primary cell lines (bovine and murine) and African green monkey kidney cells (Vero cells – Sigma-Aldrich, St. Louis, MO, USA) (Conrad et al., 1993; Hemphill et al., 1996; Stenlund et al., 1997; Hemphill, 1999; Weiss et al., 1999; Gondim et al., 2001; Vonlaufen et al., 2004; Cadore et al., 2009; Rojo-Montejo et al., 2009; Lv et al., 2010). Organotypic rat brain slice cultures, previously developed to study the physiology of the neuronal tissues *in vitro* were also used to culture *N. caninum* (Stoppini et al., 1991), as this method mimics the *in vivo* situation upon experimental infection and the three-dimensional organisation of the tissues is preserved (Hemphill et al., 2004).

Cell cultures containing *N. caninum* tachyzoites are usually maintained in Dulbecco's Modified Eagle's Medium (DMEM) (Koyama et al., 2001), minimum essential medium (MEM) (Yamane et al., 1998) or Roswell Park Memorial Institute Medium (RPMI-1640) (Stenlund et al., 1997; Hemphill et al., 2004; Bień et al., 2010; Reiterová et al., 2011). Growth medium is usually supplemented with foetal bovine/calf serum (FBS); however, care should be taken when selecting this product as many batches of commercially available FBS contain antibodies against *N. caninum* that could potentially lead to agglutination and death of the parasite once released into the medium following host cell lysis (Hemphill, 1999). One study showed that all FBS samples tested by western blot were positive for antibodies to *N. caninum* and 88% of the samples were positive on enzyme-linked immunosorbent assay (ELISA) (Torres and Ortega, 2006). In order to avoid the complications of culturing cells in FBS-supplemented medium, immunoglobulin G-free horse serum can be used as a substitute; however, cultures tend to be less prolific when horse serum is used (Hemphill, 1999). FBS has been used at different concentrations such as a 1% (Barber et al., 1995), 2% (Stenlund et al., 1997), 5% (Hemphill et al., 2004), 7% (Vonlaufen et al., 2002), 10% (Weiss et al., 1999; Lv et al., 2010) and 20% (Hemphill et al., 1996) for cell culture.

Neospora caninum tachyzoites, in contrast to *T. gondii*, are very vulnerable to the effects of extracellular maintenance and lose their infectivity rapidly if kept in growth medium extracellularly for more than a few hours (Paré et al., 1996; Hemphill, 1999; Naguleswaran et al., 2003). However, long term *in vitro* culture of *N. caninum* tachyzoites did not impair infectivity in mice and cattle (Kritzner et al., 2002; Cannas et al., 2003). However, attenuation of the virulence of *N. caninum* tachyzoites was achieved following continuous passage of the parasites in cell culture and clear differences in the *in vivo* pathogenicity was shown for parasites maintained in culture for different lengths of time (Bartley et al., 2006). When introduced back into *in vitro* cultures, the parasites showed rapid growth, which suggests that the tachyzoites may have adapted to the *in vitro* environment.

Neospora caninum tachyzoite-to-bradyzoite *in vitro* cultivation has been performed in Vero cells, a system that allowed the separation of bradyzoites from the host cells (Vonlaufen et al., 2004). The induction of bradyzoites occurred after treatment of tachyzoite-infected Vero cell cultures for 8 days with sodium nitroprusside (SNP), an inducer of apoptosis (Vonlaufen et al., 2004). This process severely scaled down the parasite proliferation rate leading to reduced expression of the tachyzoite surface antigens and induced expression of the bradyzoite marker, *N. caninum* bradyzoite antigen 1 (NcBAG1). The stage conversion of *T. gondii* occurs more efficiently and is dependent on the strains of parasites used, whereas with *N. caninum*, this is more difficult to achieve and depends more on the host cell lines and parasite isolates and requires nitric oxide such as SNP as described above (Weiss et al., 1999).

In vitro cell culture of *N. caninum* has been used for the development of tools that are used in immunodiagnosis, immunohistochemical and molecular (by PCR) detection of the parasite and for assessing the susceptibility of *N. caninum* tachyzoites to chemotherapeutic agents. It allows for the development of various ELISAs, indirect fluorescent antibody tests (IFAT) and it has also provided a means for defining ultrastructural differences between *Neospora* and *Toxoplasma* (Barr et al., 1991; Williams et al., 1997; Schares et al., 1998; Hemphill, 1999; Speer et al., 1999).

1.11 Pathological changes in *N. caninum* infected cattle

Bovine neosporosis is a disease of the placenta and foetus and is acquired either through a primary maternal infection or parasite recrudescence during pregnancy (Dubey et al., 2006). The parasite is transmitted very efficiently across the placenta and a high percentage of aborted foetuses do not exhibit gross pathological changes, while the *in utero* infected calves are generally born healthy (Dubey et al., 2006). Naturally *Neospora* aborted foetuses may be autolysed or mummified and can exhibit pale white foci in the skeletal and cardiac muscles as well as small, pale to dark foci of necrosis in the brain along with hydrocephalus (Dubey et al., 1998; Anderson et al., 2000; Piergili Fioretti et al., 2003). Gross placental lesions are limited to focal necrosis and areas of discolouration in placental cotyledons (Dubey et al., 1998; Piergili Fioretti et al., 2003).

In experimental infections, light microscopy usually reveals severe lesions in the placenta (Dubey et al., 2006). After infection, the parasite causes damage by replicating in both the maternal and foetal tissues at the foeto-maternal interface and elicits a nonsuppurative inflammatory response in the foetal liver, CNS, skeletal muscle and heart (Maley et al., 2003; Macaldowie et al., 2004; Gibney et al., 2008). After intravenous inoculation of *N. caninum* tachyzoites at 70 dg, lesions consisted of serum leakage between the maternal and foetal tissues along with nonsuppurative inflammatory infiltrates, which were in direct association with *N. caninum* tachyzoites in the maternal septa, and necrosis of foetal mesenchymal and trophoblast cells at 14 dpi (Macaldowie et al., 2004). After inoculation of cows at 70 dg when foetal death had occurred 20-22 days later, multifocal epithelial cell necrosis and focally extensive necrosis of foetal villi were the main placental lesions in all animals examined (Gibney et al., 2008). *N. caninum* tachyzoites were also detected by immunohistology and ultrastructural examination in degenerated epithelial cells and the maternal interstitial layer (Gibney et al., 2008). After 28 dpi, Macaldowie et al., (2004) observed extensive autolysis and necrosis of trophoblast cells in foetal villi, necrosis of the maternal septa and separation of foetal cotyledons from maternal caruncles. Foetuses from these animals were not alive at the time of euthanasia of the dam.

In animals inoculated subcutaneously at 70 dg with *N. caninum* and euthanised at 14 dpi, placental lesions were less severe and consisted of mild nonsuppurative inflammatory infiltrates in the maternal septa with isolated areas of serum leakage

between maternal and foetal tissues, and low numbers of degenerated foetal villi and necrotic foetal trophoblast cells (Macaldowie et al., 2004). Severe lesions were observed in the placenta of one foetus that had died within 28 dpi and consisted of necrosis and separation of the foetal chorion from the caruncles with serum leakage, haemorrhage and necrosis of both maternal and foetal tissues; however, the placenta from a live foetus showed no significant lesions at 28 dpi. In animals that were carrying dead foetuses at 42 and 56 dpi, foetal cotyledons were necrotic and had detached from the maternal caruncles, which were shrunken with sloughed maternal septa and necrotic foetal trophoblast cells (Macaldowie et al., 2004); these lesions were associated with a nonsuppurative inflammatory infiltrate within the interstitium of the detached foetal chorion and were associated with *N. caninum* tachyzoites, however it was not clear when post infection these two foetuses had died. The placentomes from cattle infected with the Nc-Spain 1H isolate (low virulence isolate) exhibited only mild serum leakage in the caruncular septa, while those infected with the Nc-1 isolate presented with multiple foci of non-suppurative inflammatory infiltrates in both the maternal and foetal interstitium, areas of epithelial cell necrosis and haemorrhage in the caruncular septa, necrosis of foetal villi, as well as cell debris and serum leakage between maternal and foetal tissues (Rojo-Montejo et al., 2009).

Dams experimentally infected subcutaneously in mid gestation showed placental lesions, represented by necrosis of small groups of foetal villi with proteinaceous exudate between affected villi and maternal caruncular septa (Maley et al., 2003). In animals infected at 210 dg, they were restricted to mild multifocal nonsuppurative inflammatory infiltration in foetal villi and the surrounding maternal epithelium, without the presence of *N. caninum* tachyzoites (Gibney et al., 2008).

Neospora caninum infection in early gestation has been associated with foetal death and extensive pathological changes in various tissues (Williams et al., 2000; Guy et al., 2001; Gibney et al., 2008; Rosbottom et al., 2008); whereas in foetuses from dams infected in late gestation, only the brain and spinal cord exhibited pathological changes (Gibney et al., 2008). It is believed that *N. caninum* tachyzoites enter the foetal bloodstream and invade the tissues with a preference for the CNS (Macaldowie et al., 2004); tachyzoites are mainly found in the brain where they multiply and cause destruction of neurons (Wouda et al., 1997). The main pathological lesion observed after infection of the dam in early gestation with 10^7 *N. caninum* tachyzoites of the Liverpool strain was multifocal necrosis in the CNS and

liver with scattered necrotic cells in skeletal muscle, the renal tubular epithelium, pulmonary and pancreatic parenchyma, thymus, spleen and bone marrow (Gibney et al., 2008). *N. caninum* tachyzoites were detected within all affected tissues in foetuses in early gestation from the latter experiment. In another study, experimental infection of cattle with 10^7 tachyzoites of the low virulent Nc-Spain 1H at 70 dg did not induce histopathological changes in the CNS of infected foetuses, whereas mild focal perivascular cuffing in the brain and multiple foci of hepatocellular necrosis in the liver were observed in foetuses that had died at 34 dpi (104 dg) following infection with the same dose of the more virulent Nc-1 isolate in the same experiment (Rojo-Montejo et al., 2009).

Foetuses in mid to late gestation had lesions in the CNS, which consisted of mild microgliosis and perivascular mononuclear infiltration in association with *N. caninum* tachyzoites; while the tongue, skeletal muscle, liver and heart exhibited moderate to severe mononuclear infiltrates (Maley et al., 2003; Gibney et al., 2008; Almería et al., 2010).

In a recent study, foetuses examined after parasite recrudescence in mid gestation showed only mild nonsuppurative infiltrates in skeletal muscles and CNS; tachyzoites were detected in the spinal nerve root of only one foetus (Rosbottom et al., 2011). The predominant lesion reported in calves born alive with clinical neosporosis (which is rare) was encephalomyelitis, with more prominent lesions in the spinal cord than the brain, represented by focal gliosis and perivascular mononuclear cuffing (Parish et al., 1987; Peters et al., 2001). One still born calf presented with extensive myocarditis, with low numbers of neutrophils and mononuclear cells, necrosis of cardiomyocytes and numerous tachyzoites throughout the myocardium, while the brain exhibited multifocal areas of necrosis with perivascular cuffing and capillary necrosis (Dubey et al., 1990b). Hepatic lesions in this calf consisted only of centrilobular necrosis without associated *N. caninum* tachyzoites.

1.12 Diagnosis of bovine neosporosis

For the diagnosis of bovine neosporosis, clinical history, epidemiological data, information about the abortion pattern and foetal age are important factors that should be considered (Ortega-Mora et al., 2006). The definitive diagnosis of neosporosis can be very difficult, because infection does not always result in abortion

and even demonstration of *N. caninum* infection, both histologically and immunohistologically, does not give conclusive evidence that the parasite is the cause of the abortion (Thurmond et al., 1999).

With regards to post-mortem diagnosis in aborted foetuses, the ideal diagnostic samples include both the aborted foetus and the placenta, together with sera from the dam. If this is not feasible, samples from brain, heart and liver of the foetus should be submitted (Ortega-Mora et al., 2006). The brain is the most reliable tissue for the diagnosis, but the probability of diagnosing the infection increases when other tissues, such as heart and liver, are analysed (Ortega-Mora et al., 2006). Histopathological examination is an important diagnostic procedure (Dubey and Schares, 2006; Ortega-Mora et al., 2006). Histology allows for the detection of tachyzoites, inflammatory and degenerative changes in foetal tissues, especially in the CNS, heart, liver and muscles (reviewed in Dubey and Lindsay, 1996). However, the inflammatory lesions are not pathognomonic for *N. caninum* infection.

Histology has been the most commonly used method for parasite detection initially, but immunohistological detection of parasites in foetal brain, lung, liver and heart has been used to confirm the presence of the agent (Lindsay and Dubey, 1989a; Boger and Hattel, 2003) . Both polyclonal and monoclonal antibodies specific to *N. caninum* can be used, but the polyclonal antibodies made in rabbits seem to be more reliable than the mouse-derived monoclonal antibodies for diagnostic purposes (Lindsay and Dubey, 1989a; Cole et al., 1994). Immunohistology is highly specific, although cross reactivity with *T. gondii* has been reported (Van Maanen et al., 2004). Polyclonal antibodies directed against *N. caninum* surface proteins Nc-p43 (specific for both *N. caninum* tachyzoites and bradyzoites) and Nc-p36 (reacts with tachyzoites only) have been evaluated for diagnostic purposes and were shown to react with two isolates of *N. caninum* (Nc-1 and Nc-Liverpool), but not *T. gondii,* indicating that they do not cross-react with *T gondii* (Hemphill and Gottstein, 1996; Hemphill et al., 1997; Fuchs et al., 1998). Another murine monoclonal antibody, which reacted specifically with *N. caninum* tachyzoites and tissue cysts had previously been generated to combat the problem of cross-reactivity between *N. caninum* and *T. gondii* in formalin-fixed paraffin-embedded tissues (Cole et al., 1993). This antibody was shown to recognise *N. caninum* tachyzoites and bradyzoites in dog, cattle, mice, rats, sheep and goats (Hemphill, 1999; Uzêda et al., 2013).

The PCR technique also plays an important role in the diagnosis of *N. caninum* infection when used in aborted foetal tissues (Gottstein et al., 1998; Baszler et al., 1999a; Sager et al., 2001; Van Maanen et al., 2004) and other samples such as amniotic fluid (Ho et al., 1997) and cerebrospinal fluid (Peters et al., 2000; Schatzberg et al., 2003). The advantage of the PCR is its high specificity and high sensitivity and therefore the ability to detect small amounts of *N. caninum* DNA in a large quantity of tissue; PCR also works well when foetal tissues are autolysed, which is often the case with *Neospora* abortions (Ortega-Mora et al., 2006). An indirect *in situ* PCR method has also been described and it combines the advantage of the extraordinarily high sensitivity and specificity of PCR and the *in situ* representation of immunohistological methods (Löschenberger et al., 2004).

Diagnosis of neosporosis by PCR is based on the detection of specific DNA sequences, such as the ITS1, 18S ribosomal (r) DNA and 28S rDNA (Ho et al., 1996; Buxton et al., 1998; Ellis et al., 1998). The sequence differences that exist among the ITS1 regions of different apicomplexan parasites, such as *N. caninum*, *T. gondii*, *Hammondia hammondi* and *H. heydorni*, allow for the establishment of species specific PCR protocols (Dubey and Schares, 2006). In addition to the single-step conventional PCR (Holmdahl and Mattsson, 1996; Payne and Ellis, 1996), two-step nested PCRs were also developed (Buxton et al., 1998; Uggla et al., 1998). The two-step nested PCRs are more sensitive, but have the disadvantage of potential carryover contaminations. This has led to the development of an alternative single-step nested PCR with high sensitivity, but with a lower risk of carryover contamination (Ellis et al., 1999).

Another technique that can be applied for the diagnosis of foetal neosporosis involves the isolation of *N. caninum* in cell culture or bioassay by inoculation in highly receptive mouse strains such as IFN-γ knock-out and Balb/c nu/nu mice (Dubey, 1999). This technique, however, is not suitable for routine diagnosis since the success of the isolation depends on the number of organisms present (Dubey, 1999). Also, it does not comply with the aim to reduce the use of laboratory animals and the replacement with alternative methods.

The diagnosis of acute versus chronic *N. caninum* infection in adult cattle is epidemiologically important (Dubey and Schares, 2011). Avidity tests have been used to distinguish between acute and chronic infection and it was shown that low avidity values are associated with acute infection, as the first antibodies produced

after a primary infection have a lower affinity (binding strength) than those produced later during the infection (Björkman et al., 1999). Two recombinant protein-based ELISAs utilising the immunodominant *N. caninum* dense granule protein (NcGRA7) and the *N. caninum* surface antigen (NcSAG4) protein were developed to investigate the usefulness of both methods in discriminating between acute and chronic infection (Aguado-Martínez et al., 2008). The results of the latter study suggested that in experimentally and naturally infected cattle, the anti-rNcGRA7 antibody levels are indicative of an acute infection (first infection, reinfection and recrudescence), whereas the presence of anti-rNcSAG4 antibodies may be associated with both acute and chronic infection (tachyzoites to bradyzoites conversion). A recent study also looked at the rNcGRA7 and rNcSAG1 antigens as an indicator for the activation stage of *N. caninum* (Hiasa et al., 2012). Its results suggested that rNcSAG1, as a marker of both acute and chronic infection, can be a useful tool for the detection of *N. caninum* infection, whereas rNcGRA7 would be an indicator of acute infection. The authors also suggested that if both antibodies are increased during pregnancy, then *N. caninum* activation and/or abortion risk should be considered.

1.13 Prevention and control of *N. caninum* in cattle

Several control measures have been proposed to reduce the risk of endogenous transplacental transmission of *N. caninum* in cattle (Dubey et al., 2007). Embryo transfer from infected dams to uninfected recipients is considered to be a cost-effective preventative measure to reduce the likelihood of endogenous transplacental transmission of *N. caninum*, but identifying suitable negative recipients is vital (Baillargeon et al., 2001). The use of this technology enables the recovery of uninfected calves from genetically valuable, but *N. caninum*-infected dams (Dubey and Schares, 2011). Infection was not detected in embryos, foetuses or calves born to seronegative recipients that received embryos from seropositive donors, whereas five out of six calves in the embryo transfer from seronegative donors to seropositive recipients were infected with *N. caninum* (Baillargeon et al., 2001; Moskwa et al., 2008). The use of artificial insemination of seropositive dams with semen from beef bulls was also suggested (López-Gatius et al., 2005). Recent studies have indicated that there is a significantly lower risk of abortion in heifers and parous cows inseminated with beef bull semen compared to those inseminated with Holstein-Friesian bull semen (Almería et al., 2009; Yániz et al., 2010).

Selective culling of seropositive cows has been advocated to eliminate infection from a herd (Larson et al., 2004; Hall et al., 2005) but whilst culling of infected cows is an effective control option, it is not always economically practical (Dubey et al., 2007). Culling decisions concerning cows with confirmed *N. caninum* abortion can be made with the knowledge that there is a high probability of repeat abortion in these animals as seropositive cows have a greater risk of abortion; these cows are likely to infect some or all of their offspring via transplacental transmission and can act as source of infection for dogs which may result in them producing oocysts which can infect other naïve cows within the herd (Moen et al., 1998; Haddad et al., 2005).

There are no licenced drugs available for treatment of *N. caninum* infected cattle and use of chemotherapy as an economical control tool in cattle is questionable due to need to treat cows during pregnancy, thus raising the issue of unacceptable milk and meat residues and withdrawal periods (Reichel and Ellis, 2002, 2009). Drugs such as toltrazuril and its derivative ponazuril have shown effect on tachyzoites in mice both *in vivo* and *in vitro*, but did not result in elimination of the parasite (Strohbusch et al., 2009). There have also been attempts to alter the course of *N. caninum* infection in cows with the use of prophylactic medicine with a slow-release monensin bolus, but results from that study were inconclusive (VanLeeuwen et al., 2011). Other drugs are being evaluated for treatment of *N. caninum* infection, but there is still a challenge in terms of clearing tissue cysts in chronically infected animals (Debache et al., 2011).

Numerous reports have discussed the possible use of vaccines in the control of *N. caninum* infection in cattle (Romero et al., 2004; Williams and Trees, 2006; Williams et al., 2007; Reichel and Ellis, 2009; Weston et al., 2012; Weber et al., 2013). An efficient vaccine would have to satisfy the criteria of protection against both infection and clinical disease and be effective in inducing a non-foetopathic, cell mediated immune response (Goodswen et al., 2013). Presently, there is no commercial vaccine available for neosporosis, but animal models have been used to test the efficacy of killed and recombinant *N. caninum* vaccines (Rojo-Montejo et al., 2011; Weston et al., 2012). The latter commercial inactivated vaccine (NeoGuard) was recently evaluated, but demonstrated no significant effect when tested in a clinical trial to assess its efficacy (Weston et al., 2012) and it has subsequently been withdrawn from the market. The development of new animal models to investigate

N. caninum vaccine has been advocated and this is due in part to the unsatisfactory levels of foetal loss in mouse models, which are limited in their capacity as predictive systems for developing vaccines against bovine abortions (Reichel and Ellis, 2009). The use of sheep or other ruminants in clinical trials of new vaccines is also of little value when cattle are the main target species (Reichel and Ellis, 2009).

1.14 Development of the bovine foetal immune response and its relevance for *N. caninum* infection

The ability of the bovine foetus to respond to various antigens develops in a sequential fashion during the approximately 280 day gestational period (Maddox et al., 1987). Bovine foetuses were able to develop mitogenic cellular responses around day 80 of gestation (Osburn et al., 1982), but spleen and thymus cells of other *N. caninum*-infected foetuses showed no evidence of cell mediated immune response before 98 day of gestation age (Bartley et al., 2012). Foetal immunocompetence starts to develop at 100 dg, but only after 150 dg is the foetus able to recognise and respond to antigens effectively (Osburn, 1986). The immune system then becomes progressively more competent at recognising and responding in full to infectious agents, as has been shown for bovine viral diarrhoea virus (BVDV) (Nettleton and Entrican, 1995) and *N. caninum* (Williams et al., 2000). These findings may help to explain why foetuses infected with *N. caninum* early in gestation die due to parasite induced lesions and those infected during mid or late gestation survive. It is evident also that the foetus is beginning to develop a parasite-specific immune response around mid-gestation that will contribute to the changing dynamics of the host parasite relationship and ultimately influence disease outcome (Innes et al., 2005). Many authors have debated the hypothesis that the bovine foetus will be unlikely to survive if infected with *N. caninum* in the first trimester as this may give rise to fulminating parasitaemia and placental or foetal lesions that can terminate pregnancy, whereas foetuses can mount an effective immune response in the middle third of pregnancy that can result in the birth of animals that are clinically normal, but persistently infected (Williams et al., 2000; Andrianarivo et al., 2001b; Almeria et al., 2003; Bartley et al., 2004; Innes et al., 2005; Rosbottom et al., 2011). In natural infection, the majority of *N. caninum*-associated abortion was reported to occur between four and seven months of gestation age, a time when the foetal immune system is developing and may be mature enough to respond to pathogens (Anderson

et al., 1991). Those findings are in contrast to the hypothesis that foetuses in early gestation die due to a lack of a competent immune response, while those in mid to late gestation are born persistently infected.

Extensive haematological and immunohistological studies have been undertaken on the immune response and lymphoid tissues in bovine embryos (<40 dg), foetuses and neonates, providing information on the development of foetal haemolymphatic tissues and immunoglobulin levels as well as the production of complement and interferon (Schultz et al., 1971b, 1973; Osburn et al., 1982; Ishino et al., 1991). When researchers first started to study the development of the bovine foetal immune response, information on the human foetal development was used as a basis, as the two species have approximately the same length of gestation period (~280). They indeed identified several similarities (Schultz et al., 1973; Namikawa et al., 1986; Lobach and Haynes, 1987; Spencer et al., 1992; Haynes and Hale, 1998; Flores et al., 2001; Szépfalusi, 2008). In 1973, a three component concept was proposed for the development of the bovine immune system where stem cells, which originate in the yolk sac, migrate to the foetal liver and subsequently to the thymus (T-cell system) and bone marrow (B cell system) (Osburn and Schultz, 1973). Lymphocytes were observed in thymus and blood of bovine foetuses at 42-43 dg (Schultz et al., 1971a; Osburn and Schultz, 1973).

In cattle, the thymus is first morphologically evident at approximately 30 dg, but T cells were only detected in the developing lobules at 42 dg, prior to the first detection of lymphocytes in the blood at 45 dg (Schultz et al., 1973). At approximately 55 dg, foetuses exhibit a thymus composed of lobules with a distinguishable cortex and medulla that contains numerous thymocytes and Hassall's corpuscules in the medulla (Schultz, 1973). In another study, conspicuous Hassall's corpuscles were regularly observed from 65 dg onwards (Schultz et al., 1973). The relevance of these corpuscular bodies has not been determined in animals, but studies on the human thymus have shown that they express lymphopoietin, which activates thymic dendritic cells that are able to induce proliferation and differentiation of specific regulatory T cells. Hassall's corpuscules also play a role in the removal of apoptotic cells and the maturation of thymocytes (Farr et al., 2002; Watanabe et al., 2005). A later study showed specifically that at 70dg, the thymic cortex contains numerous medium sized lymphocytes, whereas the medulla can often not be identified due to the presence of only few lymphocytes; at 150 dg, however, the

thymus is deeply lobulated and morphologically similar to that of new born calves (Ishino et al., 1991). Other studies focussed on the cellular composition of the thymus. They showed a relatively constant content of T lymphocytes (60-70% of cells) and B cells (only in the medulla, approximately 1%) throughout gestation, whereas macrophages were present in the medulla and increased from 1% at 3 months gestation to almost 8% at birth (Senogles et al., 1979). In addition, eosinophils were observed; their role was not further assessed (Schultz et al., 1973).

The spleen is morphologically evident at 55 dg, when it was shown to be predominantly composed of reticulocytes (Osburn and Schultz, 1973; Schultz et al., 1973). Lymphoid cells were first recognised at 60 dg (Schultz, 1973) and red and white pulp differentiation was first evident at 80-100 dg (Osburn and Schultz, 1973). The spleen showed an increasing percentage of T cells from 11% at three months gestation to over 40% at term while B lymphocytes consistently comprised two to three percent of cells from three months gestation to term (Senogles et al., 1979).

Peripheral lymph nodes (i.e. prefemoral and prescapular lymph nodes) were present in foetuses at 60 dg (Schultz et al., 1973). At 70 dg, they consisted of spindle shaped mesenchymal cells, but did not show cortex and medulla differentiation (Ishino et al., 1991); between 90 and 120 dg, lymphocytes appeared and formed the cortex and medulla; however, only few lymphocytes were present in the medulla at that time point and only after 150 dg were cortical structures distinct with mature lymphocytes (Ishino et al., 1991). Most major lymph nodes were grossly evident by 130 dg (Schultz et al., 1973). Follicular structures were described at 180 dg and after 210 dg, lymph nodes showed a similar appearance to those of neonatal calves (Ishino et al., 1991).

During foetal development, sequential appearance of immunoglobulins is observed even in the absence of obvious exogenous antigenic stimuli. Immunoglobulin M (IgM) containing cells were observed in spleen, lymph nodes and bone marrow and IgM was detected in foetal serum samples obtained at 130 dg, while IgG and IgG-containing cells were observed at 145 dg (Schultz et al., 1971a; Schultz et al., 1973). In spleen and lymph node, IgM-bearing cells were already demonstrated at 90 dg (Ishino et al., 1991) and in an earlier study even at 59 dg (Schultz et al., 1973), whereas cells expressing IgG were observed at 150 dg and 145 dg, respectively (Schultz et al., 1973; Ishino et al., 1991).

Lymphoid tissue in the gastrointestinal tract (gut-associated lymphoid tissue, GALT) was identified in foetuses older than 175 dg, although only to a minimal extent (Schultz et al., 1973); however, Ishino et al. (1991) have identified mild lymphocyte infiltration around blood vessels in the lamina propria as early as 120 dg; distinct lymphoid aggregation was seen at 150 dg and only at 180 dg were follicular structures detected (Ishino et al., 1991).

The innate immune response in bovine foetuses mediated by phagocytes (macrophages and neutrophils) does not fully develop until late gestation, but there is a decline in its functional capacity leading up to birth due to an increase in circulating cortisol levels (Barrington and Parish, 2001). Presumably, this decline is due to the suppression of phagocytic activities by cortisol, even though more neutrophils may be present in the peripheral blood close to parturition (Hulbert et al., 2011). Macrophages and neutrophils as the major phagocytic cells are very important innate immune cells comprising the first line of innate immunity (Kaufmann, 2008). These cells share a common origin and have functions such as phagocytosis of invading pathogens, similar kinetic behaviour during infection and antimicrobial as well as immunomodulatory properties (Silva, 2010). Macrophages have been observed from approximately 90 dg onwards, both in the thymus and, in a far larger quantity, the spleen (Senogles et al., 1979). Neutrophils were first observed at 130 dg and reached maximum values near parturition (Schultz et al., 1971a); while eosinophils were observed in the foetal age group nearest to parturition and were far less frequent than neutrophils (Schultz, 1973). Evidence of complement activity was found between gestation days 70 and 90 (Barta et al., 1972).

Information concerning the occurrence of haematopoietic stem cells in the bone marrow during foetal development is mostly based on studies in mice. In human foetuses, medullary haematopoiesis starts by gestation week ten (Charbord et al., 1996). Based on information extrapolated from human medicine, it was hypothesised that lymphocytes start to appear in the liver at 30-35 dg since lymphoid development in the liver precedes thymic development; cells then migrate to the thymus, after which lymphoid cells appeared in the bone marrow at 55 dg, but were difficult to recognise in the organ due to their relative paucity (Schultz, 1973).

Table 1.1: Specific components of the immune system in the bovine foetus listed sequentially according to the gestation day when they were first observed.

Immune system component/organ or function	Gestation days	References
Thymus	42	Schultz et al., 1973
Lymphocytes in blood	45	Schultz et al., 1973
Spleen and bone marrow	55	Schultz et al., 1973
IgM expressing lymphocytes	59	Schultz et al., 1973
Peripheral lymph nodes	60	Schultz et al., 1973
Bactericidal activity in serum	75	Barta et al., 1972
Phytohaemagglutinin lymphocyte blastogenesis	78	Renshaw and Osburn, 1977
Haemolytic complement activity, measurable C3 in serum	90	Schwartz and Osburn, 1974
Mesenteric lymph nodes	100	Schultz et al., 1973
Blood granulocyte (neutrophils)	130	Schultz et al., 1971a
IgG in serum	150	Ishino et al., 1991
Lymphocytes in tonsils	150	Ishino et al., 1991
IgG expressing lymphocytes	145-155	Schultz et al., 1973; Maclaren et al., 1984
Lymphoid tissue of gastrointestinal tract	175	Osburn and Schultz, 1973; Schultz et al., 1973
IgA expressing cells in prescapular lymph nodes	180	Ishino et al., 1991
IgA expressing plasma cells in intestine	Birth	Rossi et al., 1978; Yamini and Sleight, 1980; Maclaren et al., 1984

1.15 Pro- and anti-apoptotic activities of intracellular protozoan parasites

The protozoan parasites constitute a heterogeneous group of unicellular pathogens that differ considerably in their life cycles, modes of transmission from one host to the next and the localisation and cellular niche within their respective hosts; this has caused for distinct adaptations in order to accomplish their complex life cycles and to ensure continuing transmission to new hosts (Graumann et al., 2009). The obligate intracellular parasites, such as *N. caninum* and *T. gondii*, rely on intact cells to grow, propagate and differentiate; thus, these parasites, among other protozoans, have evolved mechanisms to suppress or delay host cell death (apoptosis) in infected cells (Schaumburg et al., 2006; Graumann et al., 2009). Infection of cells by intracellular parasites can provide an appropriate stress signal, thus driving cells to commit suicide via the intrinsic apoptotic pathway, thereby limiting the spread of the parasite progeny (Schaumburg et al., 2006). Apoptosis could therefore be viewed as an innate defence mechanism against intracellular pathogens (Williams, 1994). The modulation of the host cell activities is very important especially for the slow growing bradyzoite stage of the parasite, as their needs shift from growth to one of maintenance (Weiss and Kim, 2000). To guarantee their long-term survival, it is

necessary for the parasites to keep the host cell alive. Contrary to their anti-apoptotic effects, some protozoan parasites can also modulate the host cells to induce apoptosis. *T. gondii* was shown to induce apoptosis in primary human trophoblast cells *in vitro*, but interestingly, apoptosis was only observed in uninfected cells, which might indicate that the pro-apoptotic activity was blocked by the presence of the parasites (Abbasi et al., 2003). *Cryptosporidium parvum* is thought to promote host cell apoptosis, but only the sporozoite and merozoite stages were shown to be involved, whereas the trophozoite stage was mainly linked to inhibition of apoptosis (Mele et al., 2004).

Apoptosis (Fig. 1.3) is initiated and transduced via the intrinsic (mitochondrial) pathway, the extrinsic or death receptor pathway and the perforin/granzyme pathway (Schaumburg et al., 2006). The classical mitochondrial pathway is usually activated when the cell encounters stress signals, which includes DNA damage, growth factor withdrawal, toxins and importantly, infection with intracellular parasites (Schaumburg et al., 2006). These stress-related stimuli activate pro-apoptotic factors that are divided into multidomain [also called B cell lymphoma (Bcl-2 homology/BH)] and BH3-only families such as Bad (pro-apoptotic) (Bouillet and Strasser, 2002). These proteins function as sensors for cellular damage and can inactivate anti-apoptotic members of the Bcl-2 family, while activating pro-apoptotic Bax/Bak-like Bcl-2 proteins, which induce mitochondrial outer membrane permeabilisation (Schaumburg et al., 2006). This later leads to the release of a variety of apoptotic factors from the mitochondria into the cytoplasm, most importantly cytochrome c, which induce the formation of the apoptosome, a complex containing cytochrome c; caspase 9 and apoptotic protease-activating factor-1 (Adams and Cory, 2002; Cain et al., 2002); apoptosis-inducing factor (AIF) and endonuclease G (EndoG), which both translocate into the host cell nucleus and induce DNA fragmentation independently of caspases (Schaumburg et al., 2006). There are two forms of cytochrome c present within the mitochondria, one found bound to the inner mitochondrial membrane (IMM) and acts as a critical component of the electron transport chain, while the other form is freely floating between the IMM and outer MM (Cortese et al., 1998; Czerski and Nuñez, 2004). The release of cytochrome c activates the initiator caspase, caspase-9, which then activates the executioner caspase, caspase-3 (Slee et al., 1999).

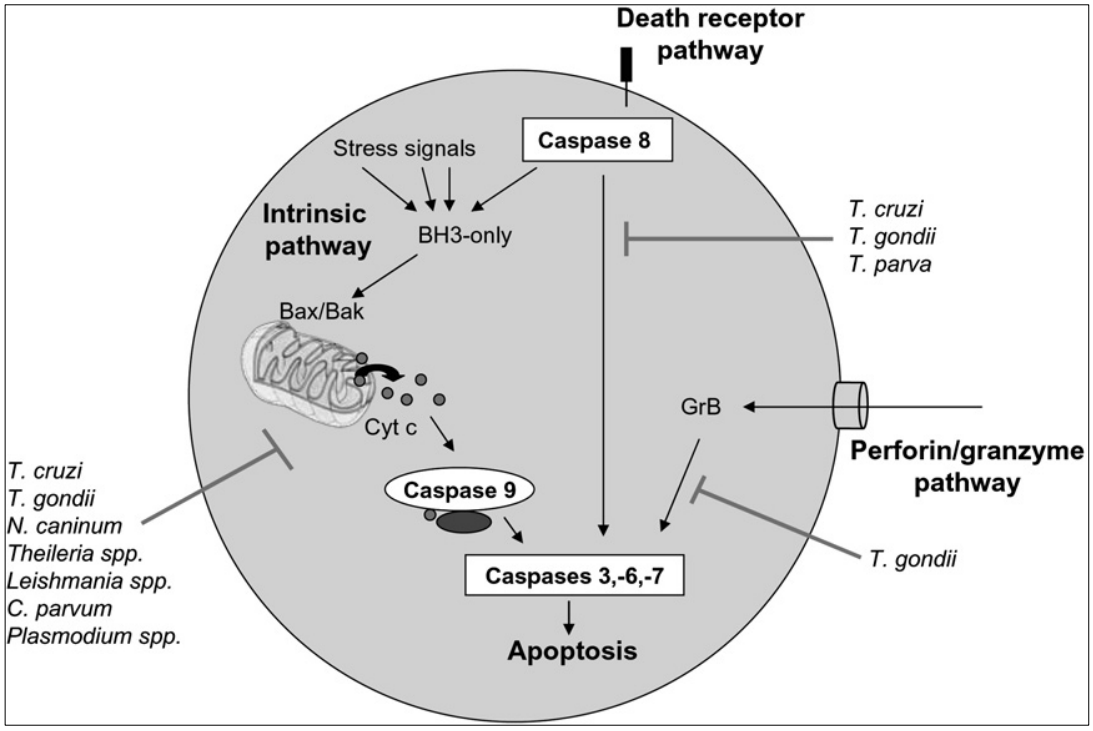

Figure 1.3. Anti-apoptotic activities of protozoan parasites. Induction of apoptosis by death receptor activation, or in response to intrinsic triggers via the mitochondrial pathway, results in the activation of caspase-8 and caspase-9, respectively. Host cell apoptosis can also occur via the perforin/granzyme pathway. Several protozoan parasites are able to inhibit apoptosis (temporarily or permanently) in all pathways. *N. caninum* among other parasites can interfere with the intrinsic apoptotic pathway leading to caspase 9 activation upstream and the effector caspases downstream. Appropriate stress signals can also lead to the release of cytochrome c and other pro-apoptotic factors via the BH3-only proteins. BH3: Bcl-2 homology; Bax: Bcl-2-associated X protein; Bak: Bcl-2 homologous antagonist/killer; cyt c: cytochrome c; GrB: granzyme B. Adopted from (Graumann et al., 2009).

The extrinsic apoptosis pathway is activated after ligation of death-receptor, namely Fas/CD95 and tumour necrosis factor-receptor 1 (TNF-R1) (Ashkenazi and Dixit, 1999). The extrinsic pathway plays a pivotal role in T and B cell development and also during the course of an immune response and is therefore of major importance for the course of parasitic infections (Dockrell, 2003). The binding of a death receptor ligand to a death receptor leads to the recruitment of the monomeric procaspase 8 protein through the death effector domain (DED) to form the death-inducing signalling complex (McIlwain et al., 2013). The outcome of the death receptor-mediated activation of caspase 8 is dependent upon the cell type, i.e. type I and II cells. In type I cells, caspase 8 initiates apoptosis directly by cleaving and further activates the executioner caspases, whereas in type II cells, caspase 8 must first activate the intrinsic apoptotic pathway to induce efficient cell death (Samraj et al., 2006). The third pathway to cell death involves cytotoxic lymphocytes, i.e. T

lymphocytes and Natural Killer cells, which eliminate pathogen-infected cells by activating caspases (Lieberman, 2003).

1.16 Parasite manipulation of host cells

Many apicomplexan parasites are known to subvert apoptotic pathways in their host cells and at the same time, modify the cells for their own development. There is evidence of death receptor-mediated apoptosis repression during *N. caninum* infection and further data also showed that the executioner caspase (cysteinyl aspartate-specific proteases), caspase 3, did not become activated in infected cells (Herman et al., 2007). *T. gondii*-infected cells were shown to be resistant to multiple inducers of the death receptor and mitochondrial pathways of apoptosis (Nash et al., 1998; Goebel et al., 2001). The inhibition is associated with a block of the caspase cascade and induction of the transcription factor, nuclear factor kappa beta (NF-κB) with concomitant upregulation of anti-apoptotic genes (Payne et al., 2003; Molestina and Sinai, 2005). *Neospora caninum*-infected cells are refractory to death receptor-mediated apoptosis, which is associated with diminished caspase activity; however, unlike in *T. gondii* infected cells, the nuclear translocation of the host transcription factor NF-κB, which is a critical component of the anti-apoptotic and pro-survival responses during *T. gondii* infection, was not observed in *N. caninum* infected cells (Ghosh, 1999; Molestina et al., 2003; Herman et al., 2007). It was later concluded by Herman et al. (2007), that infection with *N. caninum* prevents DNA degradation associated with host cell apoptosis; the absence of caspase 3 activity in cells infected with either *T. gondii* or *N. caninum* was shown to be due to a block of caspase 3 activation, but the specific mechanism(s) by which the caspase 3 activation is inhibited by *N. caninum* was not ascertained in the latter study.

The mitochondrial release of cytochrome c from the inter-membrane space is a triggering event in apoptosis (Goldstein et al., 2000). Reports have suggested that *T. gondii* infected cells can resist the release of cytochrome c in response to diverse apoptogenic triggers (Goebel et al., 2001; Sinai et al., 2004). This restriction is likely due to the activation of anti-apoptotic Bcl-2 family of proteins by the parasite, but not those on the pro-apoptotic arm (Molestina et al., 2003). The release of cytochrome c, which initiates apoptosis, is believed to occur simultaneously from all mitochondria within the dying cell (Goldstein et al., 2000); however, mitochondria that are associated with the PVM in *T. gondii* did not undergo the permeability

transition, thus retaining their cytochrome c (Carmen et al., 2006). The release of cytochrome c from non-PVM-associated mitochondria should on its own activate apoptosis, but in the presence of either endogenous or exogenous caspase inhibitors, apoptosis was blocked despite the release of cytochrome c (Deveraux et al., 1998).

1.18 Parasite egress from host cells

Parasite escape from the host cells requires the breaching of the PVM, host cytosolic organelles, the host cytoskeleton and host cell plasma membrane (Roiko and Carruthers, 2009). A reduction in potassium ions (K^+) concentration below a threshold of 80 mM has been implicated in triggering *T. gondii* egress from host cells (Moudy et al., 2001; Fruth and Arrizabalaga, 2007). Moudy et al. (2001) also showed that an increase in Ca^{2+} concentration is also needed to activate one of the mechanisms (motile apparatus) that apicomplexan parasites use in order for egress to occur. A mechanical or metabolic strain in parasite laden infected cells could cause K^+ to decrease in cells, thereby activating egress (Roiko and Carruthers, 2009). While inside the infected cell, the parasites sense a high concentration of K^+ in its surroundings and maintains a relatively non-motile state until K^+ levels fall below the threshold, then activates its motility system (Moudy et al., 2001). *Plasmodium* sporozoites are said to respond to K^+ fluxes in a similar manner (Kumar et al., 2007). Activation of phospholipase C (PLC) also seems to play an important role in the activation of parasite egress from host cells. This was shown in the related parasite, *Plasmodium falciparum* where the presence of an intracellular Ca^{2+} store has been described that can release Ca^{2+} in response to an increase in inositol 1,4,5-trisphophate (IP_3) levels (Moudy et al., 2001). The results from Moudy et al. (2001) later confirmed that the increase in Ca^{2+} during parasite egress is regulated by a PLC activity in the parasite.

The exact sequence of the egress process is to date unclear, but the following are observations published on the order of events during egress: tubular network disintegration; disassembly of the rosette formation; tachyzoite motility; protrusion of the conoids; pushing of the PVM by the tachyzoites; PVM disintegration; tachyzoites gain access into the host cell cytoplasm; migration of tachyzoites to the periphery of the host cell; and association with the host cell plasma membrane with subsequent crossing to extracellular space (Caldas et al., 2010). Lysis of the PVM and host cell membrane is considered to be caused by a pore-forming perforin-like

parasite protein (PLP) as in the case of *T. gondii*, the TgPLP1 has been implicated (Graewe et al., 2012). It has been shown that the TgPLP1 can act on both the luminal side of the PVM and the cytoplasmic side of a second vacuole within the same cell to facilitate egress (Kafsack et al., 2009). This release of TgPLP1 from the micronemes of *T. gondii* could mean that the protein may be homologues in other intracellular apicomplexan parasites.

1.19 Host cell death

Destruction of the PVM has been supported as the main cause of host cell death in parasite infected cells (Heussler et al., 2010). Several phases of parasite egress and host cell death have been suggested (Kafsack et al., 2009). Infected cells with an intact PVM and host cell plasma membrane are considered as phase zero. In phase one, there is a release of parasite proteins from micronemes which disrupt the PVM, but the host cell membrane stays intact; phase two is characterised by a breach in the host cell plasma membrane, initiating a kind of necrotic cell death; and during phase three, the parasite protease subtilisin I (SUB1) is released into the host cell cytoplasm. It is still not clear whether cell death is initiated upon rupture of the PVM or the host plasma membrane. A recent study showed supporting evidence to the idea of host cell death upon PVM destruction (Zhao et al., 2009). The authors of this study also investigated infected host cells and found that PVM destruction induced host cell death, which they described as pyronecrosis, since the features of the dead cells did not support those of apoptosis or necrosis. Heussler et al. (2010) described an ordered form of cell death in *Plasmodium*-infected hepatocytes, which was considered to be parasite-dependent and could be clearly distinguished from both necrosis and apoptosis. The key event in this case appeared to be rupture of the PVM, which occurred first during egress, and host cell death probably was dependent on the activation of cysteine proteases (Heussler et al., 2010).

1.20 The apoptosis-necrosis continuum

The morphological characteristic of apoptosis and necrosis are clearly distinct. Apoptosis is controlled process that is characterised by changes in cellular morphology, condensation of cytoplasm and nuclear fragmentation, while necrosis is a more passive process and is characterised by cell swelling and total breakdown of plasma membrane (Elmore, 2007). The mitochondria are frequently the target of

injury after stresses leading to necrotic and apoptotic cell death (Lemasters et al., 1999). Evidence indicated that necrosis and apoptosis represent morphological expressions of a shared biochemical network described as the apoptosis-necrosis continuum (Zeiss, 2003). Two clearly ascertainable factors that can alter an ongoing apoptotic process into a necrotic process include – a decrease in the availability of caspases and intracellular adenosine triphosphate (ATP) (Leist et al., 1997; Denecker et al., 2001). A decrease in cellular ATP production that ultimately leads to the generation of reactive oxygen species, both of which are consequences of cytochrome c release, can contribute to cell death in the absence of caspases (Zeiss, 2003). In the intrinsic (mitochondrial) pathway, the formation of the apoptosome is dependent on ATP for its pro-apoptotic activity and progressive energy depletion would therefore result in a greater proportion of cells being committed to necrotic cell death rather than apoptosis (Leist et al., 1997; Nicotera et al., 1998; Eguchi et al., 1999). Many insults in cells can induce apoptosis at lower doses and necrosis at higher doses; however, even in response to a certain dose of death-induced agent, morphological features of both apoptosis and necrosis may coexist in the same cell (Zong and Thompson, 2006).

During necrosis, most of the intracellular content is released out of the plasma membrane, but a small amount of molecules have been identified that can elicit necrosis-induced immune signalling; these molecules include the damage-associated molecular pattern (DAMP), high-mobility group box 1 (HMGB1) protein and heat shock proteins (Zeh Iii and Lotze, 2005; Zong and Thompson, 2006). HMGB1 is a non-histone nuclear protein ubiquitously expressed in eukaryotes, exerts distinct functions at different subcellular localisations and plays an important role in the regulation of gene transcription in the cell nucleus (Bustin, 1999; Zhou et al., 2011). Although located primarily in the cell nucleus, HMGB1 can translocate to the cytoplasm, as well as the extracellular space, during cell activation and cell death (Harris et al., 2012). Inside the cell, HMGB1 binds DNA and modulates chromosomal architecture (Ueda and Yoshida, 2010). The immune properties of necrotic and apoptotic cells can differ, therefore, the deposition of HMGB1 during cell death is of utmost importance (Rock et al., 2011). During necrosis, HMGB1 release occurs passively as cell permeability breaks down (Scaffidi et al., 2002; Rovere-Querini et al., 2004); while during apoptosis, nuclear retention of HMGB1 occurs because of post-translational modifications that affect chromatin binding

(Scaffidi et al., 2002). It has also been suggested that HMGB1 extracellular release might occur during late apoptosis (secondary necrosis) due to changes in cell permeability as well as extensive nucleosomal degradation (Harris et al., 2012). Therefore, this protein could potentially be used as a maker during necrosis-induced cell death as there is retention in the cell nucleus during apoptosis.

1.21 Aims and objectives of the study

The coccidian parasite *N. caninum* is globally distributed and causes abortion in cattle. Numerous reports have been made on the pathogenesis of the infection mainly in the placenta and foetus. Data show that foetal death occurs following infection in early gestation, while infection in mid to late gestation can result in the calf being born alive, but persistently infected. It has also been shown that the bovine foetal immune system starts to become competent only after approximately 100 days gestation age, which means that foetuses in early gestation would be unable to respond to infection. The aim of this thesis is to analyse the pathological process that lead to *N. caninum* induced foetal death.

In Chapter 2, the pathological effects of *N. caninum* tachyzoites on bovine foetuses following experimental infection of dams in early and late gestation (70 ad 210 days gestation, respectively) and of naturally infected cows after parasite recrudescence in mid to late gestation were analysed. The composition of the haemolymphatic and non-haemolymphatic tissues was evaluated along with the nature of the inflammatory response towards *N. caninum* using various leukocyte markers and marker for parasite detection.

In Chapter 2, there was evidence of hepatocellular necrosis alongside apoptotic cells in the livers of foetuses in early gestation, whereas high parasite burden was detected in cardiomyocytes, but without evidence of necrosis or apoptosis. The aim of Chapter 3 was to study the mechanism of hepatocellular cell death following *N. caninum* infection by evaluating the activation of the apoptotic pathways using an *in vitro* tissue culture model. The ultrastructural features of infected hepatocytes were also evaluated to detect subtle changes and assess the interaction between host cell organelles and *N. caninum* tachyzoites.

In Chapter 4, the seroprevalence of *N. caninum* in Jamaican dairy herds was investigated with the aim of understanding the epidemiology of the infection in the

Caribbean region. Serum samples from local dairy herds were collected and evaluated using ELISA.

CHAPTER TWO: Histological and immunohistological analysis of bovine foetuses infected with *N. caninum* in early and late gestation

2.1 ABSTRACT

Neospora caninum is a globally distributed, intracellular apicomplexan parasite and a major infectious cause of bovine abortion worldwide. The parasite was first reported as an unidentified protozoan in dogs with encephalomyelitis and myositis and later in calves with similar conditions. The major mode of transmission of the parasite is likely from infected dam to foetus via the placenta. Calves infected via this route could be born clinically healthy, but persistently infected. The pathological effects of *N. caninum* on bovine foetuses in early and late gestation (70 and 210 days gestation, respectively), and foetuses from dams following recrudescence of *N. caninum* in mid to late gestation, were assessed. An initial histological study was performed on 35 bovine foetuses and 2 new-born calves. A total of 12 foetuses/calves were subsequently chosen and subjected to more detailed histological and immunohistological examination. The haemolymphatic and non-haemolymphatic tissues were examined and stained for the presence of T and B cells, antigen presenting cells, macrophages, proliferating cells, interferon gamma producing cells and apoptotic cells. The haemolymphatic tissues of control foetuses in early gestation were moderately developed, had no histological changes and with low lymphocyte turnover. Histological changes were observed in the haemolymphatic tissues of infected foetuses in early gestation and comprised extensive lymphocyte apoptosis, low cell turnover, but with no evidence of IFN-γ production. Foetuses in late gestation had mild histological changes and evidence of IFN-γ production was seen in spleen and lymph node of infected foetuses. In the non-haemolymphatic tissues, foetuses in early gestation had the most severe lesions and exhibited severe hepatocellular necrosis and apoptosis, glial cell and/or neuroblast necrosis and apoptosis in the CNS along with high parasite loads in the CNS, liver and myocardium. Parasite loads in cardiomyocytes were not associated with cell degeneration. A mononuclear cell infiltration was observed in tissues, but not in direct association with the parasite. Histological changes were present mainly in the CNS of foetuses in late gestation where focal necrosis and mild to moderate mononuclear cell infiltrates were present. Low numbers of parasites were detected in the CNS in association with the inflammation. Other non-haemolymphatic tissues had only mild mononuclear cell infiltrates which consisted mainly of CD3-positive T cell and fewer macrophages.

2.2 INTRODUCTION

The apicomplexan parasite *N. caninum* is a major cause of reproductive failure in the cattle industry worldwide (Dubey et al., 2007). Transplacental transmission of *N. caninum* in cows is very efficient and only a proportion of infected animals abort (Trees et al., 1999). Prenatal *N. caninum* infection occurs as a result of reactivation of a persistent infection acquired before pregnancy or infection of the dam during pregnancy; while postnatal infection arise from the ingestion of oocysts shed by the definitive hosts (Trees et al., 2002; Trees and Williams, 2005). Infection via the exogenous or endogenous route of transmission can induce pathological changes in the foetus and lead to foetal death or the birth of a clinically healthy, but persistently infected calf (Dubey et al., 2006; Dubey and Schares, 2011). There are numerous reports of experimental *N. caninum* infection in animals (Williams et al., 2000; Gibney et al., 2008; Almería et al., 2010; Bartley et al., 2013a). Many different routes of challenge have been shown to lead to vertical transmission of *N. caninum* causing foetal infection and include intravenous, intramuscular, subcutaneous and oral (Uggla et al., 1998; Andrianarivo et al., 2000; Williams et al., 2003; Gibney et al., 2008). Following infection, *N. caninum* is able to gain access to the placenta probably via blood and establish itself in the maternal caruncular septum before crossing to the foetal placental villi (Dubey and Schares, 2011). For abortion to occur, the foetus and/or its placenta has to be damaged so that it is no longer viable (Gibney et al., 2008).

Neospora caninum is a significant primary cause of bovine abortion. The parasite has been identified in aborted foetuses both after natural and experimental infection (Barr et al., 1994; Wouda et al., 1997; Gibney et al., 2008). Parasite-induced pathological changes have also been described in foetuses and placenta of dams after parasite recrudescence (Barr et al., 1990; Wouda et al., 1997; Gibney, 2008; Rosbottom et al., 2011). Grossly, parasite-induced lesions are rarely seen. In aborted foetuses, pale white foci in the heart and skeletal muscle and dark foci of necrosis in the brain with hydrocephalus have been recorded (Dubey et al., 1998; Piergili Fioretti et al., 2003). In the dam, focal areas of discolouration can occasionally be seen in the placenta (Dubey et al., 1998a; Piergili Fioretti et al., 2003).

Histological changes in foetuses are variable depending on the age of the foetus. In young (< 4 months' gestation) aborted foetuses, there are focal areas of necrosis in liver and brain; while *N. caninum* tachyzoites, without evidence of necrosis in infected cells, were observed in the myocardium (Wouda et al., 1997; Maley et al., 2006; Gibney et al., 2008). Older foetuses that probably would be carried to term (>4 months' gestation age) showed focal mononuclear (lymphocytes, plasma cells and macrophages) inflammatory infiltrates in the CNS and peripheral nerves and skeletal muscles as well as a range of other organs, such as the kidneys, liver, adrenal glands and lungs, generally without parasites in the lesions (Barr et al., 1990; Wouda et al., 1997; Gibney et al., 2008; Rosbottom et al., 2011). After parasite recrudescence in naturally infected animals, *N. caninum* tachyzoites were occasionally observed in areas surrounded by mononuclear inflammatory cell infiltrates in the CNS (Rosbottom et al., 2011).

Histological changes in the placenta of foetuses that had died in early gestation are represented by multifocal epithelial cell necrosis with *N. caninum* tachyzoites within degenerated cells (Barr et al., 1990; Bergeron et al., 2001; Maley et al., 2006; Gibney et al., 2008). When foetuses were still alive 3 weeks post infection, the placenta showed necrosis of villi with moderate to severe mononuclear infiltration in the maternal caruncles. *N. caninum* tachyzoites were identified within areas of villous necrosis, but rarely in adjacent areas (Maley et al., 2006). In the surviving foetuses of dams infected in mid gestation, there were focal areas of necrosis with infiltration of neutrophils and mononuclear cells and serum exudates; tachyzoites were identified in the placenta (Almería et al., 2010). In one placenta where the foetus was found dead, there were large areas of necrosis and placentitis with mineralisation and few tachyzoites. After infection in late gestation, the histological changes were restricted to small areas of epithelial necrosis with mild mononuclear interstitial infiltration dominated by mononuclear cells in the maternal tissues (Gibney et al., 2008).

2.3 Aim of the study

There is strong evidence that *N. caninum* infection in early gestation is associated with foetal death most probably due to lack of foetal immunocompetence, whereas in mid to late gestation, infection can result in the birth of asymptomatic, persistently infected animals (Williams et al., 2000; Guy et al., 2001b; Gibney et al., 2008; Rosbottom et al., 2011). Accordingly, the immunological development of the foetus is most likely critical in determining if a foetus is killed by the infection or survives, but becomes persistently infected. Survival of the foetus will therefore depend on its ability to raise an immune response to the parasite.

The purpose of the present study was to define the immune response to *N. caninum* in bovine foetuses in early and late gestation (70 and 210 dg) and in foetuses after parasite recrudescence had occurred in mid to late gestation, by measuring the development and composition of the haemolymphatic tissue and the development of an inflammatory response to the parasites. The study was carried out on foetuses of dams experimentally infected either at 70 dg, a time when the foetal immune system is not thought to be functional, or at 210 dg when a foetus is expected to be more immunocompetent. In addition, foetuses of naturally infected dams that had evidence of parasite recrudescence in mid and late gestation and calves from persistently infected mothers that were born alive were examined.

2.4 MATERIALS AND METHODS

2.4.1 Animals and foetal tissues, histological examination

An initial histological study was performed on tissues from 37 Holstein-Friesan bovine foetuses (2 calves included, Table 2.1) that had been collected for histological examination in a previous experiment carried out at the University of Liverpool, then Faculty of Veterinary Science and The Liverpool School of Tropical Medicine, as part of the PhD project of Dr. Helen Gibney (Gibney, 2008). Briefly, three groups of foetuses were examined. Group 1 consisted of seven foetuses (including one set of twins) from 6 dams that had been infected intravenously (*iv*) with *N. caninum* tachyzoites (Liverpool strain) at 70 dg and 6 control foetuses whose dams had received uninfected Vero cells in phosphate buffered saline (PBS). Group 2 was comprised of 6 foetuses from dams that had been infected *iv* with *N. caninum* tachyzoites at 210 dg and 6 control foetuses from dams that had been inoculated with uninfected Vero cells in PBS. Group 3 consisted of 10 foetuses (including two sets of twins) and 2 new-born calves from 10 naturally persistently infected dams which had been euthanised after parasite recrudescence had occurred in mid to late gestation. Detailed information on the foetuses is provided in Table 2.1.

Dams had been euthanised within 24 h after foetal death had been diagnosed (animals infected at 70 dg, group 1) or 20–22 days post inoculation in the control groups and in all animals infected at 210 dg (group 2). Eight dams in group 3 (a total of 10 foetuses) had been euthanised one week after a 50% increase in antibody levels had been detected and levels remained high. The remaining 2 dams were allowed to calve normally, because the rise in antibody levels was detected in one animal at 37 weeks gestation and in the other only after parturition.

All foetuses had been subjected to a gross post mortem examination within an hour after euthanasia of the dams. Euthanasia and post mortem examination of calves was carried out 2 weeks after birth. Tissues or tissue samples [thymus, spleen, mesenteric lymph node, femoral bone marrow, brain, spinal cord, *Nervus femoralis*, heart (apex), lung, left liver lobe, left kidney and adrenal gland, pancreas, section of jejunum and *Musculus quadriceps femoris*] had been collected from all foetuses. Lymph nodes were not sampled in group 1 (70 dg) foetuses, because they were not grossly apparent at that stage. Tissues had been fixed in 4% buffered paraformaldehyde (pH 7.4) and routinely paraffin wax embedded after 24-48 h

(Gibney, 2008). Sections (3-5µm thick) had been prepared and stained with haematoxylin-eosin (HE). For the present initial study, these sections were retrieved from the archive and a thorough histological assessment was undertaken to identify any histopathological changes and to assess the development and composition haemolymphatic tissues. Based on the results of this study, cases for the subsequent studies were selected.

Table 2.1: Groups of foetuses included into the present study for histological screening

Groups	Number of foetuses (Infected/controls)	Inoculation (iv) (Infected/controls)	Time of inoculation (Infected/controls)	Foetal status at euthanasia of dam
Group 1	7 infected	10^7 *N. caninum* tachyzoites	70 dg	Dead, 91 ± 1 dg (all foetuses)
	6 controls	10^7 Vero cells in PBS	70 dg	Alive, 91 ± 1 dg (all foetuses)
Group 2	6 infected	10^7 *N. caninum* tachyzoites	210 dg	Alive, 231 ± 1 dg (all foetuses)
	6 controls	10^7 Vero cells in PBS	210 dg	Alive, 231 ± 1 dg (all foetuses)
Group 3 Recrudescence	10 naturally infected	NA	NA	Alive, 147 – 245 dg
	2 naturally infected	NA	NA	Alive at birth

2.4.2 Histology and immunohistology for the characterisation of pathological changes and the identification of the composition of haemolymphatic tissues

Based on the results of the initial histological screening of all 37 foetuses/calves from both control and *N. caninum* infected dams (Table 2.1), a total of 12 foetuses/calf (group 1: 3 infected and 2 controls, group 2: 2 infected and 3 controls and group 3: 1 infected and 1 uninfected control; Table 2.2) were selected. The infected foetus from group 3 was euthanised at 31 weeks gestation, while the calf (used as control) was born alive. Haemolymphatic tissues (thymus, spleen, mesenteric lymph node, femoral bone marrow) and other tissues (cardiac muscle, *Musculus quadriceps femoris*, liver, lung, brain, spinal cord, *Nervus femoralis*, intestine, kidney and adrenal gland) were subjected to a more detailed histological examination using special stains when appropriate, and an immunohistological examination to identify parasite antigen and leukocytes in tissues.

The haemolymphatic tissues of infected foetuses in early gestation (group 1) were chosen based on the presence of extensive necrotic lesions in spleen, thymus, bone marrow and liver and provided that enough tissue was present in the paraffin blocks to allow further sectioning. Infected foetuses at 210 dg (group 2) and those from the recrudescence group (group 3) with the most extensive lesions in any tissues were chosen. Control foetuses in early and late gestation were chosen based on the availability of enough tissues in the blocks, while from the recrudescence group, the calf was chosen as a control for the composition of the haemolymphatic tissues, because it was negative for *N. caninum* by PCR after birth. For other tissues, foetuses in early gestation were chosen due to the availability of enough tissues in the blocks, while those from 210 dg and the recrudescence group were chosen because they exhibited the most extensive lesions in various tissues.

Table 2.2: Foetuses selected for detailed histological and immunohistological examination

Day of inoculation	Inoculum	Foetal status at euthanasia of dam	Individual foetus number[a]	Number[b]
70 dg	*N. caninum* tachyzoites	Died 91±1 dg	I-1	H03 - 2724
70 dg	*N. caninum* tachyzoites	Died 91±1 dg	I-3	H05 - 0562
70 dg	*N. caninum* tachyzoites	Died 91±1 dg	I-4	05L – 0708
70 dg	Vero cells (control)	Alive 91±1 dg	C-3	H04 – 1517
70 dg	Vero cells (control)	Alive 91±1 dg	C-4	H04 – 1518
210 dg	*N. caninum* tachyzoites	Alive 231±1 dg	I-11	H04 – 986
210 dg	*N. caninum* tachyzoites	Alive 231±1 dg	I-12	H04 – 987
210 dg	Vero cells (control)	Alive 231±1 dg	C-8	H04 – 976
210 dg	Vero cells (control)	Alive 231±1 dg	C-9	H04 – 980
210 dg	Vero cells (control)	Alive 231±1 dg	C-11	H04 – 984
NA	NA	Alive 217 dg	R-5 [c]	05L – 2575
NA	NA	Alive: full term	R-10 [d]	05L – 3647

dg – days of gestation

NA – Not applicable

[a] Individual foetus numbers are those allocated in the original experiment (Gibney, 2008).

[b] The case numbers refer to the Histology Laboratory database numbers that were provided at the time of the initial experiments.

[c] Parasite recrudescence in mid gestation (persistently infected dams).

[d] Neonatal calf born from seropositive dam.

2.4.3 Lendrum's Carbol Chromotrope stain for the demonstration of eosinophils

In order to confirm cells identified as eosinophils in HE-stained sections, the Lendrum's stain was performed on selected consecutive sections by the Histology Laboratory, Veterinary Laboratory Services, School of Veterinary Science. Following deparaffinisation in xylene for 5 min and rehydration through each graded alcohol, sections were placed in Mayer's Haemalum (see Appendix) for 1 min, then blued in running tap water for 5 min. The sections were then stained in Carbol Chromatrope (BDH brand, VWR International, Lutterworth, UK) for 1 h (see Appendix for solutions) followed by rinsing in distilled water. This was followed by dehydration with ethanol, clearing with xylene and cover slips were mounted on slides with DPX (BDH brand, VWR International).

2.4.4 Immunohistological staining

Immunohistology was performed on 3-5 µm thick sections of formalin-fixed, paraffin-embedded tissues consecutive to those cut for the histological examination. Sections were mounted on Poly-L-Lysine treated slides and stained immunohistologically to detect *N. caninum* antigen and to identify T cells (CD3-positive), B cells (PAX5-positive), monocytes/macrophages and neutrophils (myeloid/histiocyte antigen/calprotectin-positive, hereafter refer to as calprotectin), major histocompatibility complex class II antigen (MHCII-positive), apoptotic cells (cleaved caspase 3-positive), interferon gamma (IFN-γ) expressing cells and proliferating cells (proliferating cell nuclear antigen (PCNA)-positive) in haemolymphatic tissues and in other tissues with inflammatory infiltrates. Leukocyte markers were used in other tissues of foetuses in late gestation where inflammatory infiltrates were seen. Other tissues of foetuses in early gestation were also stained with the leukocytes markers if mononuclear cells were observed histologically in these tissues. Details of the antibodies used and the cell population to which they are directed are shown in Table 2.3.

Table 2.3: Antibodies used for immunohistological staining, with references

Ligands	Antibodies and sources	Specificity
CD3	Rabbit anti-human CD3, DAKO, Glostrup, Denmark (N1580)	Pan T-cell marker (Rosbottom et al., 2008)
Proliferating cell nuclear antigen (PCNA)	Mouse anti- PCNA, clone PC10, DAKO (M0879)	Proliferating cells in S phase, late G1 and early G2 phases (Kubben et al., 1994)
PAX5	Mouse anti-human Pax-5, clone 24/Pax-5, BD Transduction Laboratories, Lexington, Kentucky, USA (610862)	Pan B-cell marker (Agostinelli et al., 2010)
MHC II	Mouse anti-human HLA-DR, clone TAL. 1B, DAKO (M0746)	Antigen presenting cells (APC), macrophages and lymphocytes (Rosbottom et al., 2011)
Cleaved caspase 3	Rabbit anti-cleaved caspase-3, Asp 1756, DAKO (5A1E)	Apoptotic cells (Gjørret et al., 2007)
Myeloid/histiocyte antigen/calprotectin	Mouse anti-human myeloid/histiocyte antigen/calprotectin, clone MAC 387, DAKO (M 0747)	Monocytes, neutrophils and recently blood-derived macrophages (Rosbottom et al., 2008)
IFN-γ	Mouse anti-bovine IFN-γ, clone MCA1964, Jackson Immunoresearch Laboratories, Suffolk, UK	Interferon-γ expressing cells (Rosbottom et al., 2008)
Neospora caninum	Rabbit anti-*N. caninum* , Parsley, University of Liverpool, Liverpool, UK	*Neospora caninum* antigen in tissues (Gibney et al., 2008)

The peroxidase anti-peroxidase (PAP) (Hsu et al., 1981; Kipar et al., 1998) and the avidin-biotin complex (ABC) (Kipar et al., 1998; Gibney et al., 2008) methods were performed as previously described (Table 2.5). Immunohistology followed standard protocols which are outlined below and antigen retrieval methods were applied for detection of some antigens (Tables 2.4 and 2.5). Three immunohistological methods (PAP mouse, PAP rabbit and ABC method) are described below for each detection system used (Table 2.5). A bovine spleen served as the positive control of each marker.

Table 2.4: Antigen retrieval methods

Antigen retrieval	Retrieval details
Protease	Incubate for 5 min in PBS (pH 7.2) at 37°C. 5 min protease treatment at 37°C: 0.05% protease (bacterial protease type XXIV, P8038, Sigma) in pre-warmed (37°C) PBS (pH 7.2); wash 3x5 min ice-cold TBST.
Citrate buffer, pH 4.0	Incubate in 96°C in pre-warmed citrate buffer for 15 min followed by 15 min cooling at room temperature. For general method – see CD3.
Microwave, 4x5 min in 10 mM EDTA	Wash with distilled water then 4x5 min in 10 Mm EDTA in plastic racks in 1 litre beaker in microwave (cover with 4 sheets of blue role and secure with elastic band; also use 0.5 litre beaker with distilled water to balance up heat in the microwave). Slides are then placed in distilled water immediately after microwaving.
Citrate buffer, pH 6.0	Incubate at 97°C in pre-warmed citrate buffer for 25-30 min then cool at room temperature for 15-20 min. Wash in TBST.

PBS – Phosphate buffered saline, TBST – Tris-buffered saline tween,
EDTA – Ethylenediaminetetraacetic acid

Table 2.5: Antibodies and immunohistological protocols

Primary antibody	Antigen retrieval	Antibody dilution	Secondary antibody	Detection system PAP/ABC
Rabbit anti-human CD3	Citrate buffer[d]	1:10 in 20% SS in TBST	Goat anti-rabbit IgG[a] biotinylated, 1: 100 in TBST	ABC, polyclonal rabbit[a], 0.9 µl A + 0.9 µl B to 100 µl TBST
Mouse anti-PCNA	Citrate buffer[e]	1:100 in TBST	Rat anti-mouse IgG[b], 1:100 in 1% BSA in TBST	PAP, monoclonal mouse[b], 1:500 in 1% BSA in TBST
Mouse anti-human PAX5	Microwave[f]	1:40 in 1% (BSA) in TBST	Rat anti-mouse IgG[b], 1:100 in TBST	PAP, monoclonal mouse[b], 1:500 in TBST
Mouse anti-human HLA-DR	Citrate buffer[d]	1:25 in TBST	Rat anti-mouse IgG[b], 1:100 in 1% BSA in TBST	PAP, monoclonal mouse[b], 1:500 in 1% BSA in TBST
Rabbit anti-cleaved caspase 3	Citrate buffer[d]	1:50 in 20% SS in TBST	Swine anti-rabbit IgG[c], 1:100 in 20% SS in TBST	PAP (rabbit), polyclonal[c], 1:100 in 20% SS in TBST
Mouse anti-human myeloid/ histiocyte antigen	Protease	1:600 in TBST	Rat anti-mouse IgG[b], 1:100 in TBST	PAP monoclonal mouse[b] 1:500 in TBST
Mouse anti-bovine IFN-γ	Citrate buffer[d]	1:50 in TBST	Rat anti-mouse IgG[b], 1:100 in TBST	PAP, monoclonal mouse[b], 1:500 in TBST
Rabbit anti-*N. caninum*	No pre-treatment	1:1000 in 20% SS in TBST	Swine anti-rabbit IgG[c] 1:100 in 20% SS in TBST	PAP rabbit[c] (1:100 in 20% SS in TBST

[a] Obtained from Vector Laboratories Ltd, Peterborough, UK; [b] Obtained from Jackson Immunoresearch Laboratories, Suffolk, UK; [c] Obtained from DAKO, Glostrup, Denmark; [d] Treatment for 30 min at 97°C in citrate buffer (pH 6.0); [e] Treatment for 15 min at 96°C in citrate buffer (pH 4.0); [f] Treatment for 10 min at 800W in 10 mM EDTA (pH 9.0); BSA – Bovine serum antigen; SS – swine serum.

The three detection methods (PAP using a mouse monoclonal primary antibody, PAP using a rabbit polyclonal primary antibody, ABC using a rabbit polyclonal primary antibody) are described, using the demonstration of myeloid/histiocyte antigen/calproectin, CD3 and *N. caninum* as examples.

2.4.5 Staining for myeloid/histiocyte antigen/calprotectin (method: PAP mouse)

The PAP method was performed as previously described (Hsu et al., 1981; Kipar et al., 1998). Tissue sections were deparaffinised in xylene for 10 min then rehydrated through each 2 min, twice in 100% ethanol and once in 96% ethanol. Following deparaffinisation, sections were incubated in methanol with 0.5% H_2O_2 (Perhydrol 30% H_2O_2 P-a, Fisher Scientific, New Jersey, USA) for 30 min at room temperature (RT) to inactivate endogenous peroxidases. The sections were washed for 5 min in Tris-buffered saline tween (TBST, pH 7.6, see Appendix) followed by protease pre-

treatment (antigen retrieval, Table 2.4). The sections were washed for 5 min in PBS (pH 7.2) at 37°C, then for 5 min in 0.05% protease treatment at 37°C (Bacterial protease type XXIV, Sigma-Aldrich, Dorset, UK) in pre-warmed (37°C) PBS, followed by 3 washes for 5 min each in ice-cold TBST. The slides were then placed in coverplates in Sequenza racks (Thermo Shandon, Pittsburgh, USA) and washed for 5 min with TBST followed by blocking of non-specific binding of antiserum by incubation in 10% rat serum in TBST for 10 min. Following blocking, the sections were incubated for 15-18 h at 4°C with monoclonal mouse anti-human myeloid/histiocyte antigen (1:600 in TBST, Table 2.5). On day 2, the slides were washed in TBST for 5 min then incubated for 30 min in rat anti-mouse IgG (1:100 in TBST, H&L, 425-055-100, Jackson ImmunoResearch, Suffolk, UK). A further 5 min wash in TBST was followed by 30 min incubation with PAP mouse (1:500 in TBST; 223005025, Jackson ImmunoResearch). The slides were washed in TBST and removed from the cover-plates and further incubated with permanent stirring for 10 min in 3,3' diaminobencidin-tetrahydrochloride (DAB, Fluka Chemie AG, Buchs, Switzerland) with 0.01% H_2O_2 (Perhydrol 30% H_2O_2 P-a, Fisher Scientific) in 0.1 M imidazole buffer (pH7.1, Fluka Chemie AG; see Appendix) at RT. The slides were then washed in TBST three times for 5 min each then once for 5 min in distilled water. Slides were counter stained with Papanicolaou's haematoxylin (Merck) for 1 min then placed in running tap water for 5 min. The sections were dehydrated in ascending ethanol (1 min 96%, 2 min 100% and 3 min 100%), cleared in xylene (2 min 100% and 2 x 3 min 100%) then cover slips were mounted on slides with Distyrene Plasticizer Xylene (DPX; BDH brand, VWR International).

2.4.6 Staining for *N. caninum* antigen (method: PAP rabbit)

The PAP method was applied as previously described (Kipar et al., 1998; Gibney et al., 2008). Tissue sections were deparaffinised in xylene for 10 min followed by rehydration through each 2 min, twice in 100% ethanol and once in 96% ethanol. The sections were incubated in methanol with 0.5% H_2O_2 (Perhydrol 30% H_2O_2 P-a, Fisher Scientific) for 30 min at room temperature to inactivate endogenous peroxidases. The slides were then placed in coverplates and Sequenza racks (Thermo Shandon) and washed for 5 min in TBST (pH 7.6, see Appendix), followed by blocking of non-specific binding of antiserum by incubation in swine serum, diluted 1:2 in TBST for 10 min. The slides were incubated for 15-18 h at 4°C with rabbit

anti-*Neospora caninum* (Gibney et al., 2008) in 20% swine serum in TBST; dilution 1:1,000. This was followed by a wash in TBST, then incubation for a further 30 min with swine anti-rabbit IgG (1:100 in 20% swine serum in TBST; DAKO). The slides were washed in TBST for 5 min then incubated for a further 30 min with PAP rabbit (1:100 in 20% in swine serum in TBST; DAKO). Following incubation, the slides were washed in TBST and removed from cover-plates followed by incubation with permanent stirring for 10 minutes with DAB (Fluka Chemie AG) with 0.01% H_2O_2 (Perhydrol 30% H_2O_2 P-a, Fisher Scientific) in 0.1 M imidazole buffer (pH7.1, Fluka Chemie AG; see Appendix) at RT. This was followed by three washes in TBST for 5 min each then once for 5 min in distilled water. Slides were counter stained with Papanicolaou's haematoxylin (Merck) for 1 min then placed in running tap water for 5 min. The sections were dehydrated in ascending ethanol (1 min 96%, 2 min 100% and 3 min 100%), cleared in xylene (2 min 100% and 2 x 3 min 100%) and cover slips were mounted on slides with DPX (BDH brand, VWR International).

2.4.7 Staining for CD3 antigen (method: ABC)

The ABC method was applied as previously described (Kipar et al., 1998; Gibney et al., 2008). Sections were deparaffinised in xylene for 10 min then rehydrated through each 2 min twice in 100% ethanol and once in 96% ethanol. The sections were incubated in methanol with 0.5% H_2O_2 (Perhydrol 30% H_2O_2 P-a, Fisher Scientific) for 30 minutes at RT to inactivate endogenous peroxidases. The slides were washed for 5 min in TBST (pH 7.6, see Appendix) followed by citrate pre-treatment (antigen retrieval, see Table 2.4) in screw top coplin jars, containing 30 ml citrate buffer pH 6, for 30 min at 97°C. Slides were removed from the water-bath and allowed to cool for approximately 20 min then later returned to distilled water. Slides were placed in cover-plates in Sequenza racks (Thermo Shandon) and washed for 5 min in TBST followed by block of non-specific binding of primary antibody by incubation in goat serum at 1:10 dilutions in TBST for 10 min. The sections were incubated for 15-18 h at 4°C with polyclonal rabbit anti-CD3 (1:10 in 20% swine serum in TBST, see table 2.5). Following incubation, the slides were washed three times in TBST for 5 min each then incubated for a further 30 min with goat anti-rabbit IgG, biotinylated at 1:100 dilutions in TBST (Vector Laboratories Ltd, Petersborough, UK). This was followed by a further 5 min wash in TBST and incubation for 30 min using the avidin biotin complex at RT with 0.9 µl A + 0.9 µl B to 100 µl TBST (Vectastain

ABC-Kit, Vector Laboratories Ltd). The slides were washed in TBST and removed from cover plates then incubated with permanent stirring for 10 min in DAB (Fluka Chemie AG) with 0.01% H_2O_2 (Perhydrol 30% H_2O_2 P-a, Fisher Scientific) in 0.1 M imidazole buffer (pH7.1, Fluka Chemie AG; see Appendix) at RT. The slides were washed in TBST three times for 5 min each and once for 5 min in distilled water. Slides were counter stained with Papanicolaou's haematoxylin (Merck) for 1 min, then placed in running tap water for 5 min. The sections were dehydrated in ascending ethanol (1 min 96%, 2 min 100% and 3 min 100%), cleared in xylene (2 min 100% and 2 x 3 min 100%) and cover slips were mounted on slides with DPX (BDH brand, VWR International).

2.4.8 Quantitative data analysis

The number of cleaved caspase 3-positive cells per 100 lymphocytes was counted under 40X magnification in 10 selected fields in the white and red pulp of the spleen and cortex and medulla of the thymus of infected and control foetuses in early gestation (91±1 dg), and the thymus of infected and control foetuses in late gestation (231±1 dg). The spleen of foetuses in late gestation was not used if a statistical difference was not found in the thymus. From each thymus and spleen from foetuses in early gestation, 10 randomly non-overlapping areas were chosen; while from foetuses in late gestation, five randomly selected non-overlapping areas in the cortex and five in the medulla were chosen. A photomicrograph was then taken of each section using a Zeiss Axio Imager M2 microscope (Carl Zeiss Ltd, Göttingen, Germany). A paper grid was then used to cover the photomicrograph and 100 cells within a rectangular section in the centre were counted. The arithmetic mean percentage and standard deviation values were calculated. Mean values were compared using the Student's *t*-test. All statistical analyses were performed using IBM SPSS Statistics 20 software (IBM Corp., Armonk, New York). Statistical significance was accepted when $p<0.05$ (*) and $p<0.01$ (**).

2.5 RESULTS

2.5.1 Histological and immunohistological findings in foetuses from dams infected in early gestation (day 70 dg) and control foetuses (91±1 dg)

An initial histological screening was carried out on 13 foetuses in early gestation (Table 2.1). Five of these foetuses (three from infected, two from uninfected dams) were subsequently examined immunohistologically to evaluate the composition and activity of the haemolymphatic tissues (Table 2.6) to identify the potential changes induced by *N. caninum*. Furthermore, the distribution and effect of the parasite in other tissues was studied (Table 2.6). The foetuses from the infected dams had all died approximately 24 h prior to euthanasia.

Table 2.6: Tissues used for histological and immunohistological study

Haemolymphatic tissues	Non-haemolymphatic (other) tissues
Thymus Spleen Mesenteric lymph node (late gestation and natural infected foetuses only) Femoral bone marrow	Brain Spinal cord Cardiac muscle Liver Lung *Musculus quadriceps femoris* *Nervus femoralis* Intestine (jejunum) Kidney Adrenal gland

2.5.1.1 Non-haemolymphatic tissues

2.5.1.1.1 Brain and spinal cord: In all foetuses at this stage of development, the histological structures in the brain and spinal cord were poorly differentiated, which made it difficult to identify the different areas. White and grey matter were undifferentiated and could not be discerned, therefore, the precise localisation of lesions in infected animals could not be determined. In all foetuses from infected dams, brain and spinal cord exhibited multifocal glial cell aggregates (Fig. 2.1A), which contained low numbers of necrotic (spinal cord only) cells and, as confirmed by immunohistology for cleaved caspase 3 (Fig. 2.1B), apoptotic cells. The latter were also found disseminated in the adjacent parenchyma (Fig. 2.1B). In one foetus, a focal area of white matter necrosis (Fig. 2.1C) with necrotic debris and few apoptotic cells (observed histologically and immunohistologically) was seen in the

spinal cord; in addition, low numbers of CD3-positve T cells (Fig. 2.1D) were randomly scattered in the grey and white matter and higher numbers were observed in the meninges. Immunohistology demonstrated numerous *N. caninum* tachyzoites in the brain of all selected foetuses (Fig. 2.2A). Tachyzoites were also identified in two of the four remaining foetuses. They were also observed in the spinal cord of all selected foetuses and three of the four remaining foetuses, within intact glial cells and sometimes cell free, but not in association with the glial cell aggregates. There was no evidence of an inflammatory cell infiltration in association with the presence of degenerated cells; immunohistology for T cells, B cells and macrophages/neutrophils was all negative; however, low numbers of CD3-positive T cells were detected within the glial cell aggregates in the brain parenchyma of the three cases examined in detail, and moderate numbers of T cells were present within blood vessels in the neuropil (Fig. 2.2B). These vessels also exhibited enlarged, bulging, i.e. activated endothelial cells (Fig. 2.2B, inset), indicating T cell recruitment into the brain parenchyma. The majority of the cells within the aggregate were positive for MHCII (morphologically consistent with microglial cells; Fig. 2.2C) and individual infiltrating calprotectin-positive cells (morphology consistent with macrophages; Fig. 2.2D) were also detected. Control foetuses neither exhibited glial nodules nor T cells within blood vessels.

2.5.1.1.2 Liver: In uninfected foetuses, distinct, though not fully developed portal areas, central veins and prominent hepatic cords were present, and the presence of numerous haematopoietic precursor cells indicated moderate haematopoietic activity (Fig. 2.3A). In infected foetuses, the hepatic architecture was disrupted and hepatocytes were disorderly arranged and markedly reduced in number. Hepatic cords, central veins and portal areas were not discernible and low to moderate numbers of necrotic hepatocytes were seen (Fig. 2.3B). Remaining hepatocytes were often hyper-eosinophilic and exhibited caspase-3 expression, indicating that they were undergoing apoptosis (Fig. 2.3C). Moderate numbers of CD3-positive T cells were present between hepatocyte clusters (Fig. 2.3D), representing either new T cells produced within areas of haematopoiesis, or infiltrating T cells. Overall, however, haematopoietic precursor cells were present in much lower numbers than in control foetuses and were often apoptotic, as indicated by the expression of caspase-3 (Fig. 2.3C). Numerous *N. caninum* tachyzoites were detected in the liver, both cell-free

and within intact hepatocytes of all examined infected foetuses (Fig. 2.3E) and in a single megakaryocyte (in foetus 1-3 only; Fig. 2.3E, inset).

2.5.1.1.3 Heart: The myocardium of infected foetuses did not exhibit distinct histological changes; however, moderate amounts of mononuclear cells were present in the tissue immediately beneath the epicardium (visceral epicardium) and sometimes within vessels (Fig. 2.4A). When tested, these cells were mainly CD3-positive T cells which were also found in low numbers in the myocardium (Fig. 2.4B). They were also generally MHCII-positive. Some infiltrating cells were apoptotic (caspase 3-positive; Fig. 2.4C). Similar mononuclear cells were also seen in the epicardium and sometimes within epicardial vessels of uninfected foetuses, which could represent haematopoiesis with new T cell production. High numbers of *N. caninum* tachyzoites were detected within intact cardiomyocytes of all foetuses, without any evidence of degeneration or cell death and no inflammatory reaction (Fig. 2.4D).

2.5.1.1.4 Lungs: Complete foetal atelectasis was seen in all lungs, which in control foetuses and five foetuses from infected dams did not exhibit any histological changes. The other two foetuses had moderate autolysis in the lung. In all infected foetuses, however, apoptotic bronchial and bronchiolar epithelial cells were present, as confirmed by the immunohistological demonstration of cleaved caspase 3 expression (Fig. 2.5A). When tested, moderate amounts of CD3-positive T cells were detected in the alveolar walls and within vessels in the lungs (Fig. 2.5B), which also contained activated endothelial cells with their typical morphology. *Neospora caninum* tachyzoites were detected in moderate numbers in two of the three selected foetuses within intact cells whose morphology was consistent with macrophages, in alveolar walls (Fig. 2.5C), while low numbers were detected within similar cells in the remaining four infected foetuses.

2.5.1.1.5 Other tissues: All infected foetuses exhibited moderate amounts of apoptotic myoblasts in the *Musculus quadriceps femoris* (Fig. 2.5D) and, when tested, occasional T cells between the myofibres. Immunohistology for *N. caninum* antigen detected low numbers of tachyzoites within tubular epithelial cells in two of the three selected foetuses and in all of the remaining foetuses (Fig. 2.5E).

The remaining tissues (adrenal glands, *Nervus femoralis*, intestine, and pancreas) did not show any histological changes. Tissues examined from the control group showed normal foetal morphology and no histological changes.

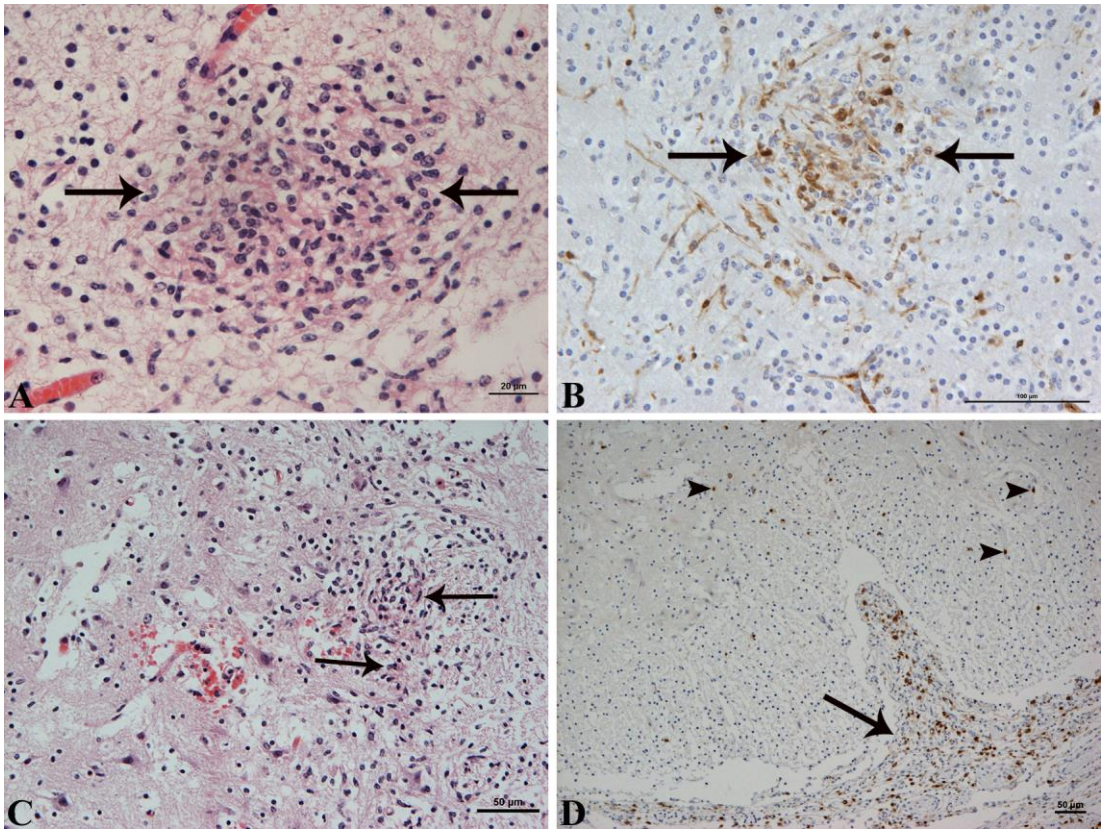

Figure 2.1. Brain and spinal cord, foetus I-3, from dam infected with *N. caninum* at 70 days gestation. **A**. A focal glial cell aggregate (glial nodule) is present in the neuropil (arrows). HE stain. Bar = 20µm. **B**. Cleaved caspase 3-positive apoptotic cells are detected within the glial aggregate (arrows) and as individual cells also in the neuropil. PAP method, Papanicolaou's haematoxylin counterstain. Bar = 100µm. **C**. A focal area of white matter necrosis (arrows) is present alongside individual apoptotic cells. HE stain. Bar = 50µm. **D**. Low numbers of CD3-positive T cells are present in the spinal cord grey and white matter (arrowheads), while higher numbers are seen in the ventral fissure and meninges (large arrow). ABC method, Papanicolaou's haematoxylin counterstain. Bar = 50µm.

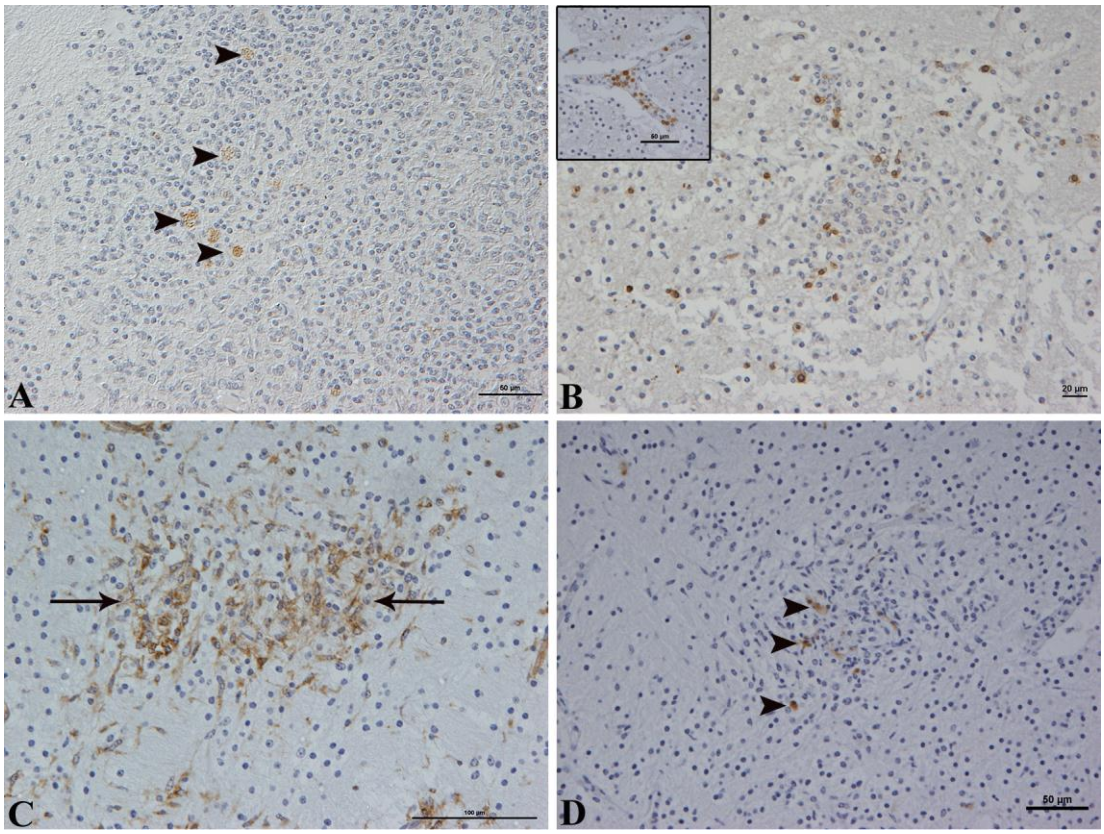

Figure 2.2. Brain, foetus I-3, from dam infected with *N. caninum* at 70 days gestation. **A**. Clusters of *N. caninum* tachyzoites are present within intact glial cells (arrowheads). PAP method, Papanicolaou's haematoxylin counterstain. Bar = 50µm. **B**. Low numbers of CD3-positive T cells are present multifocally within the glial aggregate and within blood vessels, which exhibited enlarged, i.e. activated endothelial cells (inset). ABC method, Papanicolaou's haematoxylin counterstain. Bar = 20µm. **C**. Moderate numbers of MHCII-positive activated microglial cells are present within the glial aggregate and also in the surrounding neuropil (arrows). PAP method, Papanicolaou's haematoxylin counterstain. Bar = 100µm. **D**. Individual macrophages (calprotectin-positive) are also present within the glial aggregate (arrowheads). PAP method, Papanicolaou's haematoxylin counterstain. Bar = 50µm.

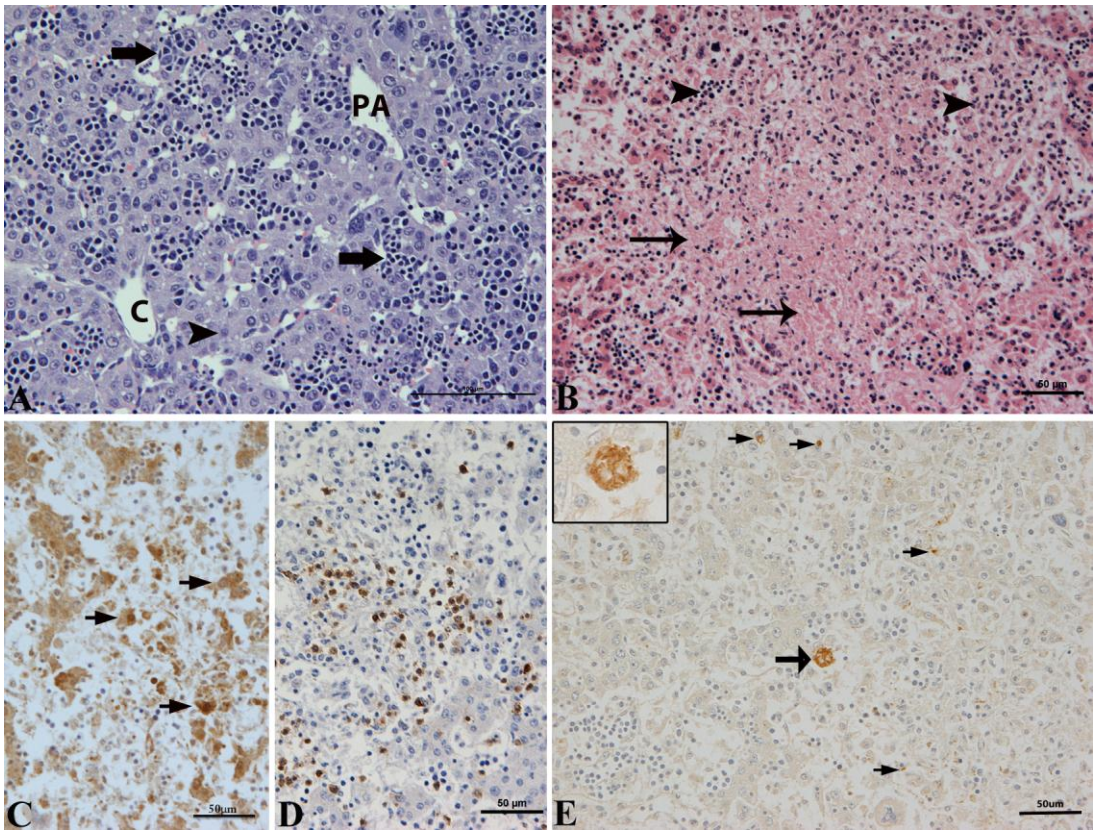

Figure 2.3. Liver, control foetus and foetuses from dams infected with *N. caninum* at 70 days gestation. **A**. Liver of control foetus (C-3) showing orderly arrangement in lobules, with hepatocytes in cords (arrowhead), central veins (C) and portal areas (PA) along with numerous haematopoietic cells (arrows). HE stain. Bar = 100µm. **B**. Liver of infected foetus (I-1) showing loss of architecture and disorderly arranged hepatocytes. Portal tracts, central veins and hepatic sinusoids are not discernible. Hepatocytes are hyper-eosinophilic (severe hepatocellular necrosis, arrows). Moderate amounts of haematopoietic cells are present and diffusely scattered (arrowheads). HE stain. Bar = 50µm. **C**. Hepatocytes exhibiting caspase 3-expression alongside necrotic cells (arrows). PAP method, Papanicolaou's haematoxylin counterstain. Bar = 50µm. **D**. Moderate amounts of CD3-positive T cells are detected and multifocally distributed between hepatocyte clusters. ABC method, Papanicolaou's haematoxylin counterstain. Bar = 50µm. **E**. Numerous *N. caninum* tachyzoites are present within intact hepatocytes and cell free (small arrows) and also in a single megakaryocyte (large arrow; inset, higher magnification). PAP method, Papanicolaou's haematoxylin counterstain. Bar = 50µm.

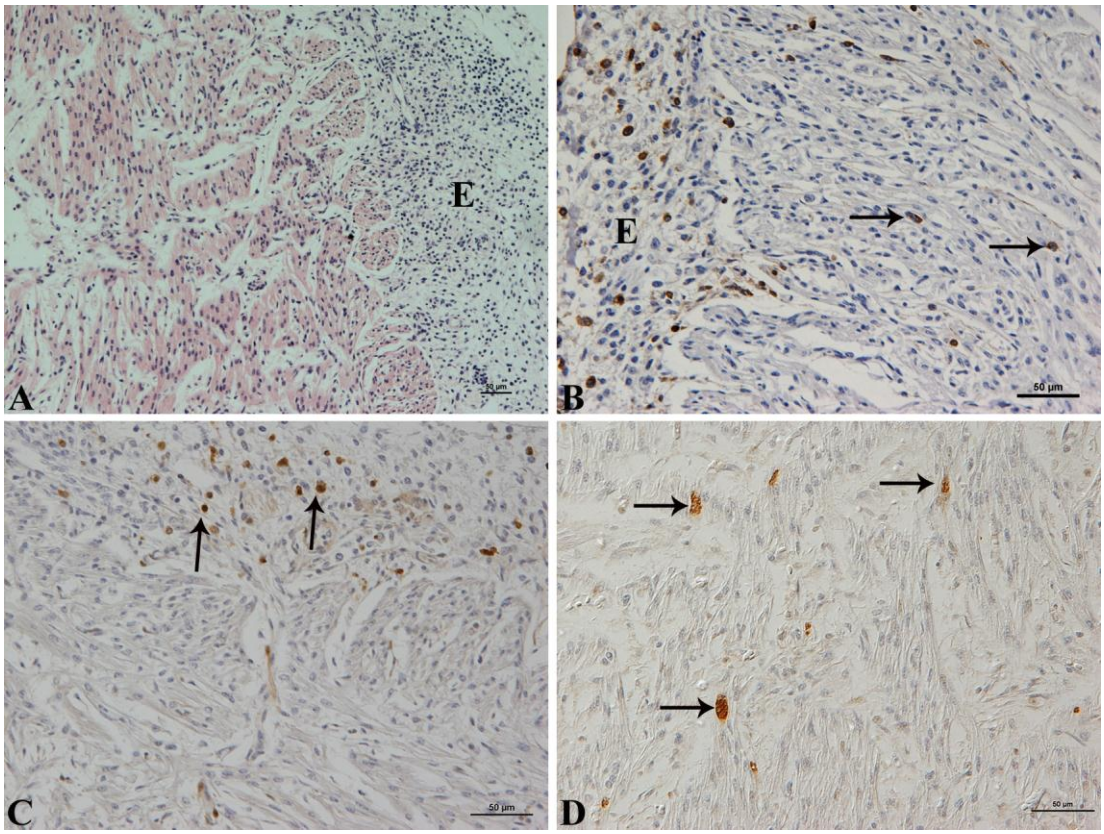

Figure 2.4. Heart, foetus I-1, from dam infected with *N. caninum* at 70 days gestation. **A**. Moderate amounts of mononuclear cells are present in the visceral epicardium (E). HE stain. Bar = 50µm. **B**. The majority of the infiltrating cells appear to be T cells, as indicated by the large number of CD3-positive cells in this location (E). Scattered T cells are also present between myoblasts (arrows). ABC method, Papanicolaou's haematoxylin counterstain. Bar = 50µm. **C**. Some infiltrating cells in the epicardium are also caspase 3-positive apoptotic cells (arrows). PAP method, Papanicolaou's haematoxylin counterstain. Bar = 50µm. **D**. Numerous *N. caninum* tachyzoites are present within intact cardiomyocytes (arrows). PAP method, Papanicolaou's haematoxylin counterstain. Bar = 50µm.

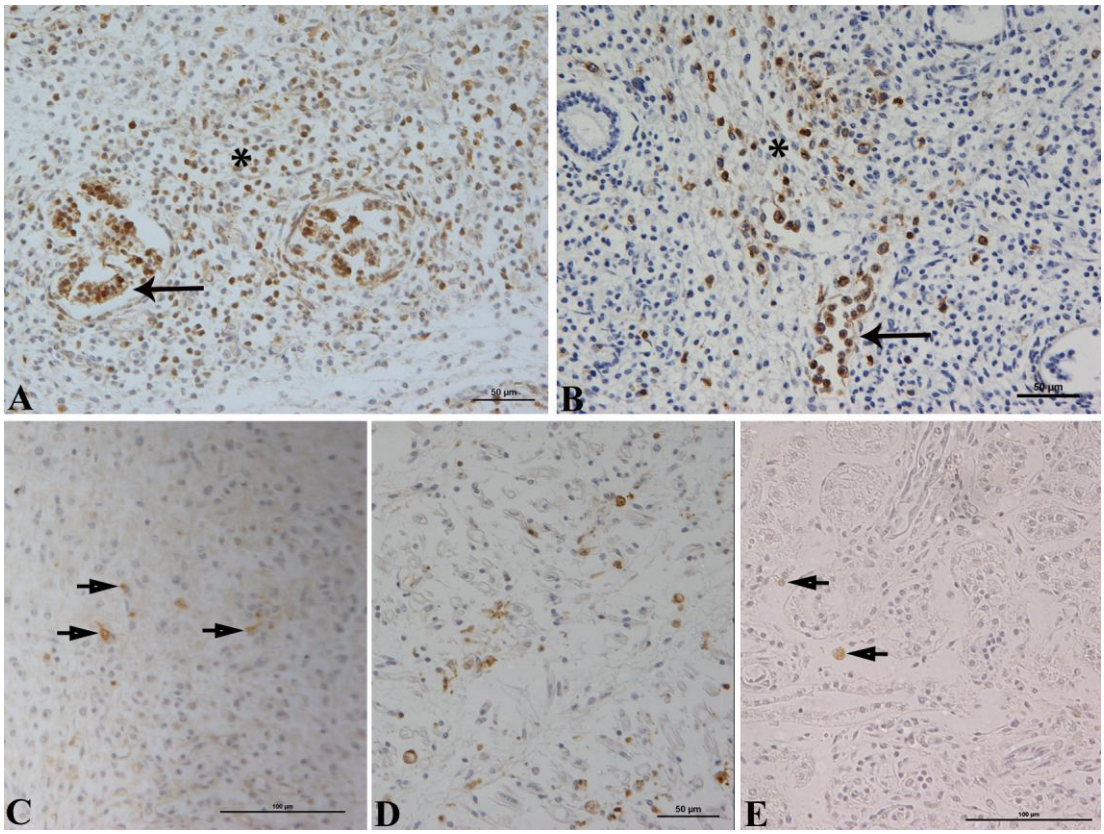

Figure 2.5. Lung, muscle and kidney, foetus I-1, from dam infected with *N. caninum* at 70 days gestation. **A**. Cells in the interstitium are often apoptotic, i.e. caspase 3-positive (asterisk, leukocytes), similar to bronchiolar epithelial cells (arrow). PAP method, Papanicolaou's haematoxylin counterstain. Bar = 50µm. **B**. Moderate amounts of CD3-positive T cells are present in the alveolar walls (asterisk) and numerous T cells are seen within blood vessels. These often show activated endothelial cells (arrow). ABC method, Papanicolaou's haematoxylin counterstain. Bar = 50µm. **C**. High numbers of *N. caninum* tachyzoites are present in the lung within intact mononuclear cells (arrows). PAP method, Papanicolaou's haematoxylin counterstain. Bar = 100µm. **D**. Moderate amounts of apoptotic myoblasts are present in the *Musculus quadriceps femoris.* PAP method, Papanicolaou's haematoxylin counterstain. Bar = 50µm. **E.** Low numbers of *N. caninum* tachyzoites are present within renal tubular epithelial cells (arrows). PAP method, Papanicolaou's haematoxylin counterstain. Bar = 100µm.

2.5.1.2 Haemolymphatic tissues

The histological and immunohistological examination of the haemolymphatic tissues of control foetuses were used to establish the composition and activity of these tissues at the foetal age of approximately 90 dg. This information was used to allow identification of changes in infected foetuses.

2.5.1.3 Thymus

2.5.1.3.1 *Control foetuses*. The thymus was examined in three control foetuses and was generally moderately lobulated, with incomplete lobules consisting of an outer cortex and an inner medulla with a distinct corticomedullary zone (Fig. 2.6A). Both cortex and medulla were distinct. The cortex was densely cellular and composed of small lymphocytes and sparse epithelial cells. The medulla comprised fewer lymphocytes, but moderate numbers of epithelial reticular cells, macrophages and ovoid epithelial structures with concentric lamellated keratinisation (Hassall's corpuscles) were present. The medullary lymphocytes were larger and had more cytoplasm than the cortical lymphocytes, consistent with the lower degree of maturation of medullary lymphocytes (Pearse, 2006). The majority of cells in both cortex and medulla were CD3-positive and could thereby be identified as T cells (Fig. 2.6B). B lymphocytes (PAX5-positive) were not observed. PCNA-positive proliferating cells (mainly lymphocytes) were detected in the cortex in low numbers and were even fewer in the medulla, whereas apoptotic cells (cleaved caspase 3-positive) were present in low numbers predominantly in the cortex. These findings indicate a low turnover (low degree of proliferation and cell death) and thereby only minimal immune activity in the thymus as it would be expected in a foetus at this stage of maturation (Linton and Dorshkind, 2004). The medulla exhibited higher numbers of MHCII-positive cells [macrophages and dendritic cells (Lemos et al., 2004; Rosbottom et al., 2011)] than the cortex, where they were dispersed among the cortical lymphocytes. IFN-γ-expressing cells were not detected, suggesting that the foetal lymphocytes were not functionally active. *Neospora caninum* antigen was not detected by immunohistology.

2.5.1.3.2 *Foetuses from infected dams*. The composition of the thymus differed from that of controls. In all infected foetuses, the cortex exhibited low cellularity (Fig. 2.6C) and a high number of these cells (mainly lymphocytes) was undergoing

apoptosis, as indicated by their caspase 3 expression (Fig 2.6D); fewer apoptotic cells were present in the medulla (Fig. 2.6D). Quantitative analysis showed that there is a significant increase in the number of apoptotic lymphocytes in the thymus of infected foetuses, compared to controls (mean number of apoptotic cells in infected foetus: 88.90±5.34, control: 16.60±6.95; $p<0.001$, Student's *t*-test, Appendix 4). The overall number of CD3-positive T cells was lower in infected foetuses (Fig. 2.6E), which is likely a consequence of the observed apoptotic cell death. B cells were also not detected. MHCII-positive cells were fewer than in controls, which indicate that macrophages and dendritic cells were also lost. PCNA-positive proliferating cells were also less numerous than in controls. This implies that the cell turnover was lower than in controls. Furthermore, IFN-γ-expressing cells were not detected as in the controls. Immunohistology identified *N. caninum* tachyzoites in the thymic medulla of infected foetuses, within large mononuclear cells consistent with macrophages (Fig. 2.6F).

2.5.1.4 Spleen

2.5.1.4.1 *Control foetuses*. The spleen was composed of numerous spindle-shaped cells; low numbers of lymphocytes and a moderate number of haematopoietic cells, with all precursor cell lineages (myeloid, erythroid and megakaryocytes) present (Fig. 2.7A). There was no specific organisation of lymphocytes into lymphoid follicles and a mixture of T and B cells was present within lymphoid aggregates. B cells were very rare (Fig. 2.7B). Accordingly, a red pulp and a white pulp could not be discerned. T cells were sometimes found arranged around small arteries, forming early periarteriolar lymphoid sheaths (PALS; Fig. 2.7C). Macrophages and splenic dendritic cells (MHCII-positive) were present in moderate amounts. PCNA-positive proliferating cells were present in low numbers and randomly scattered, consistent with the low turnover in the lymphoid organs of younger foetuses (Linton and Dorshkind, 2004). Individual caspase 3-expressing apoptotic cells were detected and randomly scattered. IFN-γ-expressing cells were not detected. *Neospora caninum* antigen was not detected by immunohistology.

2.5.1.4.2 *Foetuses from infected dams*. The spleen had a similar morphology as in control foetuses, but was of lower cellularity, i.e. fewer lymphocytes and haematopoietic precursor cells were present (Fig. 2.7D). High numbers of randomly distributed caspase 3-positive apoptotic cells (predominantly lymphocytes) were

detected by immunohistology (Fig. 2.7E). Quantitative data analysis showed a significantly higher mean percentage of apoptotic lymphocytes in the spleen of infected foetuses, compared to control (mean number of apoptotic cells in infected foetus: 34.40±13.09, control: 2.4±1.58; $p<0.001$, Student's *t*-test, Appendix 4). T cells were noticeably fewer in infected foetuses (Fig. 2.7F) compared to control foetuses, while B cells were equally low in number. Macrophages and dendritic cells (MHCII-positive) were present in amounts similar to those seen in the controls. PCNA-positive proliferating cells were present in low numbers, as in the control group. IFN-γ-expressing cells were not detected, as in the control foetuses. *Neospora caninum* tachyzoites were detected by immunohistology in moderate numbers in intact cells (consistent with macrophages) of all infected foetuses (Fig. 2.7G).

2.5.1.5 Bone marrow

2.5.1.5.1 *Control foetuses*. The femoral bone marrow was represented by small clusters of erythroid and myeloid precursor cells dispersed throughout abundant trabecular bone and cartilage (Fig. 2.8A). Numerous osteoblasts were present lining the trabecular bone. Megakaryocytes were not observed. T cells represented a small proportion and formed small clusters in the intertrabecular spaces, where B cells were also present in low numbers. A small population of MHCII-positive cells was detected. Proliferating cells were present in low numbers (haematopoietic precursor cells), whereas caspase 3-expressing, apoptotic cells were not observed. IFN-γ-expressing cells were also not detected in the bone marrow.

2.5.1.5.2 *Foetuses from infected dams*. The bone marrow had a similar composition, but was of lower cellularity than in controls (Fig. 2.8B) and, when tested, exhibited moderate amounts of caspase 3-positive apoptotic lymphocytes. T and B cells as well as MHCII-positive cells (pre-B cells and early macrophage lineage; see above) and PCNA-positive proliferating cells were present in low numbers. *Neospora caninum* tachyzoites were not present in the bone marrow of the selected foetuses, but were present as small clusters within intact mononuclear cells in one of the four remaining foetuses (Fig. 2.8C). IFN-γ-expressing cells were not detected as in the control foetuses.

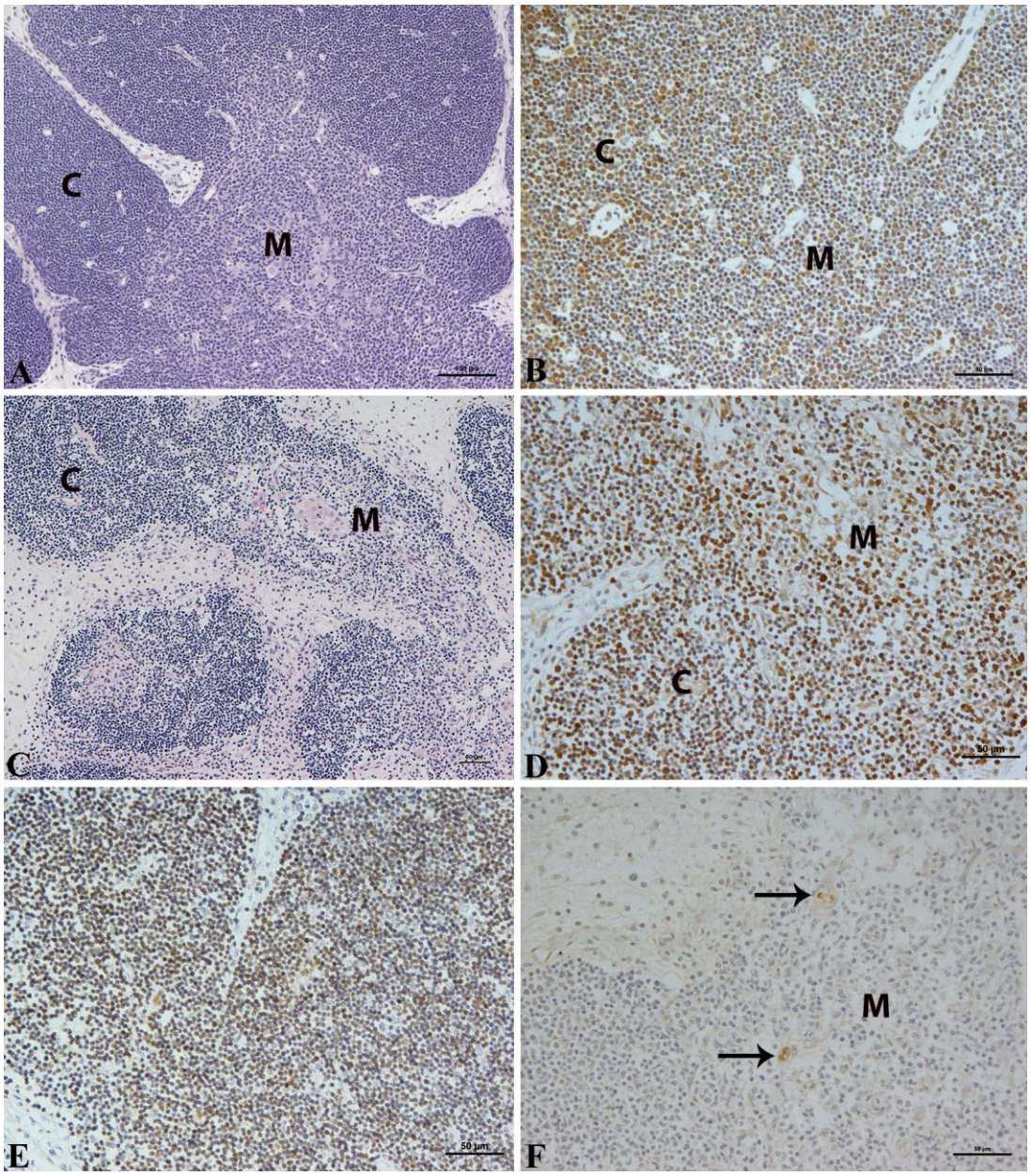

Figure 2.6. Thymus, control foetus (C-4; A and B) and foetus from dam infected with *N. caninum* at 70 days gestation (I-1; C-F). **A**. In the control foetus, the thymus comprises a distinct cortex with large numbers of lymphocytes (C) and medulla (M) that is less cell dense. HE stain. Bar = 100µm. **B**. CD3-positive T cells account for the vast majority of cells in both cortex and medulla. ABC method, Papanicolaou's haematoxylin counterstain. Bar = 50µm. **C**. In an infected foetus, the thymus is far less cellular (C: cortex, M: medulla). HE stain. Bar = 50µm. **D**. High numbers of caspase 3-positive apoptotic cells are present in both cortex and medulla. PAP method, Papanicolaou's haematoxylin counterstain. Bar = 50µm. **E**. The number of CD3-positive T cells in the thymus is also lower. ABC method, Papanicolaou's haematoxylin counterstain. Bar = 50µm. **F**. Clusters of *N. caninum* tachyzoites are present in the medulla (M) within intact mononuclear cells (arrows). PAP method, Papanicolaou's haematoxylin counterstain. Bar = 50µm.

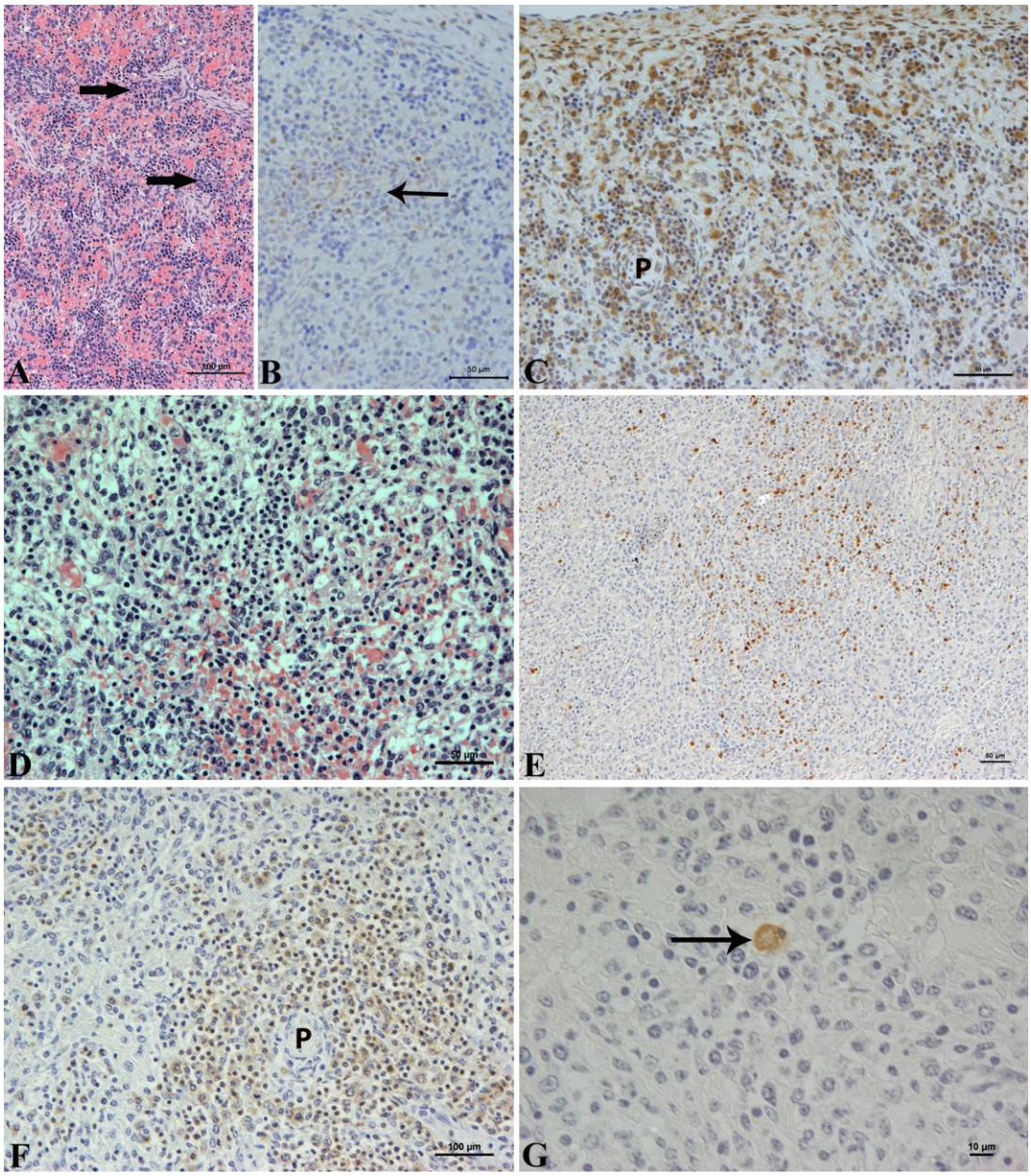

Figure 2.7. Spleen, control foetus (C-4; A-C) and foetus from dam infected with *N. caninum* at 70 days gestation (I-4; D-G). **A**. In the control foetus, the spleen comprises numerous spindle-shaped cells, low numbers of lymphocytes and moderate haematopoietic activity (arrows). HE stain. Bar = 50µm. **B**. Low numbers of PAX5-positive B cells are present within lymphoid aggregates. PAP method, Papanicolaou's haematoxylin counterstain. Bar = 50µm. **C**. CD3-positive T cells are present and sometimes found arranged around arteries forming early PALS (P). ABC method, Papanicolaou's haematoxylin counterstain. Bar = 50µm. **D**. In the infected foetuses, the overall cellularity of the spleen is lower and fewer hematopoietic cells are present. HE stain. Bar = 50µm. **E**. Caspase 3-positive apoptotic cells are present in high numbers. PAP method, Papanicolaou's haematoxylin counterstain. Bar = 50µm. **F**. The number of CD3-positive T cells are notable lower in the spleen of the infected foetus. ABC method, Papanicolaou's haematoxylin counterstain. Bar = 100µm. **G**. A cluster of *N. caninum* tachyzoites is present within an intact mononuclear cell (arrow). PAP method, Papanicolaou's haematoxylin counterstain. Bar = 10µm.

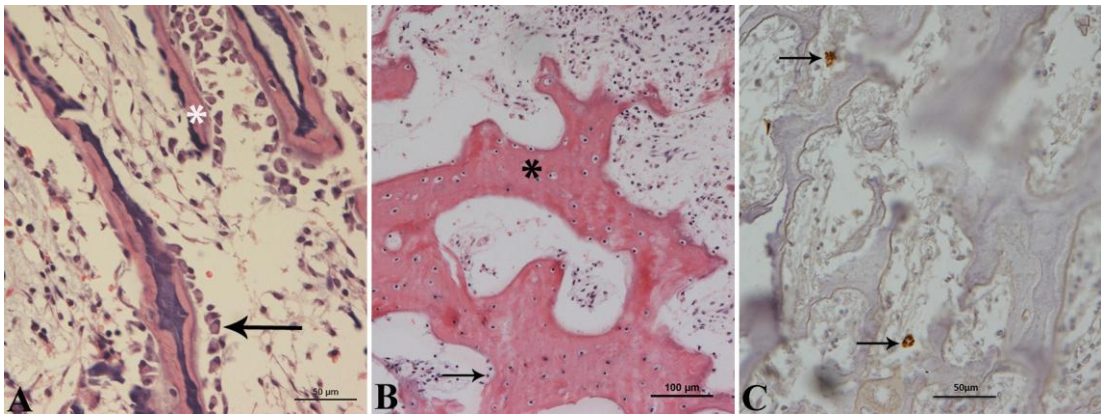

Figure 2.8. Bone marrow, control foetus (C-3) and foetuses from dams infected with *N. caninum* at 70 days gestation. **A**. In the control foetus, the bone marrow is of low cellularity with trabecular bone (asterisk) lined by numerous osteoblasts (arrow). HE stain. Bar = 50µm. **B**. In one infected foetus (I-3), low numbers of haematopoietic cells are present, abundant trabecular bone (asterisk) and fewer osteoblasts lining the trabecular bones (arrow). HE stain Bar = 100µm. **C**. In one of the four remaining infected foetuses (I-4), small clusters of *N. caninum* tachyzoites are present within intact mononuclear cells. PAP method, Papanicolaou's haematoxylin counterstain. Bar = 50µm.

In summary, haemolymphatic tissues, CNS and liver were the most severely affected organs with necrosis, apoptosis and high parasite loads especially in the liver, where tachyzoites were detected within intact cells; whereas surrounding hepatocytes were often apoptotic. *Neospora caninum* antigen was detected in all the tissues examined from infected foetuses, i.e. brain, spinal cord, liver, lung, heart, thymus, spleen, bone marrow and kidney, in early gestation, sometimes in association with cell death. Parasites were not associated with a distinct inflammatory reaction. However, there was evidence of T cell recruitment into the most affected tissues, i.e. brain, spinal cord and liver, indicated by the presence of T cells in vessel lumina and in the tissue, together with evidence of endothelial cell activation. Cardiomyocytes remained intact even with high parasite loads and were not directly associated with an inflammatory response.

2.5.2 Histological and immunohistological findings in foetuses from dams infected in late gestation (day 210) and control foetuses (231±1 dg)

The initial histological screening was carried out on 12 foetuses (Table 2.1) of which five were selected for further examinations. The five representative foetuses (two from infected, three from uninfected dams) were examined histologically and by immunohistology to evaluate the composition and activity of the haemolymphatic tissues and to assess the pathological effects of *N. caninum* on haemolymphatic and other tissues after infection of the dams at 210 dg and euthanasia within 20-22 days. All foetuses, irrespective of whether they were from infected or uninfected dams were alive when the cows were euthanized.

2.5.2.1 Non-haemolymphatic tissues

2.5.2.1.1 *Control foetuses.* All tissues exhibited the normal foetal morphology and in the vast majority no histological alterations were observed. However, in the liver of one foetus examined in detail (C-9), a multifocal mixed cellular portal infiltrate, which consisted of low numbers of CD3-positive T cells [with fewer macrophages and neutrophils (calprotectin-positive)] was observed. The haematopoietic activity in the liver was generally low and small clusters of myeloid and erythroid precursor cells with few megakaryocytes were present. *Neospora caninum* antigen was not detected.

2.5.2.1.2 *Foetuses from infected dams.* The two foetuses from dams infected at 210 dg exhibited histological changes in some organs.

2.5.2.1.3 *Brain and spinal cord*: In one foetus (I-12), a severe non-suppurative myelitis was seen. This was represented by extensive, multifocal, mononuclear inflammatory infiltrates, composed of lymphocytes and macrophages (Fig. 2.9A). These were found disseminated throughout the spinal cord and were most pronounced in the grey matter. CD3-positive T cells (Fig. 2.9B) dominated in the infiltrates and were present in moderate numbers within the grey matter, where they were admixed with fewer macrophages (calprotectin-positive). Numerous MHCII-positive cells (activated microglial cells, activated lymphocytes), were detected within the inflammatory foci mainly in the grey matter (Fig. 2.9C), while occasional

cells with a morphology consistent with plasma cells were seen. However, B lymphocytes (PAX 5-positive) were not observed. The grey and white matter also contained multifocal perivascular, mononuclear infiltrates, mainly comprised of CD3-positive T cells (Fig. 2.9B inset), with low numbers of macrophages (calprotectin-positive) and occasionally a few neutrophils. Vessels within the neuropil exhibited activated endothelial cells and leukocytes adhering (rolling) to the endothelium and accumulating in the perivascular spaces (emigration; Fig. 2.9A inset). Low numbers of apoptotic cells (identified based on their morphology and the expression of cleaved caspase-3) were also present within the inflammatory infiltrates of the grey matter and perivascular infiltrates. A small cluster of *N. caninum* tachyzoites was present within an intact glial cell (Fig. 2.9D). Moderate numbers of cells in the parenchymal and perivascular mononuclear infiltrates were found to be proliferating (PCNA-positive). In addition, this foetus also exhibited a mild radiculoneuritis of a spinal nerve root with focal leptomeningitis of the spinal cord, again with a low number of CD3-positive T cells (Fig. 2.9E) and fewer, randomly scattered calprotectin-positive macrophages. Only minimal inflammatory infiltrates were present in the brain, restricted to the grey matter of the cerebral cortex and individual proliferating glial cells were observed (PCNA-positive). IFN-γ-expressing cells were not detected in the CNS.

A second foetus (I-11) exhibited a focal area of necrosis with associated mononuclear infiltration in the white matter of the cerebral cortex (Fig. 2.9F). Low numbers of *N. caninum* tachyzoites were detected by immunohistology within an intact glial cell in association with the inflammatory infiltrate (Fig. 2.9F, inset). In addition, moderate, multifocal, mononuclear perivascular infiltrates were observed (non-suppurative encephalitis). The infiltrates could not be assessed further by immunohistology, as they were not present in the consecutive sections. The spinal cord exhibited low numbers of disseminated CD3-positive T cells mainly in the white matter.

Three of the four remaining foetuses exhibited mild mononuclear perivascular infiltrates, and the fourth foetus had a focal area of mononuclear infiltration, all in the grey matter of the brain. The spinal cord exhibited mild perivascular mononuclear infiltrates in the white matter in three foetuses; in one of these foetuses, they were also found infrequently in the grey matter. Low numbers of *N. caninum* tachyzoites were detected by immunohistology within intact glial cells in the white

matter of the latter foetus in association with the inflammatory infiltrates. Another foetus exhibited a focal area of necrosis in the white matter of the spinal cord, with mild mononuclear inflammatory infiltration, necrotic debris and occasional spheroids without the presence of *N. caninum* tachyzoites. Parasite antigen was not observed in the CNS of the remaining foetuses.

2.5.2.1.4 *Liver*: Mild, mononuclear portal infiltrates and low numbers of haematopoietic precursor cells (myeloid, erythroid precursors and a few megakaryocytes; consistent with ongoing haematopoiesis) were observed in all foetuses. In one foetus (I-12), a focal area of hepatocellular necrosis with associated predominantly mononuclear inflammatory infiltration with occasional neutrophils, was observed (Fig. 2.10A). Moderate mononuclear, portal inflammatory infiltrates were observed in both foetuses. Immunohistology on the selected foetuses showed that the portal infiltrates were comprised of low numbers of each CD3-positive T cells and PAX-5 positive B cells and fewer macrophages (calprotectin-positive). Kupffer cells were also found to express both MHCII and calprotectin. PCNA expression (moderate number of positive cells) and apoptosis (caspase 3 expression; few positive cells) was only observed in hepatocytes, and in a low number of cells, indicating parenchymal turnover (Linton and Dorshkind, 2004). Low numbers of IFN-γ-expressing cells were detected by immunohistology in portal areas and randomly scattered in the hepatic parenchyma (Fig. 2.10B). *Neospora caninum* antigen was not detected.

2.5.2.1.5 *Heart*: All foetuses exhibited mild to moderate multifocal interstitial mononuclear inflammatory infiltrates (non-suppurative myocarditis; Fig. 2.10C). In both animals tested by immunohistology, these infiltrates were comprised of CD3-positive T cells with fewer macrophages (MHCII and calprotectin-positive), but no B cells. Low numbers of PCNA-positive proliferating cardiomyocytes were seen, while caspase-3 expressing, apoptotic cells were not detected. IFN-γ-expressing lymphocytes were also present in low numbers and randomly scattered in the myocardium, indicating parasite specific cell-mediated immune (CMI) response (Fig. 2.10D). *Neospora caninum* antigen was not detected.

2.5.2.1.6 *Lung*: Low numbers of mononuclear cells were generally present in the peribronchial, peribronchiolar and alveolar septa (Figs. 2.11A). These were predominantly CD3-positive T cells. In the foetuses tested by immunohistology, high numbers of macrophages (MHCII and calprotectin-positive) were found diffusely distributed within the parenchyma. In one foetus, low numbers of mononuclear cells were also present in the pleura. Low numbers of apoptotic pulmonary epithelial cells (caspase 3-positive) were present. Small clusters of *N. caninum* tachyzoites were detected by immunohistology within intact mononuclear cells mainly within alveolar spaces and septa (Fig. 2.11B). IFN-γ was detected within the cytoplasm of mononuclear cells with morphology consistent with macrophages. These were present in high numbers in the bronchial epithelium of foetus I-11 (Fig. 2.11C); whereas in one of the remaining foetuses, numerous positive cells were also present predominantly in the bronchiolar epithelium with fewer scattered positive cells in the bronchial epithelium and alveolar septae.

2.5.2.1.7 *Other tissues:* In most foetuses (in the two selected foetuses and three of the four remaining foetuses), mild multifocal mononuclear interstitial infiltrates were present in the *Musculus quadriceps femoris* (non-suppurative myositis; Fig. 2.11D). The infiltrates were found to be composed of CD3-positive T cells with fewer macrophages (MHCII and calprotectin-positive). Low numbers of B cells (PAX5-positive) were also detected within the inflammatory infiltrates. IFN-γ-expressing cells were present in low numbers (Fig. 2.11E). *Neospora caninum* antigen was not detected.

The adrenal gland in one of the four remaining foetuses contained a focal area of eosinophil infiltration within the medulla. Other tissues did not exhibit histological changes and *N. caninum* tachyzoites were not detected by immunohistology.

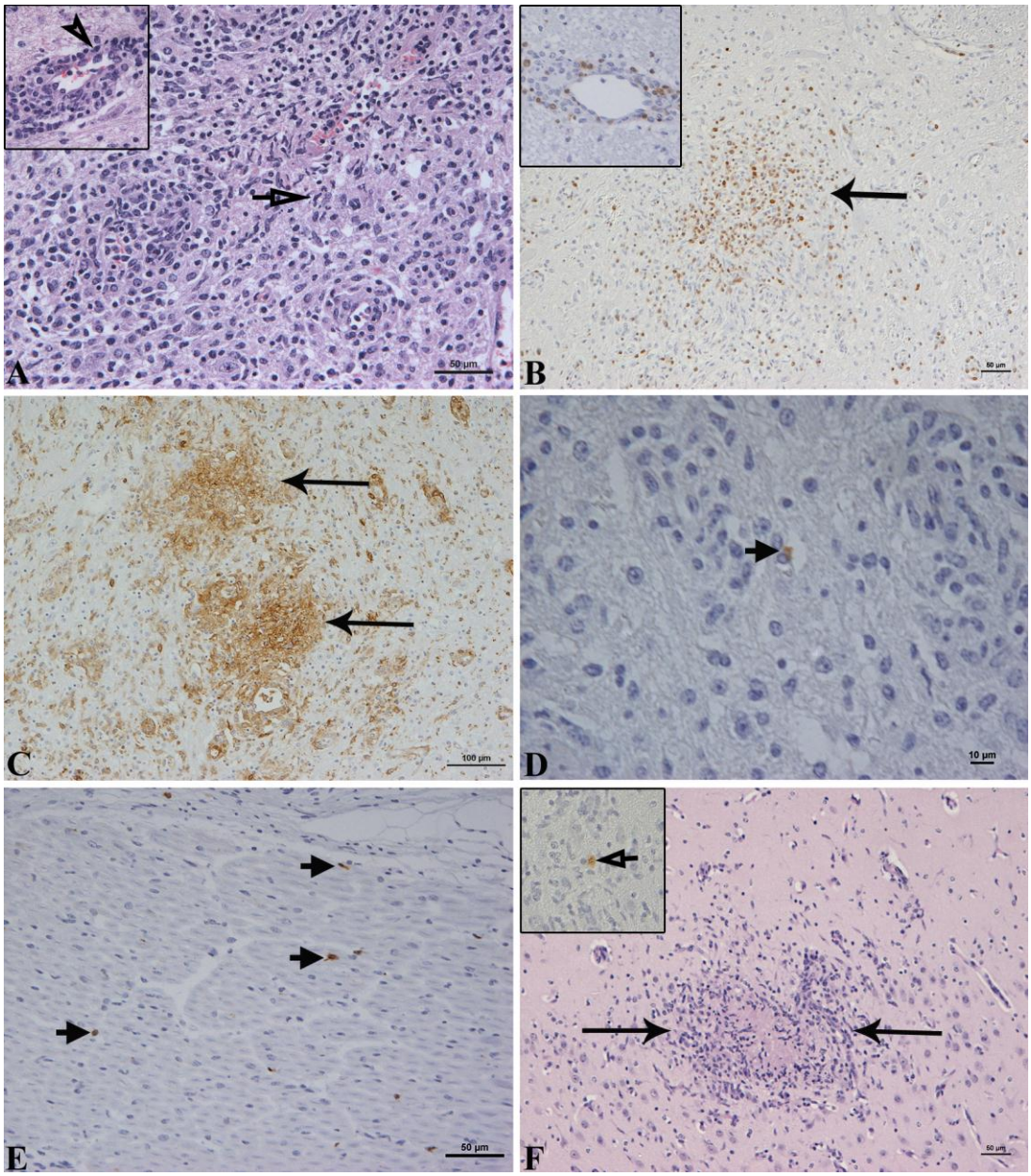

Figure 2.9. Brain and spinal cord, foetus I-12 from dam infected with *N. caninum* at 210 days gestation. **A**. Severe non-suppurative myelitis with high numbers of mononuclear cells (lymphocytes and macrophages), sparse apoptotic cells (arrow) are present within the spinal cord grey matter along with mononuclear perivascular cuffing and endothelial cell activation (inset, arrowhead). HE stain. Bar = 50µm. **B**. CD3-positive T cells are present in moderate numbers within the grey matter (arrow) and perivascular areas (inset). ABC method, Papanicolaou's haematoxylin counterstain. Bar = 50µm. **C**. Numerous MHCII-positive cells confirm microglial cell activation and infiltration of macrophages (arrows). PAP method, Papanicolaou's haematoxylin counterstain. Bar = 100µm. **D**. A small cluster of *N. caninum* tachyzoites is detected within an intact glial cell in the grey matter (arrow). PAP method, Papanicolaou's haematoxylin counterstain. Bar = 10µm. **E**. Low numbers of CD3-positive T cells are present in the spinal nerve root (arrows). ABC method, Papanicolaou's haematoxylin counterstain. Bar = 50µm. **F**. Brain of another infected foetus (I-11) with a focal area of necrosis and associated mononuclear infiltrates. HE stain. Bar = 50µm. A small cluster of *N. caninum* tachyzoites is present within an intact glial cell in direct association with the inflammatory cells (inset). PAP method, Papanicolaou's haematoxylin counterstain.

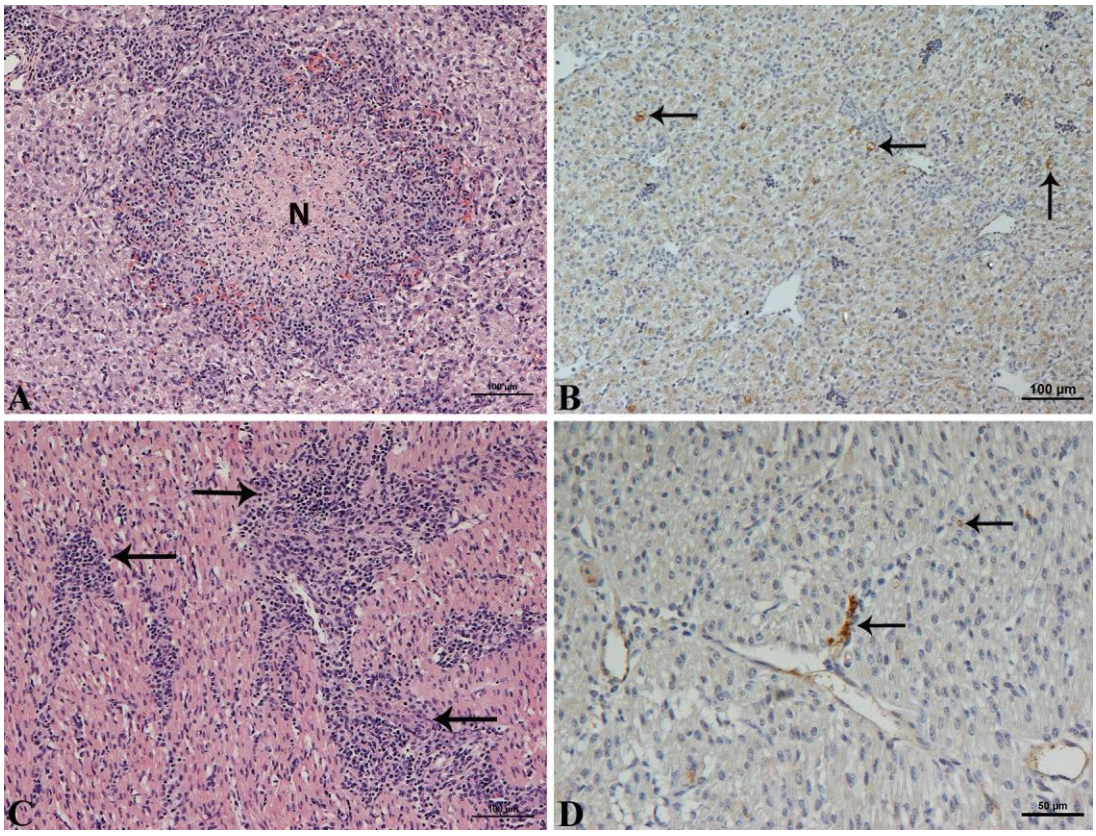

Figure 2.10. Liver, heart, lung and muscle, foetuses from dams infected with *N. caninum* at 210 days gestation. **A**. Foetus I-12 showing a focal area of hepatocellular necrosis (N) with associated mononuclear infiltrate admixed with low numbers of neutrophils. HE stain. Bar = 100µm. **B**. Liver of foetus I-11 showing low numbers of IFN-γ-expressing cells. PAP method, Papanicolaou's haematoxylin counterstain. Bar = 100µm. **C**. The heart in foetus I-11 exhibits moderate multifocal mononuclear infiltrates in the interstitium (arrows). HE stain. Bar = 100µm. **D**. Individual IFN-γ-expressing cells are present in the myocardium. PAP method, Papanicolaou's haematoxylin counterstain. Bar = 50µm.

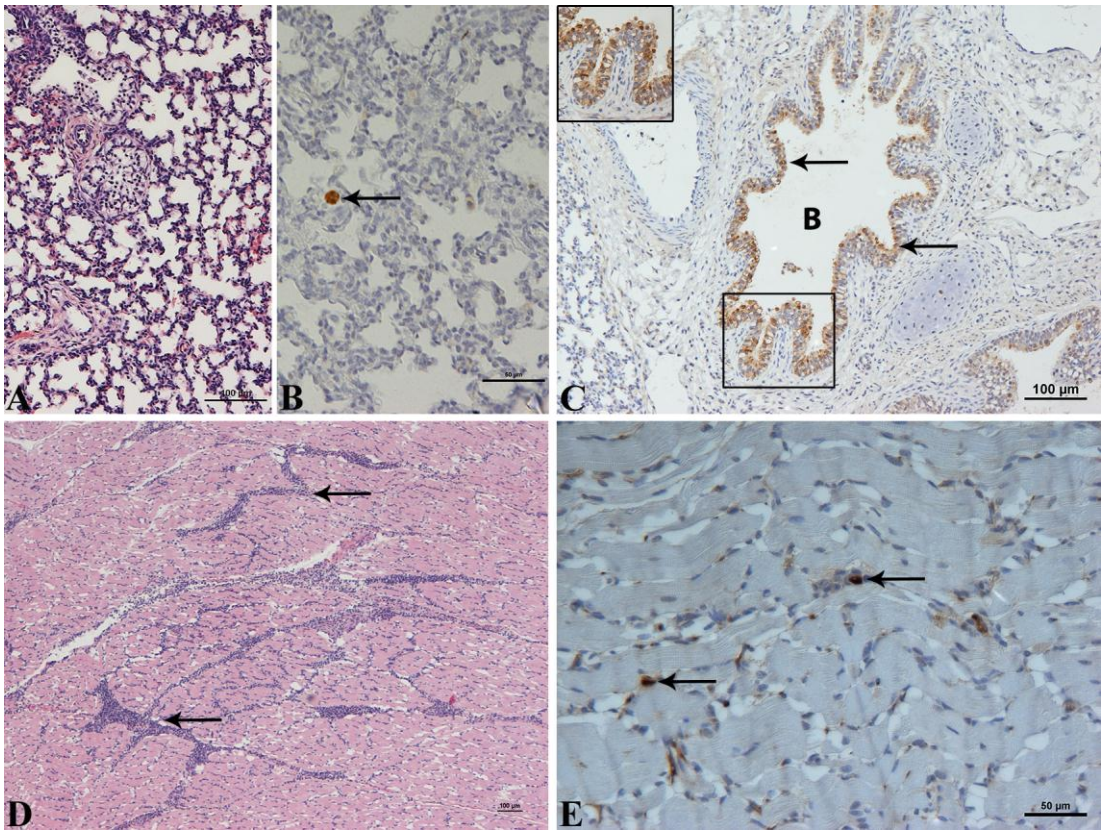

Figure 2.11. Lung and muscle, foetuses from dams infected with *N. caninum* at 210 days gestation (I-12 – A, B and D; I-11–C and E). **A**. Low numbers of mononuclear cells are also present in alveolar septa. HE stain. Bar = 100µm. **B**. A small cluster of *N. caninum* tachyzoites is detected within an intact mononuclear cell (arrow). PAP method, Papanicolaou's haematoxylin counterstain. Bar = 50µm. **C**. High numbers of IFN-γ-expressing cells are present within the bronchial epithelium (B – bronchus). The box shows an area at higher magnification (inset; 40X). PAP method, Papanicolaou's haematoxylin counterstain. Bar = 100µm. **D**. In foetus I-12, mild non-suppurative myositis with multifocal to coalescing mononuclear inflammatory infiltrates are present in the interstitium of the *Musculus quadriceps femoris.* HE stain. Bar = 100µm. **E**. Low numbers of IFN-γ-expressing cells are detected in the inflammatory infiltrates in the muscle. PAP method, Papanicolaou's haematoxylin counterstain. Bar = 50µm.

2.5.2.2 Haemolymphatic tissues

The histological examination of haemolymphatic tissues of the control foetuses euthanized at approximately 230 dg was conducted to establish the normal composition of the tissues as a basis to assess the pathological changes in infected foetuses.

2.5.2.3 Thymus

2.5.2.3.1 *Control foetuses.* In contrast to the thymuses of foetuses in early gestation, the thymus in late gestation exhibited larger lobes with a highly cellular cortex comprised of small, densely packed lymphocytes (Fig. 2.12A), which were mainly CD3-positive T cells (Fig. 2.12B). MHCII-positive cells (dendritic cells and macrophages) were detected in moderate amounts diffusely distributed in the cortex. PCNA-positive proliferating lymphocytes were present in high numbers, confirming the much higher rate of cell proliferation in the thymus at this age compared to the younger foetuses. The medulla was less cellular and comprised of larger lymphocytes (CD3-positive T cells and fewer PAX5-positive B cells), with a large population of macrophages and dendritic cells [(non-phagocytic, bone marrow derived cells; MHCII-positive) (Pearse, 2006)], prominent reticular medullary epithelial cells, Hassall's corpuscles and fewer polymorphonuclear cells that were confirmed as eosinophils by the Lendrum's Carbol Chromotrope stain. The number of PCNA-positive proliferating lymphocytes in the medulla was much lower than in the cortex (Fig. 2.12C). IFN-γ-expressing cells were not detected in the thymus. Caspase 3-positive apoptotic cells were infrequent in both medulla and cortex.

2.5.2.3.2 *Foetuses from infected dams.* The thymus generally exhibited a morphology, cellular composition (including the presence of low numbers of eosinophils in the medulla) and degree of proliferation (assessed on the basis of the number of PCNA-positive lymphocytes), similar to that of control foetuses. Histological alterations were not observed (Fig. 2.12D). However, immunohistological staining of apoptotic cells (cleaved caspase-3 positive) identified an overall slightly higher number of apoptotic cells in both cortex and medulla in infected foetuses compared to controls (Figs. 2.12E). Quantitative data analysis showed that the difference in the mean percentage (mean number of apoptotic cells) was not statistically significant (infected foetuses: 3.5±2.2; control foetuses: 4.6±3.8;

p=0.443, Student's *t*-test, Appendix 4). IFN-γ-expressing cells were not detected as in the controls. *Neospora caninum* tachyzoites were not identified by immunohistology.

2.5.2.4 Spleen

2.5.2.4.1 *Control foetuses.* Different from the spleen of foetuses in early gestation, the spleen of foetuses in late gestation exhibited a well-developed red and white pulp (Fig. 2.13A). The degree of haematopoiesis was lower than in control foetuses in early gestation, as indicated by the low number of haematopoietic precursor cells, i.e. erythroid and myeloid precursors. Megakaryocytes, however, were more abundant in the older foetuses. The white pulp was comprised of loose, poorly delineated follicle-like lymphocyte aggregates without germinal centre formation and composed of moderate amounts of PAX5-positve B cells (Fig. 2.13B) and MHCII-positive follicular dendritic cells. The PALS were composed of high numbers of CD3-positive T cells (Fig. 2.13C) intermingled with splenic macrophages and dendritic cells (MHCII-positive). Proliferating (PCNA-positive) cells were present in moderate numbers in the white pulp (PALS and lymphoid follicles). The red pulp was organised into prominent splenic cords (cords of Billroth) and venous sinuses with high numbers of erythrocytes, lymphocytes (CD3-positve T cells and fewer PAX5-positive B cells), dendritic cells and macrophages (both MHCII-positive). Occasional neutrophils and eosinophils were present in the red pulp. Low numbers of caspase 3-positive cells were detected in red pulp and lymphoid follicles (mainly lymphocytes). The presence of both proliferating and apoptotic lymphocytes in red pulp and follicles confirms lymphocyte turnover in the spleen and thereby active lymphatic tissue (Mel'nikova et al., 2006). IFN-γ-expressing cells were not detected in the spleen.

2.5.2.4.2 *Foetuses from infected dams.* The spleen of infected foetuses was similar to that of control animals; however, individual IFN-γ-expressing lymphocytes were detected. For the selected foetuses, only small tissue sections were examined due to inadequate amount of tissue in the block. One of the remaining foetuses was tested, but IFN- γ-expressing lymphocytes were not detected. There were no histological changes detected in the spleen of the infected foetuses (Fig. 2.13D) and *N. caninum* antigen was not identified.

2.5.2.5 Mesenteric lymph nodes

2.5.2.5.1 *Control foetuses.* The mesenteric lymph nodes appeared well developed (Fig. 2.14A) and exhibited a distinct superficial cortex with high numbers of densely packed B cells (Fig. 2.14B) and follicular dendritic cells (PAX5 and MHCII-positive, respectively) within prominent primary lymphoid follicles, which were surrounded by fewer CD3-positive T cells (Fig. 2.14C). The paracortex was composed of a less dense accumulation of T cells and macrophages (T cell compartment) with fewer B cells and occasional neutrophils. The medulla was less densely cellular with clearly defined medullary cords and sinuses containing a small population of lymphocytes (mainly B cells, fewer T cells), plasma cells, dendritic cells, neutrophils and macrophages. Occasional haematopoietic precursor cells were also present in the medulla. A small proportion of lymphocytes in the follicles and paracortex were found to be proliferating (PCNA-positive), a few proliferating cells were also detected in the medulla, while individual caspase 3-expressing cells were present and randomly scattered throughout the lymph node without any association to specific structures. IFN-γ-expressing cells were not detected.

2.5.2.5.2 Foetuses from infected dams. The lymph nodes of infected foetuses did not differ histologically from the control group (Fig. 2.14D). Low numbers of IFN-γ-expressing lymphocytes were present and randomly scattered mainly in the paracortex unlike in the controls (Fig. 2.14E). *Neospora caninum* antigen was not detected.

2.5.2.6 Bone marrow

2.5.2.6.1 *Control foetuses.* Compared to the bone marrow of foetuses in early gestation, the bone marrow of control foetuses in late gestation was highly cellular, with intense haematopoietic activity, represented by high numbers of erythroid and myeloid cells as well as megakaryocytes. Low numbers of adipocytes were present (Fig. 2.15A). A large population of PAX5-positive B cells was present, while CD3-positive T cells represented a minority. Moderate amounts of MHCII-positive cells (mature B cells and cells of the monocyte-macrophage lineage), were present. Few cells were found to proliferate (PCNA-positive). Apoptotic cells were not detected. IFN-γ-expressing cells and *N. caninum* tachyzoites were not detected.

2.5.2.6.1 *Foetuses from infected dams.* The bone marrow exhibited a similar morphology and activity, with all haematopoietic precursor cells present.

Histological changes were not detected (Fig. 2.15B), and IFN-γ-expressing cells were detected in low numbers compared to controls (Fig. 2.15C). *Neospora caninum* tachyzoites were not identified.

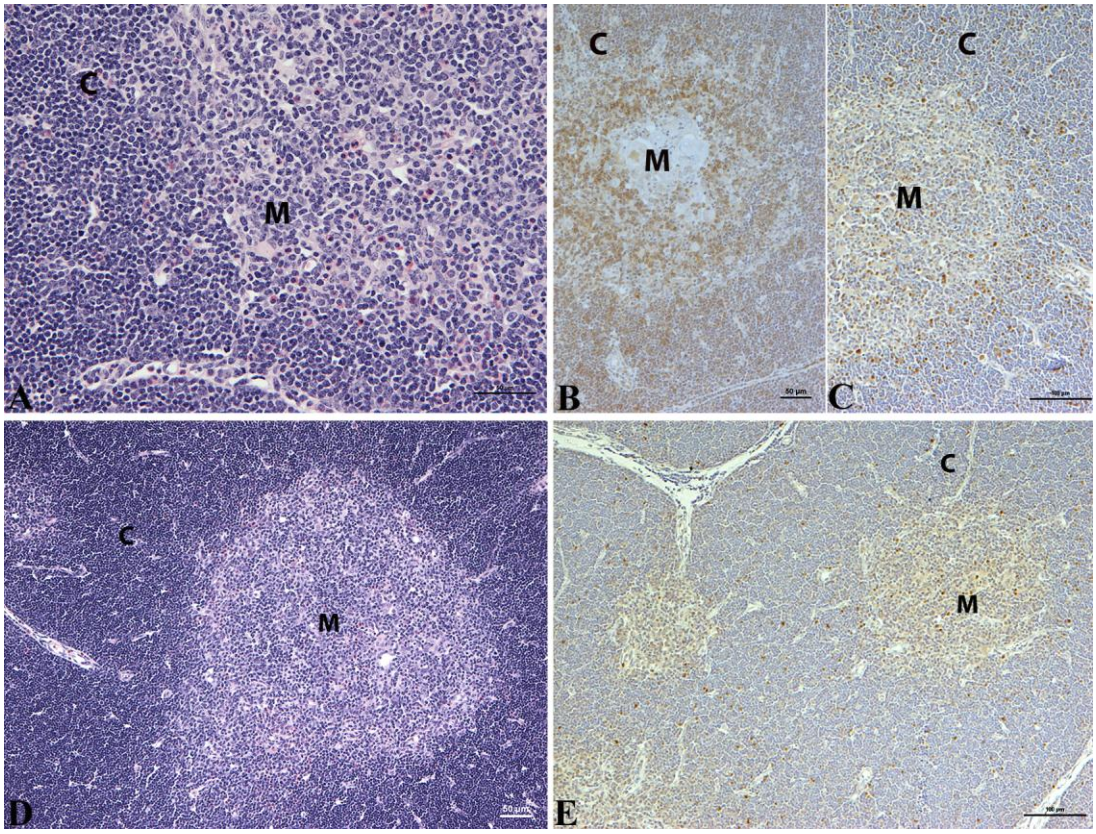

Figure 2.12. Thymus, control foetus (C-11; A-C) and foetus from dam infected with *N. caninum* at 210 days gestation (I-11; D and E). **A**. The cortex in highly cellular with densely packed lymphocytes (C), while the medulla (M) is less cell-dense and contains numerous eosinophils HE stain. Bar = 50µm. **B**. CD3-positive T cells are the predominant cell type in the cortex and medulla. ABC method, Papanicolaou's haematoxylin counterstain. Bar = 50µm. **C**. PCNA-positive proliferating cells are more frequent in the cortex than the medulla. PAP method, Papanicolaou's haematoxylin counterstain. Bar = 50µm. **D**. The cortex (C) is highly cellular as in the control foetus and medulla is less cell dense with high numbers of eosinophils. HE stain. Bar = 50µm. **E**. Low numbers of caspase 3-positive apoptotic cells are present in the cortex and even fewer in the medulla. PAP method, Papanicolaou's haematoxylin counterstain. Bar = 50µm.

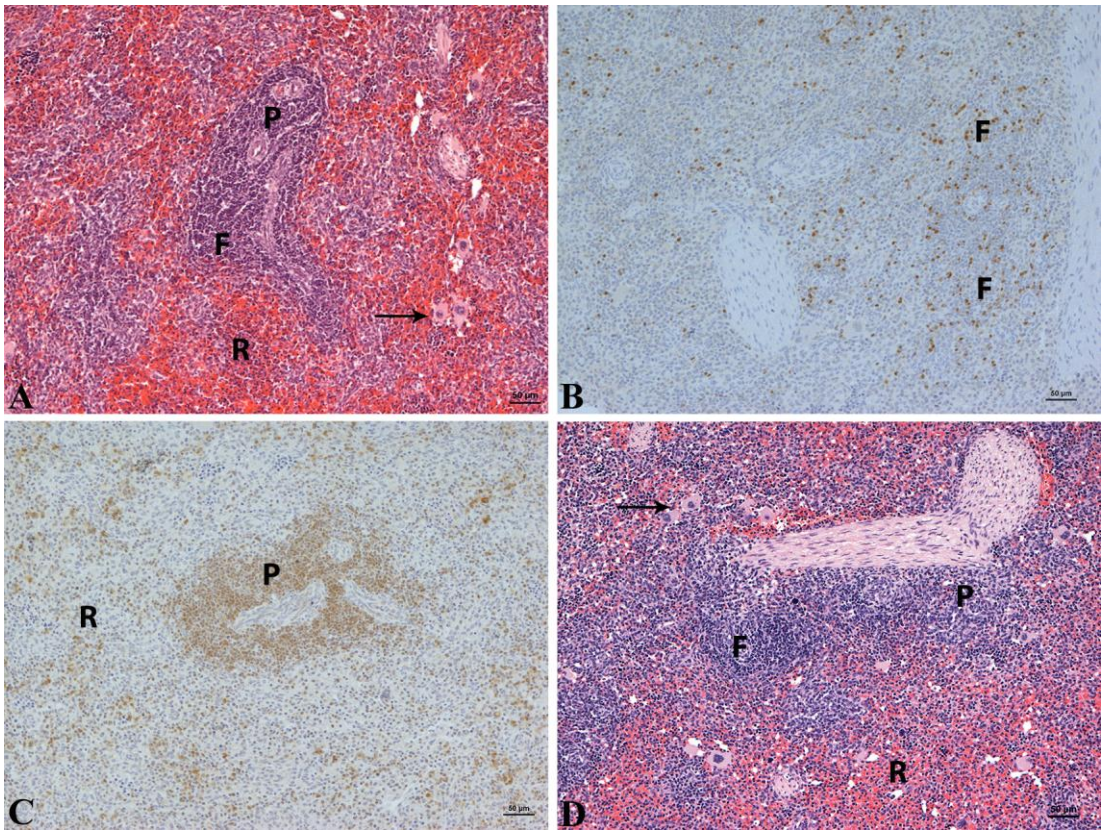

Figure 2.13. Spleen, control foetus (C-8; A-C) and foetus from dam infected with *N. caninum* at 210 days gestation (I-11; D). **A**. Red pulp (R) and white pulp [PALS (P) and follicles (F)] are well differentiated. High numbers of lymphocytes are present in the PALS (P) and follicles are not well demarcated (F). Haematopoietic cells are few (arrow). HE stain. Bar = 50µm. **B**. Moderate amounts of PAX5-positive B cells are forming lymphoid follicle-like structures (F). PAP method, Papanicolaou's haematoxylin counterstain. Bar = 50µm. **C**. The PALS (P) consists of high numbers of CD3-positive T cells and low numbers are scattered in the red pulp. ABC method, Papanicolaou's haematoxylin counterstain. Bar = 50µm. **D**. In the infected foetus, the spleen has a similar morphology as in control foetuses. White pulp (P+F) and red pulp (R) are well differentiated and follicle-like structures (F) are present. Haematopoiesis is low (arrow). HE stain. Bar = 50µm.

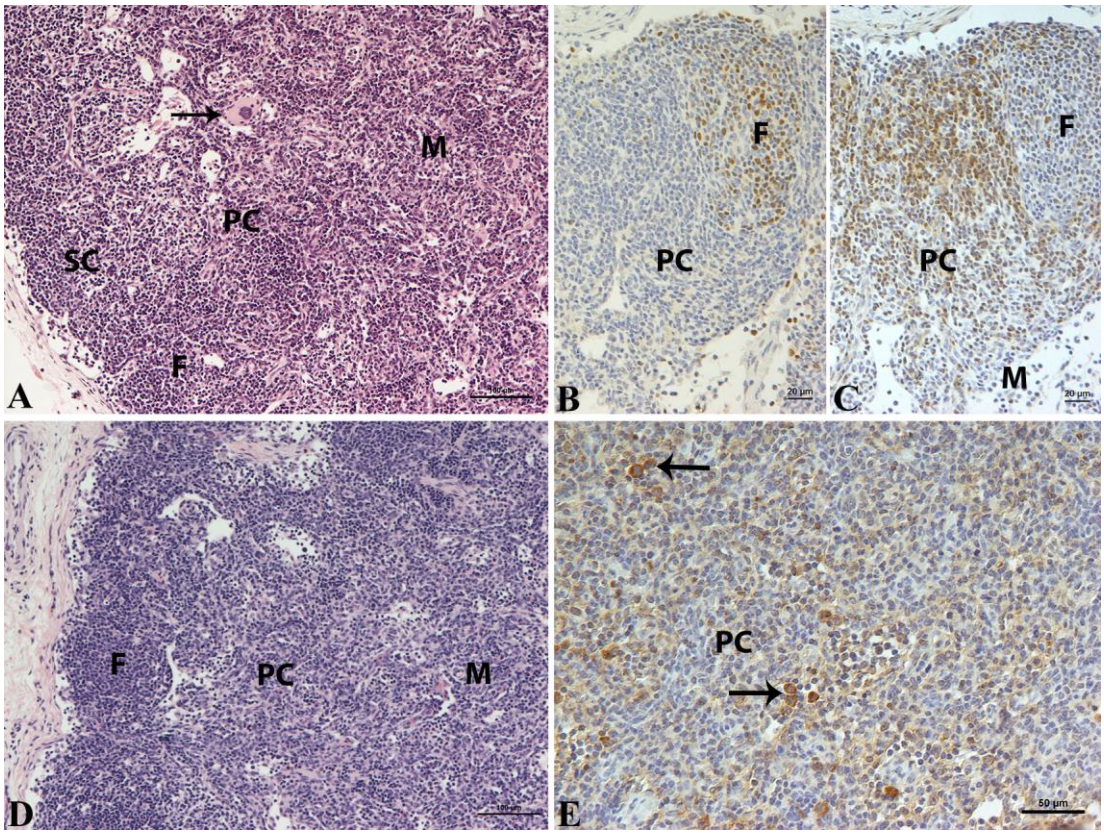

Figure 2.14. Mesenteric lymph nodes, control foetus (C-8; A-C) and foetus from dam infected with *N. caninum* at 210 days gestation (I-11; D and E). **A**. The lymph node has well distinct superficial cortex (SC) with primary lymphoid follicles (F), densely cellular paracortex (PC) and extension of cortical cells into the medulla (M). Mild haematopoiesis is also observed in the medulla (arrow). HE stain. Bar = 100µm. **B**. Lymphoid follicles (F) contain high numbers of PAX5-positive B cells with fewer present in the medulla. PAP method, Papanicolaou's haematoxylin counterstain. Bar = 20µm. **C**. The paracortex (PC) has numerous CD3-positive T cells, while low numbers are present within lymphoid follicles (F) and medulla (M). ABC method, Papanicolaou's haematoxylin counterstain. Bar = 20µm. **D**. In the infected foetus, the lymph node is structurally similar to that of the control foetus with highly developed superficial cortex (SC), paracortex (PC) and medulla (M). Primary lymphoid follicles are also prominent (F). HE stain. Bar = 100µm. **E**. Low numbers of IFN-γ-expressing cells are present mainly in the paracortex (arrows). PAP method, Papanicolaou's haematoxylin counterstain. Bar = 50µm.

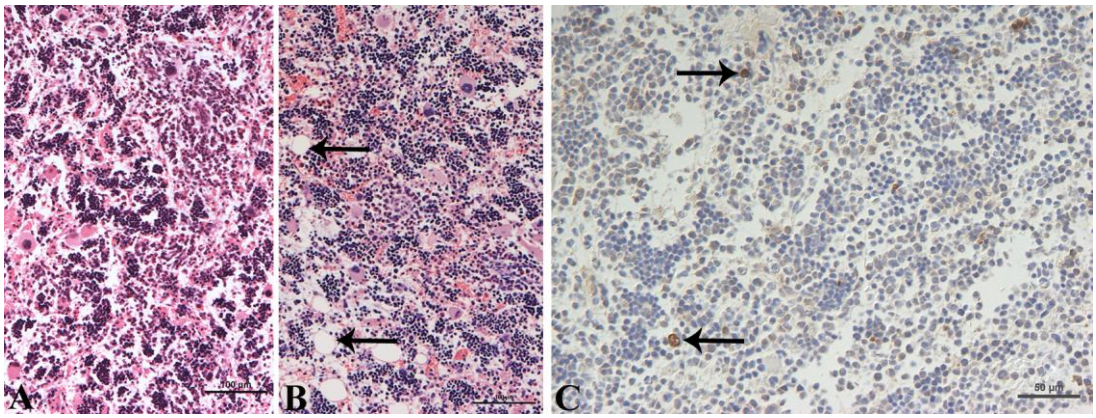

Figure 2.15. Bone marrow, control foetus (C-11; A) and foetus from dam infected with *N. caninum* at 210 days gestation (I-12; B and C). **A**. The bone marrow is of high cellularity with intense haematopoietic activity. All haematopoietic precursor cells are present. HE stain. Bar = 100µm. **B**. The bone marrow of the infected foetus is structurally similar to that of the control foetus and contains moderate amount of adipocytes (arrows). HE stain. Bar = 100µm. **C**. Low numbers of IFN-γ-expressing cells are present (arrows). PAP method, Papanicolaou's haematoxylin counterstain. Bar = 50µm.

2.5.3 Histological and immunohistological findings in a foetus and a new-born calf from naturally infected dams after recrudescence of *N. caninum* in mid to late gestation

A total of ten foetuses and two new-born calves were subjected to the initial histological examination. All ten foetuses exhibited mild to moderate mononuclear inflammatory infiltrates in various tissues. Parasite DNA had been detected by PCR in the brain (7/10) and heart (1/10) of these foetuses (Gibney, 2008). The foetus with the most severe inflammatory infiltrations in which *N. caninum* tachyzoites were demonstrated by immunohistology in a spinal nerve root with associated mononuclear inflammatory infiltrates, and in *Nervus femoralis*, *Musculus quadriceps femoris*, myocardium and liver, and in which parasite DNA had been detected in the heart and brain (Gibney, 2008), was selected for more detailed examination (R-5; 217 dg).

One of the new-born calves (R-10) was chosen for comparison. In the dam of this animal, a rise in the *N. caninum* antibody level had been detected at the end of gestation (week 40) and a pre-colostrum serum antibody level showed that the calf was serologically positive for *N. caninum* infection (persistently infected) (Gibney, 2008). The calf exhibited minor histological findings consistent with *N. caninum* infection in some tissues (mononuclear infiltration in brain, spinal cord, liver and heart), but the immunohistology for *N. caninum* antigen failed to detect parasite

antigen in the tissues. Parasite DNA was not detected by PCR in brain, heart or liver from this calf (Gibney, 2008). The second new-born calf did not exhibit histological changes in any of the tissues examined and *N. caninum* antigen was not detected by immunohistology.

2.5.3.1 Non-haemolymphatic tissues of naturally infected foetus

2.5.3.1.1 *Brain and spinal cord:* The grey matter of the brain exhibited perivascular inflammatory infiltrates that were dominated by CD3-positive T cells (Fig. 2.16A). Moderate MHCII expression was detected diffusely on glial cells with morphology consistent with activated microglial cells (Fig. 2.16B). B cells were not detected within the inflammatory infiltrates. PCNA-positive ependymal cells were observed, but caspase 3-positive cells were not identified. *Neospora caninum* antigen was not detected in the brain of the foetus.

The spinal cord exhibited the most severe lesions, and consisted of multifocal, mononuclear infiltrates mainly in the white matter (Fig. 2.17A), together with the presence of fewer leukocytes in grey matter. In addition, moderate mononuclear perivascular inflammatory infiltrates were observed in the white matter (Fig. 2.17A) along with severe leptomeningitis, while severe, non-suppurative radiculoneuritis, which was composed of similar inflammatory cells, was observed (Fig. 2.17B). CD3-positive T cells comprised the majority of the inflammatory cells and were detected in moderate numbers within the perivascular, spinal cord , meningeal (Fig. 2.17C) and spinal nerve root infiltrates. PAX5-positive B cells were also present within the spinal nerve root (Fig. 2.17D), but were less numerous than T cells. Low numbers of macrophages (calprotectin-positive) were detected within the inflammatory infiltrates of the spinal cord and leptomeninges (non-suppurative meningitis), while numerous strongly MHCII-positive cells were observed in the inflammatory infiltrates of the spinal cord parenchyma (microglia), meninges (macrophages, activated T lymphocytes and B cells (Holling et al., 2004) and spinal nerve roots (Fig. 2.17E). Low numbers of caspase 3-positive apoptotic cells were present within the inflammatory foci in the white matter and even fewer in the spinal nerve root. A small cluster of *N. caninum* tachyzoites was detected by immunohistology in a spinal nerve root within an intact glial cell in association with the inflammatory infiltrates (Fig. 2.17F).

The histological changes in the brains of the remaining nine naturally infected foetuses were limited to mild, focal and sometimes multifocal, mononuclear inflammatory infiltrates in the grey and white matter. In addition, perivascular cuffing was identified in the grey matter in two of nine foetuses. The spinal cord exhibited low numbers of scattered mononuclear inflammatory cells mainly in the grey matter, while mild perivascular mononuclear cell infiltrates were present in both grey matter and white matter in all foetuses. Parasite antigen was not detected in the CNS of these nine foetuses.

2.5.3.1.2 *Liver:* The liver of the selected foetus exhibited mild, multifocal, mononuclear portal infiltrates and CD3-positive T cells were the predominant inflammatory cell type within these infiltrates (Fig. 2.18A and 2.18B), while low numbers of PAX5-positive B cells were admixed with these. MHCII-positive cells were numerous, mainly in portal areas (mainly macrophages) and in individual cells between hepatic cords (Kupffer cells). Low haematopoietic activity was seen, represented by the presence of erythroid and myeloid precursors and fewer megakaryocytes. PCNA-positive proliferating cells were present in high numbers (hepatocytes and fewer haematopoietic precursor cells), while individual caspase 3-positive apoptotic hepatocytes were detected and randomly scattered in the parenchyma, indicating parenchymal turnover. Low numbers of IFN-γ-expressing cells were present within hepatic sinusoids and *N. caninum* antigen was not detected. Mild, multifocal, mononuclear portal infiltrates were identified in eight of the nine remaining foetuses and extramedullary haematopoiesis was present in all foetuses. Parasite antigen was not detected.

2.5.3.1.3 *Heart:* The myocardium of the selected foetus exhibited low numbers of mononuclear inflammatory cells (non-suppurative myocarditis) among which CD3-positive T cells predominated, with fewer PAX5-positive B cells. Some cells within these mononuclear infiltrates were MHCII-positive (macrophages, activated T lymphocytes and B cells). Myocardial endothelial cells were also MHCII-positive. Myocardial endothelial cell activation was less prominent in control foetuses. There was evidence of low-rate cardiomyocyte proliferation, indicated by the expression of PCNA in a few cardiomyocytes. Caspase 3 expression was not observed and *N. caninum* antigen was not detected. Mild non-suppurative myocarditis, represented by

low numbers of mononuclear cells was observed in eight of the nine remaining foetuses, but without the presence of *N. caninum* antigen.

2.5.3.1.4 *Lung*: The lung of the selected foetus exhibited low numbers of mononuclear cells in alveolar septa and BALT (Fig. 2.18C), represented by both CD3-positive T cells and PAX5-positive B cells. MHCII expression was seen in numerous cells, some disseminated in the BALT, others in cells attached to the alveolar walls (macrophages and type II alveolar epithelial cells), alveolar septa and the interstitium (mononuclear cells consistent with macrophages). Caspase 3-positive apoptotic cells were few and located mainly within alveolar spaces (desquamated type II alveolar epithelial cells and macrophages). IFN-γ-expressing cells, with morphology consistent with macrophages, were present in moderate numbers mainly in bronchiolar epithelium, alveolar septa and alveolar spaces (Fig. 2.18D). *N. caninum* antigen was not detected. In six of the nine remaining foetuses, the lungs exhibited low numbers of mononuclear cells mainly in the alveolar septa. Parasite antigen was not detected.

2.5.3.1.5 *Muscle:* The *Musculus quadriceps femoris* of the selected foetus exhibited mild multifocal mononuclear interstitial inflammatory infiltration (non-suppurative myositis, Fig. 2.18E), mainly by CD3-positive T cells (Fig. 2.18F) and fewer B cells (PAX5-positive) within the inflammatory infiltrates. MHCII expression was also observed in the infiltrating cells and diffusely in endothelial cells, indicating their activation. Proliferating cells or apoptotic cells were not observed. *N. caninum* antigen was not detected. Mild, multifocal non-suppurative myositis was observed in eight of the nine remaining foetuses and low numbers of *N. caninum* tachyzoites were detected by immunohistology in an intact myocyte immediately adjacent to the inflammatory infiltrate in one foetus.

2.5.3.1.6 *Other tissues:* The kidney of the selected foetus exhibited low numbers of CD3-positive T cells, which were multifocally distributed within the cortex with MHCII expression mainly in the areas of T cell infiltration. The adrenal gland of the selected foetus did not exhibit histological changes. Three of the nine remaining foetuses exhibited only occasional mononuclear inflammatory infiltrates in the interstitial areas of the kidneys, while the adrenal glands in two of the nine foetuses

had low numbers of the latter inflammatory cells in the medulla. The *Nervus femoralis* of the selected foetus contained a focal area of mononuclear infiltration within which low numbers of CD3-positive T cells, with mild expression of MHCII, were present. The pancreas and intestine of the latter foetus only exhibited individual CD3-positive T cells in the interstitium and lamina propria, respectively. The remaining tissues in the selected and remaining foetuses showed no histological abnormalities or *N. caninum* antigen.

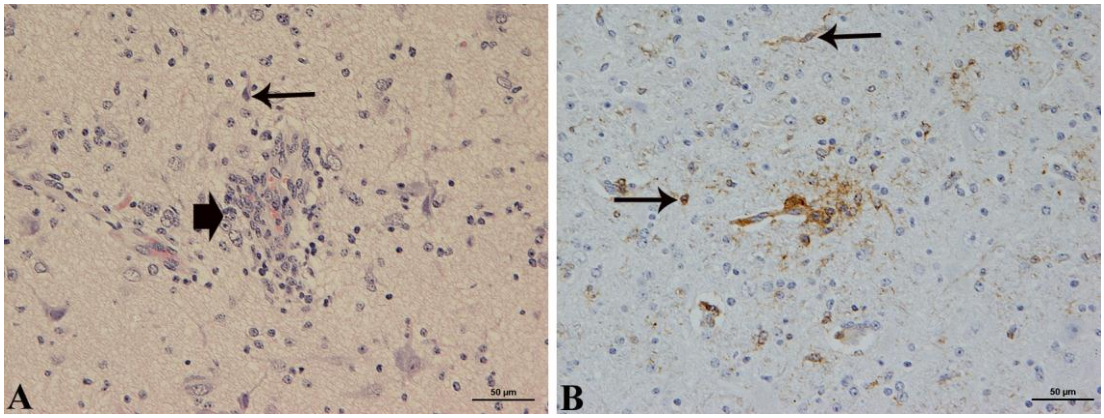

Figure 2.16. Brain, naturally infected foetus (R-5), from naturally infected dam after parasite recrudescence of *N. caninum* in mid to late gestation. **A**. Perivascular mononuclear infiltrates are present in the grey matter (large arrow) and activated microglial cells are seen in the surrounding neuropil (small arrow). HE stain. Bar = 50µm. **B**. The activated microglial cells are MHCII-positive (arrows). PAP method, Papanicolaou's haematoxylin counterstain. Bar = 50µm.

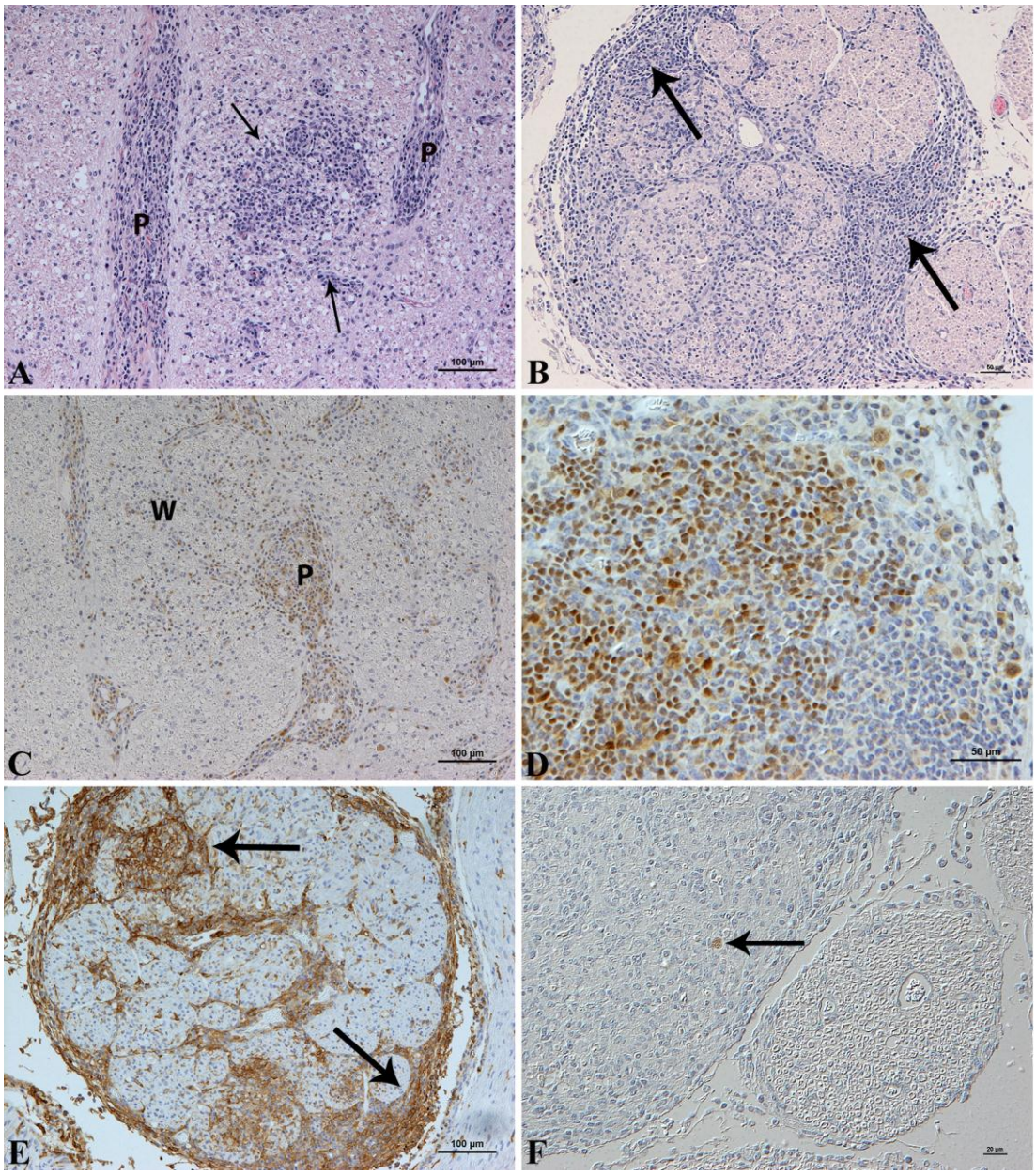

Figure 2.17. Spinal cord, naturally infected foetus (R-5), from naturally infected dam after parasite recrudescence of *N. caninum* in mid to late gestation. **A**. A focal area of mononuclear infiltrate (arrows) along with moderate perivascular infiltrates (P) is present in the ventral funiculi of the spinal cord white matter. HE stain. Bar = 100µm. **B**. Severe radiculoneuritis with high numbers of mononuclear inflammatory cells (arrows). HE stain. Bar = 50µm.**C**. The majority of the inflammatory cells in the white matter (W) and perivascular cuffing (P) are CD3-positive T cells. ABC method, Papanicolaou's haematoxylin counterstain. Bar = 100µm. **D**. Moderate amounts of PAX5-positive B cells are present within the inflammatory infiltrates of the spinal nerve root. PAP method, Papanicolaou's haematoxylin counterstain. Bar = 50µm. **E**. MHCII-positive cells, macrophages and activated lymphocytes are present in high numbers in the spinal nerve root. PAP method, Papanicolaou's haematoxylin counterstain. Bar = 100µm. **F**. A cluster of *N. caninum* tachyzoites is present within an intact glial cell in the spinal nerve root in association with the inflammatory infiltrates (arrow). PAP method, Papanicolaou's haematoxylin counterstain. Bar = 20µm.

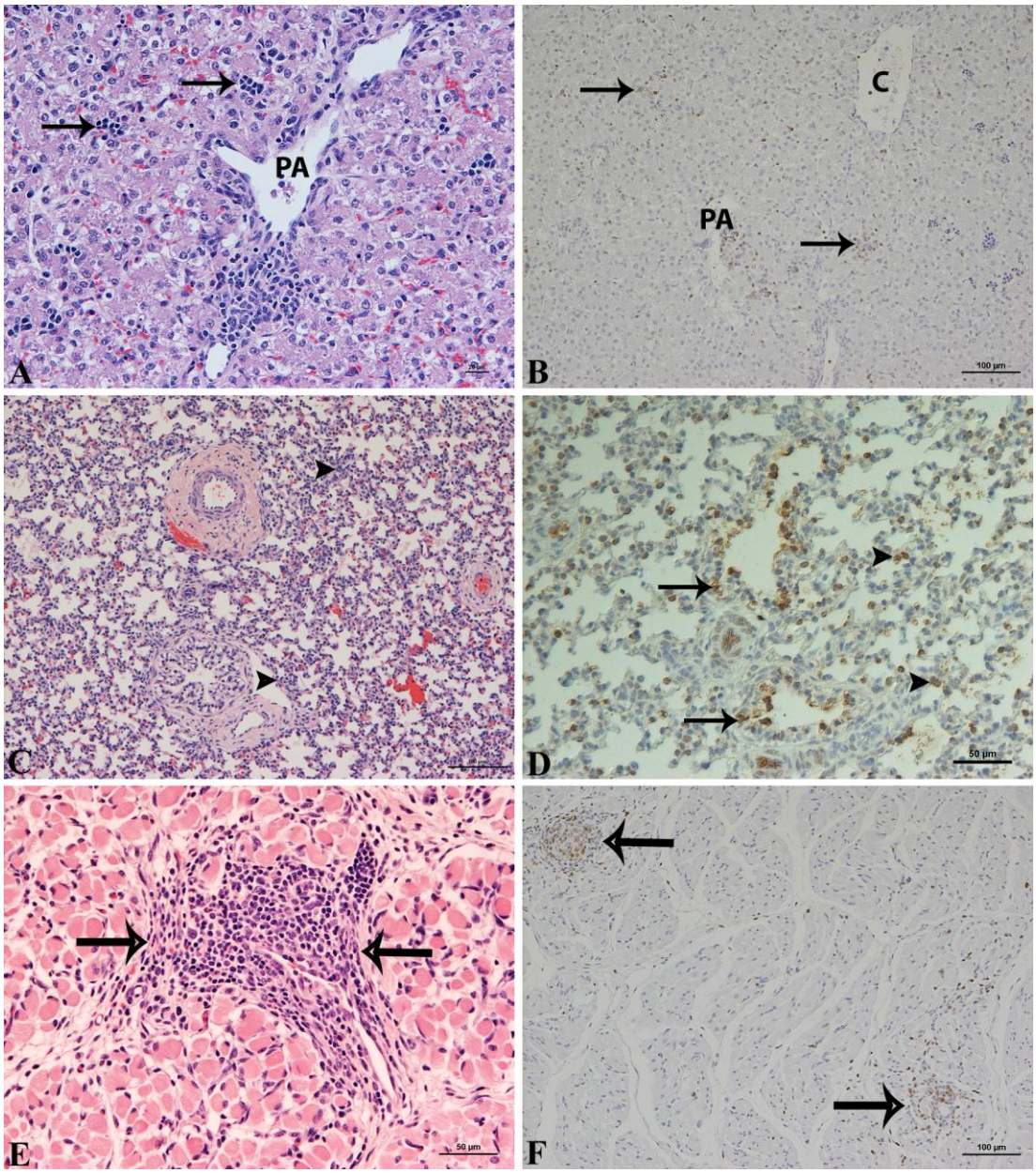

Figure 2.18. Liver and muscle, naturally infected foetus (R-5) from naturally infected dam after parasite recrudescence of *N. caninum* in mid to late gestation. **A**. Mild mononuclear portal infiltrates are present in the portal areas (PA). Haematopoietic activity is low (arrows). HE stain. Bar = 20µm. **B**. The majority of the infiltrating cells in the PA are CD3-positive and low numbers are present in hepatic cords (arrows). ABC method, Papanicolaou's haematoxylin counterstain. Bar = 100µm. **C**. The lung contains low numbers of mononuclear cells mainly in alveolar septa (arrowheads). HE stain. Bar = 100µm. **D**. Moderate numbers of IFN-γ-expressing cells are detected in the bronchiolar epithelium (arrows), alveolar septa and alveolar spaces (arrowheads). PAP method, Papanicolaou's haematoxylin counterstain. Bar = 50µm. **E**. Mild non-suppurative myositis with moderate amounts of mononuclear cells. HE stain. Bar = 50µm. **F**. The majority of the infiltrating cells in the *Musculus quadriceps femoris* are CD3-positive T cells (arrows). ABC method, Papanicolaou's haematoxylin counterstain. Bar = 100µm.

2.5.3.2 Non-haemolymphatic tissues of new-born calf

2.5.3.2.1 *Brain and spinal cord:* the naturally infected foetus differed from foetuses from experimentally infected dams in late gestation; histological changes in the CNS of the new-born calf were limited to mild mononuclear infiltration in the grey matter and white matter of the brain and spinal cord, respectively. These were mainly represented by CD3-positive T cell aggregates in the grey matter of the cerebral cortex (Fig. 2.19A) and mild T cell dominated perivascular infiltrates in the spinal cord white matter and meninges (Fig. 2.19B). Admixed within the inflammatory infiltrates in both brain and spinal cord were low numbers of macrophages and activated microglial cells (calprotectin and MHCII-positive, respectively). Caspase 3-positive apoptotic cells or *N. caninum* antigen was not detected in the CNS.

2.5.3.2.2 *Liver:* Mild portal mononuclear inflammatory infiltrates (Fig. 2.19C) dominated by CD3-positive T cells, with moderate amounts of macrophages (MHCII and calprotectin-positive) were present. B cells were not observed. Low numbers of caspase 3-positive apoptotic cells (mainly biliary epithelial cells and mononuclear cells within the inflammatory infiltrates) were present. A small proportion of hepatocytes were proliferating, as indicated by the low number of PCNA-positive hepatocytes. Haematopoietic precursor cells were present in low numbers and represented by myeloid and erythroid precursors. Moderate numbers of IFN-γ-expressing cells (macrophages and lymphocytes) were detected in the hepatic sinusoids, indicating their activation (Fig. 2.19D). *Neospora caninum* antigen was not detected.

2.5.3.2.3 *Heart:* Low numbers of CD3-positive T cells were present in the myocardium along with individual macrophages (calprotectin-positive). Low numbers of cardiomyocytes were found to be proliferating (PCNA-positive). *Neospora caninum* antigen was not detected.

2.5.3.2.4 *Lung:* Similar to the foetus, the lung exhibited a small number of mononuclear cells in the alveolar septa. These were mainly CD3-positive T cells and macrophages (calprotectin-positive), high numbers of MHCII-positive mononuclear cells along alveolar walls and desquamated within alveolar spaces (type II

pneumocytes). B cells were not detected. Low numbers of caspase 3-positive, apoptotic alveolar epithelial cells/alveolar macrophages were present. IFN-γ-expressing cells were present in low numbers and detected only within blood vessels. *Neospora caninum* antigen was not detected.

2.5.3.2.5 *Muscle:* The *Musculus quadriceps femoris* did not exhibit any histological changes in the new-born calf and *N. caninum* antigen was not detected.

2.5.3.2.6 *Other tissues:* The intestine contained high numbers of mononuclear cells within the mucosa along with low numbers of polymorphonuclear cells with large eosinophil granules (eosinophils). CD3-positive T cells represented the majority of cells within the mucosa and low numbers of PAX5-positive B cells and fewer macrophages (calprotectin-positive) were admixed with the infiltrate. The gut associated lymphoid tissues (GALT) were composed of numerous B cells and a large proportion of these were PCNA-positive proliferating cells. Also, moderate amounts of caspase 3-positive apoptotic cells (mainly B cells) were present in the GALT, indicating ongoing lymphocyte turnover. The kidney exhibited minimal numbers of CD3-positiveT cells, which were randomly scattered in the interstitium along with low numbers of macrophages (calprotectin-positive). The pancreas exhibited individual CD3-positive T cells randomly scattered within the lobules. No other abnormalities or *N. caninum* antigen were observed in the tissues of the calf.

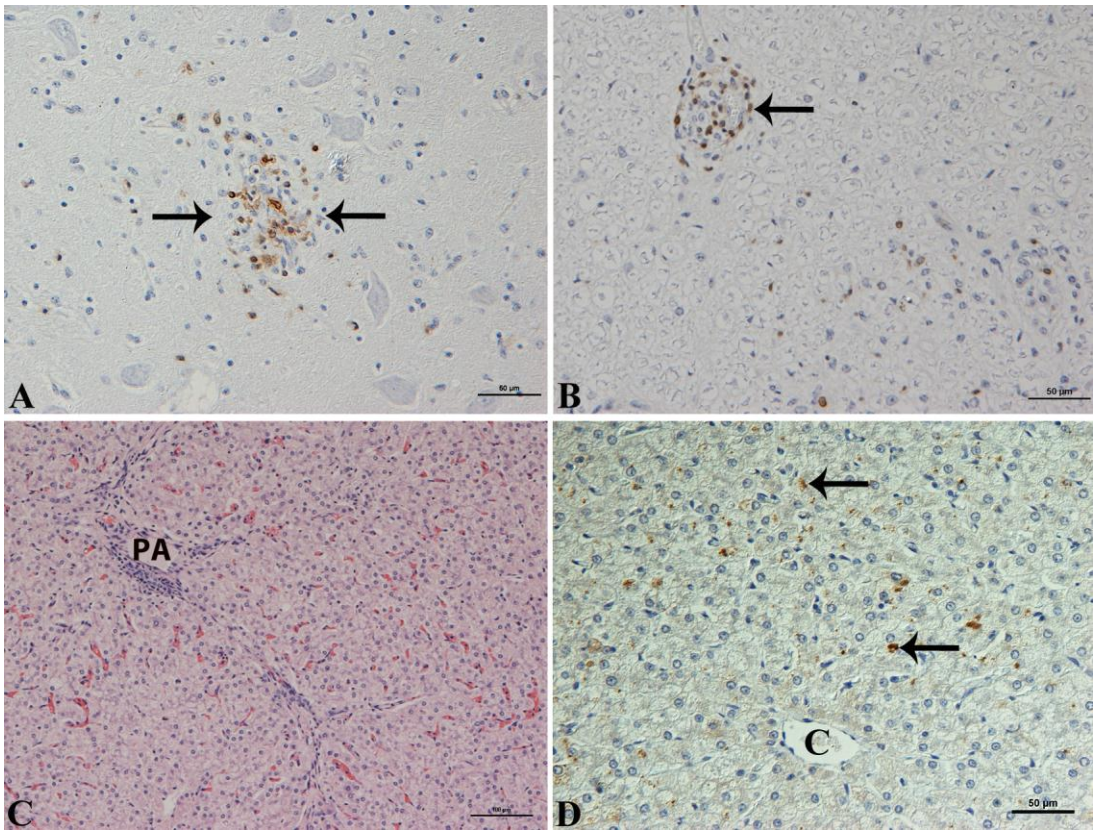

Figure 2.19. Brain, spinal cord, liver and muscle, new-born calf (R-10), from naturally infected dam after parasite recrudescence of *N. caninum* in late gestation. **A**. A focal aggregate of CD3-positive T cells is present in the grey matter of the brain (arrows). ABC method, Papanicolaou's haematoxylin counterstain. Bar = 50µm. **B**. Mild perivascular cuffing (arrow) with low numbers of CD3-positive T cells and occasional positive cells are present in the spinal cord white matter. ABC method, Papanicolaou's haematoxylin counterstain. Bar = 50µm. **C**. Occasional mononuclear portal infiltrates (PA) are present in the liver. HE stain. Bar = 100µm. **D**. Moderate numbers of IFN-γ-expressing mononuclear cells (mainly macrophages and fewer lymphocytes) are present in hepatic sinusoids (arrows; C – central vein). PAP method, Papanicolaou's haematoxylin counterstain. Bar = 50µm.

2.5.3.3 Haemolymphatic tissues

Haemolymphatic tissues (thymus, spleen, lymph node and bone marrow) of the foetus and new-born calf were studied histologically and immunohistologically to evaluate any pathological effects due to *N. caninum* after parasite recrudescence in the dams.

2.5.3.4 Thymus

2.5.3.4.1 *Naturally infected foetus.* The thymus was morphologically similar to that of foetuses from dams experimentally infected in late gestation (Fig. 2.20A). The cortex was highly cellular and contained high numbers of compact small lymphocytes (mainly CD3-positive T cells), while fewer larger T cells with more

cytoplasm were present in the medulla (Fig. 2.20B). High numbers of macrophages and dendritic cells (MHCII-positive), reticular medullary epithelial cells, Hassall's corpuscles and a large population of polymorphonuclear cells, identified as eosinophils by the Lendrum's Carbol Chromotrope stain, were also present in the medulla. PAX5-positive B cells were detected in low numbers within the medulla. High numbers of PCNA-positive proliferating cells (lymphocytes) were detected in the cortex with fewer in the medulla, while moderate amount of caspase 3-positive apoptotic cells were detected in both cortex and medulla, consistent with high cell turnover. IFN-γ-expressing cells, however, were not detected. The thymus of the remaining nine foetuses was morphologically similar to that of the selected foetus and *N. caninum* antigen was not detected in any foetus.

2.5.3.4.2 *New-born calf.* The thymus was structurally similar to that of the foetuses; however, slightly lower numbers of eosinophils were present in the medulla (Fig. 2.20C). The thymus of the other new-born calf was structurally similar to the selected calf. PCNA-positive proliferating cells (Fig. 2.20D) were numerous with low numbers of caspase 3-positive apoptotic cells, indicating cell turnover. No histological alterations were observed and *N. caninum* antigen was not detected in both animals.

2.5.3.5 Spleen

2.5.3.5.1 *Naturally infected foetus.* The spleen appeared fully developed and structurally similar to that of foetuses from dams experimentally infected in late gestation. It was composed of a well-developed red and white pulp, the latter consisting of the PALS and follicle-like structures (Fig. 2.21A). High numbers of lymphocytes were present within the PALS and were mainly CD3-positive T cells (Fig. 2.21B) with scattered B cells (PAX5-positive, Fig. 2.21C). Follicles contained numerous PAX5-positive B cells and strongly MHCII-positive cells were observed in the white pulp (dendritic cells, follicular dendritic cell, splenic macrophages and B cells). The red pulp was comprised of a smaller population of T and B cells, numerous erythrocytes, macrophages (calprotectin-positive) and splenic dendritic cells (MHCII-positive). Myeloid and erythroid cells as well megakaryocytes were present in moderate numbers (moderate haematopoiesis). PCNA-positive proliferating cells were present in high numbers mainly within lymphoid follicles,

PALS (predominantly lymphocytes) and fewer randomly scattered mononuclear cells in the red pulp. Low numbers of caspase 3-positive apoptotic cells were present predominantly in the PALS and follicles, confirming T and B cell turnover. IFN-γ-expressing cells were detected in low numbers, indicating that splenic lymphocytes were activated. The spleen appeared equally highly developed in all nine remaining foetuses. However, primary lymphoid follicles and PALS were poorly discernible in the white pulp of three of the nine foetuses that were between 21 and 24 weeks of gestation age. *Neospora caninum* antigen was not detected in any foetus.

2.5.3.5.2 *New-born calf.* The spleen of the calf was structurally similar to that of the foetuses, however, prominent lymphoid follicles with conspicuous germinal centres (secondary follicles), were present in the white pulp (Fig. 2.21D). Different from the foetuses, the calf's red pulp exhibited low numbers of neutrophils in the red pulp. The spleen of the other new-born calf was morphologically similar. Histological changes or *N. caninum* antigen were not observed in both calves.

2.5.3.6 Mesenteric lymph node

2.5.3.6.1 *Naturally infected foetus.* The lymph node was morphologically similar to that of foetuses from dams experimentally infected in late gestation. It was highly developed and exhibited a distinct cortex and medulla (Fig. 2.22A). The superficial cortex contained prominent primary lymphoid follicles with high numbers of PAX5-positive B cells (Fig. 2.22B) and occasional CD3-positive T cells. T cells also formed a concentric rim around the follicles, but were more abundant in the paracortex (T cell compartment, Fig. 2.22C). The superficial and paracortex contained high numbers of MHCII-positive cells (follicular dendritic cells, dendritic cells, B cells and macrophages, Fig. 2.22D) and fewer were present in the medulla. The medulla consisted of a smaller population of T cells (Fig. 2.22C), high numbers of B cells (Fig. 2.22B) and plasma cells within a network of reticular cells. Moderate numbers of PCNA-positive proliferating cells (mainly lymphocytes) were present predominantly in the lymphoid follicles with fewer in the paracortex. Caspase 3-positive apoptotic cells were present in low numbers mainly in the lymphoid follicles. IFN-γ-expressing cells were detected in minimal numbers in paracortex. The lymph nodes of seven of the nine remaining foetuses were available for histological assessment. All lymph nodes appeared well developed and exhibited

distinct superficial cortex, paracortex and medulla. In the older foetuses (31 and 34 weeks' gestation, the cortex was comprised of well-developed primary lymphoid follicles, whereas in the younger foetuses (21 to 27 weeks' gestation age), only immature primary lymphoid follicles, represented by small aggregates of B cells were observed. Parasite antigen was not detected in any foetus.

2.5.3.6.2 *New-born calf.* The lymph node of the calf was morphologically similar to that of the foetuses (Fig. 2.22E). However, it exhibited higher numbers of caspase 3-positive apoptotic lymphocytes in the paracortex and medulla (corticomedullary junction) with low numbers in the superficial cortex and lymphoid follicles (Fig. 2.22F). The lymph node in the other new-born calf was similar morphological and parasite antigen was also not observed in both calves.

2.5.3.7 Bone marrow

2.5.3.7.1 *Naturally infected foetus.* The bone marrow was structurally similar to that of foetuses from dams experimentally infected in late gestation. It was of high cellularity with all precursor cell lineages present, together with low numbers of adipocytes. PAX5-positive B cells were the predominant cell type detected by immunohistology, while CD3-positive T cells were present in moderate amounts. Marked MHCII expression was observed (cells of the monocyte-macrophage lineage and B cells). PCNA-positive proliferating cells (haematopoietic precursor cells and lymphocytes) were present in moderate amounts. Occasional caspase 3-positive cells were detected and individual IFN-γ-expressing cells were also present, indicating their activation. *Neospora caninum* antigen was not detected. In 3 of the 9 remaining foetuses the bone marrow was available for histological examination. It was generally of high cellularity with all haematopoietic cell lines present. High numbers of adipocytes were also observed. Parasite antigen was not detected. The bone marrow of both the selected new-calf and the other new-born calf was not available for histological examination.

Table 2.7. Summary of histological and immunohistological findings in foetuses/calf from dams experimentally infected in early and late gestation and from naturally infected dams

Tissues	Early gestation	Late gestation	Natural infection
Brain	Apoptosis + Tachyzoites ++ T cells + MHCII ++ IFN-γ –	Necrosis + Tachyzoites + T cells + MHCII + IFN-γ –	T cells + PVC + Tachyzoites – MHCII + IFN-γ –
Spinal cord	Necrosis + Apoptosis + Tachyzoites ++ T cells + MHCII ++ IFN-γ –	Apoptosis + Tachyzoites + T cells ++ MHCII ++ IFN-γ –	T and B cells ++ PVC ++ Tachyzoites + MHCII +++ IFN-γ –
Liver	Necrosis +++ Apoptosis +++ Tachyzoites +++ MHCII + T cells ++ IFN-γ –	Necrosis + Tachyzoites – T cells + MHCII ++ IFN-γ +	T cells + Tachyzoites – MHCII ++ IFN-γ +
Cardiac muscle	Tachyzoites +++ T cells + MHCII + IFN-γ –	T cells + Tachyzoites – MHCII + IFN-γ +	T cells + Tachyzoites – MHCII + IFN-γ –
Lung	Apoptosis + Tachyzoites + T cells ++ MHCII + IFN-γ –	T cells + Tachyzoites + MHCII ++ IFN-γ ++	T and B cells + Tachyzoites – MHCII ++ IFN-γ ++
Musculus quadriceps femoris	Apoptosis + T cells + Tachyzoites – MHCII + IFN-γ –	T and B cells + Tachyzoites – MHCII + IFN-γ +	T cells + Tachyzoites – MHCII + IFN-γ –
Adrenal glands	NHAIR Tachyzoites –	Eosinophils + Tachyzoites –	NHAIR Tachyzoites –
Nervus femoralis	NHAIR Tachyzoites –	NHAIR Tachyzoites –	T cells + Tachyzoites –
Intestine (jejunum)	NHAIR Tachyzoites –	NHAIR Tachyzoites –	T cells + Tachyzoites –
Kidney	T cells + Tachyzoites +	NHAIR Tachyzoites –	T cells + Tachyzoites –
Haemolymphatic tissues			
Thymus	Apoptosis +++ Tachyzoites + IFN-γ –	NHAIR Tachyzoites – IFN-γ –	NHAIR Tachyzoites – IFN-γ –
Spleen	Apoptosis ++ Tachyzoites + IFN-γ –	Tachyzoites – IFN-γ +	Tachyzoites – IFN-γ +
Mesenteric lymph node	NS	IFN-γ + Tachyzoites –	Tachyzoites – IFN-γ +
Femoral bone marrow	Apoptosis + Tachyzoites + IFN-γ –	Tachyzoites – IFN-γ +	Tachyzoites – IFN-γ +

+ - mild; ++ - moderate; +++ - severe; '–' – not detected; NHAIR – no histological abnormality is recognised; NS – not sampled; PVC – perivascular cuffing

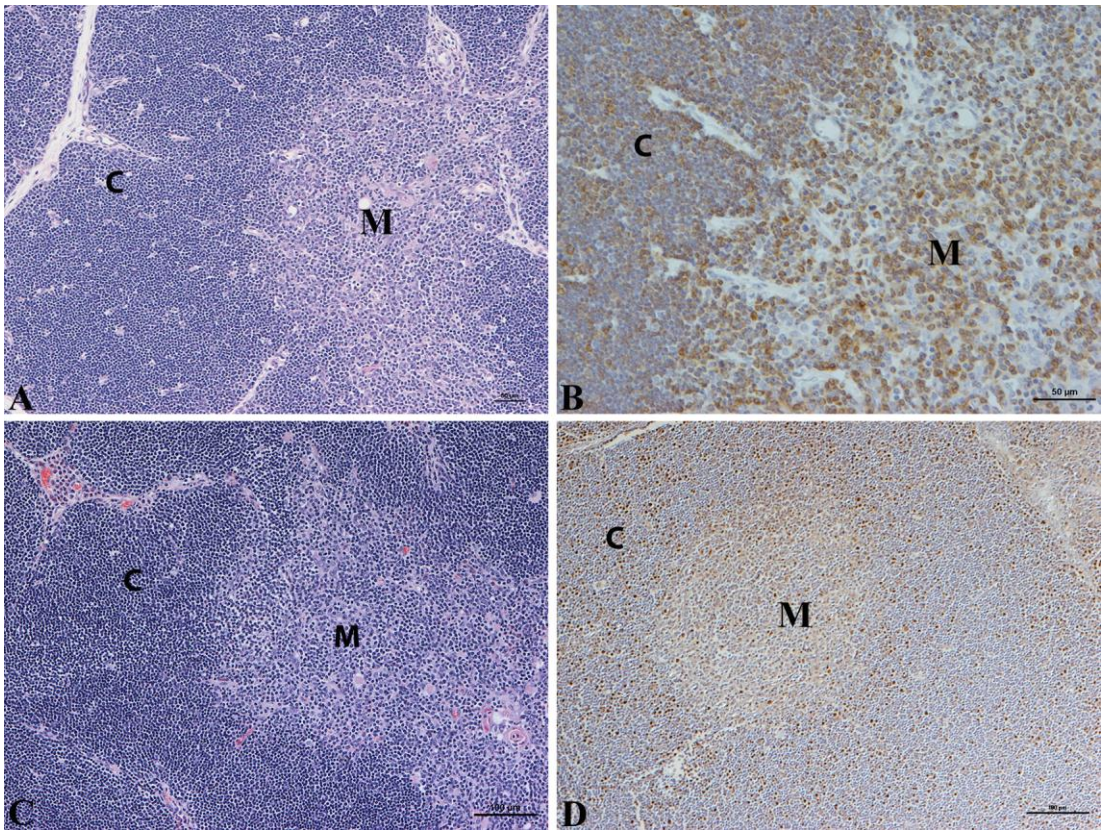

Figure 2.20. Thymus, naturally infected foetus (R-5; A and B) and new-born calf (R-10; C and D) from naturally infected dams after parasite recrudescence of *N. caninum* in mid to late gestation. **A**. The cortex (C) and medulla (M) are well differentiated. High numbers of lymphocytes are present in the cortex, with fewer in the medulla and low numbers of eosinophils (arrows). HE stain. Bar = 50µm. **B**. The majority of cells in the cortex are CD3 positive, while lower numbers are present in the medulla. ABC method, Papanicolaou's haematoxylin counterstain. Bar = 50µm. **C**. Cortex and medulla are well differentiated . Cortex has high numbers of lymphocytes and fewer are present in the medulla. HE stain. Bar = 100µm. **D**. PCNA-positive proliferating cells are present in high numbers in both cortex and medulla. PAP method, Papanicolaou's haematoxylin counterstain. Bar = 100µm.

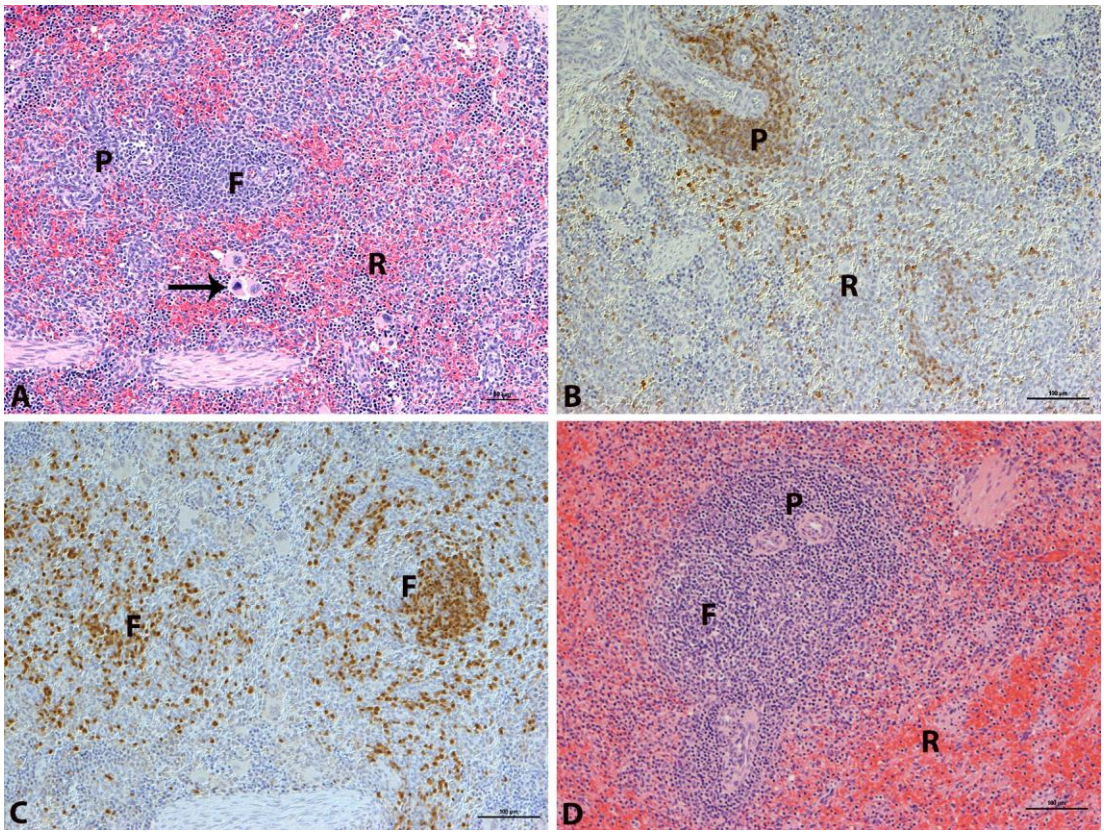

Figure 2.21. Spleen, naturally infected foetus (R-5; A-C), and new-born calf (R-10; D) from naturally infected dams after parasite recrudescence of *N. caninum* in mid to late gestation. **A**. The spleen is highly developed with well differentiated red (R) and white pulp (P+F). Low numbers of haematopoietic cells are present in the red pulp (arrow). HE stain. Bar = 50µm. **B**. High numbers of CD3-positive T cells are present in the PALS and few are scattered in the red pulp (R). ABC method, Papanicolaou's haematoxylin counterstain. Bar = 100µm. **C**. Numerous PAX5-positive B cells are present within the primary lymphoid follicle-like structures (F) and fewer positive cells are present in red pulp (R). PAP method, Papanicolaou's haematoxylin counterstain. Bar = 100µm. **D**. The spleen of the calf is highly developed with well differentiated red and (R) white pulp (P+F). HE stain. Bar = 100µm.

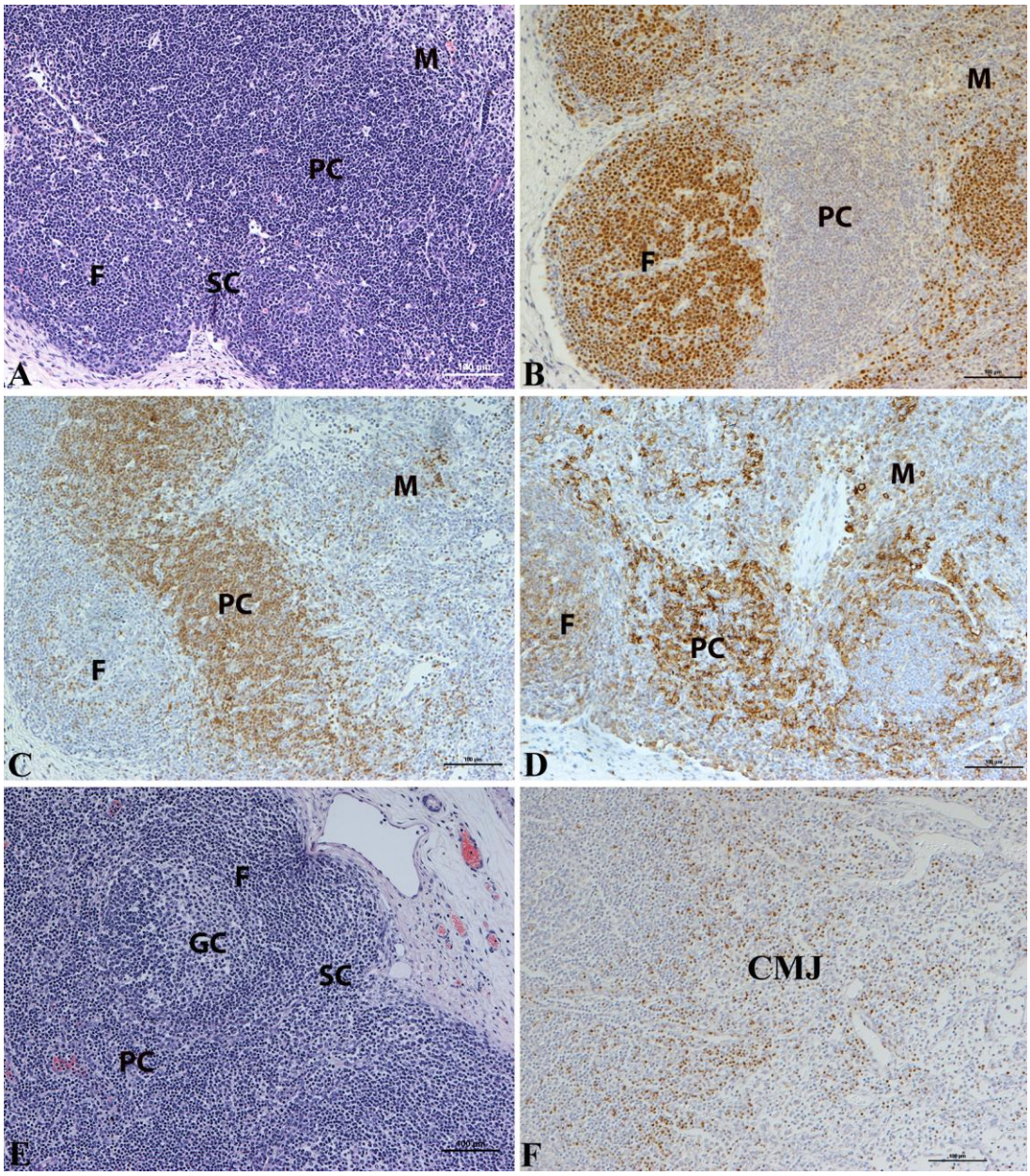

Figure 2.22. Mesenteric lymph node, naturally infected foetus (R-5; A-D) and new-born calf (R-10; E and F) from naturally infected dams after parasite recrudescence of *N. caninum* in mid to late gestation. **A**. The lymph node is highly developed and contains distinct superficial cortex and paracortex (SC and PC) with prominent lymphoid follicles (F). The medulla (M) is less cell-dense. HE stain. Bar = 100µm. **B**. Numerous PAX5-positive B cells are present in primary lymphoid follicles and fewer are observed in medulla. PAP method, Papanicolaou's haematoxylin counterstain. Bar = 100µm. **C**. CD3-positive T cells are present in high numbers in the paracortex with fewer in the medulla. Occasional positive cells are also observed in lymphoid follicles. ABC method, Papanicolaou's haematoxylin counterstain. Bar = 100µm. **D**. Numerous MHCII-expressing cells are present in the paracortex and follicles with fewer in the medulla. PAP method, Papanicolaou's haematoxylin counterstain. Bar = 100µm. **E**. The lymph node of the new-born calf is highly developed as in the foetus and consists of prominent primary lymphoid follicles (F) with germinal centres (GC). HE stain. Bar = 100µm. **F**. Numerous caspase 3-positive cells are present in the cortico-medullary junction (CMJ). PAP method, Papanicolaou's haematoxylin counterstain.

2.6 DISCUSSION

The present study examined the pathological effects of *N. caninum* in bovine foetuses in early and late gestation (70 and 210 days respectively) and in foetuses/calves after parasite recrudescence had occurred in naturally infected dams in mid to late gestation. It represents an extension of an earlier study in which parasite distribution and lesions, following infection of cattle with *N. caninum* tachyzoites in early and late gestation or after parasite recrudescence in chronically infected cattle, were described (Gibney, 2008). Evidence of foetal death in dams that had been infected in early gestation was shown by Gibney (2008) but the developmental and structural changes in the same foetuses are described and compared in this present study.

Previous experimental studies have shown that *N. caninum* infection in early gestation results in foetal death, while foetuses survive when the infection occurs later in gestation (Barr et al., 1994; Williams et al., 2000; Macaldowie et al., 2004; Gibney et al., 2008; Rosbottom et al., 2008). It was suggested that the reason for foetal death was the direct damage to the placenta and/or foetus by unhindered parasite multiplication, occurring due to a lack of immunocompetence in foetuses during early gestation (Gibney et al., 2008; Almería et al., 2010). In our study, foetal infection occurred regardless of the stage of gestation when the infection was established, and the resulting lesions were similar; however, the lesions in early gestation foetuses were more widely distributed, more extensive and more severe compared to those seen in foetuses in late gestation. In the placenta, they were represented by multifocal necrosis of both foetal and maternal epithelial cells (Gibney et al., 2008). Maley et al. (2006) also observed extensive damage with high numbers of parasites in the placenta of an experimentally infected dam (infected at 70 dg) with a dead foetus at 98 dg compared to others with live foetuses. The severity of the placental lesions thus appears to determine foetal survival or death, since with more extensive damage foetal life cannot be sustained. In another study, the lesions comprised extensive multifocal epithelial cell necrosis in all the placentomes examined, together with cell loss in a range of organs, including myocytes in skeletal muscle, renal tubular epithelial cells, pulmonary epithelial cells and lymphocytes in the thymus, spleen and bone marrow in animals where foetal death had occurred after infection at 70 dg (Gibney et al., 2008). These findings

prompted the present study that aimed to shed more light on the processes leading to foetal death, i.e. lack of foetal immune response or placental insufficiency from maternal immune response.

Immunocompetence in the bovine foetus is thought to develop from around 120 dg (Swift and Kennedy, 1972). While foetal lymphocytes are capable of mitogenic responses earlier during gestation, as early as 78 dg, they are unable to recognise and respond to pathogens (Osburn et al., 1982). Experimentally infected foetuses have been shown to mount a significant cellular immune response to *N. caninum* from approximately 120 dg (Almeria et al., 2003).

In the experiment that generated the material for the present study, all infected foetuses in early gestation died within 3 weeks of infection of the dams. The maternal immune response in the placenta can be harmful to the foetus although studies have shown that a Th1 immune response, which is linked to the production of IFN-γ, could protect against *N. caninum* abortion (López-Gatius et al., 2007; Williams et al., 2007b). However, a strong IFN-γ response was detected in a foetus that died 6 weeks post infection after experimental infection of the dam at 110 dg (Almeria et al., 2010). The authors believed that this high IFN-γ level occurred in response to high parasitaemia and was sufficient to cause placental damage and/or foetal pathological changes severe enough to kill the foetus. It was suggested that IFN-γ production and the direct damage to the placenta and foetus by multiplying parasites were likely complementary factors in foetal death in early gestation (Maley et al., 2006; Rosbottom et al., 2008).

In the present study, we aimed to further investigate the foetal immune response to *N. caninum*, in particular to characterise the inflammatory response elicited by the infection. In order to assess this, the composition of the haemolymphatic tissues was studied in control foetuses and, by comparison with the tissues in the infected group, served to detect any changes in response to the parasite infection.

2.6.1 The haemolymphatic tissues of control foetuses in early and late gestation

The haemolymphatic tissues of control foetuses in early gestation (approximately 13 weeks) were structurally similar and exhibited morphological features consistent with those described in previous studies on the development of bovine lymphoid tissues and the foetal immune response (Schultz, 1973; Schultz et al., 1973; Ishino et

al., 1991). The haemolymphatic tissues comprised mainly T cells and showed a low degree of lymphocyte turnover, as indicated by the detection of only few PCNA-positive cells and scarce apoptotic cells. Also, there was no immunohistological evidence of IFN-γ expression by lymphocytes, all findings are consistent with low immune activity at this stage of development (Linton and Dorshkind, 2004).

The composition of the haemolymphatic tissues of foetuses in late gestation differed from early gestation. The thymus appeared fully developed with numerous lymphocytes and prominent primary lymphoid follicles were seen in spleen and lymph nodes with high numbers of B cells, all of which are indications of a mature immune system. The control foetuses in late gestation (approximately 230 dg) also exhibited low numbers of apoptotic, cleaved caspase 3-positive lymphocytes, which were found randomly distributed in haemolymphatic tissues, and in similar amounts. Along with the few apoptotic lymphocytes, high numbers of PCNA-positive lymphocytes were present which is consistent with a relatively high cell turnover in late gestation compared to foetuses in early gestation.

2.6.2 The effect of N. caninum infection on haemolymphatic tissues of foetuses in early gestation

In early gestation, around day 92 of gestation, the haemolymphatic tissues of infected foetuses exhibited significantly higher numbers of apoptotic, cleaved caspase 3-expressing cells than control foetuses. Since there was no evidence of a direct association between the parasite infection and lymphocyte death, it might be the result of stress leading up to foetal death. All foetuses died within 24 h prior to euthanasia of the dams and this could account for the high numbers of lymphocyte apoptosis observed in the haemolymphatic tissues. A recent study showed that corticosterone, released from the adrenal gland into the plasma of human foetuses, caused apoptotic cell death of lymphocytes in haemolymphatic tissues as well as the delayed and decreased output of pre-T-cells from bone marrow and thymus (Yan, 2012). Extensive apoptosis of lymphocytes was also detected in the thymus of a rat 12 h after dexamethasone (synthetic glucocorticoid) treatment (Elmore, 2007), while accelerated apoptosis of thymocytes was also observed in Bcl-2 $^{-/-}$ knockout mice as early as 4 h following dexamethasone treatment, thus demonstrating its apoptotic effect on lymphocytes. Likewise, high and low doses of dexamethasone (20 mg/kg and 8 mg/kg, respectively) also induced atrophy and a dose-dependent lymphocyte

apoptosis in the thymus of BALB/c mice following intraperitoneal inoculation (Niknafs et al., 1998). The mechanism of glucocorticoid-induced apoptosis is poorly understood, but there is evidence supporting a receptor-mediated regulation of gene transactivation; however, the specific gene that is involved is not known (Distelhorst, 2002). The process involves an initial stage where the glucocorticoid receptors mediate changes in the gene expression, which affects the influence of proapoptotic factors and finally leads to activation of the executioner caspase. It is not certain if cytochrome c is released during glucocorticoid-induced apoptosis (Veis et al., 1993). Furthermore, studies carried out on bovine foetuses showed that adrenal 17α-hydroxylase cytochrome P-450 (P-$450_{17\alpha}$) mRNA expression, which correlates with foetal episodic cortisol production, is high at 50dg and reaches a maximum at 60-70dg, then declines and becomes undetectable by 100dg, but then increases again after 240dg (Lund et al., 1988), indicating that the foetal adrenal is capable of cortisol production in the early stages of gestation. A return like this observed in human foetuses was thought to be a requirement for the maturation of a number of organs such as the lung and gut (Ballard, 1980). The immunoreactive hormone corticotropin was also detected in bovine foetal blood at 40-50dg. The findings in the current study are consistent with a stress-induced release of cortisol from the adrenal glands with resulting apoptosis of lymphocytes in the haemolymphatic tissues in the foetuses that died within 3 weeks after infection of the dams at 70dg.

Caspase 3 activation and thereby apoptosis of lymphocytes could also result from initiation of the death receptor pathway, via binding of the death ligand (Fas ligand (FasL) or TNF-α) to the corresponding death receptors, Fas or TNF receptor-1 (TNFR1), respectively (Czerski and Nuñez, 2004). The Fas molecule is a cell-surface receptor that belongs to the TNF receptor family and is important for the selection of T cells, the clonal deletion of peripheral lymphocytes and the activation of cell-death induction (Watkin et al., 2001; Silva et al., 2013). The binding of Fas to the FasL is important and results in the activation of the Fas-associated death domain (FADD) and, subsequently, caspase 8 activation which in turn activates the downstream signalling pathway leading to apoptosis (Silva et al., 2013). On the other hand, the activation of the death receptor TNFR1 by TNF-α leads the recruitment of TNFR1-associated death domain protein (TRADD), which serves as a platform for the formation of various signalling complexes (Ichikawa et al., 2006). The TRADD can recruit FADD and lead to caspase 8 activation and apoptosis (Baud and Karin, 2001).

Rosbottom et al. (2008) had detected high levels of TNF-α mRNA in the cotyledons of the foetuses used in our study and concluded that the cytokine could have been either of foetal origin or expressed by infiltrating maternal macrophages. There is also evidence of TNF-α expression by human foetal trophoblast cells in early gestation (King et al., 1995); therefore, it is plausible that expression of TNF-α by foetal cells and also maternal macrophages, possibly due to placental impairment, could be one of the factors responsible for the high levels of apoptotic cell death in the haemolymphatic tissues of infected foetuses in early gestation.

IFN-γ can mediate the upregulation of Fas or FasL-expression in cells infected with *N. caninum* (Nishikawa et al., 2001). Indeed, FasL was significantly increased on IFN-γ-treated cells in an *in vitro* cell culture model following infection with *N. caninum*. It was later concluded that both Fas and FasL are involved in apoptosis in *N. caninum* infected cells in the presence of IFN-γ (Nishikawa et al., 2001). In line with this, Rosbottom et al. (2008) detected a significant increase in the IFN-γ mRNA levels in the placenta of dams infected with *N. caninum* in early gestation. Furthermore, the results of that study showed that only a small percentage of the total cytokine mRNA was detected in the foetal cotyledons; nevertheless, there was a significant upregulation in the cotyledons of infected foetuses in early gestation compared to the controls. It was, however, unsure whether the cytokines, mainly IFN-γ, were from foetal cells or maternally derived mononuclear cell which were shown to be expressing IFN-γ in the maternal interstitium. Circulating IFN-γ, either of foetal or maternal origin, could also have been a factor in the high level of lymphocyte apoptosis detected in the haemolymphatic tissues of early gestation foetuses in the current study.

Foetal immunocompetence develops gradually throughout gestation and strong *N. caninum*-specific CMI response (proliferative response and IFN-γ) was detected in infected foetuses around midgestation (Andrianarivo et al., 2001b; Bartley et al., 2004). However, similar proliferative responses were not observed in foetuses in early gestation, but bovine foetal splenocytes and thymocytes (98 dg) were able to produce detectable levels of IFN-γ following concanavalin A (ConA) stimulation (Bartley et al., 2012). In our study, the lack of any detectable IFN-γ expression in the haemolymphatic tissues and inflammatory infiltrates in the CNS, liver, heart, lung and skeletal muscle suggests that the T cells recruited into these tissues are immature and non-functional. Osburn et al. (1982) showed that foetal lymphocytes were

capable of mitogenic response and cytokine production when stimulated with ConA at around day 80 of gestation, but were not able to respond to infection. Our data indicate that the components of the CMI were not fully developed and T cells recruited to the tissues of foetuses did not respond to the antigenic stimulation from *N. caninum*.

B cells were very rare in the foetuses at early gestation, were only seen in spleen and bone marrow and in small numbers. They were not detected in the thymus, where they have been shown to be generally present in the medulla of foetuses in late gestation (Senogles et al., 1979). The production of B cells in species other than rodents and man is thought to depend on the GALT as the B cells are generated in the ileal Peyer's patches from late gestation onwards, but little is known about when and where B cell lymphopoiesis first occurs (Ekman et al., 2010). Results from Ekman et al. (2010) suggest that the bovine foetal bone marrow and lymph node support B cell lymphopoiesis via a pre-B cell like stage before and concomitantly with the development of the Peyer's patches, and our findings do not contradict this hypothesis.

Foetuses in early gestation (approximately 13 weeks) exhibited low numbers of haematopoietic precursor cells within the bone marrow, without evidence of megakaryocytes. Instead, the liver and spleen were the main haematopoietic organs at this stage. In murine embryos, haematopoiesis commences in the yolk sac blood islands, aorta-gonad-mesonephros region and placenta before it occurs also in the liver, after spreading from one or more of the former sites, and remains in the liver for the remainder the foetal life (Medvinsky et al., 2011). At this stage, i.e. early to midgestation, haematopoiesis gradually shifts from the liver to the spleen in a time-dependent manner that varies with species and cell lineage (Johns and Christopher, 2012). Human foetal bone marrow erythropoiesis, for example, begins between 16 and 18 weeks' gestation as hepatocyte proliferation challenges haematopoiesis (Forestier et al., 1991). The fact that mild haematopoiesis was detected in the bone marrow of foetuses in our study, at approximately 13 weeks gestation, suggests that it starts earlier in cattle than in humans, although both species have approximately the same length of gestation. Also, in bovine foetuses, foetal macrophages that originated in the bone marrow were detected by Senogles et al. (1979) in the spleen after 12 weeks gestation age.

We did not observe megakaryocytes in the bone marrow of the early gestation foetuses, although they were prominent in the liver and spleen at this stage. Megakaryopoiesis consists of two distinct phases of cell size and nuclear to cytoplasmic ratio (Matsumura and Sasaki, 1989). The first phase is seen when megakaryopoiesis takes place in the yolk sac and in the liver ("early phase"), the second in the "late phase" of hepatic megakaryopoiesis, at the time when it begins to shift to the bone marrow, which then takes over the production of megakaryocytes (Matsumura and Sasaki, 1989). Numerous *N. caninum* tachyzoites were observed in a megakaryocyte in the liver of one infected foetus, which indicates that haematopoietic cells are target cells for the parasite at this stage.

After infection in early gestation, all foetuses exhibited widespread histological changes (apoptosis, single cell necrosis and high parasite loads) in haemolymphatic tissues. In addition, low lymphocyte turnover in the haemolymphatic tissues similar to controls was observed, but with a significant increase in apoptotic lymphocytes compared to controls and without evidence of IFN-γ production by lymphocytes in the spleen. These findings provide further evidence that foetuses from dams infected in early gestation were immunologically immature. The presence of numerous *N. caninum* tachyzoites within mononuclear cells, most likely macrophages in these tissues at this stage provides further evidence that the parasites were multiplying rapidly (Maley et al., 2003; Macaldowie et al., 2004; Gibney et al., 2008).

2.6.3 The effect of N. caninum infection on non-haemolymphatic tissues of foetuses in early gestation

Infected foetuses in early gestation exhibited pathological changes of parenchymal cells (extensive hepatocellular necrosis and apoptosis, and necrosis and apoptosis of glial cells in the brain and spinal cord). This was seen in close association with the presence of numerous parasites. In the CNS parasites were far more frequent in these young foetuses than in foetuses in late gestation, where the CNS and lung were the only organs that contained immunohistologically detectable amounts of parasites. These findings are in accordance with those of Collantes-Fernández et al. (2006b) who observed highest parasite burdens and most severe lesions in foetuses in the first trimester of pregnancy.

In foetuses in early gestation, the presence of *N. caninum* tachyzoites within tissues appeared not to induce a substantial inflammatory reaction. However, there was evidence of T cell recruitment in association with damage and the presence of parasites in tissues. T cells were also present within blood vessels in the brain, and, though generally few in number, were found in the brain parenchyma and the spinal cord, where they were seen among the glial aggregates when *N. caninum* was detected by immunohistology, although not in direct association with the parasites. They were also found in the liver, heart, lungs and skeletal muscle (*Musculus quadriceps femoris*) in association with the presence of parasites in the tissue. These findings provide the first immunohistological evidence of a T cell response to *N. caninum* in early gestation foetuses. T cell infiltrates were not detected in the brain of control foetuses, and there was no evidence of T cells within blood vessels, suggesting that the T cell recruitment seen in the infected foetuses was a specific response to the parasites. However, it appears to be restricted to the recruitment of the cells, indicating that adhesion molecules are expressed and interact with T cells and endothelial cells at this stage, while the lack of immunohistological evidence of IFN-γ expression by these T cells indicates that they were not functionally active (Hughes et al., 1990).

A recent study showed foetal death between 28 and 35 days post infection after inoculation of dams with 10^8 Nc-Spain 7 tachyzoites at 65 dg. It also describes extensive inflammatory infiltrates in the brain, liver, heart, lung, muscle and tongue (Caspe et al., 2012). The CNS of all 5 foetuses (examined at 93 days gestation age), in that study, had "severe multifocal, mononuclear, meningoencephalitis; while perivascular cuffing and haemorrhage was associated with necrosis and microgliosis in the brainstem" in two of five foetuses. These findings are only in partial agreement with those of our study, which examined the foetuses at 91-92 dg, since we found T cells infiltrating the parenchyma in low numbers, not forming perivascular cuffs, even fewer infiltrating macrophages, and no other infiltrating cells. Instead, we observed microglial aggregates. Our findings were confirmed by immunohistology that identified the cells as CD3-positive T cells, MHC-positive activated microglial cells and calprotectin-positive macrophages. Microglial cells are resident macrophages in the brain and spinal cord and are present even at early gestation (Billiards et al., 2006); they comprise the main form of active immune defence in the CNS (Aloisi, 2001). Microglial cells become activated after CNS infection or any

inflammatory stimuli to perform innate immune functions and are not specifically recruited to the CNS during infection. The activated microglial cells, which we identified on the basis of their morphology and MHCII expression in the brains of the infected foetuses in our study, formed prominent (glial) aggregates. It is likely that these formed the mononuclear cell infiltrates described by Caspe et al. (2012).

In the current study, hepatocellular necrosis and apoptosis was seen in the foetal liver following infection in early gestation and numerous *N. caninum* tachyzoites were detected within intact hepatocytes and sometimes extra-cellularly. These were not detected in direct association with the moderate numbers of scattered CD3-positive T cells, which could represent not only recruited inflammatory cells, like in other tissues (see above), but also new T cells generated as part of the observed haematopoiesis. The intracellular pathogens can induce stress-related signals, which could trigger cell death via the intrinsic pathway of apoptosis in an effort to prevent further development of the pathogen (Schaumburg et al., 2006). However, protozoan parasites (*Trypanosoma cruzi, Leishmania sp., Cryptosporidium parvum, T. gondii*) have developed anti-apoptotic mechanisms to counteract the potentially protective response of apoptosis (Heussler et al., 2001; Sinai et al., 2004; Herman et al., 2007). While intracellular protozoan parasites can manipulate the host cells' caspases to deactivate cell death for their own survival, it is also important to note that the parasites produce cysteine proteinases during egress that could potentially lead to death of the surrounding cells (Graumann et al., 2009; Heussler et al., 2010). The high number of apoptotic hepatocytes could also be the result of a defence mechanism to induce pathological changes in the organ in an attempt to reduce the number of parasites. In one study, infection of mice with the RH strain of *T. gondii* led to high levels of Th1 type pro-inflammatory cytokines (IFN-γ, TNF-α, IL-12 and IL-18), which corresponded with high levels of apoptotic cell death in the livers (Mordue et al., 2001). Necrotic cells can also induce a strong inflammatory response by secreting pro-inflammatory cytokines, such as TNF-α and IFN-γ (Bruchhaus et al., 2007). However, IFN-γ expression was not observed in the livers of foetuses in early gestation in the current study, suggesting this was not the mechanism leading to hepatocyte apoptosis. Further infection studies to assess the potential transcription and translation of these cytokines in the foetal liver would be required to address this hypothesis.

Hepatocellular necrosis in association with *N. caninum*, following infection of foetuses in early gestation, has previously been confirmed by transmission electron microscopy (Gibney et al., 2008). The mechanism(s) by which hepatocytes undergo necrosis in response to the parasite is/are unknown. However, the findings clearly demonstrate the relevance of the liver as a target organ for *N. caninum* (Wouda et al., 1997; Gibney et al., 2008). Another study has also reported hepatocellular necrosis in foetuses following *N. caninum* infection in early gestation, however, staining for apoptotic cells was not performed (Caspe et al., 2012). Infection in foetuses during midgestation resulted in focal hepatocellular necrosis with associated mononuclear infiltration along with lower parasite numbers, compared to those reported in early gestation, indicating a role of the inflammatory response in controlling the pathological effects of the parasite in the liver (Almería et al., 2010).

In our study, immunohistology provided evidence of higher parasite burden in the liver compared to the brain and spinal cord of all foetuses infected in early gestation, as indicated by the presence of higher numbers of tachyzoites. Similarly, naturally infected foetuses (approximately 5 months' gestation age) exhibited more prominent lesions and larger quantities of *N. caninum* tachyzoites in the liver than in the brain (Wouda et al., 1997; Collantes-Fernández et al., 2006a). The higher parasite load detected in the liver compared to the brain is probably due in part to the chronicity of the infection; the higher parasite burden observed in the liver is consistent with acute infections, and this is in line with our findings, since the brain is more involved in chronic infections (Collantes-Fernández et al., 2006a).

Neospora caninum tachyzoites were detected in renal tubular epithelial cells, cardiomyocytes and within mononuclear cells morphologically consistent with macrophages in the lungs of the day 70 foetuses, but were not in direct association with the inflammatory infiltrates observed in these organs. Apoptosis was observed in desquamated pulmonary type II epithelial cells/alveolar macrophages in the lungs, but this did not appear to be parasite associated. Necrotic cells were not detected even when parasites were present. The kidneys were moderately autolytic, which was most likely the consequence of hypoperfusion due to the compromised placenta and foetal circulation. However, there was no evidence of tubular epithelial cell necrosis.

The high parasite loads detected by immunohistology within intact cardiomyocytes was not associated with any evidence of cell death or degeneration. Low numbers of T cells were present, but these were not in direct association with

the parasites. Low numbers of apoptotic, cleaved caspase 3 expressing cells were detected within the visceral epicardium and probably represent areas of extramedullary haematopoiesis. These observations suggest that *N. caninum* can multiply within cardiomyocytes without cell degeneration. One study has shown that *Trypanosoma cruzi* does not induce apoptosis in murine fibroblasts as the parasites are able to regulate apoptosis (Clark and Kuhn, 1999), but others have found evidence of cell death in cardiomyocytes during *T. cruzi* infection both *in vivo* and *in vitro* (De Souza et al., 2003). In a canine model of *T. cruzi* infection in cardiomyocytes, apoptosis was only found in cells in close proximity to infiltrating mononuclear inflammatory cells (Zhang et al., 1999). It is therefore tempting to speculate that cardiomyocyte degeneration was not observed in the foetuses in our study due to the lack of sufficient and functional immune cells in direct association with the parasites. *N. caninum* has been shown to inhibit caspase 3 activity and block apoptosis in mouse embryonic fibroblasts (Herman et al., 2007). The present findings are consistent with those of previous studies in which aggregates of *N. caninum* tachyzoites were observed within intact cardiomyocytes without associated necrosis or inflammation (Wouda et al., 1997; Gibney et al., 2008). This, however, does not exclude the possibility of degenerative changes via direct action of the parasites on cardiomyocytes as focal myocardial necrosis was occasionally seen in young naturally infected foetuses (90-120 dg) (Wouda et al., 1997).

The results presented here show that *N. caninum* tachyzoites have a wide range of target cells in foetuses in early gestation, in the brain and spinal cord, heart, lung, liver, kidney, and haemolymphatic tissues. Equally, it has been shown elsewhere that the placenta from the dams exhibited extensive necrosis of foetal and maternal epithelial cells and parasites were also detected within necrotic and intact cells, both in association with inflammation (Gibney et al., 2008). This suggests that the parasites, invade the placenta and establish a local maternal immune response (Rosbottom et al., 2008). This immune response may have initially limited parasite dissemination within the placenta, but was unable to control the high parasite loads following the uncontrollable multiplication in the foetus, and reinvasion of the placenta by the parasites, leading to the severe pathological changes observed in maternal and foetal epithelial cells (Gibney et al., 2008). The fact that these changes led to the death of all foetuses in early gestation, within 3 weeks of infection, is consistent with other experimental studies where infection of cattle in the first

trimester resulted in foetal death (Barr et al., 1994; Williams et al., 2000; Gibney et al., 2008). Infection acquired in early gestation was accompanied by a Th1 type cytokine response in the dam with the production of TNF-α, IFN-γ and IL-12, all of which may be lethal to the foetus through the production of free oxygen radicals (Maley et al., 2003). In the present study, there was no evidence of foetal CMI response to *N. caninum* and it would be reasonable to conclude that the direct placental damage and the parasite multiplication in the foetus contributed to foetal death in early gestation.

2.6.4 The effect of N. caninum infection on foetuses in late gestation and new born calves

In comparison to foetuses in early gestation, the foetuses experimentally infected in late gestation exhibited no histological changes in haemolymphatic tissues, although all dams had been infected with the same dose of parasite inoculum as in early gestation and were euthanised at the same time post infection. Parasites were not detected in the haemolymphatic tissues, which suggest either that the tachyzoites were not able to spread to all tissues or that there are no target cells in these tissues in the older foetuses. Immunohistology detected IFN-γ expression in lymphocytes in the spleen and lymph node of the infected foetuses, which indicates a *N. caninum*-specific CMI response to the parasites, since no IFN-γ was detected in control foetuses of the same age. The IFN-γ response may have limited parasite establishment in the haemolymphatic tissues. It is also another indication of the maturity of the foetal immune system. The role of IFN-γ in protective immunity against *N. caninum* has been established in a murine model (Khan et al., 1997). A similar experimental study in which dams had been infected with *N. caninum* at 110 dg, found a 34.3 fold higher expression of IFN-γ mRNA in the spleen of infected foetuses compared to controls (Almeria et al., 2003). The presence of IFN-γ within the tissues may have served to limit parasite numbers and multiplication, thus reducing parasite-induced pathological changes (necrosis, apoptosis and inflammation) in the tissues compared to foetuses in early gestation (Bartley et al., 2013a). In addition, infected foetuses in late gestation, in the current study, showed profoundly higher lymphocyte proliferation in the haemolymphatic tissues compared to foetuses in early gestation and apoptotic lymphocytes were significantly lower, suggesting high cell turnover in older foetuses.

In the thymus, low numbers of eosinophilic granulocytes were detected within the thymic medulla. Schultz et al. (1973) had observed these cells in the thymus of normal disease-free bovine foetuses close to parturition and suggested that they might be present at the sites of antigen-antibody reactions. Eosinophils were also detected in placental lesions of *N. caninum* infected cows following experimental infection in early gestation with subsequent foetal death (Macaldowie et al., 2004). Eosinophils were also observed, but in higher numbers in the thymic medulla of the naturally infected foetus compared to the new-born calf. The thymus of the dams did not exhibit eosinophils and this might suggest that with age, the number of these cells in the thymic medulla decreases and disappear in a time dependent manner.

Foetuses in late gestation had inflammatory infiltrates in the brain, spinal cord, myocardium, *Musculus quadriceps femoris*, *Nervus femoralis*, lung and liver, represented by a mild lymphocyte-dominated mononuclear cell infiltration. The most severe changes were seen in the CNS and included focal necrosis and perivascular cuffs in the brain, a tissue response commonly reported in bovine neosporosis (Nishimura et al., 2013); the spinal cord exhibited severe mononuclear inflammatory infiltrates, which were dominated mainly by T cells and fewer macrophages. Low numbers of parasites were detected within an intact glial cell in one foetus in direct association with the necrosis and inflammation in the brain, while a small cluster of parasites was present in the spinal cord, also within an intact glial cell in the second selected foetus in direct association with the inflammatory infiltrates. This active inflammatory response supports our hypothesis that older foetuses can respond to the presence of the parasites and mount a protective CMI response. The glial cell activation and inflammation in direct association with the parasites is supporting this hypothesis.

Low numbers of cells with morphology consistent with plasma cells were observed in the spinal cord, although B cells were not detected in the inflammatory infiltrates. Marginal zone B cells can be activated during protozoan infection and generate short lived plasma cells, which can provide a rapid antibody response (Amezcua Vesely et al., 2012). However, secondary lymphoid follicles were not present in spleen or lymph nodes in infected foetuses and plasma cells were not observed in any other tissues.

The liver of foetuses infected in late gestation had a mild periportal non-suppurative inflammatory infiltrate, dominated mainly by CD3-positive T cells, low

numbers of macrophages and a complete absence of *N. caninum* tachyzoites. The mild inflammatory response might indicate that parasites had invaded the liver, but had been controlled by the immune response. The one foetus that had a focal area of necrosis had a lymphocyte-dominated mononuclear infiltrate surrounding the necrotic foci with scant neutrophils. This may have been a site of parasite multiplication and necrotic cell death. Overall, the older foetuses had fewer apoptotic, cleaved caspase 3-positve hepatocytes than the younger infected foetuses and moderate hepatocyte proliferation was observed, indicating parenchymal turnover.

Evidence suggests that *N. caninum* tachyzoites cross the placenta and reach the foetus approximately 10 days after maternal infection (Barr et al., 1994). This might imply that the parasites invade the foetus and multiply within the foetal tissues before reinvading the placenta where they cause massive placental necrosis, as observed in foetuses in early gestation (Gibney et al., 2008). On the other hand, the opposite should be true for older foetuses with a mature immune system that can detect and respond to the parasite. This leads to the theory that parasites were able to invade foetal tissues, but multiplication was controlled by the mature foetal immune response with little to no reinvasion to the placenta. Previous work done on the placentae from the animals (infected in late gestation) used in our study revealed only small areas of epithelial cell necrosis affecting usually one foetal villus in the surrounding maternal epithelium.

In all the naturally, persistently infected cattle in the present study, parasite recrudescence had occurred after 20 weeks of gestation age, and there is evidence that the parasites had reached the foetuses at the time of euthanasia since parasite DNA was detected in 7 of 10 foetuses (Gibney, 2008). Recrudescence in the dam of foetus examined in detail in the present study occurred at 26 weeks gestation when a rise in the *N. caninum* specific antibody level was detected and euthanasia was subsequently carried out at 31 weeks gestation (Gibney, 2008). Data from a previous study showed that foetuses survived to term when recrudescence occurred after the second half of gestation (Guy et al., 2001b); therefore, it would be plausible to assume that this foetus would have survived to term, had the dam not been euthanised (Williams et al., 2000; Maley et al., 2003; Bartley et al., 2004). Similar to the foetuses experimentally infected in late gestation, the haemolymphatic tissues of the foetus and the calf born alive from a naturally, persistently infected dam were

similar. Secondary lymphoid follicles were present in the spleen of the calf which might suggest B cell activation as a consequence of infection. These two animals did also not show evidence of parasites in any of the haemolymphatic tissues, an observation consistent with the foetuses experimentally infected in late gestation.

Neospora caninum tachyzoites were only found in the CNS (spinal nerve root) in the naturally infected foetus and in direct association with the lymphocyte-dominated mononuclear inflammatory infiltrates (T cells, fewer B cells and macrophages). MHCII-positive microglial cells, identified on the basis of their morphology, were also present in high numbers indicating their activation in response to the presence of the parasites. Mononuclear inflammatory cells were also observed in the liver, heart, *Nervus femoralis* and skeletal muscle (*Musculus quadriceps femoris*), though only mild to moderate, but without the presence of parasites. These findings are consistent with those observed in canine neosporosis where meningoencephalitis, hepatitis, radiculoneuritis, myositis, myocarditis and neuritis predominantly with lymphocytes, histiocytes, plasma cells and occasional neutrophils were described (Peters et al., 2000).

Similar inflammatory infiltrates were observed in the remaining nine naturally infected foetuses, but the extent of the inflammation was lower. Infiltrates were present in CNS, liver, heart, lungs, *Musculus quadriceps femoris*, kidney and adrenal glands. This shows that the most severe lesions were found in the foetus at 31 weeks gestation age, while those at 20-26 weeks' gestation age had fewer and milder lesions. This is in contrast to what is observed in experimentally infected foetuses, whose dams had been inoculated with *N. caninum* tachyzoites at 140 dg and euthanised at 14, 28, 42 and 56 days post infection (Maley et al., 2003). The most severe lesions in this study were found in younger foetuses examined at 14 and 28 days post infection and comprised "foci of coagulative necrosis in the brain and spinal cord, surrounded by microglial cells and lymphocytes, perivascular cuffs, meningitis and periportal infiltrates"; while similar lesions were present in foetuses examined at 28 days post infection, but were fewer and milder. Interestingly, no lesions were found in foetuses examined after 56 days post infection. Others have also shown that the intensity of infection decreases with increasing foetal age in naturally infected foetuses (Collantes-Fernández et al., 2006b). As the foetal immune system gradually develops, it is expected that it would respond more rapidly to invading pathogens. This means that more severe lesions would be expected in

younger foetuses, while older animals would have a more mature immune response against the infection and therefore, milder lesions. These results from the naturally infected foetus could be due to the fact that parasite recrudescence was first detected at 26 week's post infection and the dam was euthanised at 31 week's gestation age (Gibney, 2008). Consequently, this would mean that the parasite would have a much longer time to replicate in this foetus and elicit a strong immune response; whereas the remaining foetuses, which were euthanised as soon as possible after parasite recrudescence was detected, would not have had enough time for a stronger immune response.

It has previously been shown that the placenta of the naturally infected cows had little evidence of parasite-induced necrosis in the foetal villi which were associated with a T cell-dominated inflammatory infiltrate and a highly significant increase of IFN-γ as well as other pro-inflammatory cytokines (TNF-α, IL-12p40, IL-2 and IL-18) (Rosbottom et al., 2011). Other studies have reported the concomitant protective effect of IFN-γ and IL-12 (Marks et al., 1998; Baszler et al., 1999b; Almeria et al., 2011). The inflammatory response noted in the naturally infected foetus indicates that they were responding to the infection, while the IFN-γ response may have contributed to the control of parasite dissemination and protection from parasite-induced pathological changes in foetuses.

The calf born alive to the naturally, persistently infected dam, exhibited only minimal histological changes. These comprised mild T cell-dominated mononuclear infiltrates in the brain, spinal cord, liver and heart. However, *N. caninum* tachyzoites were not detected in any tissues examined. A rising maternal antibody level to *N. caninum* was detected only at week 40 of gestation age, which suggests that recrudescence occurred at the end of the gestation period. It was, however, not possible to determine whether the parasites had crossed the placenta and infected the foetus, as immunohistology and PCR failed to detect the parasite in the brain, heart and liver (Gibney, 2008). However, the high pre-colostral antibody level detected in the calf at birth indicated that tachyzoites had crossed the placenta and infected the foetus before parturition (Gibney, 2008). The mild inflammatory reaction observed in the heart, liver and CNS (target organs) suggests parasite invasion into these tissues, supporting the view that the calf was infected and probably a persistently infected animal. The lesions described in the tissues of the foetus and calf are consistent with those of other studies (Barr et al., 1994; Wouda et al., 1997; Gibney

et al., 2008). Inflammatory infiltrates were more numerous in the naturally and experimentally infected foetuses compared to the calf and again, this might be dependent on the time when the infection occurred.

The virulence of different *Neospora* isolates is also of relevance for the assessment of parasite-induced changes, as highly virulent isolates will induce more widespread lesions and foetal death, while those of low virulence usually have a low capacity for multiplication in host tissues and for transplacental infection (Rojo-Montejo et al., 2009a; Rojo-Montejo et al., 2009b). Low virulent isolates, such as Nc-Spain 1H failed to induce clinical signs or mortality in a non-pregnant mouse model and led to low levels of transplacental transmission and neonatal mortality in pregnant mice (Rojo-Montejo et al., 2009b). The Nc-Spain 1H did also not induce foetal death in cattle, different from more virulent isolates, such as Nc-Liverpool and Nc-1 (Rojo-Montejo et al., 2009a). Therefore, the unavailability of data such as the strain that was involved in the initial infection of the naturally infected dams used in this study, its virulence and route of infection may have affected the results. These are important factors that could determine the outcome of the pregnancy and the effects the parasites would have had on the foetus. However, the lesions detected in the tissues of the naturally infected foetus and new-born calf, even though mild, were consistent with lesions observed in other *N. caninum* infected animals; these were classified as non-suppurative myositis, myocarditis and pneumonia, focal necrosis and necrotising non-suppurative encephalitis (Pescador et al., 2007).

We have shown here the characteristic differences in foetuses infected in early and late gestation and have compared them with uninfected control foetuses at the same gestation age. We have shown evidence of parasite-induced lesions in a foetus and new-born calf from naturally, persistently infected dams in which parasite recrudescence had occurred in mid to late gestation and compared these to experimentally infected foetuses in early and late gestation. Foetuses infected in early gestation had no evidence of a functional inflammatory immune response to *N. caninum*, suggesting a lack of ability to control parasite multiplication and all foetuses died within 3 weeks of the infection with widespread histological changes (apoptosis, single cell necrosis in haemolymphatic tissues, hepatocellular and glial cell necrosis and apoptosis). Unlike younger foetuses, those foetuses infected in late gestation and naturally infected foetuses all survived and evidence of an inflammatory response in response to the parasite was described. The results

demonstrated that the timing when *N. caninum* occurs can be crucial in determining whether the foetus lives or dies and the inflammatory response detected in older foetuses (experimentally and naturally infected), might have been linked with protection from the parasites. This means that infection in early gestation can lead to foetal death and abortion, while in mid to late gestation the foetus could survive to term. High parasite loads were detected in the liver with evidence of hepatocellular necrosis and apoptosis, whereas similarly high parasite burden was present within cardiomyocytes without evidence of cell degeneration.

CHAPTER THREE: Investigation of parasite-induced apoptosis in hepatocyte and cardiomyocyte cell lines

3.1 ABSTRACT

Neospora caninum is a causative agent of bovine abortion and is closely related to *T. gondii*, which infects a wide range of animals and humans. In order for intracellular parasites to survive and propagate, they must be capable of modulating the host cell functions, which includes inhibiting apoptosis. The present study aimed to investigate in more detail the finding that *N. caninum* infection appears to induce degeneration and death in hepatocytes, but not cardiomyocytes. An *in vitro* tissue culture system, utilising human hepatocyte HepG2 and murine HL-1 cardiomyocyte cell lines, was used to study the cellular alterations in association with *N. caninum* infection, focusing on the apoptotic pathway, i.e. the activation of the initiator caspases 8 and 9, and the effector caspase 3. Mitochondrial organisation in infected hepatocytes and cardiomyocytes was also evaluated, using double staining techniques with anti-COX 1 (mitochondrial marker) and anti-*N. caninum* polyclonal antisera, to further understand the host-parasite interaction within infected cells. Quantitative (caspase 3) and semi-quantitative (caspases 8 and 9) analyses were used to assess differences in caspase activation in hepatocytes and cardiomyocytes. The quantitative analysis of caspase 3 expression revealed a significant difference in the numbers of caspase 3-expressing hepatocytes in infected cultures compared to controls between 20 and 36 hours post infection (p=0.029, Mann-Whitney U test). However, caspase 3 expression was detected exclusively within uninfected cells in the infected cultures, and infected hepatocytes remained unlabelled. Significant differences in caspase 3 expression between infected and control cultures were not observed for HL-1 cardiomyocytes; infected cells were unlabelled for caspase 3, suggesting inhibition of the effector caspase. Semi-quantitative analysis for caspases 8 and 9 expression in infected HepG2 and HL-1 cultures revealed no significant differences in the number of positive cells in infected cultures compared to controls at each time point. Caspase 8 and 9 expression was mainly detected in uninfected cells, but infected hepatocytes were occasionally positive as well. Assessment of the mitochondrial organisation in HepG2 and HL-1 cells identified aggregated mitochondria along the parasitophorous vacuole membrane (PVM) in infected cells, while uninfected cells in the infected cultures exhibited large clusters of mitochondria. These cells often exhibited a punctate cytoplasmic distribution of the mitochondria, a finding consistent with mitochondrial fragmentation in association

with apoptosis. The results suggest that *N. caninum* inhibits apoptosis in infected hepatocytes in association with increased apoptosis of uninfected bystander cells. In contrast there was no evidence of parasite-induced apoptosis in either bystander or infected cardiomyocytes.

3.2 INTRODUCTION

Apoptosis is a form of caspase-mediated cell death with particular morphological features and anti-inflammatory outcome (Fink and Cookson, 2005). Apoptosis signalling occurs via the activation of caspase cysteine proteases and there are two initial pathways leading to caspase activation; the extrinsic pathway via the death receptors that process caspase 8, and the intrinsic pathway that is initiated following cytosolic release of mitochondria derived cytochrome c, in which caspase 9 is activated (Dorn, 2013). Both pathways terminate with the activation of the effector caspase, caspase 3. Apoptosis is often regarded as an active or programmed form of cell death due to its morphological and bioenergetic features (Zong and Thompson, 2006). However, in the absence of phagocytosis, apoptotic cells/bodies could lose their integrity and subsequently undergo the so-called secondary or apoptotic necrosis (Fink and Cookson, 2005). Necrosis is a term used for non-apoptotic cell death. It is signalled by irreversible changes within the nucleus and cytoplasm and includes karyolysis, pyknosis, karyorhexis, condensation and intense eosinophilia of the cytoplasm, loss of structure and fragmentation (Majno and Joris, 1995). In response to a death stimulus, there exists a continuum of apoptosis and necrosis and many agents can induce apoptosis at lower doses and necrosis at higher doses or features of both could coexist in the same cell (Zong and Thompson, 2006). Apoptosis often precedes necrosis in cells as the former is an active energy dependent process that requires adenosine triphosphate (ATP), while the latter is passive and does not require energy (Elmore, 2007).

The Apicomplexa, among other obligate intracellular parasites, are known to extensively modify their host cells to ensure their own survival (Lüder et al., 2009). The parasites invade the host as their reproduction is entirely reliant on intracellular resources and they acquire nutrients for their own benefit (Leirião et al., 2004). Once inside the host cells, parasites reside in a parasitophorous vacuole (PV) surrounded by a PVM, which is derived from the host plasma membrane (Hemphill et al., 2006). So far, there have not been extensive studies on the changes that develop in *N.*

caninum infected host cells. For their own survival, the parasites must avoid the harsh environment within a cell, circumvent the host defences, acquire nutrients, and kill or maintain the cell according to their needs (Leirião et al., 2004). *T. gondii* was shown to inhibit apoptosis of their infected host cells (Nash et al., 1998; Herman et al., 2007); however, *in vitro* infection of IFN-γ-treated BALB/3T3 clone A31 fibroblasts with *N. caninum* resulted in apoptotic cell death (Nishikawa et al., 2001). The results of the latter study indicated that the bcl-2 protein played a role as its expression was upregulated by the infection, but was inhibited by IFN-γ. Bcl-2 is a member of the bcl-2 superfamily of mitochondrial proteins that play a major role in regulating apoptosis and prolongation of cell survival (Adams and Cory, 1998).

Multiple inducers of apoptosis, including gamma and ultra-violet irradiation, drug-mediated apoptosis and IL-2 deprivation, failed to induce apoptotic cell death in different types of cells infected with tachyzoites of the closely related parasite *T. gondii* (Nash et al., 1998). It was later shown that *N. caninum* tachyzoites are able to inhibit apoptosis of host cells, as indicated by the lack of apoptosis-associated DNA degradation (Herman et al., 2007). This was confirmed through the induction of apoptosis via the death receptor pathway by treating the *N. caninum*-infected cultures with TNF-α and the protein synthesis inhibitor cycloheximide. The study, which used the terminal deoxynucleotidyl transferase dUTP nick end labelling (TUNEL) method as a means to demonstrate apoptosis, showed that more than 20% of uninfected cells within the infected cultures were apoptotic, while only approximately 4% of *N. caninum*-infected cells were apoptotic. One of the major findings in the latter study was also the inhibition of caspase 3 by *N. caninum* in infected cells (Herman et al., 2007). This defence mechanism strongly supports a survival strategy of the parasites that modulates the apoptotic machinery of the host cells to their favour.

Mitochondrial association to the PVM has been reported for many organisms including *T. gondii* and *Chlamydia psittaci* (Jones and Hirsch, 1972; Matsumoto et al., 1991; Sinai et al., 1997). This association is dependent on active parasite invasion of the cell and is thought to be achieved either during or soon after invasion and is not disrupted thereafter, even if the parasite is killed after cell entry (Sinai et al., 1997). The association is thought to be a mechanism to acquire nutrients from the host cell cytoplasm (Sinai and Joiner, 1997). However, it was shown that *T. gondii* was able to inhibit ultraviolet light-induced apoptosis via inhibition of cytochrome c

release from the mitochondria that were in close association with the PVM (Carmen et al., 2006). Similar to *T. gondii*, *N. caninum* could potentially regulate host cell apoptosis via manipulation of the mitochondrial pathways (Payne et al., 2003). A similar association of host cell organelles has been reported for *N. caninum*, though fewer mitochondria were found to physically attach to the PVM compared to *T. gondii* (Hemphill et al., 1996).

3.3 Aims of the study

Hepatocellular necrosis was observed histologically in the livers of foetuses from dams infected in early gestation (70 dg) in association with high parasite loads, however, immunohistology also detected numerous cleaved caspase 3-positive, apoptotic hepatocytes (see Chapter 2 for details). The parasites were detected mainly within intact hepatocytes, while hepatocellular necrosis was observed in the surrounding uninfected cells. Hepatocellular necrosis has been confirmed by transmission electron microscopy (TEM), but the mechanism by which the hepatocytes undergo necrosis in response to the presence of *N. caninum* has not been ascertained (Gibney, 2008). High parasite loads were also observed within intact cardiomyocytes of infected foetuses in early gestation; however, these were not associated with necrosis, apoptosis or an inflammatory reaction (see Chapter 2 for details). To further understand the role of the parasite in the pathogenesis of neosporosis in the liver and heart of bovine foetuses, an *in vitro* tissue culture system utilising primary bovine hepatocytes, an established human hepatoma cell line (HepG2) and a murine cardiomyocyte cell line (HL-1) was used to investigate parasite-induced apoptosis at a cellular level.

The aims of this study were to establish the mechanism of hepatocyte cell death following *N. caninum* infection, focusing on the mode of cell death and activation of the apoptotic pathways, i.e. the dissection of the apoptotic cascade – activation of initiator caspases (caspases 8 and 9) and effector caspase (caspase 3) - should it occur, and also to assess the mitochondrial organisation of *N. caninum*-infected hepatocytes and cardiomyocytes.

3.4 MATERIALS AND METHODS

A human hepatoma cell line (HepG2, ATCC HB-8065, kindly provided by the Department of Molecular and Clinical Pharmacology, University of Liverpool), primary bovine hepatocytes (derived from liver samples obtained from a local abattoir in Birkenhead, Liverpool, UK), a murine cardiomyocyte cell line (HL-1, kindly provided by Dr. William Claycomb, Health Science Centre, Louisiana State University, New Orleans, LA), an African Green Monkey kidney epithelial cell line (Vero cells, ATCC CCL-81) and *N. caninum* tachyzoites (Nc-Liverpool), both maintained at the Department of Infection Biology, University of Liverpool, were used for the *in vitro* studies.

3.4.1 Culturing and maintenance of Vero cells

Vero cells were maintained in RPMI-1640 medium supplemented with 2% (v/v) horse serum (Invitrogen, Paisley, UK), 50 IU/ml penicillin, and 50 µg/ml streptomycin (Lonza Bio-Whittaker, Walkersville, USA) [growth medium] at 37°C with 5% CO_2 in T-75 tissue culture flasks (Nunc, Roskilde, Denmark). Flasks were inoculated with $3x10^5$ cells in 15 ml growth medium. When the Vero cell layer became confluent, it was washed with PBS/ethylenediaminetetraacetic acid (EDTA) [PE; 1 ml/wash] to remove all traces of medium and serum. Excess PE was then tipped off and replaced with 0.5 ml of 0.25% PBS/EDTA/Trypsin (PET). Excess PET was then removed leaving only enough to cover the cell layer, and the flask was incubated at 37°C for 5 min. Cells were then washed from the flask with 10 ml of growth medium and transferred to a centrifuge tube. A cell count was carried out using a Neubauer haemocytometer. New flasks were inoculated with $3x10^5$ cells/75 cm^2.

3.4.2 Culturing and maintenance of *N. caninum* parasites

N. caninum tachyzoites of the NC-Liverpool isolate (Barber et al., 1995) were maintained in Vero cells grown in RPMI-1640 medium supplemented with 2% (v/v) horse serum, penicillin 50 IU/ml, streptomycin 50 µg/ml (Lonza Bio-Whittaker), as previously described (Williams et al., 1997). Tachyzoites were harvested from the Vero cell monolayers after the cells had been destroyed following parasite egress, which resulted in the presence of numerous free tachyzoites in the culture medium. A sterile cell scraper (Fisher Scientific, New Jersey, USA) was used to remove the

parasite-infected cell monolayers. The suspension of parasites and Vero cells was homogenised by passages through a 25 gauge needle until all Vero cells had been disrupted and the intracellular tachyzoites released. The preparation containing the parasites and cell debris was washed twice in cold sterile phosphate buffered saline (PBS, pH 7.2) by centrifugation at 858 x g at 4°C. The final pellet was then passed through a Sephadex G-25M PD-10 Desalting column (Pharmacia, Uppsala, Sweden) that had been equilibrated with PBS as per the manufacture's instruction. The eluted purified parasites were counted using a Neubauer haemocytometer and used to infect cell cultures or centrifuged at 12,000 x g and the pellet stored at -20ºC until needed.

3.4.3 Isolation and culturing of primary bovine hepatocytes

3.4.3.1 Reagents and solutions

Collagenase type II (1 mg/ml), Hank's balanced salt solution (HBSS), Dulbecco's modified eagle medium (DMEM), bovine serum albumin fraction (BSA-fraction V), fungizone antimycotic (250 µg amphotericin B + 250 µg sodium desoxycholate/ml), gentamycin (250 mg), penicillin 10,000 U/ml/streptomycin 10 mg/ml, ethylene glycol tetraacetic acid (EGTA; 3.8g/L), sodium hydroxide (NaOH; 0.8g/L), calcium chloride ($CaCl_2$; 5 mmol/L), HEPES 1.0 mM, PBS, foetal bovine serum (10% FBS). HBSS and fungizone were purchased from Life Technologies, Paisley, UK. All other chemicals were purchased from Sigma-Aldrich, Dorset, UK. Perfusate solutions and culture media were prepared as follows: perfusate A (wash buffer pH 7.0) contained 1,000 ml PBS, 380 g/100 ml EGTA and 800 mg NaOH; perfusate B consisted of 500 ml PBS, 250 mg gentamycin and 6 ml penicillin/streptomycin; perfusate C comprised 500 mg collagenase type II, 500 ml HBSS, 1M HEPES solution and 210 mg $CaCl_2$. The growth medium used for culturing the primary cells contained DMEM + HBSS (100 ml) 10% (v/v) FBS, fungizone antimycotic (250 µg amphotericin B + 250 µg sodium desoxycholate/ml) and 1 g/L of BSA-V.

3.4.3.2 Isolation of primary bovine hepatocytes

Each liver (four from the apical region of the caudate process with intact capsule from adult cows) was collected in cold NaCl solution (0.9 g/L) and transported to the lab within approximately 30 min. The procedure was carried out in a designated sterile lab used for primary cell isolation. The liver specimen was placed in a sterile Petri dish and a large vein on the cut surface was cannulated with a 14G needle. All

other vessels were ligated with either suture material or forceps to keep the fluid from escaping through the cut surface. The lobe was perfused for 15 min at a flow rate of 50 ml/min with perfusate A (37°C). Perfusate B was then administered for 3 min at the same flow rate, after which the collagenase solution (perfusate C) was administered for 7 min at 50 ml/min (with the collagenase added to the buffer approximately 2 min before perfusion). The caudate process was then moved to a sterile plate in perfusate B and fine forceps were used to gently disrupt the liver capsule and release the cells into the buffer. Residual tissue was removed and the cell suspension was filtered into a sterile beaker through a 125 µm nylon blotting cloth, which was pre-treated with the same buffer to facilitate drainage. The cell suspension was allowed to settle for approximately 10 min on ice in 50 ml Falcon tubes after which the supernatant was removed and cells were washed three times with perfusate B (4°C, centrifugation for 3 min at 50 x g) before re-suspension in 20 ml PBS. The cell suspension was then layered over 20 ml of Lymphoprep solution (Progen Biotechnik, Heidelberg, Germany) and spun at 4°C for 20 min at 1,000 x g. Cells were retrieved from the top of the Lymphoprep solution and re-suspended in PBS for viability determination by 0.4% (w/v) trypan blue (Sigma-Aldrich, Dorset, UK) exclusion and cell enumeration with a Neubauer haemocytometer.

3.4.3.3 Culturing and maintenance of primary bovine hepatocytes

The hepatocyte cell density was adjusted to $2x10^6$ cells per 25 cm^2 collagen-coated flask (Sigma-Aldrich) in DMEM + HBSS growth medium containing 10% (v/v) FBS, BSA-V and fungizone and maintained at 37°C in a humidified atmosphere of 95% O_2 and 5% CO_2. After 24 h incubation, 50% of the growth medium was removed and fresh medium added, followed by complete replacement by fresh medium each 24 h. The monolayer was monitored daily using an inverted phase contrast microscope; morphological changes were assessed using a DCM900 digital camera (Oplenic Optronics Equipment Company Ltd, China). The monolayers were infected with different multiplicities of infection (MOI), i.e. $1x10^6$, $2x10^6$ and $4x10^6$ *N. caninum* tachyzoites, after reaching confluence. Parasites were allowed to interact with the host cells for 1 h after which the monolayer was washed and new growth medium added. Uninfected hepatocytes were used as controls and were treated similarly without the parasites. At the end of the experiment, the cell layers were harvested using a sterile cell scraper (Fisher Scientific) and the suspension was

collected into 15 ml tubes and centrifuged at 215 x g for 10 min. The cell pellets were washed twice in PBS then transferred to 1.5 ml Eppendorf tubes in PBS and centrifuged at 100 x g for 10 min. PBS was removed and the pellets were fixed in 4% paraformaldehyde (PFA).

3.4.4 Culturing and maintenance of hepatocyte cell lines

HepG2 cells were grown in T75 (Nunc, Roskilde, Denmark) tissue culture flasks in 15 ml of growth medium (Lonza Bio-Whittaker). To prepare the growth medium, 450 ml DMEM was supplemented with 50 ml of 10% (v/v) (FBS; heat inactivated at 56°C for 30 min) and 100 U/ml penicillin and 100 µg/ml streptomycin (both from Lonza Bio-Whittaker). Cell monolayers were washed with PBS, then trypsinised with 0.25% trypsin/EDTA (Lonza Bio-Whittaker) and incubated for 5 min at 37°C. Cells were washed from the flasks using growth medium and collected in 25 ml Falcon tubes. One hundred microlitres of the cell preparation was removed and added to an Eppendorf tube with 100 µl of 0.4% trypan blue to determine cell viability. Cell viability was greater than 95% at all times. Cells were counted using a Neubauer haemocytometer. A volume containing $3x10^6$ cells was added to each flask in growth medium and incubated in a humidified atmosphere with 5% CO_2 in air at 37°C. The cell layer was infected with $6x10^6$ *N. caninum* tachyzoites when approximately 80% confluent. Tachyzoites were allowed to interact with the cell layer for 1 h after which time the monolayer was washed twice with PBS (37°C) to remove free parasites, and new growth medium added. Uninfected HepG2 cells, treated similarly but without the parasites, were used as controls and were included for each time point to account for any spontaneous changes that might have occurred during culture. At harvesting, the monolayers were scraped from the flasks using a sterile cell scraper (Fisher Scientific). The suspension was collected in 15 ml tubes and centrifuged at 215 x g for 10 min followed by 2 washes with PBS at 215 x g for 10 min each. Cells were transferred to 1.5 ml Eppendorf tubes in PBS and centrifuged at 380 x g for 10 min. PBS was removed and cell pellets were fixed in 4% PFA. Cells were harvested every hour over a 48 h period. The same protocol was used to culture the human hepatoma cell line (HuH7) and a mouse hepatoma cell line (Hepa1C) in conjunction with HepG2 cells. All cell lines were cultured and HepG2 cells were subsequently chosen for the study due to their ability to survive longer periods in culture and with fewer cell deaths compared to the other two cell lines.

3.4.5 N. caninum in vitro invasion-egression study

To ascertain the length of time that *N. caninum* tachyzoites take to egress from infected cells following invasion, an invasion-egression study was performed. To do this, $3x10^4$ HepG2 cells/well were seeded on 8-well Lab-Tek chamber slides (Nunc) in DMEM with 10% (v/v) FBS. Cells were infected with *N. caninum* tachyzoites after reaching confluence, using an MOI of 2:1 and 5:1 (tachyzoites to host cell), respectively. The experiment was undertaken twice under similar conditions. At 1 h post infection, the wells were washed twice with pre-warmed PBS (37°C) to remove all free parasites and new growth medium was added. Chamber slides were checked every 3 h after the first 12 h for the first signs of parasite egress from infected cells. Once this was seen, slides were washed twice with PBS and cells were fixed in 4% PFA at the end of the study.

3.4.6 Culturing and maintenance of murine cardiomyocyte cell line

HL-1 cells were maintained in Claycomb's medium (Sigma-Aldrich), according to the protocol supplied by the Claycomb laboratory (see Appendix 3), supplemented with 2 mM L-glutamine (Sigma-Aldrich), 0.1 mM norepinephrine, 10% (v/v) FBS (Sigma-Aldrich) 100 U/ml penicillin and 100 µg/ml streptomycin (Lonza Bio-Whittaker) in 5% CO_2 at 37°C and 95% humidity. The cells were passaged every 3 days (d) after reaching confluence by trypsinisation (trypsin/EDTA, Lonza Bio-Whittaker) and seeded onto T75 flasks. Flasks were gently washed with 6 ml of 0.05% (v/v) trypsin/EDTA warmed to 37°C. The trypsin/EDTA was aspirated and another 3 ml was added and incubated for 2 min. This volume of trypsin/EDTA was then removed and a second 3 ml volume was added and incubated for a further 3-8 min. Flasks were examined microscopically for cell detachment and gentle tapping on the flasks helped to dislodge adhering cells. Following trypsin digestion, an equal amount of Soybean Trypsin inhibitor (Sigma-Aldrich) was added directly onto the cells to inactivate the enzyme followed by the addition of Claycomb's wash medium (Claycomb's medium supplemented with 5% (v/v) FBS, 100 U/ml penicillin and 100 µg/ml streptomycin) to the suspended cells, which were further pelleted by gentle centrifugation (5 min at 500 x g). The cells were resuspended in the supplemented Claycomb's medium, cell viability was determined using trypan blue exclusion, and a total of $3x10^6$ viable cardiomyocytes were transferred to T75 flasks. The flasks were precoated with 6 ml of gelatin/fibronectin (Bacto-Gelatin and fibronectin;

Sigma-Aldrich) and incubated for approximately 12 h at 37°C before use (see Appendix 3). Cells were infected with $6x10^6$ tachyzoites (MOI of 2:1), when the monolayer was approximately 80% confluent, and cultured in humidified atmosphere of 5% CO_2 in air at 37°C. The monolayer was washed with PBS (37°C) to remove all free parasites 1 h after seeding and new growth medium was added. Uninfected HL-1 cells were used as controls for each time point and were treated similarly without the parasites. Cells were harvested at the relevant time points (every 4 h over a 48 h period) using a sterile cell scraper (Fisher Scientific) and the suspension collected in a 15ml tube. The cell suspension was centrifuged at 500 x g for 5 minutes followed by 2 washes in PBS. Cells were transferred to 1.5 ml Eppendorf tubes in PBS and centrifuged at 500 x g for 5 min. Cell pellets were fixed in 4% PFA.

3.4.7 Processing for histology, haematoxylin and eosin and Giemsa stain

Processing for histology (i.e. paraffin wax embedding), the preparation of sections for light microscopy, and all routine immunohistology and immunofluorescence staining were performed by the technical staff in the Histology Laboratory, Veterinary Laboratory Services, School of Veterinary Science, University of Liverpool. After fixation in 4% PFA for 15-18 h, cell pellets were routinely embedded in paraffin wax. Series of sections (3-5 µm thick) were cut and mounted on Poly-L-Lysine treated slides and allowed to dry at 37ºC. They were deparaffinised in xylene for 10 min, then rehydrated in graded alcohols to distilled water and subjected to the haematoxylin-eosin (HE) and Giemsa stain and the various other staining protocols (Table 3.1).

Table 3.1: Specimens and staining protocols applied to cell pellets

Cell type	Staining protocols	Time point
HepG2 cells	IH caspases 3, 8 and 9 (single stain)	0-48 h
	IH + IF caspase 3	24 and 36 h
	IH + IF caspase 8	32 h
	IH + IF caspase 9	36 h
	IF (anti-Neospora + anti-COX 1)	32 h
HL-1 cardiomyocytes	Caspases 3, 8 and 9 (single stain)	0-48 h
	IH + IF caspase 3	24 h
	IH + IF caspase 8	32 h
	IH + IF caspase 9	32 h
	IF (anti-Neospora + ant-COX 1)	28 and 32 h

IH – immunohistology; IF – immunofluorescence

Time points were over a 48 h period (48 separate cultures plus controls). One time point was subsequently chosen randomly for each caspases 3, 8 and 9 between 24 and 36 h and shown in detail (time of parasite sgression).

For the HE stain, sections were stained in Mayer's haemalum (see Appendix 2) for 5 min, blued in tap water for 6 min and then stained in a working solution of eosin (see Appendix 2) for 2 min. After that, slides were transferred directly to 95% ethanol for 7 dips and then submerged for 1 min. This process was repeated twice. Sections were then dehydrated in absolute alcohol, cleared in xylene and mounted in DPX (BHD brand, VWR International, Lutterworth, UK).

The Giemsa stain was performed for the initial identification of *N. caninum* tachyzoites in sections processed for routine histology. Sections were stained in a coplin jar in a mixture of 1 ml of Giemsa stock (see Appendix) and 45 ml distilled water in a water bath at 56°C for 20 min, then rinsed in distilled water. They were differentiated by passing them through acetic acid (1/1500) for approximately 30s, then washed in distilled water. Sections were blot-dried, rinsed briefly in alcohol and cleared and mounted with DPX. Parasites are stained blue to dark blue.

3.4.8 Immunohistology and immunofluorescence

The peroxidase anti-peroxidase (PAP) method was applied (Kipar et al., 1998) as outlined in Table 3.3, following standard protocols described in Chapter 2, section 2.4.4. Immunohistology (IH) was performed to identify cells undergoing apoptosis, i.e. expressing caspase 8 (extrinsic pathway of apoptosis), caspase 9 (intrinsic pathway of apoptosis) and cleaved caspase 3 (effector caspase) in *N. caninum*-infected and uninfected cells. Section from a bovine foetal thymus and spleen served as positive controls and for optimisation of the protocols. Details of the antibodies used and the epitope to which they are directed are provided in table 3.2, information on antigen retrieval, antibody dilution, secondary antibodies and detection systems are given in table 3.3.

Consecutive sections from each tissue served as negative controls in which the primary antibody was replaced by TBS.

Table 3.2: Antibodies used for immunohistological and immunofluorescence staining

Ligands	Antibodies and sources	Specificity
Cleaved caspase 3	Monoclonal rabbit anti-cleaved caspase 3, (ASP175, 5A1E; Cell signalling), DAKO, Glostrup, Denmark.	Apoptotic cells, effector caspase (Eckle et al., 2004)
Caspase 8	Polyclonal rabbit anti-human caspase 8, LS-B2225, Lifespan Bioscience Inc., Nottingham, UK.	Initiator caspase, extrinsic pathway (Csak et al., 2011)
Caspase 9	Polyclonal rabbit anti-caspase 9, PA1-21141, Thermo Fisher Scientific, Loughborough, UK.	Initiator caspase, intrinsic pathway
MTCO1	Monoclonal mouse anti-MTCO1, clone 1D6E1A8, Abcam, Cambridge, UK.	Mitochondrial marker, inner membrane (Clemente et al., 2013)
N. caninum	Monoclonal mouse anti-*N. caninum* (gp65) antibody, clone 5B6, Accurate Chemical and Scientific Co., New York, USA.	*N. caninum* antigen (Uzêda et al., 2013)
N. caninum	Polyclonal rabbit anti-*N. caninum* , Parsley, University of Liverpool, Liverpool, UK	*N. caninum* antigen (Gibney et al., 2008)

Table 3.3: Immunohistological protocols: antigen retrieval, antibody dilution, secondary antibodies and detection systems

Antibody	Antigen retrieval	Antibody dilution	Secondary antibody	Detection system
Anti-cleaved caspase 3 (mAb)	Citrate buffer [a]	1:50 in 20% SS in TBST	Swine anti-rabbit [b], 1:100 in 20% SS in TBST	PAP rabbit [b], pAb (1:250 in 20% SS in TBST)
Anti-caspase 8 (pAb)	Citrate buffer [a]	1:100 in 20% SS in TBST	Swine anti-rabbit [b], 1:100 in 20% SS in TBST	PAP rabbit [b], pAb in 20% SS in TBST)
Anti-caspase 9 (pAb)	Citrate buffer [a]	1:4 in 20% SS in TBST	Swine anti-rabbit [b], 1:100 in 20% SS in TBST	PAP rabbit [b], pAb in 20% SS in TBST)
Rabbit anti-*N. caninum* (pAb)	No pre-treatment	1:1000 in 20% SS in TBST	Swine anti-rabbit IgG [b], 1:100 in 20% SS in TBST	PAP rabbit [b] (1:100 in 20% SS in TBST
Mouse anti-*N. caninum* (mAb)	Protease	1:200 in TBST	Rat anti-mouse [c], 1:200 in TBST	PAP mouse [c], mAb (1:500 in TBST)

[a] Treatment for 30 min at 97°C in citrate buffer (pH 6.0); [b] Obtained from DAKO, Glostrup, Denmark; [c] Obtained from Jackson Immunoresearch Laboratories, Suffolk, UK; SS – swine serum; pAb – polyclonal antibody; mAb – monoclonal antibody

3.4.8.1 Demonstration of N. caninum

After deparaffination, sections were incubated in methanol with 0.5% H_2O_2 (Perhydrol 30% H_2O_2 P-a, Fisher Scientific) for 30 min at room temperature (RT) to inactivate endogenous peroxidase, followed by a 5 min wash in Tris-buffered saline tween (TBST, pH 7.6, see Appendix). Protease pretreatment (antigen retrieval, see

Table 2.4, Chapter 2) was performed by washing the slides in PBS (pH 7.2) at 37°C for 5 min, followed by 0.05% protease treatment at 37°C (Bacterial protease type XXIV, Sigma-Aldrich) in pre-warmed (37°C) PBS for a further 5 min, then three washes for 5 min each in ice-cold TBST. The slides were placed in cover plates and Sequenza racks (Thermo Shandon, Pittsburgh, USA) and washed for 3 x 5 min in TBST, then non-specific binding of antiserum was blocked by incubation in 10% rat serum in TBST for 10 min. The sections were incubated overnight (15-18 h) at 4°C with mouse anti-*N. caninum* in TBST. Slides were washed in TBST 3 x 5 min, then incubated for 30 min with the secondary antibody. Following another wash in TBST, slides were incubated for 30 min with PAP mouse, then washed in TBST 3 x 5 min and removed from the cover plates. The sections were then incubated with permanent stirring for 10 min in DAB (Fluka Chemie AG, Buchs, Switzerland) with 0.01% H_2O_2 (Perhydrol 30% H_2O_2 P-a, Fisher Scientific) in 0.1 M imidazole buffer (pH7.1, Fluka Chemie AG; see Appendix) at RT. The slides were washed in TBST for 3 x 5 min and 1 x 5 min in distilled water, counterstained with Papanicolaou's haematoxylin (Merck) for 1 min, and placed in running tap water for 5 min. Sections were dehydrated in ascending ethanol (1 min 96%, 2 min 100% and 3 min 100%), cleared in xylene (2 min 100% and 2 x 3 min 100%), then cover slips mounted with DPX (BDH brand, VWR International).

3.4.8.2 Double immunoperoxidase (IP) and immunofluorescence (IF) labelling for the demonstration of N. caninum and caspases in N. caninum-infected cell cultures

A double IP and IF staining procedure was chosen since all primary antibodies (anti-*N. caninum* and caspases had been generated in rabbit. The alternative use of the monoclonal mouse anti-*N. caninum* antibody was decided against since this antibody generated no reaction in the single immunohistological labelling. Prior to the use in the double staining, single labelling with each antibody had shown the presence of the target antigens in the tissues.

The double IP and IF staining method followed previously described protocols (Ressel and Poli, 2010). The staining was performed in sequential steps with IP to detect the parasites (first antigen) and IF to detect a caspase (second antigen), followed by counterstaining with 4,6´-diamindino-2-phenylindole (DAPI). Details of the antibodies used and the detection systems are provided in table 3.4.

Table 3.4: Antibodies and protocols for sequential double immunoperoxidase-immunofluorescence and double immunofluorescence labelling

Immunoperoxidase		**Immunofluorescence**	
Primary antibody[a]	**Secondary antibody[b]**	**Primary antibody[c]**	**Secondary antibody[d]**
pAb rabbit anti-*Neospora caninum* 1:1000 in 20% SS in TBST	3x drops DAKO anti-rabbit (EnVision)	Rabbit anti-cleaved caspase 3 (1:50) in 20% SS in TBST	Anti-rabbit Dylight 549 (1:200) in antibody diluent
pAb rabbit anti-*Neospora caninum* 1:1000 in 20% SS in TBST	3x drops DAKO anti-rabbit (EnVision)	Rabbit anti-human caspase 8 (1:100) in 20% SS in TBST	Anti-rabbit Dylight 549 (1:200) in antibody diluent
pAb rabbit anti-*Neospora caninum* 1:1000 in 20% SS in TBST	3x drops DAKO anti-rabbit (EnVision)	pAb rabbit anti-caspase 9 (Neat)	Anti-rabbit Dylight 549 (1:200) in antibody diluent
NA	NA	mAb mouse anti-MTC01 (1:100) + pAb rabbit anti-*N. caninum* (1:1000) in TBST	Anti-mouse Dylight 488 (1:200) + Anti-rabbit Dylight 549 (1:200) in antibody diluent

pAb – polyclonal antibody; mAb – monoclonal antibody ; NA – not applicable

[a] Produced at the University of Liverpool; [b] purchased from DAKO; [c] For antibody details, refer to Table 3.2 above; [d] purchased from Vector Laboratories Ltd

Deparaffinised sectioned pellets were washed in distilled water for 5 min, followed by antigen retrieval with citrate buffer (Table 3.3. For detailed description see Chapter 2, Table 2.4). Following incubation, the slides were removed and allowed to cool for 20 min, then returned to distilled water. The slides were placed on a flatbed and washed 3 times with TBST for 2 min, followed by incubation with 100 µl DAKO REAL peroxidase blocking solution for 10 min at RT. This was followed by three washes with TBST for 2 min each. Slides were later incubated for 1 h at RT with polyclonal rabbit anti-*N. caninum* antibody, then washed 3 times with TBST for 2 min each and incubated with DAKO EnVision+ System-Peroxidase solution for 30 min at RT. The solution was removed by three washes in TBST for 2 min each, followed by incubation of the sections with permanent stirring for 10 min in DAB (Fluka Chemie AG) with 0.01% H_2O_2 (Perhydrol 30% H_2O_2 P-a, Fisher Scientific) in 0.1 M imidazole buffer (pH7.1, Fluka Chemie AG; see Appendix 2) at RT. The slides were then washed three times in distilled water and placed back on the flatbed. This was followed by 3 washes with TBST for 2 min each and incubation for 15-18 h at 4°C with the primary antibody for the second antigen. Slides were then washed three times with TBST for 2 min each followed by incubation with a fluorescence labelled secondary antibody (Table 3.4 for antibodies and dilutions) for a further 30 min in the dark to demonstrate the caspases. This was followed by three

washes in TBST for 2 min each and washing with distilled water 3 times after which VECTASHIELD Hard Set mounting medium with DAPI (Vector Laboratories Ltd, Cambridgeshire, UK) was applied. The slides were then kept in the dark at 4°C until viewing.

3.4.8.3 Double immunofluorescence staining for detection N. caninum tachyzoites and host cell mitochondria

For evaluation of the host cell mitochondrial organisation in *N. caninum*-infected and uninfected HepG2 and HL-1 cells, the double immunofluorescence labelling technique was performed, using a mouse monoclonal antibody against the mitochondrial MTCO1 marker (from here on refer to as COX 1) as described (Clemente et al., 2013) and the rabbit anti-*N. caninum* polyclonal antibody for the detection of the parasites (Table 3.4). After deparaffinisation, slides were washed in distilled water for 5 min and placed on a flatbed followed by three washes with TBST for 2 min each. The sections were incubated for 15-18 h at 4°C with 100 µl of the primary antibody cocktail, then washed 3 times with TBST for 2 min each and incubated for a further 1 h in the dark with the fluorescence labelled secondary antibodies. This was followed by 2 washes with TBST for 2 min each. Slides were then passed through distilled water 3 times, and the VECTASHIELD Hard Set mounting medium with DAPI was applied. Slides were kept in the dark at 4°C until viewing.

3.4.8.4 Image acquisition and editing

Stained slides were examined with a Nikon Eclipse 80*i* microscope equipped with a digital sight DS-5Mc camera (Nikon Corporation, town, Japan). For the double IP and IF stained sections, an appropriate 400 x high power field (HPF) was chosen and two images were captured. The first was a red-green-blue (RGB) image from a DAB-stained section that was acquired under bright-field light, and a brown precipitate following the shape of the parasite was considered a positive reaction. Without changing the microscopic field or magnification, a second image was generated changing only the settings of the microscope to capture the fluorescence stain in the same field. This was captured and merged with DAPI at the same time. All images were saved as TIFF files, with 2,560 x 1,920 pixels (width x height) and 8-bit depth. Images were processed using Adobe Photoshop CS6 software, version

13.0.1 (Adobe System Incorporated, San Jose, California, USA). The bright field image (layer one) was adjusted for contrast and resolution (300 pixels/inch) and layered onto a white background. The same resolution was set for the second image (fluorescence), then the Photoshop colour range was selected and the image copied and pasted over the bright field image, creating a second layer. The layers were merged using the transparency setting (blending options) creating a composite image of the two signals. The single images for histology and immunohistology were captured similarly as described above (first image). For the double IF, slides were examined with a Zeiss Axio Imager M2 microscope equipped with an AxioCam MRc camera (Carl Zeiss Ltd, Jena, Germany). All images were captured at 630 x HPF. Four images were automatically generated by the microscope (three single channels and one composite) and processing of images was performed using the Zen 2012 Digital Imaging software (Carl Zeiss Ltd).

3.4.9 Quantitative, semi-quantitative assessment and statistical data analysis

Quantitative analysis for cleaved caspase 3-positive cells (HepG2 and HL-1 cell lines) was performed by counting 4 non-overlapping, representative 400 x HPF in one section of each infected and control cell pellets. The antibody selectively stained the cytoplasm of cells with morphological changes consistent with apoptosis and of cells without visible morphological changes. Four fields were used due to the relatively small size of the samples (cell pellets). A photomicrograph of each section was taken with the Zeiss Axio Imager M2 microscope (Carl Zeiss Ltd). The number of positive and negative cells was counted in each section and the mean percentage was given for infected and uninfected cells. The Kruskal-Wallis test was performed separately for the infected and control groups to test for differences across time points (0-48 h), then the Mann-Whitney U test was applied to test differences at each time point (infected versus control).

To assess the number of caspases 8 and 9-positive cells, a subjective grading system was used to determine the intensity of the IH reaction in cells (0 = no reaction, 1 = weak staining, 2 = moderate staining, 3 = intense staining). Positive cells were identified based on both nuclear and cytoplasmic (caspase 8 - cytoplasmic only) reaction. In addition, a semi-quantitative scoring system of the percentage of positively labelled cells (proportion), independent of intensity, was applied (0 = negative, 1 = 1-25% positive cells, 2 = 26-50% positive cells, 3 = 51-75% positive

cells, 4 = >75% positive cells). Each section was divided into 4 non-overlapping representative 400 x HPF, and a number (0, 1, 2 or 3) was applied to represent each staining intensity and the proportion of positively stained cells (0, 1, 2, 3 or 4). The average of these 4 numbers generated from the four microscopic fields provided a single number for intensity (I) and for the proportion of positive cells (P), respectively. The mean immunohistological score ($\bar{IS}$) was obtained by multiplying the average staining intensity by the average proportion of positives ($\bar{I}$ x $\bar{P}$ = $\bar{IS}$). The data were analysed using the Kruskal-Wallis test to check for differences between infected and control specimens separately, then the Mann-Whitney U test was applied to specimens from corresponding time points to check for statistical differences (scores) between infected and control cells (0-48 h). All statistical analyses were performed using the IBM SPSS Statistics 20 software (IBM Corp., Armonk, NY). Statistical significance was accepted when $p<0.05$ (*****).

3.4.10 One-dimensional poly-acrylamide gel electrophoresis (1-DE) and immunoblot analysis

In sections from pellets prepared with both HepG2 and HL-1 cells stained with IH and IF, there was evidence that the cleaved caspase 3, caspases 8 and 9 antibodies cross-reacted with *N. caninum* tachyzoites. In order to confirm this cross reaction, a 1-DE and immunoblot blot analysis was performed, using a *N. caninum* tachyzoite lysate prepared from cell-free tachyzoites from cultures maintained under the same conditions as those used for the initial immunohistological staining (Table 3.3). Vero cell protein extract was used as a positive control for caspases 3, 8 and 9 to show that the antibodies recognise the target proteins.

3.4.10.1 Parasite and Vero cell preparation

Neospora caninum tachyzoites and Vero cells were cultured and harvested as described above in section 3.4.2 and 3.4.1, respectively. A total of $1x10^8$ tachyzoites and $1x10^5$ Vero cells (grown in T75 flask) were used for protein extraction.

3.4.10.2 Preparation of tachyzoite and Vero cell lysates

Cell samples were lysed in a loading buffer containing 50 mM Tris-HCl (pH 6.8), 1% (v/v) Triton X-100 and 10 µl/ml protease inhibitor (Sigma-Aldrich). The suspension was incubated on ice for 10 min after which tachyzoites and Vero cells

were disrupted by incubation in an ultrasonic bath sonicator (Thermo Fisher Scientific) at 4°C, followed by centrifugation at 12,000 x g for 10 min. Supernatants were collected and the remaining unlysed pellets discarded.

3.4.10.3 Bradford protein assay

The protein concentration of both the *N. caninum* and Vero cell extract was determined with the Bradford protein assay. The sample and standards (10 µl of each in triplicate) were pipetted into a 96-well plate, and 200 µl Coomassie protein assay reagent (Bradford Protein Assay Kit; Thermo Fisher Scientific) was added to each well and mixed thoroughly. The plate was incubated at RT for approximately 5 min and the absorbance measured with an Infinite F50 ELISA plate reader (Tecan, Salzburg, Austria) at 595 nm. A standard curve was generated from the absorbance and the sample concentration was calculated accordingly in µg/µl.

3.4.10.4 Sodium-dodecyl sulphate polyacrylamide gel electrophoresis (SDS-PAGE)

The protein extracts of the *N. caninum* Liverpool isolate and Vero cell lysates were processed for SDS-PAGE. Resolving and stacking gels were prepared according to previously published protocols (Goebel et al., 2001). Acrylamide gel was made up with 30% acrylamide in 0.8% Bis-acrylamide stock solution (BDH brand, VWR International). The resolving gel solution [10 ml acrylamide, 5 ml 1.5M Tris-HCl (pH 8.8), 4.6 ml double distilled water (ddH_2O), 200 µl 10% (w/v) ammonium persulphate (APS), 200 µl SDS and 20 µl tetramethylethylenediamine (TEMED)] was poured between two clean glass plates which were stabilised in a pouring stand, and a small volume of water was added to provide a smooth gel interface. Following the polymerisation of the resolving gel and water removal, the stacking gel [830 µl acrylamide, 630 µl 1M Tris-HCl (pH 6.8), 3.4 ml ddH_2O, 50 µl 10% (w/v) APS, 50 µl 10% (w/v) SDS and 5 µl TEMED] solution was poured on top of the resolving gel and a comb was added. Following stacking gel polymerisation, the comb was removed and the wells were washed with 1x SDS-PAGE running buffer [25 mM Tris-HCl (pH 7.5), 250 mM glycine, 0.1 % (w/v) SDS]. *N. caninum* and Vero cell protein samples were prepared using 4x LDS sample buffer (Invitrogen, Paisley, UK) supplemented with 10% β-mercaptoethanol (BME) reducing agent and denatured at 95℃ for 10 min. A total of 7.5 µl ColorPlus pre-stained protein ladder [New England Biolabs: 10-230 kDa (P7711S)] was loaded as a reference for molecular weights, and

N. caninum and Vero cell protein extracts were loaded at a concentration of 10 µg each to separate wells. SDS-PAGE gel was run at 150V in 1x SDS-PAGE running buffer for approximately1 h, until optimum resolution of the marker was achieved.

3.4.10.5 Western blot and immunoblot analysis

Poly-vinylidine fluoride (PVDF) membranes (Millipore U.K. LTD, Feltham, UK) were primed in 100% methanol and equilibrated in SDS-PAGE transfer buffer [25 mM Tris-HCl (pH 8.3), 192 mM glycine and 20% (v/v) methanol]. Two thick pieces of filter paper were also soaked in the transfer buffer. One piece of soaked filter paper was placed on the surface of a Bio-Rad semi-dry transfer apparatus, the soaked PVDF membrane was placed on top of this, followed by the complete SDS-PAGE gel. Finally, the second piece of soaked filter paper was placed on top of the SDS-PAGE gel. Electrophoretic transfer was performed according to the manufacturer's instructions at 150V for 1 h using a Hoefer TE 70 Semi-Dry transfer apparatus (GE Healthcare, Buckinghamshire, UK). Following the transfer, the PVDF membrane was blocked in 10% (w/v) non-fat skimmed milk powder (Sigma) prepared in Tris-buffered saline [50 mM Tris-HCl (pH 8.3), 150 mM NaCl] containing 0.5% (v/v) Tween-20 (TBST). After blocking, the membrane was washed twice quickly with approximately 10 ml TBS-T, and 3 times for 5 min each with TBST, then cut into strips. Membranes were then incubated for 15-18 h at 4^{o}C on a rocker with the primary antibodies, i.e. rabbit anti-cleaved caspase 3 mAb (1:1,000), rabbit anti-human caspase 8 pAb (1:1,000), rabbit anti-caspase 9 pAb (1:1,000) and rabbit anti-*N. caninum* pAb (1:500) diluted in antibody diluent (Abcam, Cambridge, UK). For antibody and manufacturers' details, refer to Table 3.2 above. Following incubation, the strips were washed 3 times for 5 min each with TBST.

Binding of the primary antibodies was detected with the goat anti-rabbit HRP-conjugated secondary antibody (1:2,500; Abcam) diluted in antibody diluent (Abcam) and applied for 1 h at RT on a rocker. Following incubation, the strips were washed twice quickly with approximately 10 ml TBS-T, then 3 times for 5 min each with TBS-T. Binding of the secondary antibody was detected by enhanced chemi-luminescence (ECL)-Plus (GE Healthcare). Antibody-bound proteins were visualised on a Bio-Rad Molecular Imager ChemiDoc XRS+ with Image Lab Software (Bio-Rad laboratories Ltd, CA, USA) and images saved as TIFF files.

3.4.11 Ultrastructural examination of *N. caninum*-infected cells by transmission electron microscopy (TEM)

Cultures containing $3x10^6$ HepG2 cells grown in T75 tissue culture flasks were infected with $6x10^6$ *N. caninum* tachyzoites (Liverpool strain, MOI of 2:1) and harvested at 40, 42 and 44 h post infection. Cell culture monolayers were harvested from flasks using a sterile cell scraper (Fisher Scientific). Cells were centrifuged at 858 x g for 10 min and the resulting cell pellet was washed twice and resuspended in PBS in 1.5 ml Eppendorf tubes, then centrifuged at 1,000 x g for 10 min. Pellets were fixed in 2.5% glutaraldehyde in 0.1 M sodium cacodylate buffer, pH 7.4, at 4°C until further processing. Processing of the pellets for TEM was undertaken by the technician in the Electron Microscopy Unit, Veterinary Laboratory Services, School of Veterinary Science, University of Liverpool (conventional TEM) and the Electron Microscopy Unit, Institute of Veterinary Pathology, Vetsuisse Faculty, and the Centre for Microscopy and Image Analysis, University of Zurich, Switzerland (3D-TEM).

For the conventional TEM processing, samples were washed in 0.1 M sodium cacodylate buffer for 10 min and post-fixed in 1% (w/v) osmium tetraxide for 40 min. Subsequently, specimens were washed in distilled water for 10 min then prestained in uranyl acetate (2% UA in 0.69% maleic acid) for 40 min. Specimens were then dehydrated in graded series of ethanol (50, 70, 90 and 3 x 100%), and in acetone 100% (3 x 5 min each). Samples were then routinely embedded and went through a graded acetone series in resin, 30:70 Taab resin in acetone for 40 min, 70:30 mix and the procedure was repeated twice using 100% resin for 1 h each. Specimens were then transferred into polyethylene moulds of undiluted resin for embedding and incubated at 60°C overnight (15-18 h). Semi-thin sections were cut, stained with methylene blue and examined to select areas of interest for ultrastructural examination. Ultrathin sections were then cut from the polymerised blocks with a diamond knife (Diatome Ltd, Biel, Switzerland) on an ultracut ultramicrotome (Reichert Jung, Vienna, Austria) then loaded onto 200 mesh copper grids (Agar Scientific, Essex, UK). Staining with uranyl acetate and lead citrate was performed. Sections were viewed on a Philips EM208S (FEI UK Limited, Cambridge, UK) operating at 80 kV.

For the 3D-EM, tissue blocks were fixed in 2.5 glutaraldehyde in 0.1 M sodium cacodylate buffer, pH 7.4, overnight at 4ºC, washed in 0.1 M PB for 3 x 15 min, and post-fixed in 1% osmium tetroxide in 0.1 M PB for 1-2 h at RT. Specimens were washed 3 times for 10 min in distilled water and en-bloc stained with 2% aqueous uranyl acetate for 1 h at RT, then washed 3 x 5 min in distilled water. For dehydration, specimens were immersed in 50/70/95% ethanol for 10 min each, then in 100% ethanol and 100% propylene oxide for 3 x 15 min. For infiltration with resin, they were subsequently immersed in 1:1 EMBed 812 and propylene oxide overnight at RT in capped vials on a shaker and finally embedded in 100% EMBed 812 for 2 h at RT with subsequent polymerisation at 60–70ºC (~65 ºC) in an oven for 48 h. Semithin sectioning and staining was performed as described above. Preevaluation of sections and digital imaging was performed with a Philips CM 10 (Philips, Eindhoven, Netherlands) and a Gatan Orius Sc1000 (832) digital camera, (Gatan Inc., Pleasanton, USA). For FIB-SEM nanotomography ("3D-EM"), ultrathin sections from these blocks were imaged with a TEM (Leo 912, Zeiss, Oberkochen, Germany) to localise *N. caninum* tachyzoites. Epoxy blocks were then glued onto an aluminum SEM sample holder by applying conductive carbon cement at the bottom and the sides. The sample was sputter coated with 10 nm of carbon. Milling and imaging was performed continuously in an Auriga 40 cross beam system (Zeiss, Oberkochen, Germany) using the FIBICS Nanopatterning software (Fibics Inc., Canada). Milling was carried out with a gallium-ion beam at 30 kV, 600 pA current, and a *z*-spacing of 15 nm. SEM images were acquired at an acceleration voltage of 1.5 kV using an in-lens energy selective backscattered electron dectector (ESB) with a grid voltage of 1.3 kV and 14 µs dwell time. The pixel-size was set to 15 nm and tilt-corrected to obtain isotropic voxels. The obtained stack of serial images was registered and aligned with the software Fiji and the plugin TrackEM2. The 3D model of the data was visualized by loading the image stack into Imaris (Bitplane AG, Zurich, Switzerland).

The distance between the PVM and associated outer mitochondrial membrane (OMM) was measured on images of known magnification and the mean and standard deviation calculated using IBM SPSS Statistics 20 software (IBM Corp.).

3.5 RESULTS

3.5.1 Culturing and infection of primary bovine hepatocytes

Primary bovine hepatocytes were isolated from livers of cows and infected with *N. caninum* tachyzoites to evaluate their effects on bovine hepatocytes *in vitro*. Livers from adult animals were used since it was impossible to acquire viable bovine foetal tissues at a slaughterhouse for the isolation of hepatocytes. Assessment of cell viability in freshly isolated bovine adult hepatocytes (Fig. 3.1A), using trypan blue exclusion, showed an average viability of 76% (range 67.5 - 84.5%). Hepatocytes seeded onto T25 collagen-coated flasks began to adhere to the culture flasks after approximately 2 h in culture. After 24 h, numerous non-adherent, i.e. non-viable cells were observed floating in the medium and subsequently removed together with the old growth medium. Adhering hepatocytes exhibited an epithelial phenotype and survived in culture for approximately 8 d while maintaining their morphology (flat cells with one or two round nuclei, granular and sometimes vacuolated cytoplasm). After a week in culture, a heterogeneous population of cells, with high numbers of spindle-shaped cells (consistent with myofibroblasts), was observed among the hepatocytes. The proliferation of fibroblasts subsequently resulted in the overgrowth and death of the hepatocytes.

Following infection of the isolated hepatocytes (approximately 24 h post isolation) with *N. caninum* tachyzoites at different MOI (0.5, 1 and 2 tachyzoites to 1 hepatocyte), numerous dead, detached cells were observed in the flasks during the first 12-24 hpi. Remaining adhering hepatocytes appeared normal or shrunken, but the hepatocyte population was greatly reduced and therefore unsuitable for further investigation. The light microscopic examination of PFA-fixed, paraffin embedded cell pellets harvested at 24 hpi revealed that the majority of hepatocytes underwent coagulative necrosis, based on their morphology (Fig. 3.1B). Low numbers of viable hepatocytes, with distinct nuclei and cell borders, were observed in the infected culture. The majority of hepatocytes in the control cultures remained unaltered and the cellular morphology was retained, with a flattened appearance (Fig. 3.1C). Low numbers of detached hepatocytes were present in the culture flasks of the uninfected controls, but this did not significantly affect the quantity of viable cells. Due to the high rate of cell death in culture following infection, further studies on isolated bovine hepatocytes were not attempted and the human hepatoma cell line (HepG2)

was subsequently used to study the effects of the parasites and to understand the mechanism of cell death following infection.

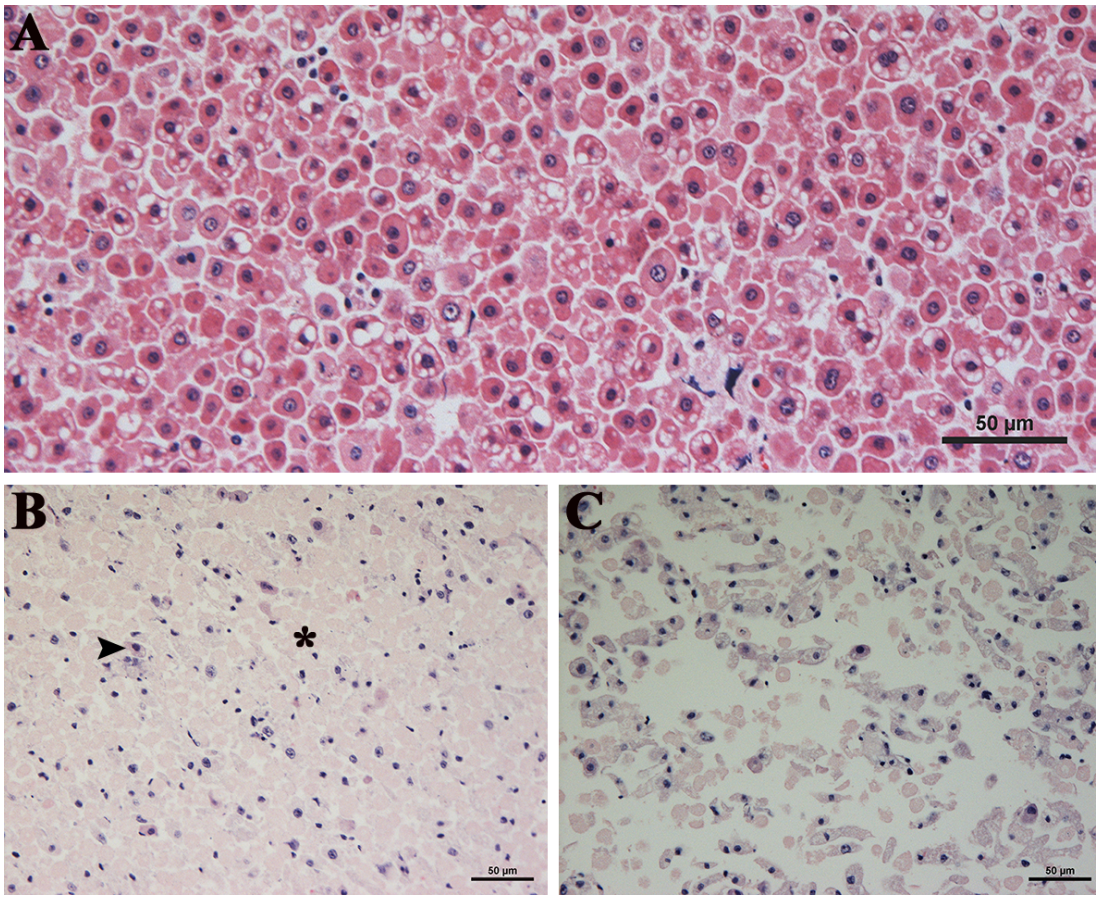

Figure 3.1. Primary bovine hepatocytes, isolated, cultured and infected with *N. caninum* tachyzoites. **A**. Overview of primary bovine hepatocytes 2 h after isolation, presenting as a homogenous cell population. **B**. Hepatocytes following infection with *N. caninum* tachyzoites (MOI of 0.5) and harvested approximately 24 hpi. Low numbers of viable hepatocytes (arrowhead) are present, while the majority of cells are necrotic, with loss of cell borders and nuclei and poorly discernable cytoplasm (asterisk). **C**. Control culture with higher numbers of viable hepatocytes harvested at the same time as the infected culture. HE stains. Bars = 50µm.

3.5.2 *Neospora caninum in vitro* invasion-egression time-course study

Initially, human HepG2, HuH7 and murine Hepa1C cell lines were cultured and infected with *N. caninum* tachyzoites to assess the optimum cell line in terms of growth efficiency and survivability following *N. caninum* infection. All cell lines were harvested, stained immunohistologically and processed for TEM. The HepG2 cell line was subsequently chosen due to its high survivability, uniform monolayer and high growth rate. The *in vitro* invasion-egression study was carried out to ascertain the approximate length of time *N. caninum* takes to invade, replicate and egress from the infected cells (the of invasion has been kept unchanged while studying the time of egression). To ensure that free tachyzoites were removed from

wells after infection, each well was washed twice with sterile PBS after 1 h incubation, to remove all remaining parasites. Extracellular tachyzoites were not observed between 12 and 24 hpi. The first sign of parasite egress was seen at approximately 36 hpi on a chamber slide culture infected with an MOI of 2:1 (parasites/cells). In a repeat experiment under the same conditions and an MOI of 5:1, parasite egress was first observed at approximately 48 hpi. Following egress, abundant cell debris was present within infected wells compared to controls, suggesting increased cell death around the time of parasite egress. Immunohistological demonstration of *N. caninum* antigen in the monolayer on the chamber slides revealed numerous large intact PV with high numbers of tachyzoites (Fig. 3.2A). Cell death was more extensive in the infected cultures following parasite egress, with large empty spaces observed on the monolayer, compared to the uniform growth on the control slides (Fig. 3.2B). Based on these results, all subsequent *in vitro* infections were carried out with an MOI of 2:1.

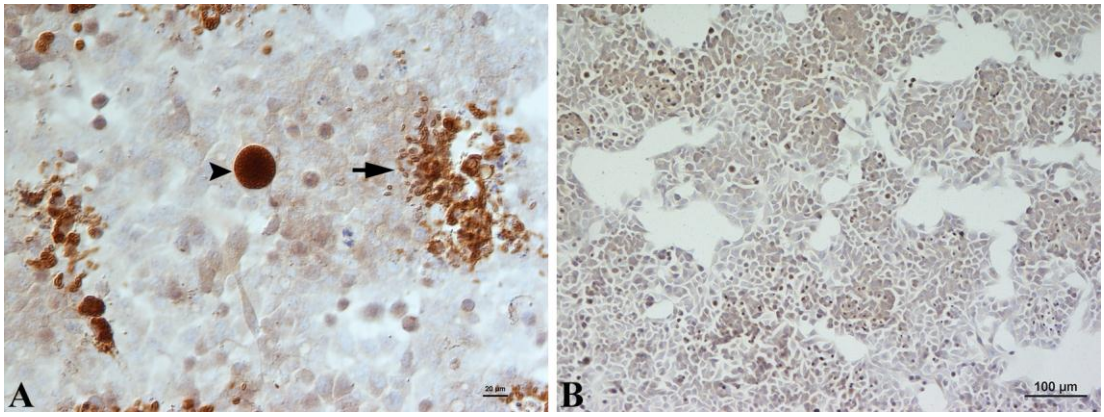

Figure 3.2. HepG2 cells following infection with *N. caninum* tachyzoites and harvested at 60 hpi (for methods, see Chapter 2, section 2.4.6). **A**. Numerous intact PVs with high numbers of tachyzoites (arrowhead) are present. The majority are undergoing parasite egress (arrow). Bar = 20 µm. **B**. Control culture showing 100% confluence. Bar = 100 µm. PAP method, Papanicolaou's haematoxylin counterstain.

3.5.3 SDS-PAGE and immunoblot analysis

The results of the immunohistological and immunofluorescence stains provided strong evidence of cross reaction of the primary antibodies against caspases 3, 8 and 9 with *N. caninum* tachyzoites in both HepG2 and HL-1 cells. Tachyzoites within intact hepatocytes and cardiomyocytes were stained with the respective antibodies, while the specific cytoplasmic (all caspases) and/or nuclear (caspase 9) reaction was not observed in the cells (Figs. 3.5 and 3.17). To ascertain whether the binding of the antibodies to the parasites was non-specific, protein extract from free *N. caninum*

tachyzoites cultured under the same condition as those used for the initial immunohistological staining, was analysed by SDS-PAGE and immunoblotting with the same primary antibodies. Vero cell protein extract served as a positive control, and the immunoblots yielded a complex of immunoreactive banding specific for their respective antigens (Fig. 3.3): a 12 KDa protein representing the small subunit (cleaved) caspase 3 and a band representing pro-caspase 3 (approximately 32 KDa); a band of approximately 30 KDa detected by anti-human caspase 8; while anti-caspase 9 detected 2 bands, a 25 and 35 KDa protein, representing the full length and cleaved intermediate caspase 9, respectively. These results confirm the specificity of the antibodies for the respective caspase. In contrast, immunoblots on the parasite extracts showed that the antibodies react with unknown proteins, ranging in size from approximately 10 to 40 KDa, with a similar pattern for all three antibodies. The rabbit anti-human caspase-8 antibody yielded the strongest bands, which correlated with the intensity of the immunohistological reaction that prompted the immunoblot analysis. These findings are consistent with non-specific binding of the anti-caspase antibodies to *N. caninum* antigens.

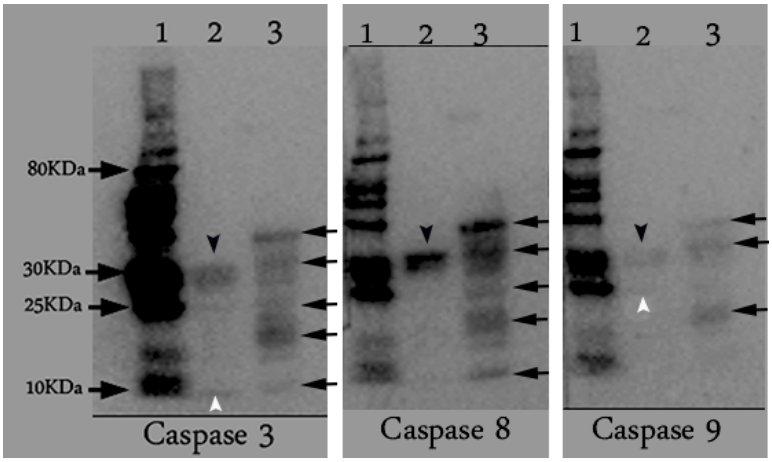

Figure 3.3. SDS-PAGE and immunoblot analysis of *N. caninum* (Nc-Liverpool) and Vero cell (positive control) protein extract run under reducing condition with rabbit antibodies against cleaved caspase 3, caspase 8 and caspase 9. Lane 1 – molecular weight markers; Lane 2 –Vero cell protein extract (positive control); Lane 3 – *N. caninum* protein extract. **Caspase 3**. Vero cells and *N. caninum* protein extract (10 µg) incubated with rabbit anti-cleaved caspase 3 and detected by immunoblot. A 32 KDa (pro-caspase 3, black arrowhead) and a 12 KDa (small subunit caspase 3, white arrowhead) are detected. The primary antibody also binds to several parasite proteins ranging from approximately 10-40 KDa (arrows, lane 3). **Caspase 8**. Vero cells and *N. caninum* protein extract (10 µg) incubated with rabbit anti-human caspase 8 and detected by immunoblot. Lane 2 – 30 KDa protein (arrowhead, Vero cells). The primary antibody also binds to several parasite proteins ranging from approximately 10-40 KDa (arrows, lane 3). **Caspase 9**. Vero cells and *N. caninum* protein extract (10 µg) incubated with rabbit anti-caspase 9 and detected by immunoblot. Lane 2 – 35 KDa protein (black arrowhead, cleaved intermediate) and a 25 KDa protein (white arrowhead, full length caspase 9) are identified.

The primary antibody also binds to several parasite proteins ranging from approximately 10-40 KDa (arrows, lane 3).

3.5.4 Cytopathic effects of *N. caninum* in HepG2 hepatoma cells

In vivo studies (Chapter 2) showed evidence of hepatocellular necrosis and apoptosis in foetuses from dams infected at 70 dg, and the presence of large numbers of cleaved caspase 3-positive apoptotic, uninfected hepatocytes. To further assess the effect of the parasite on hepatocytes, the expression of cleaved caspase 3, caspase 8 and caspase 9 was evaluated by immunohistology in an immortalised human hepatoma cell line, HepG2, *in vitro*. By light microscopy, both uninfected and infected hepatoma cells exhibited a normal morphology, while low numbers of apoptotic bodies were observed (Figs. 3.4A-F). In infected culture, moderate numbers of *N. caninum* tachyzoites were detected in intact hepatocytes during early time points and increased with time. Cleaved caspase 3-positive hepatocytes were detected in infected cultures at all time points studied, but tachyzoites were only found within intact, cleaved caspase 3-negative hepatocytes (Fig. 3.5A). In comparison, the uninfected control cultures (16-32 hpi) contained lower numbers of caspase 3-expressing apoptotic hepatocytes (Fig. 3.5D; 32 hpi) at the corresponding time points. Quantitative analysis of cleaved caspase 3 expression revealed no significant differences in the mean numbers of apoptotic cells between infected cultures and uninfected control cultures from 0-16 hpi (Fig. 3.6; $p>0.05$, Mann-Whitney U test). At 20 hpi, however, the number of cleaved caspase 3-positive apoptotic hepatocytes was significantly increased and remained high until 36 hpi in infected cultures compared to controls (Fig. 3.6; $p=0.029$, Mann-Whitney U test). No significant differences were observed between infected and control cultures after the 36 hpi time point, although slightly higher numbers of apoptotic cells were present in infected cultures.

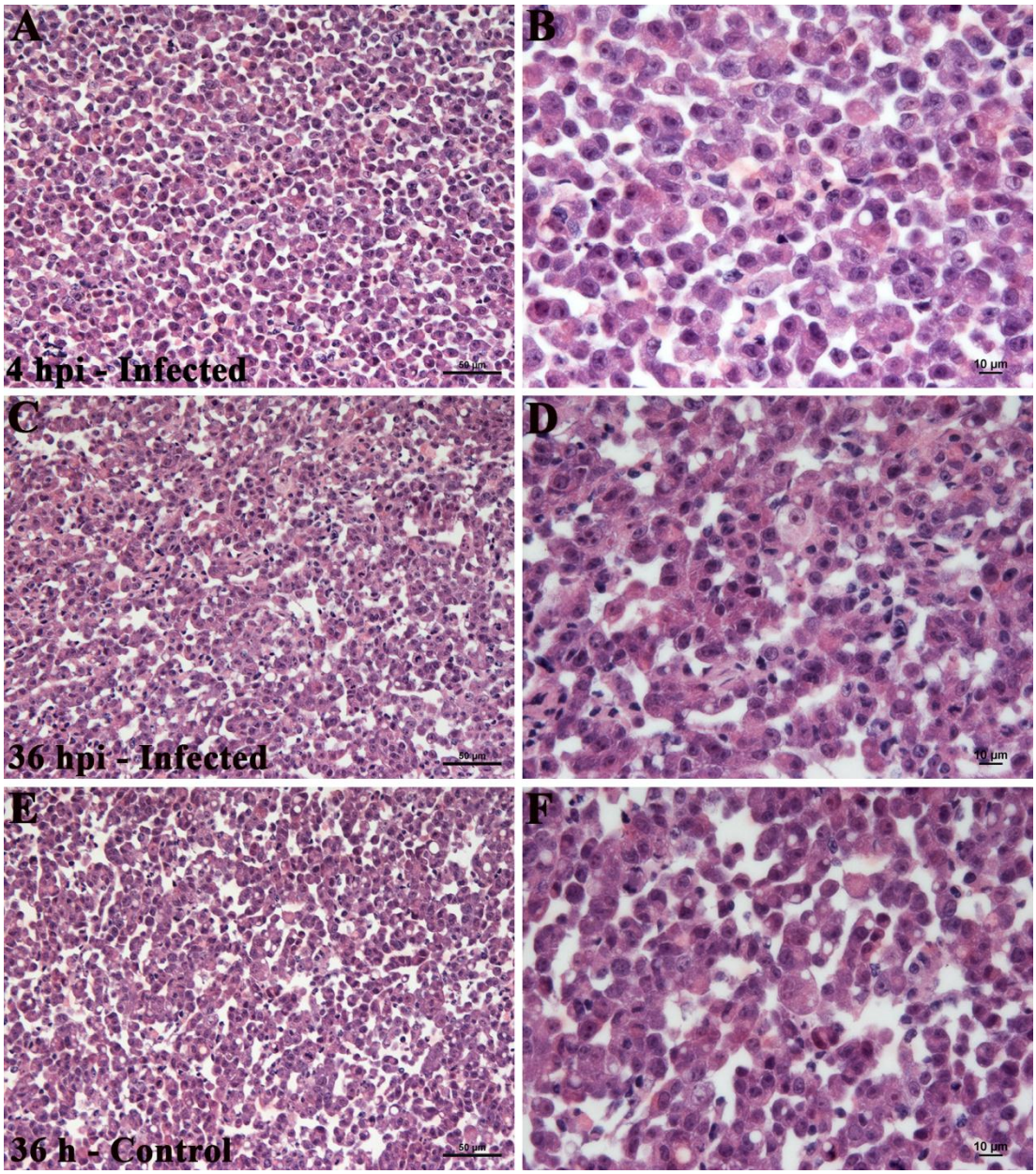

Figure 3.4. Overview of cell pellet from *N. caninum*-infected (MOI of 2:1) and uninfected cultured HepG2 cells harvested at 4 hpi (A, B) and 36 hpi (C-F). **A**. At 4 hpi, hepatocytes are generally viable. HE stain. Bar = 50µm. **B**. Higher magnification of A. HE stain. Bar = 10µm. **C**. At 36 hpi, *N. caninum*-infected culture has high numbers of viable hepatocytes. HE stain. Bar = 50µm. **D**. Higher magnification of C showing viable hepatocytes. HE stain. Bar = 10µm. **E**. At 36 hpi, uninfected control cultures exhibit high numbers of viable hepatocytes. HE stain. Bar = 50µm. **F.** Higher magnification of E. HE stain. Bar = 10µm.

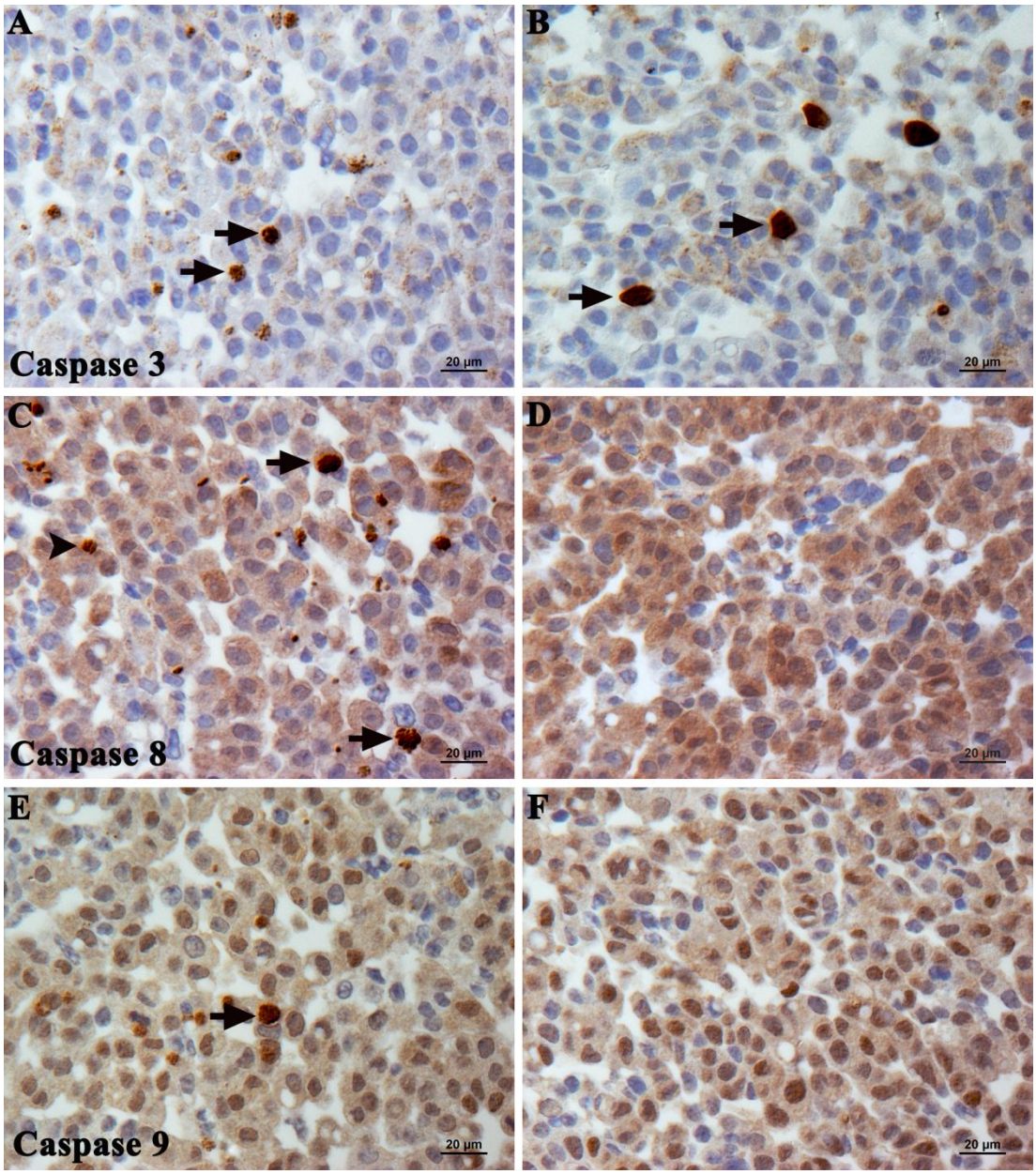

Figure 3.5. Cell pellet from *N. caninum*-infected (A, C, E) and uninfected (B, D, F) HepG2 cells harvested at 36 hpi, stained for the expression of cleaved caspase 3 (A, B), caspase 8 (C, D) and caspase 9 (E, F). **A**. *N. caninum* tachyzoites (cross reaction with caspase antibody, discern based on parasite morphology) are detected within intact hepatocytes that are not labelled for caspase 3 (arrows). **B**. Uninfected control culture showing caspase 3 expression. **C.** *N. caninum* tachyzoites are detected within viable cells not labelled for caspase 8 (arrow) and within caspase 8-positive hepatocytes (arrowhead). **D.** Uninfected control culture showing similar caspase 8 expression. **E**. High numbers of caspase 9-expressing hepatocytes are detected and *N. caninum* are present with an intact cell not labelled for caspase 9 (arrow). **F**. Caspase 9-expressing cells are detected in high numbers as in the infected cultures. Figs A-F: PAP method, Papanicolaou's haematoxylin counterstain. Bars = 20µm.

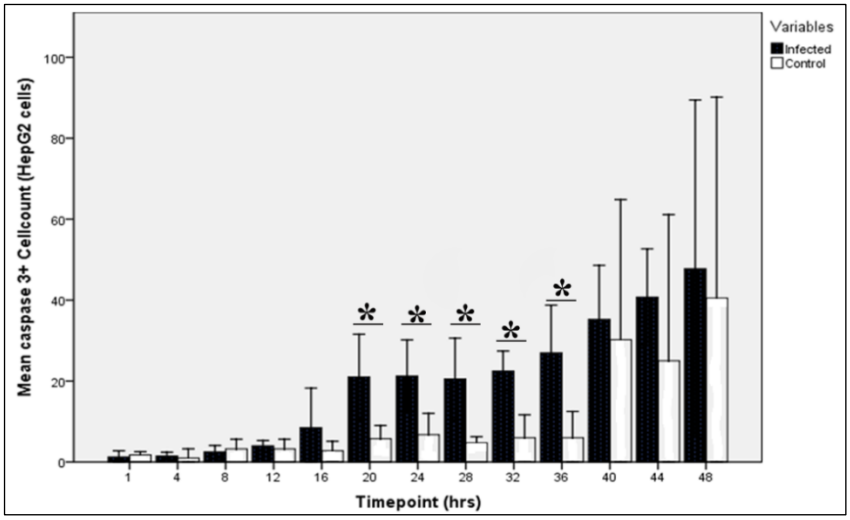

Figure 3.6. Quantitative analysis of caspase 3 expression in *N. caninum*-infected and uninfected HepG2 cells. Cultures were infected with *N. caninum* tachyzoites and apoptotic hepatocytes in 4 randomly selected, non-overlapping, representative HPF were counted and compared with controls at corresponding time points. Significantly higher numbers of caspase 3-expressing hepatocytes were detected in infected cultures compared to controls at 20-36 hpi (asterisk, $p<0.05$). Whiskers represent 95% confidence intervals.

3.5.4.1 Caspase 3 expression in individual N. caninum infected cells using double immuno-labelling. The expression of cleaved caspase 3 was assessed in *N. caninum*-infected cells using the combined IP and IF labelling technique for *N. caninum* tachyzoites and cleaved caspase 3, respectively. Sequential sections, following those used for the individual immunohistological staining for both antigens, were used for the double IP and IF staining. The IP-staining revealed high numbers of *N. caninum* tachyzoites within intact hepatocytes, which exhibited normal cellular morphology (Figs. 3.7A (24 hpi) and 3.7D (36 hpi). No cleaved caspase 3 expression was detected within infected cells by IF; however, surrounding uninfected hepatocytes were clearly positive [Figs. 3.7B, C (24 hpi) and E, F (36 hpi)], confirming the results of the single IH. Lower numbers of caspase 3-positive cells were detected in the control culture, also confirming the result of the single IH.

3.5.4.2 Evaluation of the apoptotic pathways in N. caninum-infected and uninfected HepG2 cells: caspase 8 expression. Immunohistological staining for caspase 8 used sections from PFA-fixed paraffin embedded cultured hepatocytes cut after those used to analyse caspase 3 expression. Caspase 8 expression was characterised by intense cytoplasmic staining in hepatocytes with normal morphology. The semi-quantitative assessment (mean proportion, intensity and immunohistological score) of caspase 8

expressing hepatocytes in four HPF was undertaken and uninfected control and infected cultures compared between 0 and 48 hpi (Figs. 3.8A, B). Despite the apparent cross reaction of the anti-human caspase 8 antibody with *N. caninum* tachyzoites, it was possible to distinguish between parasites (based on their morphology) and host cell caspase 8 expression. *N. caninum* tachyzoites were clearly identified in hepatocytes not labelled for caspase 8 at different time points and were sometimes detected within intact caspase 8 expressing cells with normal morphology (Fig. 3.5B). The number of caspase 8-positive hepatocytes (normal cellular morphology) in infected cultures at each time point was generally high and considerably higher than the number of cleaved caspase 3 expressing cells at each corresponding time point. Control cultures had equally high numbers of caspase 8-expressing cells as the infected cultures (Fig. 3.8E). Semi-quantitative data analysis of caspase 8-expressing hepatocytes in both infected and control cultures revealed a steady decline from the initial mean proportion at 0-20 hpi, followed by a plateau at 20-24 hpi (Fig. 3.8A). An increased number of caspase 8-positive cells was observed at 28 hpi, followed by a gradual decrease up to 48 hpi. This pattern was apparent in both infected and control cultures and there was no significant difference between the two at corresponding time points (Figs. 3.8A-B; $p>0.05$, Mann-Whitney U test).

The double IP and IF technique was used to detect tachyzoites and expression of caspase 8 in individual *N. caninum*-infected and uninfected HepG2 cells. Staining was performed on sections consecutive to those used for single IH. Clusters of *N. caninum* tachyzoites were detected within intact hepatocytes, which exhibited normal cellular morphology (Fig. 3.9A). Caspase 8 expression was detected by IF in high numbers of hepatocytes in the same section (Fig. 3.9B). The merged IP and IF image revealed that the majority of infected hepatocytes did not express caspase 8 (Fig. 3.9C). However, unlike caspase 3, caspase 8 was also expressed by a few *N. caninum*-infected hepatocytes; these had normal cellular morphology (Fig. 3.9C). High numbers of caspase 8-positive uninfected hepatocytes were detected within the infected culture, and in the control cultures, similar numbers of caspase 8 expressing hepatocytes were evident (Fig. 3.9D-F).

3.5.4.3 Evaluation of the apoptotic pathways in N. caninum-infected and uninfected HepG2 cells: caspase 9 expression. Expression of the mitochondria-dependent caspase 9 was assessed in *N. caninum*-infected HepG2 cells. Immunohistological

staining for caspase 9 was performed on sections from PFA-fixed paraffin embedded cultured hepatocytes cut after those stained for caspase 3 and 8. Caspase 9 expression was detected within intact hepatocytes with normal cellular morphology, and was represented by an intense nuclear (Ritter et al., 2000; Eckle et al., 2004) and cytoplasmic reaction.

Semi-quantitative analysis was carried out as described above for caspase 8. No significant differences were observed between infected and control cells with regard to the mean proportion and immunohistological scores of caspase 9-positive hepatocytes (Fig. 3.10A-B; $p>0.05$, Mann-Whitney U test). A slight increase in the number of caspase 9-positive hepatocytes was observed in the infected cultures at 1, 4, 16, 32 and 44 hpi compared to controls at corresponding time points, but this was not significant. Caspase 9 expression was predominantly detected in uninfected hepatocytes within the infected cultures (Fig. 3.5C). In control cultures, the expression was similar to that observed in infected cultures (Fig. 3.5F). The number of caspase 9 expressing cells increased slightly (0-16 hpi), followed by a moderate decrease (20-28 hpi; Fig. 3.10A). In comparison, the number of positive cells in the infected cultures increased modestly with time and plateaued at the time when parasite egress was observed (32-36 hpi), but similar numbers of positive cells were present in the controls. A fluctuation in the number of positive cells was observed after 36 hpi.

To further evaluate the activation of the intrinsic, mitochondrial pathway in *N. caninum*-infected and uninfected cells, double IP and IF labelling for *N. caninum* and caspase 9 was performed on a pellet harvested at 36 hpi. Staining was undertaken on sections consecutive to those used for single IH. Clusters of *N. caninum* tachyzoites were detected within intact hepatocytes with normal cellular morphology (Fig. 3.11A). IF of the same section showed high numbers of caspase 9-positive hepatocytes, but *N. caninum*-infected cells were caspase 9-negative (Fig. 3.11B, C). Hepatocytes within the control cultures exhibited similar cellular morphology as infected cells at corresponding time points and similar numbers of caspase 9-expressing hepatocytes (Fig. 3.11D-F), which suggests that factors other than the parasites are responsible for cell death in the *in vitro* model.

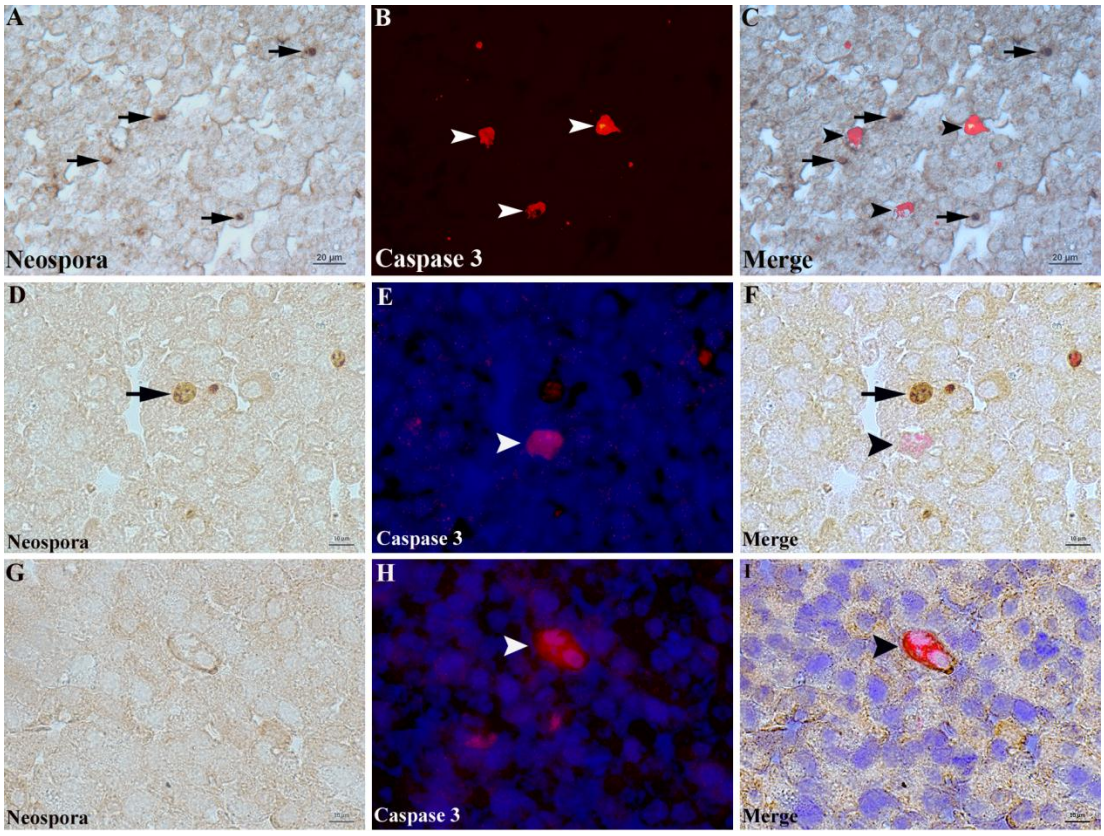

Figure 3.7. Combined immunoperoxidase (IP) and immunofluorescence (IF) labelling of *N. caninum*-infected and uninfected HepG2 cells. IP staining of *N. caninum*-infected and uninfected HepG2 cells using rabbit anti-*N. caninum* pAb with DAKO anti-rabbit EnVision (DAB; A, D, G) and further IF staining using rabbit anti-cleaved caspase 3 labelled with anti-rabbit Dylight 549 (red; B, E, H). Bars = 20 µm. Merged (C, F, I). **A-C**. At 24hpi, *N. caninum* tachyzoites are evident as a brown reaction (DAB) within the cytoplasm of hepatocytes under bright field light (arrows; **A**). IF shows caspase 3 expresson in hepatocytes (arrowheads; **B**). Overlay of images A and B showing no co-localisation of *N. caninum* tachyzoites (arrows) and caspase 3 expressing cells (arrowheads) (**C**). **D-F**. At 36hpi, clusters of *N. caninum* tachyzoites are detected as a brown reaction (DAB) within intact hepatocytes (arrow, **D**). IF shows caspase 3 expressing hepatocyte (arrowhead, **E**). Overlay of D and E showing no co-localisation of caspase 3 expressing hepatocyte (arrowhead) with *N. caninum* tachyzoites (arrow) (**F**). **G-I**. At 36hpi, uninfected controls culture without *N. caninum* tachyzoites (**G**). IF reveals caspase 3 expressing hepatocytes with diffuse cytoplasmic staining (arrowhead; **H**). Overlay of G and H showing caspase 3 expression in an uninfected hepatocyte (arrowhead; **I**).

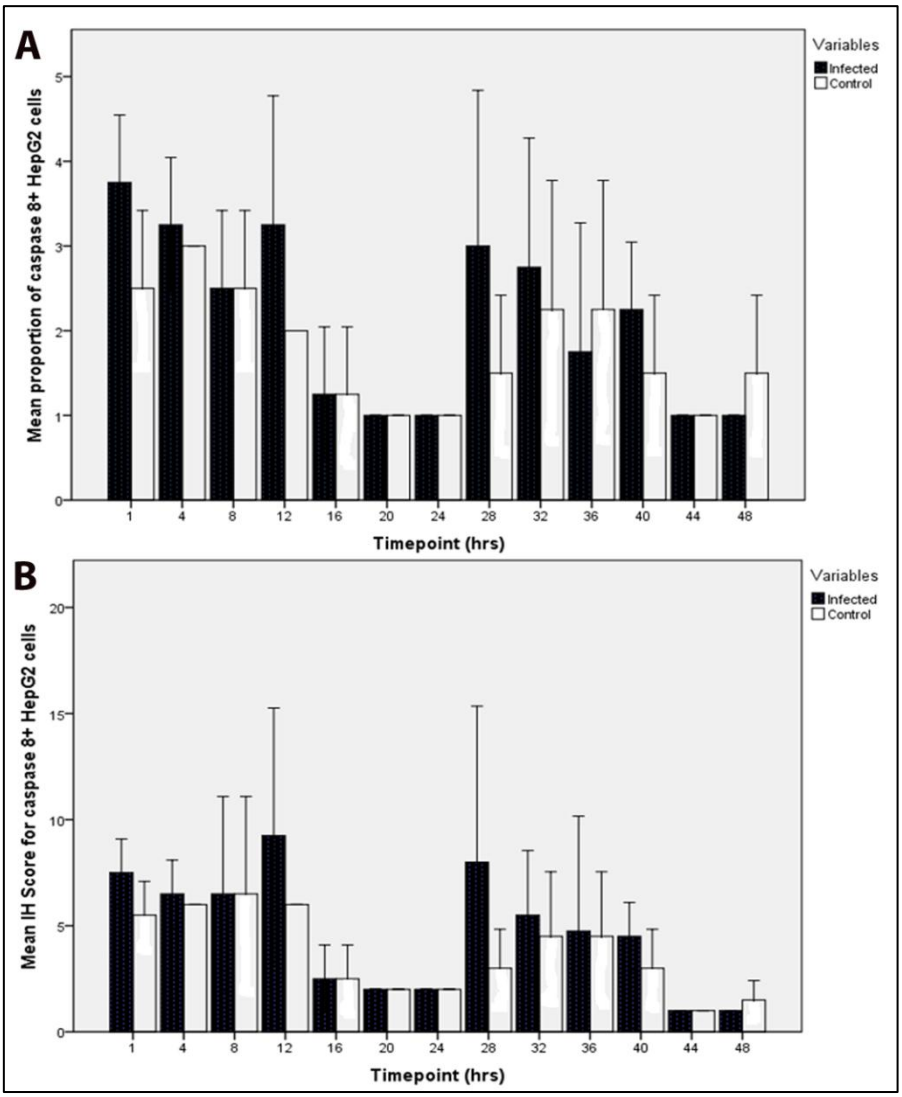

Figure 3.8. Semi-quantitative analysis of caspase 8 expression in *N. caninum*-infected and uninfected HepG2 cells. **A**. Mean proportion of caspase 8-expressing hepatocytes in infected (black bars) and control cultures (white bars). No significant differences are observed between infected and control cultures at corresponding time point. **B**. Mean immunohistological scores for caspase 8 expression at corresponding time points. No significant differences were observed between infected (black bars) and uninfected control (white bars) cultures. Whiskers represent 95% confidence intervals.

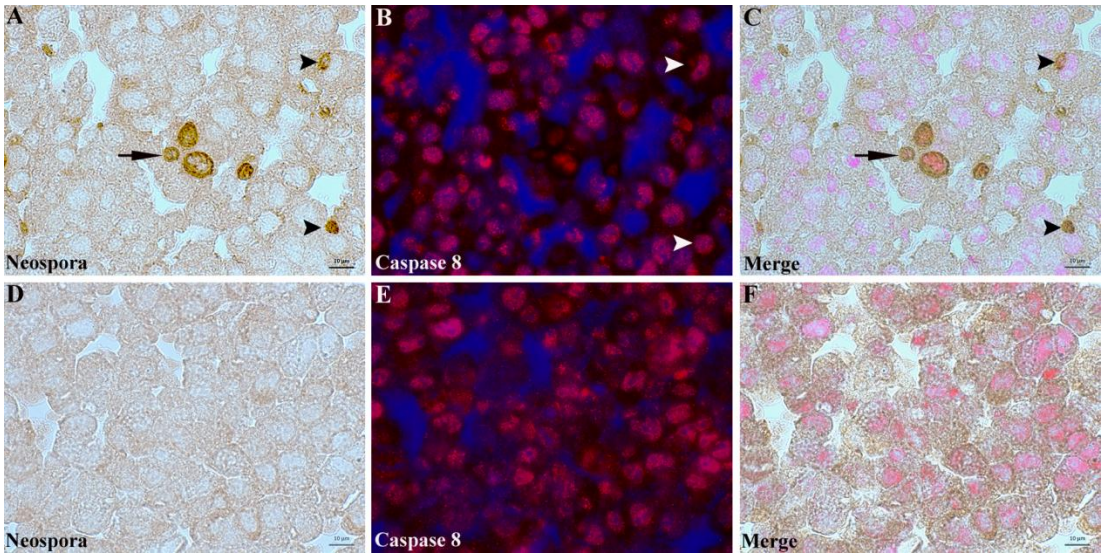

Figure 3.9. Combined immunoperoxidase (IP) and immunofluorescence (IF) labelling of *N. caninum*-infected and uninfected HepG2 cells using rabbit anti-*N. caninum* pAb with DAKO anti-rabbit EnVision (DAB; A, D) and further IF staining using rabbit anti-human caspase 8 labelled with anti-rabbit Dylight 549 (red; B, E). Bars = 10µm. Merge (C, F). **A-C**. At 32hpi, *N. caninum* tachyzoites are evident (DAB) in the cytoplasm of intact hepatocytes (arrow) and two clusters within caspase 8-expressing hepatocytes (arrowheads) (A). IF staining reveals high numbers of caspase 8 expressing hepatocytes and two cells where *N. caninum* tachyzoites are detected under bright field light (arrowheads) (B). Overlay of A and B showing clusters of tachyzoites within intact hepatocytes (arrow) and *N. caninum* tachyzoites within caspase 8 expressing cells (arrowheads) (C). **D-F**. At 36hpi, uninfected control culture under bright field is negative for *N. caninum* tachyzoites (D). IF shows high numbers of caspase 8 expressing hepatocytes (E). Overlay of D and E showing caspase 8 expression in uninfected HepG2 cells (F).

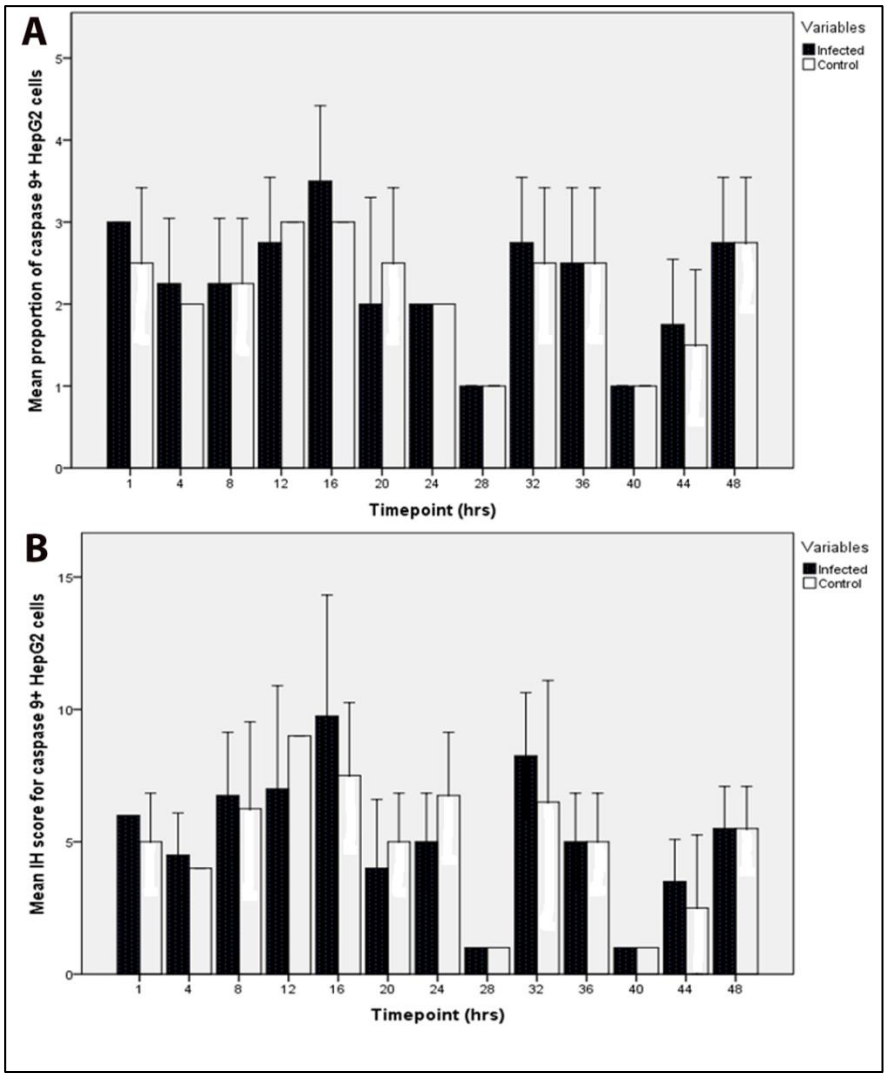

Figure 3.10. Semi-quantitative analysis of caspase 9-expression in *N. caninum*-infected and uninfected HepG2 cells. **A**. The mean proportion of caspase 9-expressing cells in infected (black bars) and control cultures (white bars). Significant differences were not observed in caspase 9-expression. **B**. Mean immunohistological score for caspase 9-expression in *N. caninum*-infected hepatocytes (black bars) and controls (white bars). Significant differences were not observed between infected and controls. Whiskers represent 95% confidence intervals.

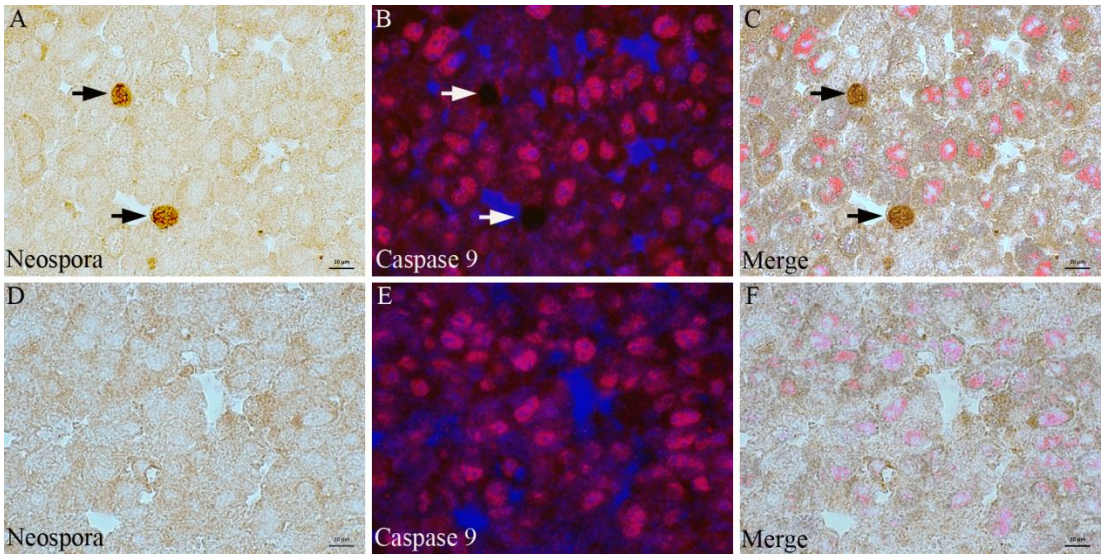

Figure 3.11. Combined immunoperoxidase (IP) and immunofluorescence (IF) labelling of *N. caninum*-infected and uninfected HepG2 cells using rabbit anti-*N. caninum* pAb with DAKO anti-rabbit EnVision (DAB; A, D) and further IF staining with rabbit anti-caspase 9 labelled with anti-rabbit Dylight 549 (red; B, E). Bars = 10µm. Merge (C, F). **A-C**. At 36hpi, large clusters of *N. caninum* tachyzoites are detected within intact hepatocytes (arrows; **A**). IF reveals high numbers of caspase 9 expressing hepatocytes. Arrows point to areas where tachyzoites are detected under bright field light (**B**). Overlay of A and B showing clusters of tachyzoites in hepatocytes not labelled for caspase 9 (arrows; **C**). **D-F**. At 36hpi, uninfected control culture under bright field light is negative for *N. caninum* tachyzoites (**D**). IF reveals high numbers of caspase 9 expressing hepatocytes in the control culture (**E**). Overlay of D and E showing the distribution of caspase 9 expressing cells in the control culture (**F**).

3.5.5 Mitochondrial organisation in *N. caninum* infected HepG2 cells

The HepG2 cell line was used to assess the organisation of host cell mitochondria during *N. caninum* infection. In infected cultures at 24 and 32 hpi, *N. caninum* tachyzoites were detected within intact hepatocytes in which aggregates of host cell mitochondria were seen in close association with the PVM (Figs. 3.12A-C; 24 hpi and D-F; 32 hpi). Mitochondria were clumped in close proximity to the PVM. In contrast, uninfected hepatocytes in the infected cultures had large clusters of mitochondria which aggregated mainly in the perinuclear region. Other uninfected bystander hepatocytes in the infected cultures had a more diffuse, homogenous distribution of mitochondria, often with an unaltered reticular pattern consistent with the normal cellular morphology.

In the control cultures, a large population of hepatocytes exhibited diffusely distributed mitochondria or mitochondrial aggregates with a punctate pattern and localised mainly in the perinuclear regions (Figs. 3.12G-I; 32 hpi), similar to uninfected cells in the infected cultures.

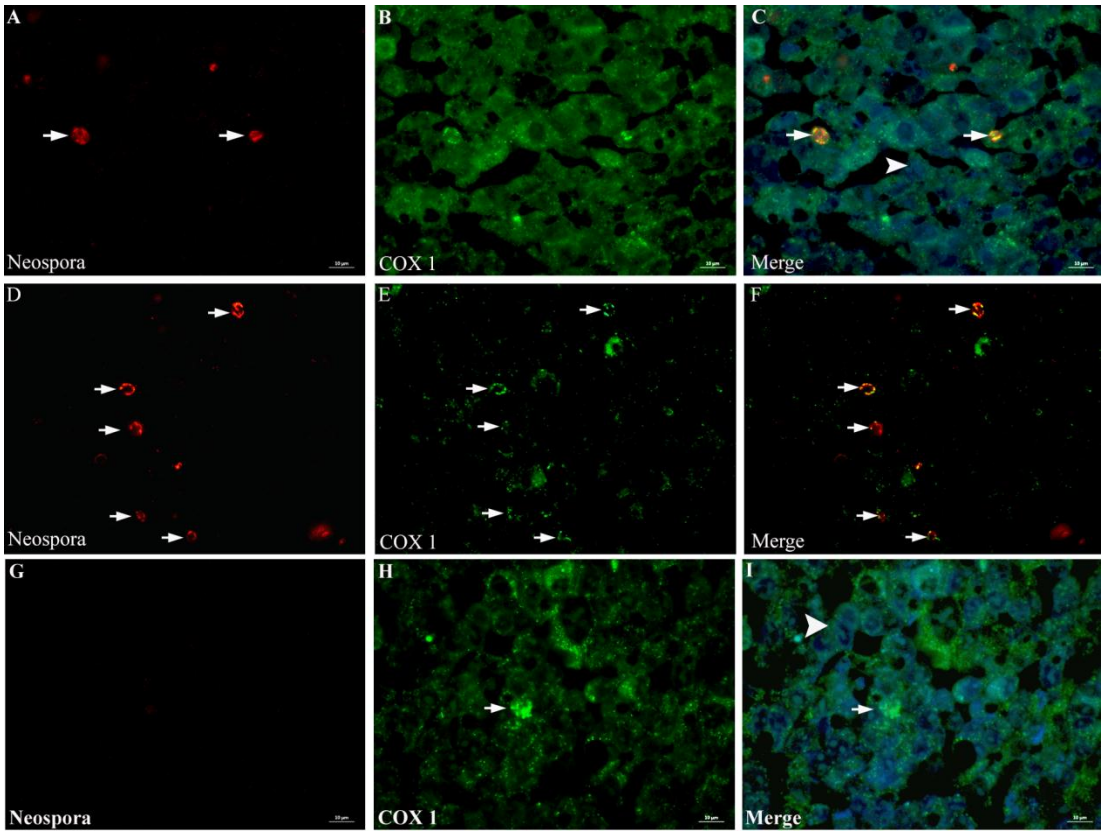

Figure 3.12. Double immunofluorescence (IF) labelling of *N. caninum*-infected and uninfected HepG2 cells with rabbit pAb and labelled with anti-rabbit Dylight 549 (red) and host cell mitochondria detected with mouse anti-MTCO1 mAb and labelled with anti-mouse Dylight 488 (green). Bars = 10µm. A-C. At 24hpi, high numbers of *N. caninum* tachyzoites are detected within hepatocytes (arrows; **A**). Diffuse distribution of host cell mitochondria is detected with clumped pattern observed in cells with *N. caninum* tachyzoites (**B**). Overlay showing close contact of the host cell mitochondria with PVM (arrows; **C**). Arrowhead points to a more diffuse distribution of mitochondria. D-F. At 32hpi, high numbers of parasites are detected within hepatocytes (arrows; **D**). Clumped mitochondria are observed in hepatocytes containing tachyzoites (arrows; **E**). Overlay reveals the close association of the parasites with the host cell mitochondria (arrows; **F**). **G-I**. At 32hpi, tachyzoites are not present in uninfected control culture (**G**). A diffuse distribution of host cell mitochondria is shown within uninfected hepatocytes with clumping and large aggregate, punctate pattern (arrow, COX 1; **H**). Overlay shows the distribution of mitochondria in uninfected hepatocytes and cells with clumping of mitochondria (arrow, COX 1 and DAPI), while others exhibit normal, homogenous distribution in the cytoplasm (arrowhead; **I**).

3.5.6 Ultrastructural characterisation of *N. caninum*-infected hepatocytes

TEM served to closer examine the distribution of host cell mitochondria in *N. caninum*-infected HepG2 cells. In the infected cultures, harvested at 42 hpi, uninfected cells exhibited a normal morphology. Infected cells containing tachyzoites appeared intact, i.e. exhibited morphology similar to uninfected cells (Fig. 3.13). However, a close association of the host cell mitochondria with the *N. caninum* PVM was observed (Figs. 3.14A-B). A few mitochondria even appeared to be in direct physical contact with the PVM (Figs. 3.14A-B and 3.15A-B), while others formed small clusters in close apposition. Despite this, mitochondria were of homogenous size and structure, with unaltered membranes and matrices. The mean distance between the OMM and PVM was 140.30±118.70 nm (n=12) and range from approximately 25 to 375 nm. In viable hepatocytes from the control cultures, mitochondria were randomly distributed throughout the cytoplasm, although found mainly in the perinuclear region (Figs. 3.14C-D and 3.15A-B). Mitochondria were morphologically similar to those observed in the infected cells. Other cells within the control cultures were characterised by cytoplasmic vacuolation and mitochondrial clumping, which are features of early apoptosis (Fig. 3.14D; Haga et al., 2003). These features were not observed in infected cells with viable parasites at similar time points. In infected cells, the endoplasmic reticulum (ER) was often observed in close association with the PVM especially in the perinuclear region (Fig. 3.15B).

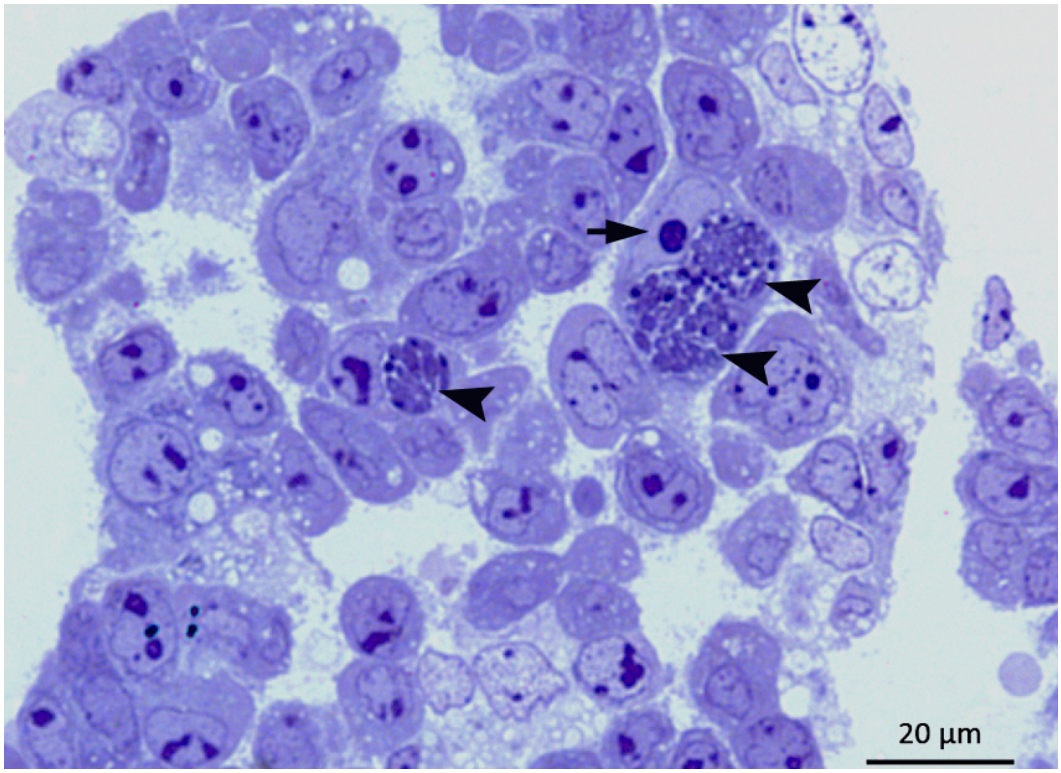

Figure 3.13. Semithin section of a *N. caninum*-infected HepG2 cell pellet harvested at 42 hpi. Clusters of *N. caninum* tachyzoites (arrowheads) are present with intact hepatocytes, exhibiting normal cellular morphology (arrow points to the nucleus of the infected cell). Toluidin blue stain, Bar = 20µm.

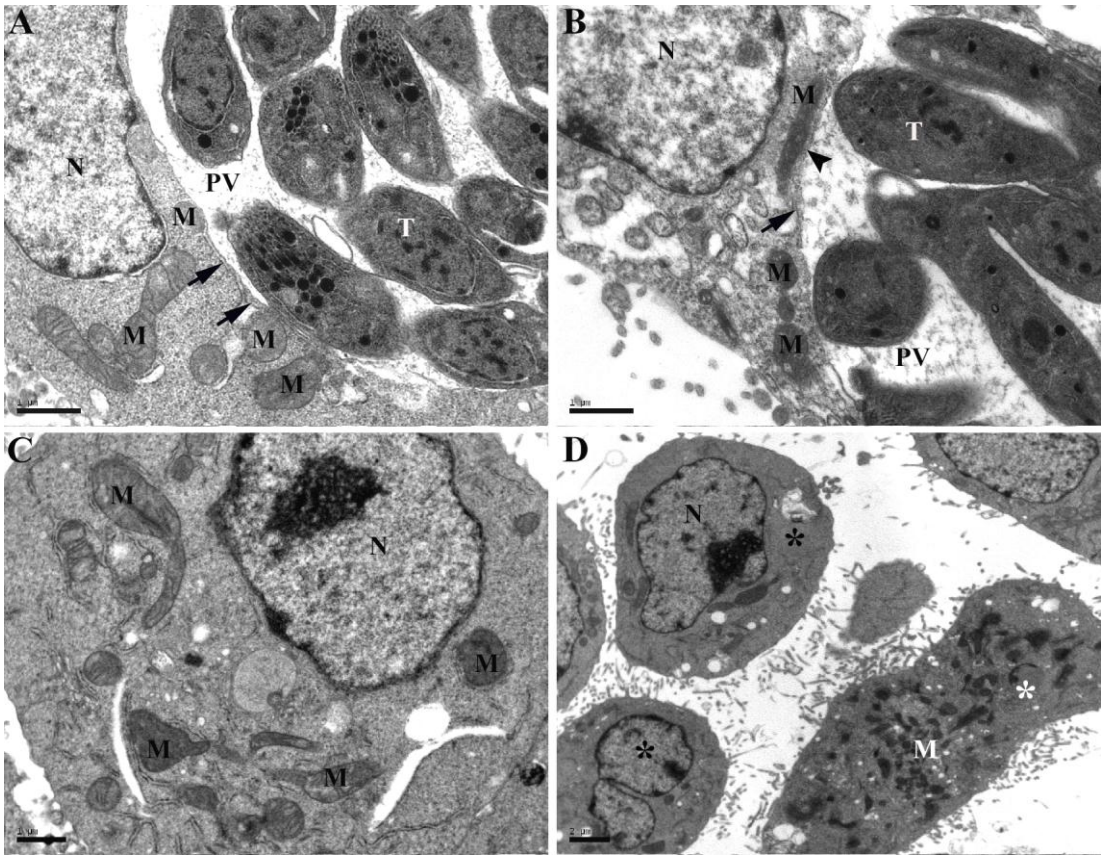

Figure 3.14. Ultrastructural features of *N. caninum*-infected and uninfected HepG2 cells harvested at 42 hpi. **A**. Numerous *N. caninum* tachyzoites (T) are present within the PV in a hepatocyte which otherwise exhibits the normal cellular morphology. A cluster of mitochondria (M) is seen in close contact with the PVM (arrows). Bar = 11,000X. **B**. Hepatocyte with numerous tachyzoites (T) in a PV. A small cluster of mitochondria (M) is located in close apposition to the PVM (arrow) and a single mitochondrium is in direct contact with the PVM (arrowhead). **C**. Uninfected hepatocyte from the control culture with randomly distributed mitochondria (M) in the cytoplasm and surrounding the nucleus (N). Bar = 8,900X. **D**. Control culture. Hepatocytes with normal morphology and randomly distributed mitochondria (black asterisks) and a single apoptotic hepatocyte with clumped mitochondria (M) and small cytoplasmic vacuoles (white asterisk) Bar = 3,500X. Lead citrate/uranyl acetate staining.

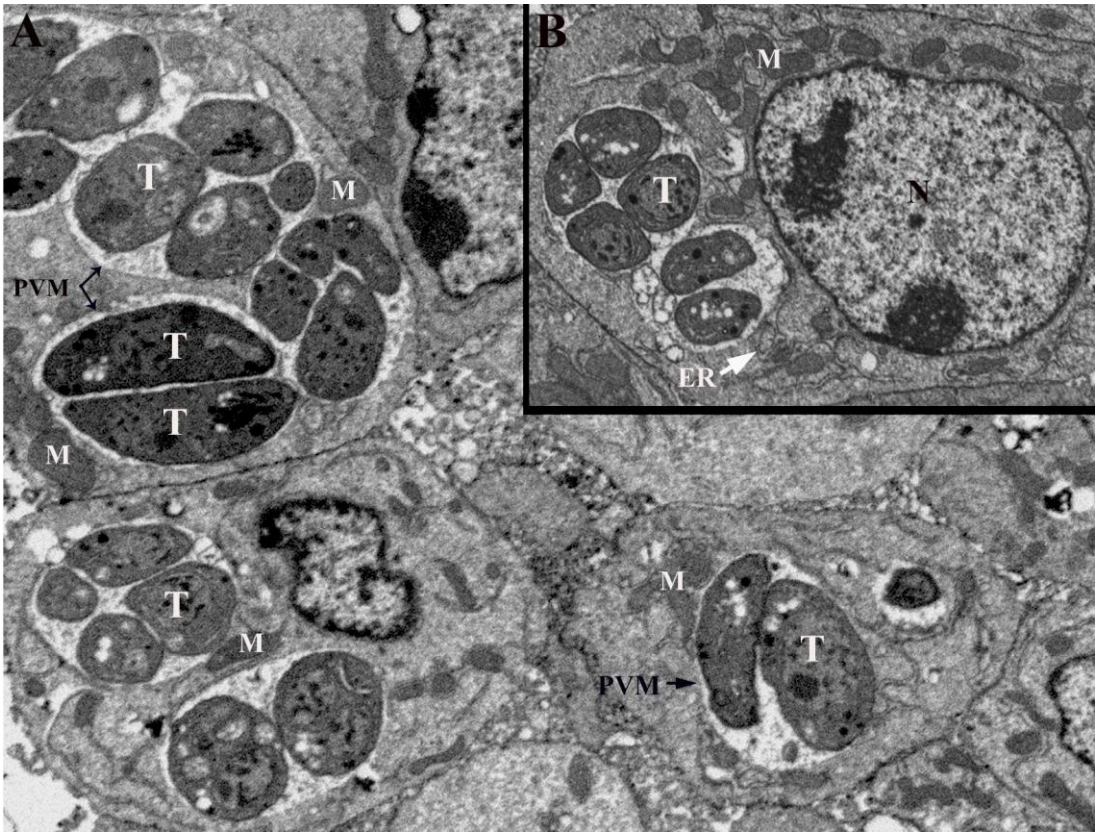

Figure 3.15. Ultrastructural features of *N. caninum*-infected HepG2 cells harvested at 46 hpi. **A**. *N. caninum* tachyzoites (T) are present in hepatocytes with numerous mitochondria (M) that are predominantly located in close contact with the PVM. **B**. Hepatocyte with two PV filled with tachyzoites (T). Numerous mitochondria (M) are located in the perinuclear region and in association with the PVM. Endoplasmic reticulum (ER) is also closely associated with the PVM. Lead citrate/uranyl acetate staining, FIB-SEM Nanotomography.

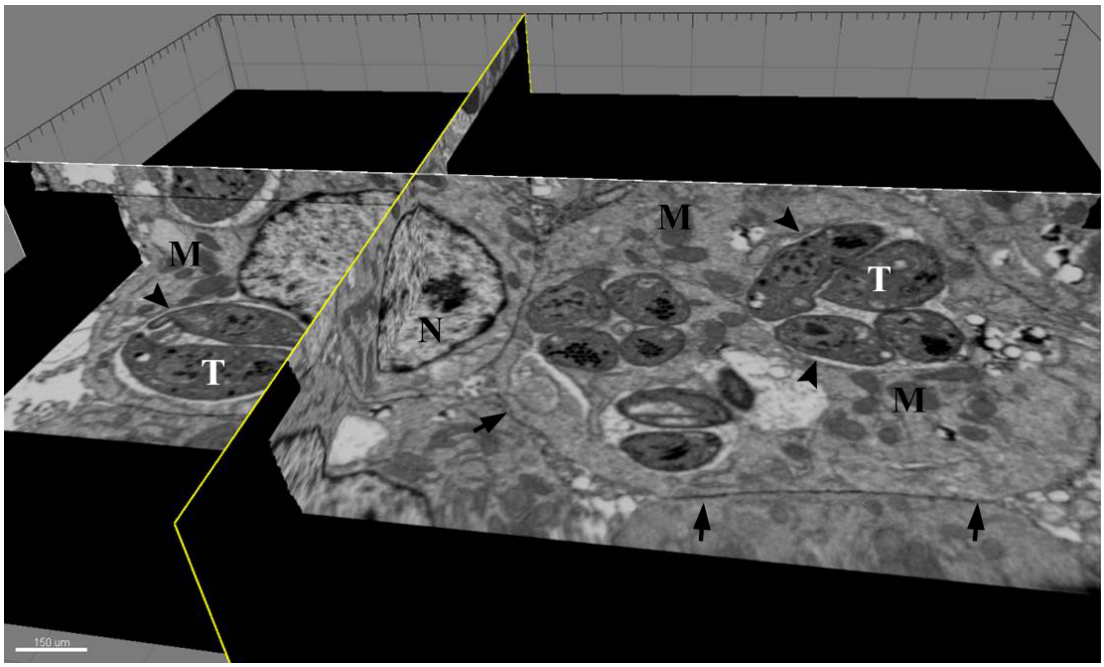

Figure 3.16. Example of the 3D model image stack of *N. caninum*-infected HepG2 cells harvested at 46 hpi (same as in Fig. 3.15) and visualised using the Imaris software. Tachyzoites (T) are present within vable hepatocytes (arrows, cell border). Mitochondria (M) are seen in the cytoplasm surrounding the nucleus (N) and in association with PVM (arrowhead). Lead citrate/uranyl acetate staining, FIB-SEM Nanotomography.

3.5.7 Effects of *N. caninum* on HL-1 murine cardiomyocytes

Large numbers of *N. caninum* tachyzoites were detected within intact cardiomyocytes of foetuses from experimentally infected cows in early gestation without evidence of cell degeneration (Gibney et al., 2008). To further investigate these *in vivo* observations, the interaction between *N. caninum* and cardiomyocytes was investigated to understand why the parasites appear to have a different effect in these cells compared to hepatocytes. For this purpose, an *in vitro* cardiomyocyte culture system was used. Activation of the intrinsic (caspase 9) and extrinsic (caspase 8) apoptotic cascade, along with expression of the effector caspase 3 was evaluated for evidence of apoptotic cell death in cardiomyocytes in association with *N. caninum* infection, either as a result of the direct impact of the parasites in infected cells or indirectly in neighbouring uninfected cells, similar to the effect in cultured hepatocytes. In the HE-stained sections of the PFA-fixed and paraffin embedded cardiomyocyte pellets, a uniform population of cardiomyocytes, with low numbers of apoptotic bodies was observed in both the infected and control cultures (Figs. 3.17A-F). Cleaved caspase 3 was detected in the cytoplasm of cells with the morphology of apoptotic cells. Morphological assessment and quantification of cleaved caspase 3-

positive cells showed that in the infected cultures, *N. caninum* tachyzoites were only detected within cleaved caspase 3-negative, viable cardiomyocytes, whereas a proportion of uninfected cells was found to be cleaved caspase 3-positive (Figs. 3.18A). Their numbers were similar to the numbers of caspase 3-positive cells in control cultures at corresponding time points (Fig. 3.18D). Mean numbers of positive cells fluctuated mildly in both infected and control cultures, but there were no significant differences in the mean numbers between them (Fig. 3.19; $p>0.05$, Mann-Whitney U test), suggesting that caspase 3-activation in the infected cultures is not parasite dependent.

To further characterise the effects of *N. caninum* on HL-1 cardiomyocytes, the simultaneous double IP and IF staining technique to detect *N. caninum* and cleaved caspase 3 expression was employed on sequential sections consecutive to those cut for single IH. Again, *N. caninum*-infected cardiomyocytes exhibited normal cellular morphology, similar to cells in the control cultures at each time point. *N. caninum* tachyzoites were observed within intact cardiomyocytes in the IP-stained sections (Fig. 3.19A), and IF on the same sections revealed cleaved caspase 3 expression in uninfected cardiomyocytes, whereas infected cells remained unlabelled, (Fig. 3.20A-C; 24 hpi). In the control cultures, similar numbers of cleaved caspase 3-positive cardiomyocytes were detected (Fig. 3.20D-F; 24 hpi).

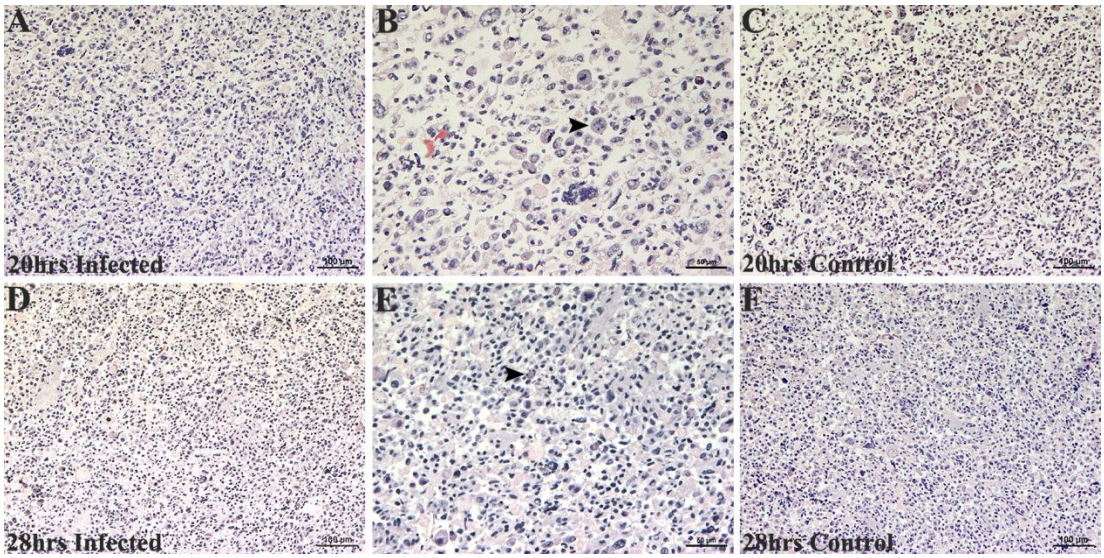

Figure 3.17. *N. caninum*-infected (MOI of 2:1) and uninfected HL-1 cardiomyocytes at 20 hpi (A-C) and 28 hpi (D-F). **A**. At 20 hpi, infected cultures show predominantly viable cells. **B**. Higher magnification of A, showing uninfected apoptotic cells (arrowhead) among viable cells. **C**. Uninfected control culture harvested at 20 hpi, with similar morphological features as the infected culture. **D**. Infected HL-1 culture harvested at 28 hpi, showing high cell numbers and similar morphological features as in A. **E**. Higher magnification of D showing apoptotic (arrowhead) and viable cells. **F**. Uninfected control culture harvested at 28 hpi, exhibiting high cell numbers and similar to the infected culture. Figs A and D: HE stain. Bars = 100µm. Figs. B and E: HE stain. Bars = 50µm. Figs. C and F: HE stain. Bars = 100µm.

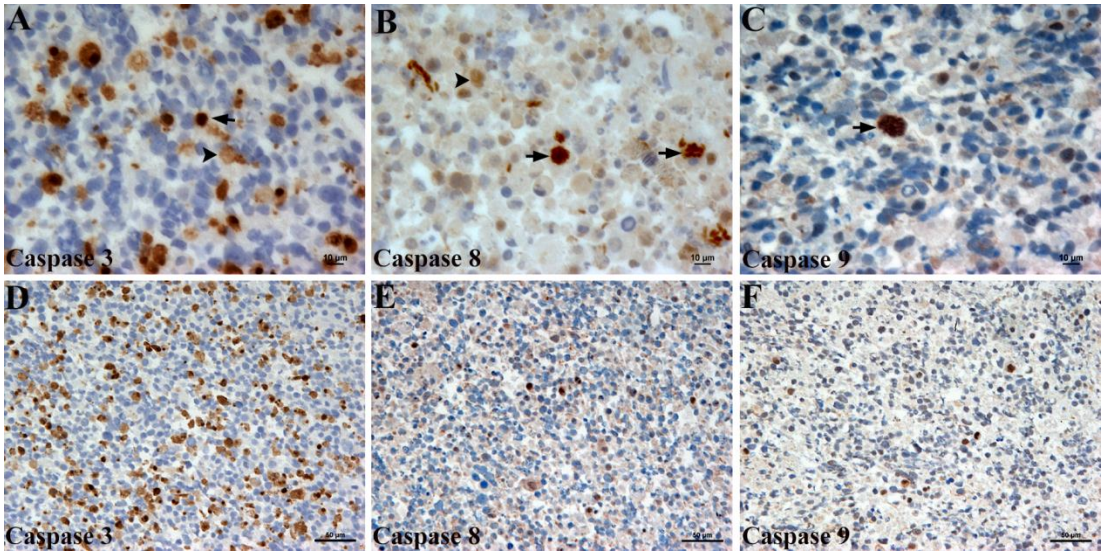

Figure 3.18. Immunohistological staining of *N. caninum*-infected (A-C) and uninfected (D-F) HL-1 cardiomyocytes harvested at 32 hpi for the expression of caspase 3 (A, D), caspase 8 (B, E) and caspase 9 (C, F). **A**. High numbers of caspase 3 expressing, apoptotic uninfected cells are detected in the infected culture (arrowhead), whereas *N. caninum* tachyzoites are present within intact cells not labelled for caspase 3 (arrow). **B**. *N. caninum* tachyzoites (arrows) are detected within intact caspase 8-negative cells. Uninfected cells in the infected culture are expressing caspase 8 (arrowhead). **C**. Tachyzoites are detected within intact caspase 9-negative cells (arrow), while uninfected cells express caspase 9. **D**. Caspase 3 expression is detected in high numbers of cells in the control culture. **E**. Similar numbers of caspase 8-expressing cell are detected in the control culture. **F**. Uninfected control culture showing caspase 9 expression in a moderate number of cells. PFA-fixed and paraffin embedded cell cultures. PAP method, Papanicolaou's haematoxylin counterstain. Figs A-C: Bars = 10µm. Figs D-F: Bars = 50µm.

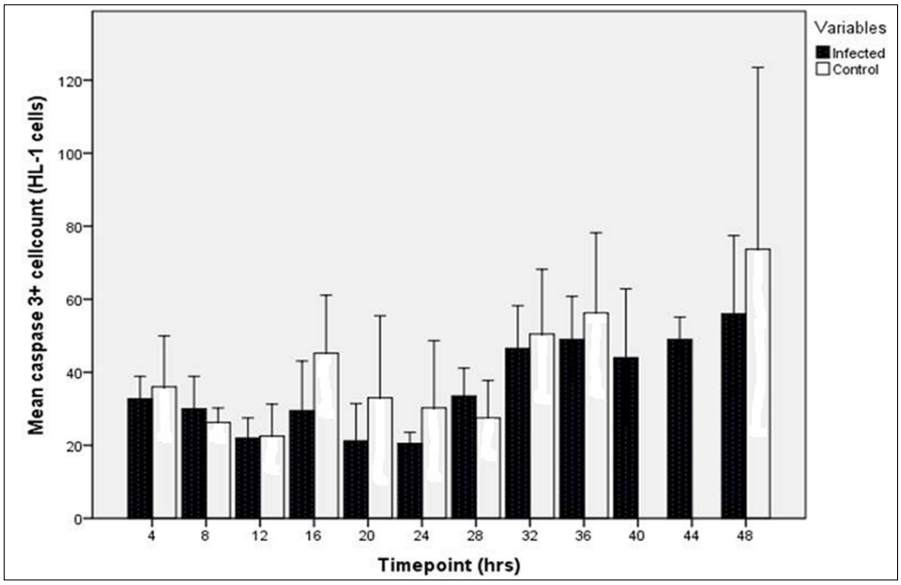

Figure 3.19. Quantitative analysis of caspase 3 expression in *N. caninum*-infected and uninfected HL-1 murine cardiomyocytes. Four randomly selected, non-overlapping 40X high power fields were selected and assessed quantitatively for both infected (black bars) and control (white bars) cultures. No significant differences were observed in the numbers of caspase 3-expressing cardiomyocytes between infected and control cultures at corresponding time points. Whiskers represent 95% confidence interval.

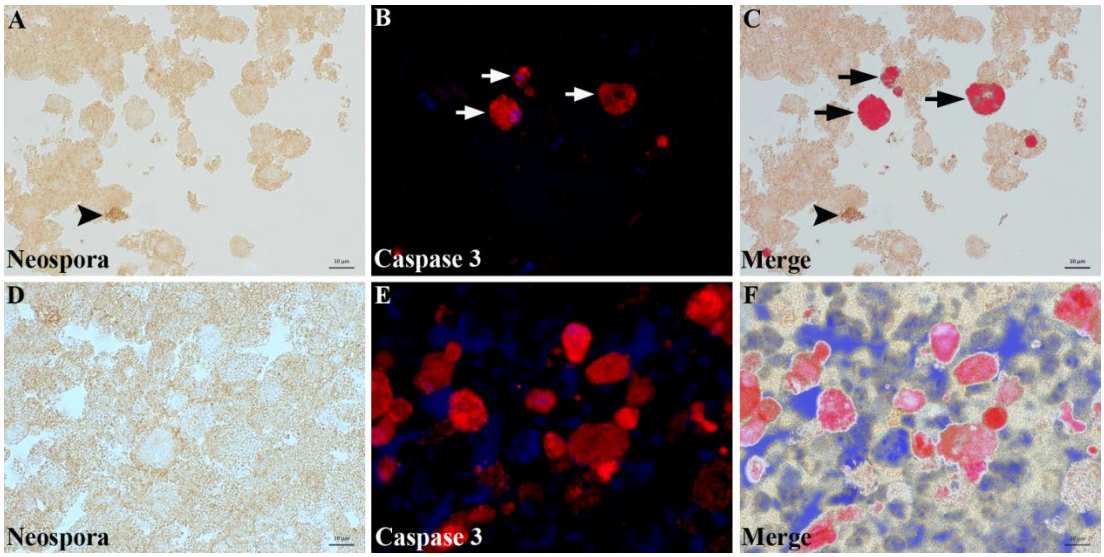

Figure 3.20. Combined immunoperoxidase (IP) and immunofluorescence (IF) labelling of *N. caninum*-infected (A-C) and uninfected (D-F) HL-1 murine cardiomyocytes harvested at 24 hpi. **A**. A cluster of *N. caninum* tachyzoite is detected within a cardiomyocyte (arrowhead). **B**. IF staining reveals low numbers of cleaved caspase 3-expressing cardiomyocytes (arrows). **C**. Merged image of A and B in which tachyzoites are evident as brown staining (arrowhead) and neighbouring, uninfected caspase 3-expressing cardiomyocytes as red fluorescent labelling (arrows). **D-F**. Uninfected control cultures at 24 hpi. **D**. *N. caninum* tachyzoites are not detected in uninfected cultures under bright field light. **E**. High numbers of cardiomyocytes are labelled for cleaved caspase 3. **F**. Merged image of D and E showing distribution of cleaved caspase 3-expressing uninfected cardiomyocytes. IP staining of *N. caninum*-infected HL-1 cardiomyocytes using rabbit anti-*N. caninum* pAb with DAKO anti-rabbit EnVision (DAB: A, D) and further IF staining with rabbit anti-cleaved caspase 3 labelled with anti-rabbit Dylight 549 (red: B, E). Merged images: C, F. Bars = 10 µm.

3.5.7.1 Evaluation of the apoptotic pathways in N. caninum-infected and uninfected HL-1 murine cardiomyocytes: caspase 8 expression. Caspase 8 expression was characterised by intense cytoplasmic staining. To assess the extent of caspase 8 expression in *N. caninum*-infected HL-1 cells, a semi-quantitative analysis, using the same approach as for the HepG2 cells, was conducted on immunohistologically stained sections consecutive to those used above. Within the infected cultures, caspase 8 expression was observed in large numbers of uninfected cardiomyocytes, whereas *N. caninum*-infected cells were caspase 8-negative (Fig. 3.18B). Similar numbers of caspase 8-expressing cells were detected in both infected and control cultures (Fig. 3.18E), and the statistical analysis of the mean proportion of caspase 8-expressing cardiomyocytes confirmed this for all time points (Fig. 3.21A; $p>0.05$, Mann-Whitney U test). The mean IH score for caspase 8-expression also showed no significant difference between infected and control cultures (Fig. 3.21B; $p>0.05$, Mann-Whitney U test), except at 44 hpi, where the expression was significantly more intense in the control cultures. These findings indicate that *N. caninum* had no effect on caspase 8-activation following infection in the *in vitro* model.

To further evaluate the caspase 8-expression in *N. caninum*-infected HL-1 cells, the double IP and IF-labelling technique was performed, using the rabbit anti-*N. caninum* and rabbit anti-human caspase 8 pAbs on sequential sections consecutive to those used above. Cardiomyocytes in both infected and control cultures exhibited normal cellular morphology at corresponding time points. *N. caninum* tachyzoites were detected by IP staining within intact, caspase 8-negative cardiomyocytes (Fig. 3.22A). IF revealed caspase 8 expression with strong cytoplasmic staining in uninfected cardiomyocytes, while infected cells were caspase 8-negative (caspase 8 antibody cross reaction is observed in the section, but parasites are identified based on their morphology) (Fig. 3.22B, C). Similar numbers of caspase 8-expressing cardiomyocytes were detected in the control cultures (Fig. 3.22D-F).

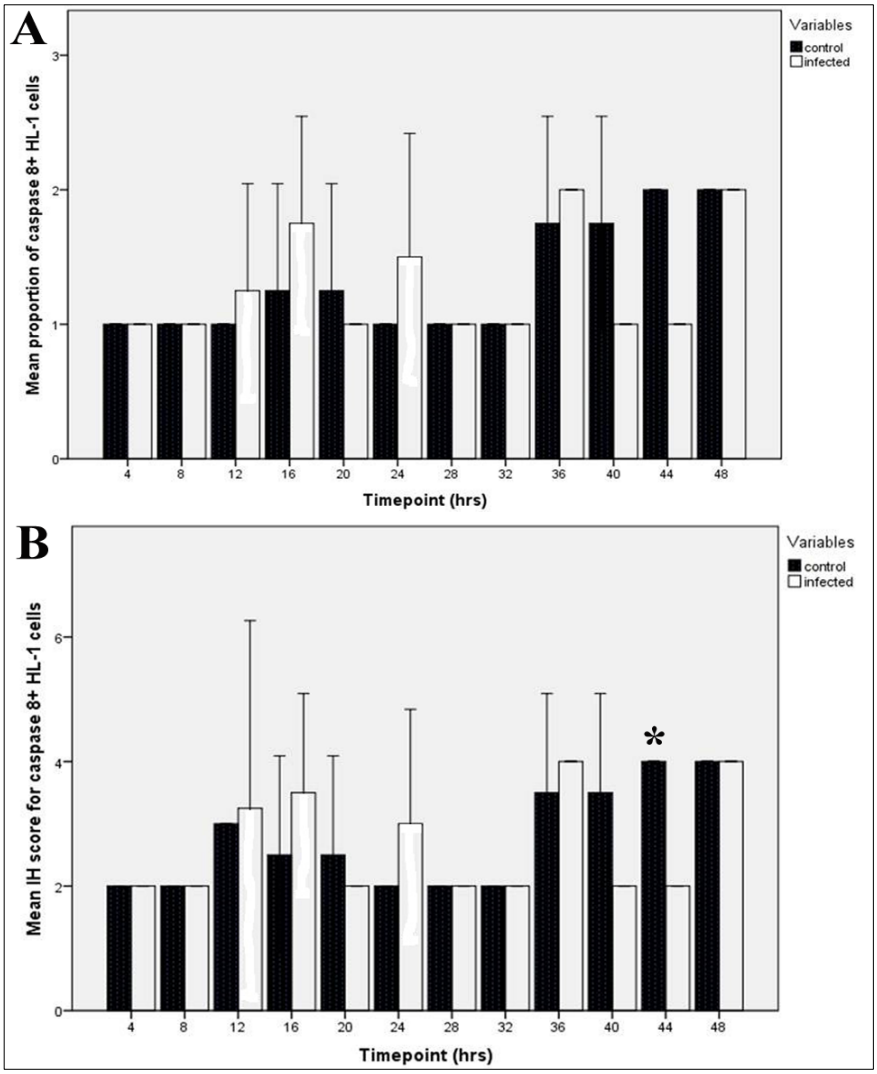

Figure 3.21. Semi-quantitative analysis of caspase 8 expression in *N. caninum*-infected and uninfected HL-1 murine cardiomyocytes. **A**. The mean proportion of caspase 8-expressing hepatocytes is slightly higher in infected cultures (white bars) at 12, 16, 24 and 36 hpi ($p>0.05$) compared to controls (black bars). **B**. The mean immunohistological scores for infected (white bars) and control cultures (black bars) are shown. A significant difference is observed at 44 hpi when the expression is more intense in control cultures. Asterisk denotes a p value of <0.05 and whiskers represent 95% confidence intervals.

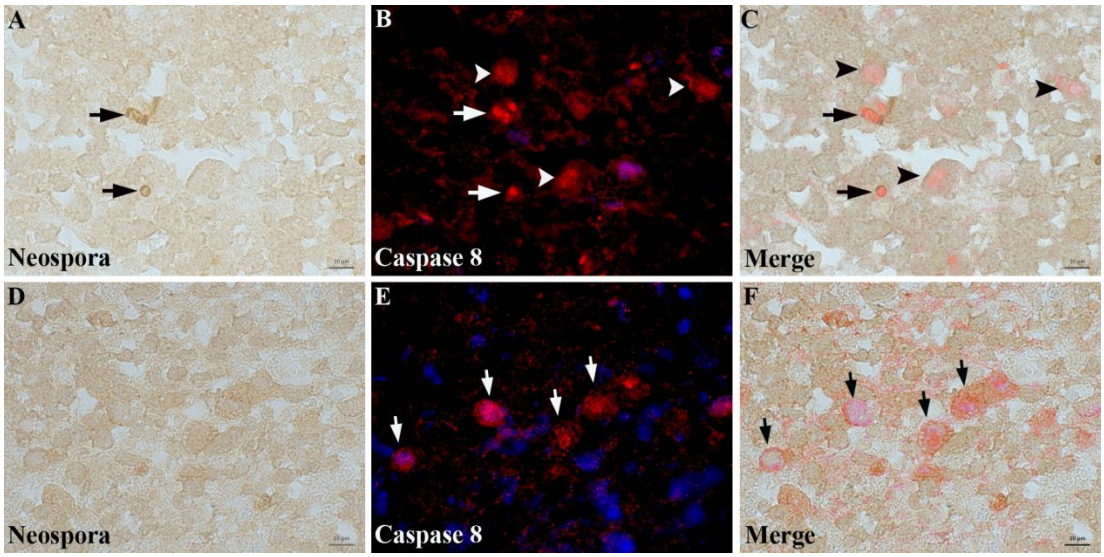

Figure 3.22. Combined immunoperoxidase (IP) and immunofluorescence (IF) labelling of *N. caninum*-infected and uninfected HL-1 murine cardiomyocytes harvested at 32 hpi. **A**. Clusters of *N. caninum* tachyzoites are detected within intact cardiomyocytes (arrows). **B**. IF staining reveals caspase 8 expression in the cytoplasm of cardiomyocytes (arrowheads). Arrows point to the clusters of tachyzoites with caspase 8 antibody cross-reaction (discerned based on parasite morphology). **C**. Overlay of A and B showing caspase-8 expressing cells (arrowheads) and localisation of tachyzoites (arrows). **D-F**. Uninfected controls culture harvested at 32 hpi. **D**. *N. caninum* tachyzoites are not detected in control cultures under bright field light. **E**. IF staining for caspase 8 reveals red fluorescent staining within the cytoplasm of uninfected cardiomyocytes (arrows). **F**. Overlay of D and E showing the distribution of caspase 8 expressing cells in the control culture. IP staining of *N. caninum*-infected HL-1 cardiomyocytes using rabbit anti-*N. caninum* pAb with DAKO anti-rabbit EnVision (DAB; A, D) and further IF staining with rabbit anti-human caspase 8 labelled with anti-rabbit Dylight 549 (red: B, E). Merged images: C, F. Bars = 10 µm.

3.5.7.2 Evaluation of the apoptotic pathways in N. caninum-infected and uninfected HL-1 murine cardiomyocytes: caspase 9 expression. Caspase 9-expression in cardiomyocytes was characterised by a nuclear or both nuclear and cytoplasmic reaction (Eckle et al., 2004). Cells expressing caspase 9 exhibited the normal cellular morphology and were found in both infected and control cultures. The semi-quantitative analysis was performed as described for HepG2 cells. In the infected cultures, IH detected *N. caninum* tachyzoites within intact, caspase 9-negative cardiomyocytes, whereas numerous uninfected cells were found to be caspase 9-positive (Fig. 3.18C; 32 hpi). In the control cultures (Fig. 3.18F; 32 hpi), caspase 9 expressing cells were less numerous than in the infected cultures at the corresponding time points. A significantly higher proportion of caspase 9-positive cells was observed in control cultures at 20, 32 and 48 hpi (Fig. 3.23A, B; $p<0.05$, Mann-Whitney U test). No differences were observed at other time points, although

caspase 9-positive cells were slightly more numerous in control cultures compared to infected cultures.

To further evaluate the expression of caspase 9 in *N. caninum*-infected HL-1 cardiomyocytes, the double IP and IF labelling technique was performed using the rabbit anti-*N. caninum* and the rabbit anti-caspase 9 pAbs on sequential sections consecutive to those used for the single IH staining. As was previously observed in *N. caninum*-infected HepG2 cells, tachyzoites were detected within intact HL-1 cardiomyocytes exhibiting normal cellular morphology (Fig. 3.24A, 32 hpi). IF revealed high numbers of caspase 9 expressing cells in the same section, but *N. caninum*-infected cardiomyocytes remained unlabelled (Fig. 3.24B, C), thus confirming the IH results. Similarly high numbers of caspase 9-positive cardiomyocytes were detected in the control cultures (Fig. 3.24D-F).

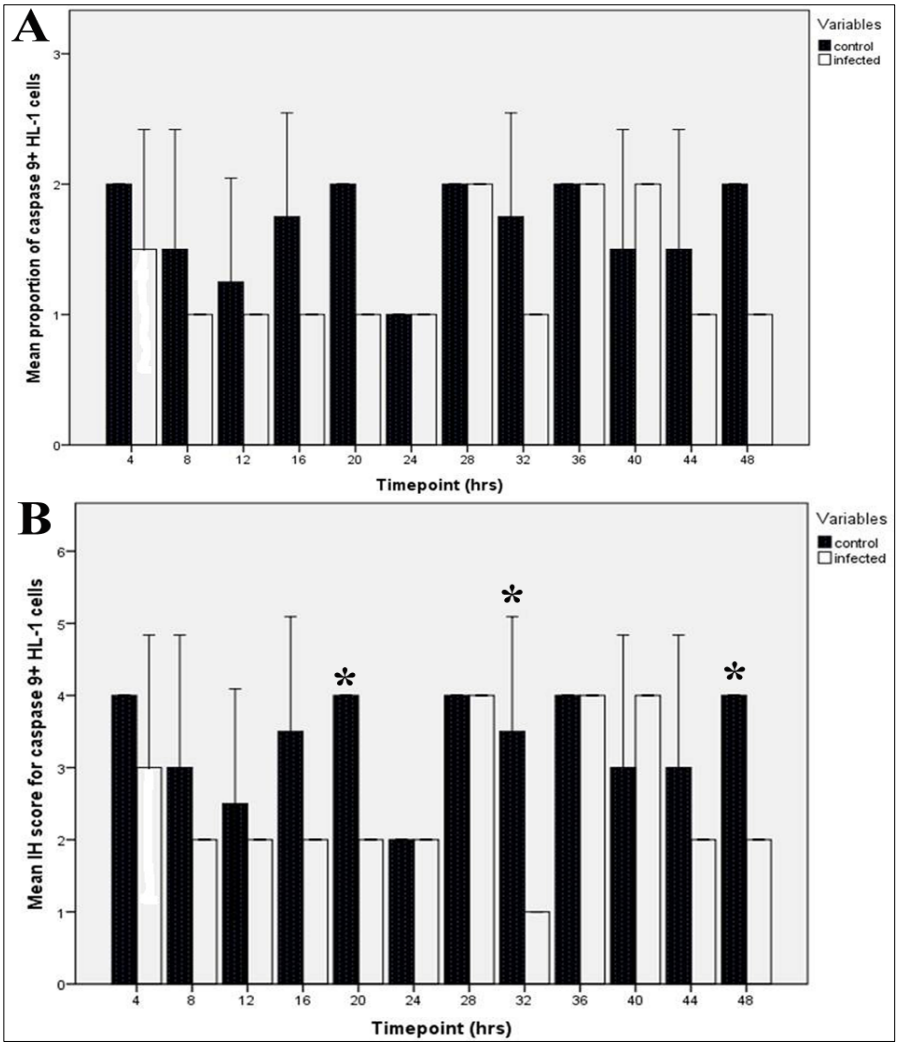

Figure 3.23. Semi-quantitative analysis of caspase 9 expression in *N. caninum*-infected and uninfected HL-1 murine cardiomyocytes. **A**. A mild increase in the mean proportion of caspase 9-expressing cells is observed in control HL-1 cultures (black bars) compared to infected cultures (white bars) at corresponding time points. **B**. Significant differences in the mean immunohistological scores of control cultures were observed 20, 32 and 52 hpi (black bars). Asterisk denotes a *p* value of <0.05 and whiskers represent 95% confidence intervals.

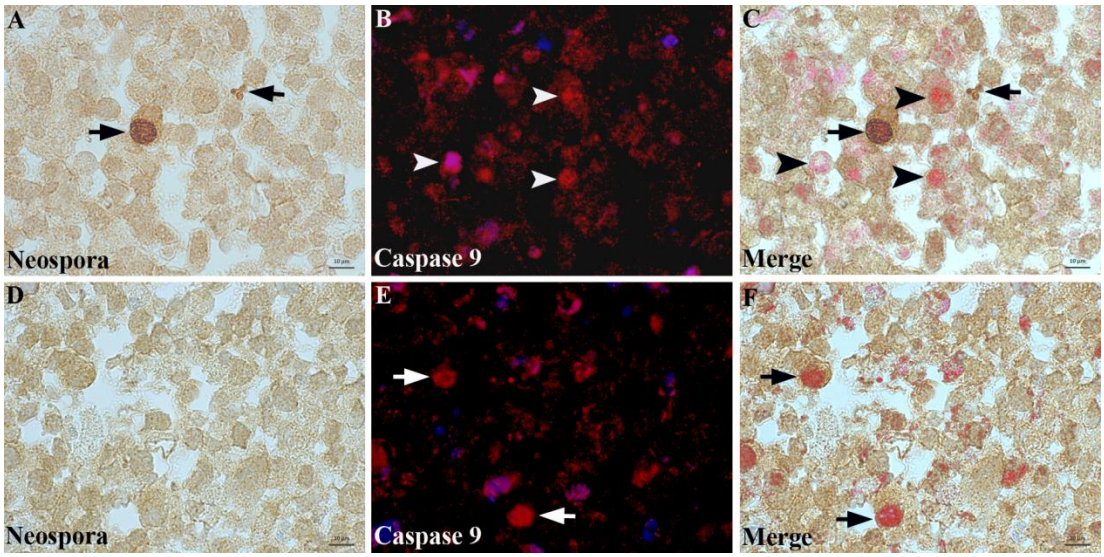

Figure 3.24. Combined immunoperoxidase (IP) and immunofluorescence (IF) labelling of *N. caninum*-infected (A-C) and uninfected (D-F) HL-1 murine cardiomyocytes harvested at 32 hpi. **A**. Two clusters of *N. caninum* tachyzoites are detected by IP staining (arrows). **B**. IF detected caspase 9 expressing cardiomyocytes with diffuse nuclear and cytoplasmic staining (arrowheads). **C**. Overlay of A and B showing caspase 9 expressing cardiomyocytes (arrowheads) and intact cells with *N. caninum* tachyzoites not labelled for caspase 9 (arrows). **D-F**. Uninfected controls culture harvested at 32 hpi. **D**. *N. caninum* tachyzoites are not present within the control culture. **E**. IF reveals caspase 9 expressing cardiomyocytes in the nucleus and cytoplasm of uninfected cells (arrows). **F**. Overlay of D and E shows the distribution of caspase 9-positive cardiomyocytes in uninfected cells (arrows). IP staining of *N. caninum*-infected HL-1 cardiomyocytes using rabbit anti-*N. caninum* pAb with DAKO anti-rabbit EnVision (DAB: A, D) and further IF staining with rabbit anti-caspase 9 labelled with anti-rabbit Dylight 549 (red: B, E). Merged images: C, F Bars = 10 µm.

3.5.8 Mitochondrial organisation in *N. caninum* infected HL-1 cells

To analyse the potential effect of *N. caninum* on mitochondrial organisation in cardiomyocytes, the double IF staining was performed with rabbit anti-*N. caninum* pAb for detection of the parasites and mouse anti-COX 1 mAb for labelling of the mitochondria on sequential sections of the infected HL-1 cell culture pellets consecutive to those used for the caspase staining described above. In the infected cultures, *N. caninum* tachyzoites were detected by IF (red fluorescence) within PV (Figs. 3.25A, D) in close association with mitochondria (green fluorescence) that formed aggregates surrounding the PVM (Figs. 3.25B, C; 28 hpi, 3.25E, F; 32 hpi). Among uninfected cells, approximately 40% comprised a uniform population of viable cells with a homogenous cytoplasmic distribution of mitochondria. The remaining uninfected cells exhibited clumps of mitochondria. These were represented by large aggregates of mitochondria with a punctate pattern and localised predominantly in the perinuclear region (Figs. 3.25B-C and E-F). In the control

cultures, a similar pattern of mitochondrial organisation was observed (Figs. 3.25H, I). A large proportion of cells exhibited a homogenous distribution of mitochondria, represented by a reticular pattern throughout the cytoplasm. The remaining approximately 40-50% of cells exhibited mitochondrial clumping, with large aggregates of cytosolic punctate mitochondria.

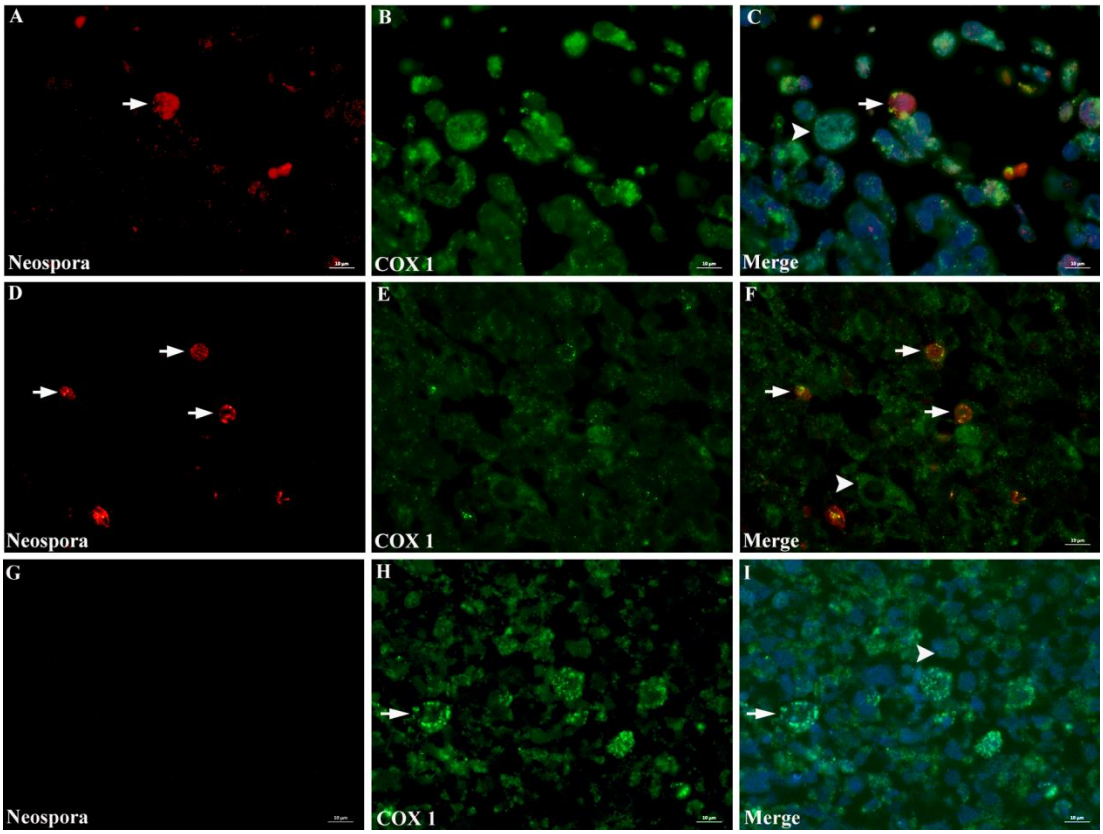

Figure 3.25. Double immunofluorescence labelling of *N. caninum*-infected (A-F) and uninfected (G-I) HL-1 murine cardiomyocytes at 28 hpi (A-C) and 32 hpi (D-I). **A-F. A**. A large cluster of tachyzoites is detected within a cardiomyocyte (arrow). **B**. IF reveals mitochondrial distribution in the cytoplasm of cardiomyocytes in the infected culture. **C**. The overlay shows a close association of the clumped host cell mitochondria with the PVM (arrow) and a diffuse homogenous distribution of the mitochondria in an uninfected cell (arrowhead). **D**. At 32 hpi, high numbers of tachyzoites are detected within cardiomyocytes (arrows). **E**. Host cell mitochondria are observed in aggregates surrounding areas where parasites are detected. **F**. Aggregated host cell mitochondria are present in close association with the PVM (arrows), while a homogenous diffuse pattern is observed in uninfected cells (arrowhead). **G.** Control HL-1 cells are negative for *N. caninum* tachyzoites. **H**. Large aggregates of mitochondrial clumping are observed in the cytoplasm of uninfected cells (arrow). **I**. Merged image showing distribution of host cell mitochondria forming large aggregates in uninfected HL-1 cells (arrow) along with an even distribution of mitochondria in other cells (arrowhead). Immunolabelling of infected cardiomyocytes using rabbit anti-*N. caninum* pAb with anti-rabbit Dylight 549 (red; A, D, G) to identify the parasites and mouse anti-MTCO1 mAb followed by anti-mouse Dylight 488 was used for detection of host cell mitochondria (B, E, H). Merged images: C, F, I. Bars = 10 µm.

3.6 DISCUSSION

The current study sought to further investigate the observation that *N. caninum* tachyzoites induced hepatocellular death (necrosis and apoptosis) in foetuses following infection in early gestation, but did not lead to the death of cardiomyocytes. The analysis of the tissues of foetuses from experimentally infected dams detected tachyzoites mainly within intact foetal hepatocytes and cardiomyocytes which both exhibited normal cellular morphology. In the foetal liver, hepatocellular necrosis was observed along with high numbers of hyper-eosinophilic, cleaved caspase 3-positive, apoptotic cells. These observations indicated that hepatocytes that were infected with *N. caninum,* remained intact while surrounding uninfected cells underwent necrosis and/or apoptosis. Evidence of hepatocellular necrosis, in association with *N. caninum* infection in early gestation, was confirmed in these same foetuses by TEM in an earlier study (Gibney et al., 2008). To define the mechanisms underlying these findings, the impact of *N. caninum* infection on hepatocytes and cardiomyocytes was evaluated using an *in vitro* tissue culture system, focusing on the demonstration of initiator and effector caspases of the apoptotic pathways in infected and uninfected cells.

3.6.1 The effects of N. caninum on primary bovine hepatocytes

Cells isolated *ex vivo* more closely represent the physiology of cells *in vivo* and for this reason were chosen to further assess the mechanism of cell death following *N. caninum* infection (Zhang et al., 2011). Primary hepatocytes were isolated from the caudate process of adult bovine livers using the collagenase perfusion method to separate hepatocytes from the surrounding extracellular matrix. This method is widely used and produces a relatively large number of hepatocytes, which can be maintained for up to 10 days in culture (Risal et al., 2011; Zhang et al., 2011). We obtained a mean viability of 78% which was consistent with other studies of bovine primary hepatocyte isolation where viability of approximate 81% and 86% were recorded (Forsell et al., 1985; Zhang et al., 2011). Following the inoculation with *N. caninum* tachyzoites at different MOI, the viability of hepatocytes was significantly reduced after 24 h. This loss of viability could be due to several causes. For example, the culture conditions and growth medium are important factors; they ensure the survival of cells in the *in vitro* environment and can result in a significant reduction

of viable cells if not optimal (Clouet et al., 1998). When infected cultures were compared with control cultures after 24 h, a profound difference was observed in that control cultures exhibited almost full viability, which suggests that the addition of parasites to the primary cultures resulted in substantial cell death. Similarly, a high level of apoptotic cell death was observed in an *in vitro* model with primary human trophoblasts infected with *T. gondii* (Abbasi et al., 2003). This indicates that primary hepatocyte cultures may not be an ideal *in vitro* model for assessing the pathogenesis of *N. caninum*. Due to the findings in the initial experiments, any further experiments with primary bovine hepatocyte isolates were deemed unfeasible and further attempts not made.

3.6.2 The effects of N. caninum on HepG2 cells

The assessment of infected HepG2 cell cultures provided evidence that *N. caninum* inhibits apoptosis of infected cells. Both mitochondrial and death receptor pathways appeared inhibited in infected hepatocytes, but not in uninfected bystander cells. Evidence of necrotic cell death was shown in foetuses following *N. caninum* infection in early gestation (Gibney, 2008), but immunohistological staining of sections from the same paraffin blocks revealed high numbers of cleaved caspase 3-positive, apoptotic cells alongside necrotic hepatocytes (described in Chapter 2). Previous reports have shown that the protozoan parasite *T. gondii* targets the caspases and inhibits apoptosis induced in different cell types by a variety of pro-apoptotic agents either through the intrinsic or extrinsic pathway (Nash et al., 1998; Goebel et al., 2001). Hence, the quantitative and semi-quantitative analyses undertaken in the present study were conducted to evaluate the type and degree of caspase activation in *N. caninum*-infected and uninfected control cultures. Antibodies that detect the active subunits of the caspases are valuable tools to identify apoptotic cells since the activation of the enzymes is a key molecular event during apoptotic cell death (Eckle et al., 2004). The use of antibody-based methods was chosen rather than using other methods such as TUNEL-assays which only label cells that already exhibit morphological changes of apoptosis and cannot discriminate between apoptotic, necrotic and autolytic cell death (Grasl-Kraupp et al., 1995).

Based on the obvious lack of caspase 3 expression in *N. caninum* infected cells, the present data show that cells infected with *N. caninum* did not undergo apoptosis; in contrast, a proportion of uninfected cells in the infected cultures was found to

express cleaved caspase 3, i.e. to be apoptotic. There were higher numbers of caspase 3-positive hepatocytes in the infected cultures compared to controls between 20 and 36 hpi, indicating parasite-induced apoptotic cell death in uninfected bystander cells. Likewise, caspase 3 activation was not detected in *T. gondii*-infected murine fibroblasts and immunoblot analysis revealed caspase 3 activation in uninfected cells undergoing apoptosis (Payne et al., 2003), thus reinforcing the evidence that infected cells are refractory to apoptosis. A more recent study also reported inhibition of caspase 3 expression in mouse embryonic fibroblasts infected with both *N. caninum* and *T. gondii* (Herman et al., 2007). Immunoblot analysis of infected cultures in the latter study failed to detect the αII-spectrin cleavage, which is a major substrate for cysteine proteases involved in both necrotic cell death, which involves the activation of the Ca^{2+} dependent calpain proteases (Liu et al., 2004), and apoptotic cell death (caspase 3 activation). The αII-spectrin cleavage was, however, detected in uninfected cultures, suggesting apoptotic cell death rather than necrosis (Herman et al., 2007). These findings support the results of the present study and provide further evidence that *N. caninum* blocks apoptosis in infected cells, but not in uninfected bystander cells. The mechanism by which uninfected bystander cells undergo apoptosis is not clear, but others have assessed the role of the *T. gondii* programmed cell death 5 gene (TgPDCD5) in Chinese hamster ovary epithelial cells, mouse macrophages and a human promyelocytic leukaemia cell line (HL-60 cells). PDCD5 is a homologue of the human apoptosis-related molecule and was found to be located close to the rhoptries or vesicle-like structures of the parasite surface membrane in *T. gondii* (Bannai et al., 2008). The authors showed that TgPDCD5 was secreted from the parasite and also speculated that the heparin sulphate proteoglycan-binding motif-dependent internalisation of TgPDCD5 could lead to apoptosis of bystander cells, as was observed when recombinant TgPDCD5 was added to growth medium of *T. gondii*-infected cells along with IFN-γ. It was further argued that the pro-apoptotic effect of TgPDCD5 may not have sufficed to trigger apoptosis in the *T. gondii*-infected cells, or the effect could have been counteracted by the anti-apoptotic effect of the parasites. It is believed that TgPDCD5 contributes to the activation of apoptosis in cooperation with other factors, such as IFN-γ, TNF-α and IL-12, but its mechanism *in vitro* is not clear (Bannai et al., 2008). Since *N. caninum* is the closest relative of *T. gondii* and comparison of their genome shows a high degree of sequence conservation and synteny (Reid et al., 2012), a similar mechanism could

contribute to apoptosis of uninfected bystander cells in *N. caninum*-infected cultures, which would explain why significantly higher numbers of uninfected apoptotic hepatocytes were detected leading up to the time when parasite egress usually occurs (approximately 36 hpi). The NcPDCD5 (hypothetical protein) is also expressed in *N. caninum* tachyzoites (NCLIV_002640) and have orthologs in *T. gondii* (toxodb.org/toxo/, version 11), which suggest it could play a similar role as proposed for *T. gondii*.

Triggering of apoptosis is dependent on a balance between pro- and anti-apoptotic stimuli. The apoptotic cascade will run its course when the caspase activity reaches a certain threshold, which means that if the stimulus is insufficient, cells could escape overt proteolytic destruction and recover or, alternatively, die via necrosis (Zhivotovsky, 2004). Moreover, it was shown that while caspases are necessary for apoptosis, they are not sufficient to exert it (Lukovic et al., 2003). Inhibition of the caspases does not always prevent cell death (Denecker et al., 2001). In the absence of caspase activation in a murine fibrosarcoma cell line (L929 cells), the death domain-containing components of the signalling pathway were activated which resulted in necrotic cell death (Vercammen et al., 1998a). This would suggest that both necrotic and apoptotic cells could develop in the same tissue following induction of cell death. Accordingly, this could at least partly explain why hepatocellular necrosis was observed alongside apoptosis in foetuses following infection in early gestation (Gibney et al., 2008).

Caspase 8 and 9 expression was detected in high numbers of hepatocytes in both infected and control cultures, without significant difference between the two at corresponding time points, indicating that activation of the initiator caspases in infected cultures is not parasite driven or that other factors can contribute to the induction of apoptosis. However, a mild increase in the number of caspase 8 and 9 expressing hepatocytes was observed in infected cultures, suggesting that parasite infection might play a role in activation of the initiator caspases. Infection by intracellular parasites can trigger the mitochondrial pathway of apoptosis mainly due to cell stress, but this natural cell response can be counterbalanced by the presence of viable tachyzoites that can offer protection from cell death (Schaumburg et al., 2006). The mitochondrial pathway of apoptosis is of particular importance during infection with the intracellular protozoan parasites, as was observed in the present study; however, activation of the death receptor pathway was also detected during *N.*

caninum infection. Since activation of both pathways was mainly observed in uninfected cells and not in *N. caninum* infected cells, there is evidence that the parasites interfere with both the initiator and effector caspases. The results also indicate that the parasites might provide only partial protection from activation of the initiator caspases, but completely inhibit activation of the effector caspase. Similar findings were reported for *T. gondii* that inhibited caspase 3 following induction of apoptosis *in vitro* (Goebel et al., 1998; Goebel et al., 2001; Payne et al., 2003). The data obtained from the immunohistological studies were confirmed by the double IP and IF staining and these results further support the suggestion that *N. caninum* inhibits apoptosis to enhance its survival in the cell. They also support the findings in foetuses from dams infected in early gestation, where parasites were detected within intact hepatocytes, whereas the surrounding uninfected cells were caspase 3-positive or exhibited features of necrosis (Chapter 2).

So far it is not known whether and how the PVM interferes with mitochondria in *N. caninum* infection. Mitochondria play a key role in apoptotic signalling pathways, as they are involved in the release of proteins such as cytochrome c into the cytoplasm, leading to activation of the caspase cascade (Desagher and Martinou, 2000). In addition, mitochondria have been shown to be closely associated with the PVM in *T. gondii*-infected cells, and this mechanism is believed to be involved in energy acquisition of the parasite from host cells and, purportedly, the inhibition of cytochrome c and thereby the inhibition of caspase activation (De Melo et al., 1992; Sinai et al., 1997; Magno et al., 2005). De Melo et al. (1992) have also shown that the mitochondria of *T. gondii* were not labelled with rhodamine 123 after the parasite had entered a cell, whereas those in the extracellular parasites were labelled, indicating that the parasites' mitochondria become inactive once within the PV and would depend on host cell energy sources whilst inside the cell. In the present study, the mitochondrial organisation in *N. caninum*-infected hepatocytes was assessed by double IF labelling and TEM. In *N. caninum*-infected HepG2 hepatocytes, mitochondria were found to accumulate in close association with the PVM. They also formed large perinuclear aggregates in the cytoplasm of both infected and uninfected cells in infected cultures and in uninfected control cultures. Mitochondrial aggregation and cytochrome c release was shown in uninfected HeLa cells undergoing apoptosis following transient overexpression of the pro-apoptotic protein bax, through transfection with a DNA encoding a His-tagged bax (Eskes et al.,

1998). Accordingly, our results imply that mitochondrial aggregation in both infected and uninfected cells may be a consequence of stimulation of the mitochondria dependent apoptotic pathway. Overall, our results suggest that during *N. caninum* infection, the presence of parasites is associated with a stress signal that can trigger apoptotic cell death in uninfected and infected cells. However, the anti-apoptotic activity of the parasites may inhibit the pro-apoptotic pathway of its host cells, enhancing their survival whilst the parasites replicate, whereas uninfected bystander cells continue to undergo apoptosis. Furthermore, it was shown in cells induced to undergo apoptosis that following the first exposure to an apoptotic stimulus, mitochondria became aggregated and was followed by the release of cytochrome c to the cytoplasm triggering caspase 3 activation (Haga et al., 2003). This indicates that infected cells can remain viable due to the parasite's anti-apoptotic effect, but will go on to die following parasite egress. Such a death mechanism was termed pyronecrosis since the morphological features were neither those of necrosis nor apoptosis (Heussler et al., 2010).

The ultrastructural examination of parasite-infected cells further confirmed mitochondrial clumping and their association with the PVM in viable infected cells. Soon after invasion, the parasites multiply and the rapidly expanding PV will affect the host cell organelles mechanically since it will cause them to move to the periphery of the cell (Sinai et al., 1997). An older study has shown that other parasites, such as *Leishmania amazonensis* and *Coxiella burnetti*, grow within vacuoles that are sometimes considerably larger than those of *T. gondii*, but these were not found in close contact with host cell organelles (Veras et al., 1994). Instead, a distance of approximately 30-50 nm was maintained between PVM and host cell organelle membranes; this was considered to be the minimum distance that could occur due to the repulsive forces, which create the so called exclusion zone between organelles (Sinai et al., 1997). This would imply that the closer association between the PV and host cell organelles observed with *N. caninum* infection (range from approximately 25-375 nm in this study) is an active process that overcomes the above-mentioned normal repulsive forces that keep organelles apart. The close contact observed between the PV and other organelles in a *T. gondii* infected cell is thought to be essential for the intracellular development of the parasite in so far as it enables the direct transfer of lipids from the host cell to the parasite at the site of PVM-organelle association (Sinai et al., 1997). However, others have suggested that

the PVM-organelle association is merely for physical strengthening of the PVM while it expands within the cell (Magno et al., 2005), as the protozoan parasites do not depend on host cell biosynthesis for most of their needs and only some small molecules are transported from the host cell cytoplasm to the PV via transport channels in the PVM (reviewed in (Saliba and Kirk, 2001)). The close association of mitochondria within the exclusion zone could be interpreted as a potential protein-protein interaction, since the organelles were not affected by the repulsive forces (Sinai et al., 1997). Further studies are warranted to fully understand this interaction.

The mitochondria play a key role in mediating apoptosis via the intrinsic pathway, also in cells infected with obligate intracellular parasites (Green and Reed, 1998). Inhibition of the initiator (caspases 8 and 9) and effector caspase 3 was observed in *T. gondii* infected, but not the uninfected cells *in vitro* (Goebel et al., 2001). The present study yielded similar findings, i.e. the effector caspase 3 was not expressed in *N. caninum*-infected cells; however, caspases 8 and 9 were infrequently expressed in infected cells, suggesting that parasites inhibited apoptosis only downstream of the initiator caspases. It has been shown that cytochrome c was released from the mitochondria of both *T. gondii*-infected and uninfected cells in culture, but the release in the latter was more rapid and led to activation of the initiator and executor caspases, while caspase 3 was not activated in infected cells (Carmen et al., 2006). This suggests that although cytochrome c is released from the mitochondria of infected cells, it does not result in effective activation of the initiator caspase. The question then arises how the parasite contributes to the inhibition of caspase activation in the face of cytochrome c release. PVM-associated mitochondria appear to have undergone distinct functional changes compared to non-PVM-associated mitochondria; this small subset of mitochondria could be involved in anti-apoptotic responses, which probably protect infected cells from activation of the initiator caspases (Sinai et al., 1997). It is likely that the association of host cell mitochondria with the PVM in *N. caninum*-infected cells is also linked to anti-apoptotic mechanisms or a means of the parasites' energy acquisition from the host cell. Mitochondrial clumping, which is associated with early apoptosis (Haga et al., 2003), was confirmed ultrastructurally. This morphological feature was also seen in a proportion of cells within the uninfected culture, but the vast majority of viable cells had a more diffuse distribution of mitochondria in the cytoplasm. This therefore suggests that the presence of the parasites might act as a stimulus for apoptosis

activation, which may have resulted in mitochondrial clumping, but not apoptosis activation (Schaumburg et al., 2006).

3.6.3 The effects of N. caninum on HL-1 cardiomyocytes

HL-1 is a cardiac muscle cell line derived from a mouse atrial cardiomyocyte tumour, which has retained the ability to contract and the morphological and biochemical properties and the phenotype of differentiated cardiomyocytes during extended culturing, which renders it particularly useful for studies on cardiomyocyte function (Claycomb et al., 1998). The current study aimed to further assess and evaluate the findings documented in Chapter 2 where high parasite loads of *N. caninum* tachyzoites were detected within intact cardiomyocytes of foetuses following infection in early gestation. It also intended to assess if cardiomyocytes can be infected readily with *N. caninum* and responded to infection in the same way as hepatocytes. Previous *in vivo* studies have also reported *N. caninum* tachyzoites in cardiomyocytes without evidence of cellular degeneration (Wouda et al., 1997; Gibney et al., 2008). Apoptotic cell death was recorded in a canine model of *T. cruzi* infection, but only cardiomyocytes associated with inflammatory cells were affected (Zhang et al., 1999). Here, the quantitative and semi-quantitative analyses were performed to assess activation of the initiator and effector caspases in *N. caninum*-infected and uninfected murine HL-1 cardiomyocytes. Following infection of cardiomyocytes with *N. caninum* tachyzoites, cleaved caspase 3-positive, apoptotic cells were observed; however, these were exclusively uninfected bystander cells. The numbers of cleaved caspase 3 expressing cardiomyocytes were similar in both infected and control cultures, indicating that *N. caninum* did not induce apoptosis in the infected cultures. These findings suggest that *N. caninum* inhibits caspase 3 expression in cardiomyocytes, but has no effect on uninfected cells that appear to undergo apoptosis as part of the normal cell death in culture in association with cell turnover (Al-Rubeai and Singh, 1998). The double IF study confirmed the IH findings and revealed cleaved caspase 3-positive apoptotic uninfected cells in the infected cultures, whereas *N. caninum*-infected cardiomyocytes were caspase 3-negative. These findings confirm the results in Chapter 2 where high parasite loads were detected within cardiomyocytes without evidence of necrosis or apoptosis. A similar study revealed cardiomyocyte apoptosis following infection with *T. cruzi* in

both an *in vivo* mouse model and in primary cultures of mouse embryonic cardiomyocytes *in vitro* (De Souza et al., 2003). The authors reported apoptosis of infected cardiomyocytes in both models. Their data are in contrast to our findings which indicate inhibition of the effector caspase by the parasites.

The expression of the initiator caspases (8 and 9) was also assessed in *N. caninum*-infected cardiomyocytes. The results suggest that activation of the initiator caspases is also inhibited in *N. caninum*-infected cardiomyocytes. Either of the initiator caspases is generally required to activate the effector caspase 3, which was shown to likely be inhibited (see above). Semi-quantitative analysis of caspase 8 and 9 expression was performed to evaluate activation of the initiator caspases following *N. caninum* infection. Interestingly, activation of the initiator caspases was observed exclusively in uninfected bystander cells in the infected cultures, whereas cardiomyocytes containing viable parasites were unlabelled, suggesting that *N. caninum* inhibits host cell apoptosis in cardiomyocytes starting at the level of the initiator caspases. The comparison with the control cultures at corresponding time points did not reveal significant differences in the numbers of caspase 8 and caspase 9 expressing cardiomyocytes, indicating that other factors influence the induction of apoptosis in both infected and control cultures. Some of these factors that may have influenced the induction of apoptosis in cell culture have been outlined in previous reports and include pH and nutrient levels in the growth medium and failure to passage cells regularly after becoming confluent (Singh et al., 1997; Al-Rubeai and Singh, 1998; Singh and al-Rubeai, 1998) and these might be of particular importance in the induction of cell death in our *in vitro* model. The IH results of the current study are in accord with findings from the double IF labelling. Here *N. caninum*-infected cardiomyocytes remained unlabelled, while high numbers of uninfected bystander cells express caspases 8 and/or 9. This suggests that *N. caninum* is able to block apoptosis in cardiomyocytes by manipulating both the intrinsic and extrinsic caspase pathways. Furthermore, the absence of cleaved caspase 3 activation in *N. caninum*-infected cardiomyocytes in the *in vitro* model suggests that the parasites are able to block apoptosis at all levels of the apoptotic cascade in their host cells. These findings are in agreement with results from other studies utilising the closely related parasite *T. gondii* (Payne et al., 2003).

Apoptosis is a highly regulated form of cell death that is mediated by mitochondrial outer membrane permeabilisation and endoplasmic reticulum stress,

together with other factors (Lee and Gustafsson, 2009). Mitochondria play an important role in apoptosis triggered by various stimuli (Desagher et al., 1999). To further understand the processes involved in host cell death/manipulation following infection with *N. caninum*, cardiomyocytes were also evaluated by double IF labelling to assess the effect of *N. caninum* infection on the mitochondrial dynamics. As was observed in *N. caninum*-infected hepatocytes, a close association of aggregated mitochondria with the PVM was also detected in cardiomyocytes. Mitochondrial clumping in the cytoplasm, which is suggestive of early apoptosis, was seen substantially less frequently in infected cells than in uninfected bystander cells, indicating that the mitochondrial network in infected cells is less affected. Furthermore, the uninfected bystander cells exhibited large aggregates of mitochondrial clumps, which is a feature of early apoptosis. Mitochondrial fission is an early apoptotic event that occurs prior to the release of proteins involved in apoptosis, caspase 3 activation and membrane blebbing (reviewed by (Suen et al., 2008)). Based on these findings, it is likely that the mitochondrial aggregation observed in the uninfected cardiomyocytes was an associated feature of early apoptosis of these cells. Though mitochondrial fragmentation and clumping is universally accepted as an early event of apoptosis, it is also important to note that excessive fission can occur following exposure to agents that can disrupt the inner mitochondrial membrane electrochemical potential and is not always associated with apoptosis (Suen et al., 2008).

Cross-reactivity between *N. caninum* and the primary antibodies used for the detection of caspase activation was observed in the immunohistologically stained sections and occasionally following IF labelling. The antibody reaction occurred with unknown parasite proteins of molecular weights ranging from approximately 10-40 KDa. The antibody cross-reaction appeared to concern surface proteins and possibly proteins located in interior organelles based, since the staining was diffuse over the parasites. A previous study has shown that mouse Fc fragments can also bind to *T. gondii* even at low concentrations, whereas parasites incubated with the Fab fragments do not bind even at very high concentrations (Vercammen et al., 1998b). These findings corroborate our results that the binding of the Fc, but not the Fab fragments of the rabbit antibodies, represents a non-specific binding of immunoglobulin to the parasite. Fc-receptors (FcR) are expressed by protozoan parasites, and metazoa, bacteria and some viruses induce FcR expression on infected

cells (Daëron, 1997). The presence of the FcR on *N. caninum* tachyzoites has not been examined so far; however, extensive work has been done on *T. gondii* and showed FcR expression with different degrees of affinity to ligands (Ferreira De Miranda-Santos and Campos-Neto, 1981; Budzko et al., 1989). It is therefore possible that the reaction observed in the current study constitutes a nonspecific binding of FcR on the surface of the parasites to Fc fragments of the antibodies. It is, however, not clear, whether this is a phenomenon of these antibodies only, but it is surprising that it should affect both mouse and rabbit antibodies.

In summary, the present study demonstrates that *N. caninum* infection induces apoptosis in bystander hepatocytes as indicated by increased caspase 3 expression, but not in infected cells. In contrast to hepatocytes, the infection is established in cardiomyocytes without evidence of apoptosis in both infected and uninfected cells, as shown by the lack of increased caspase 3 expression in infected cultures compared to controls. There is a difference in the pathogenesis of *N. caninum* infection in hepatocytes and cardiomyocytes, as indicated by the cytopathic effect induced by the parasite in liver cultures, but it is still not clear why in infected cultures, uninfected hepatocytes but not cardiomyocytes undergo apoptosis. It is likely that the degree of response to *N. caninum* infection varies with different host cell types, but this is yet to be clarified. Different from previous studies using fibroblasts, the current *in vitro* study was undertaken on hepatocytes and cardiomyocytes in order to reflect the *in vivo* environment; it also focussed on the first 36 hpi, i.e. before parasite egress was observed *in vitro*, but this is likely to be different *in vivo*. Importantly, the results corroborate the findings of cytopathic effects observed in hepatocytes following *N. caninum* infection. The mechanism underlying the effect of the parasite on the activation of the intrinsic and extrinsic apoptotic pathways in host cells is unclear and warrants further investigation to fully understand how *N. caninum* is able to subvert host cell functions. It is also unclear if *N. caninum* actively recruits mitochondria to its PVM and the role of this organelle in parasite-host cell interaction.

CHAPTER FOUR: Seroprevalence of *N. caninum* in Jamaican dairy herds

4.1 ABSTRACT

Neospora caninum is a cyst-forming protozoan parasite which causes abortion in cattle and neuromuscular disease in dogs. Appropriate techniques have been developed for the diagnosis of neosporosis both *in vivo* and in aborted foetuses. In cattle, the detection of *N. caninum* specific antibodies in serum or milk has been shown to be an efficient diagnostic option in live animals at both the herd and individual level. Blood samples were collected from 499 Holstein-Friesian and Holstein-Friesian crossbreed cattle in Jamaica and the serum aliquoted and used for the detection of *N. caninum* specific antibodies in order to study the seroprevalence of *N. caninum* in the country. A seroprevalence of approximately 26% was detected, with the majority of animals being between 0 and 2 years old, while the lowest seroprevalence was found in animals over 13 years of age. The status of pregnancy was shown to influence the seropositivity of animals, but age was not significant in influencing seropositivity, indicating that vertical transmission is the major route of transmission in Jamaican dairy herds.

4.2 INTRODUCTION

Neospora caninum is a coccidian parasite which is an important cause of abortion in cows and neuromuscular disease in dogs (Dubey and Lindsay, 1996; Borsuk et al., 2011). It is morphologically similar to *Toxoplasma gondii*, but is biologically different (Dubey and Schares, 2011). Abortion in *N. caninum* infected cows is a direct result of transplacental transfer of tachyzoites to the foetus during gestation (Björkman et al., 1996; Anderson et al., 1997). These tachyzoites may have arisen from either reactivation of a latent *N. caninum* infection or by ingestion of *N. caninum* oocysts (Jenkins et al., 2002).

Considerable differences have been reported in the seroprevalence of *N. caninum* within countries, regions and between beef and dairy cattle (Dubey and Schares, 2011). Most of the surveys were carried out by testing sera from individual cattle; although bulk milk antibody detection is also an economical way of estimating *N. caninum* prevalence within a herd (Wapenaar et al., 2007; Frössling et al., 2008; Schares et al., 2009; Dubey and Schares, 2011).

Serological tests have the advantage that they can be applied *intra vitam* and are suitable techniques for processing large numbers of samples (Dubey and Schares, 2006). There are a variety of serological assays available for the detection of *N. caninum* antibodies in cattle (for review see Table 2, Dubey et al., 2006). The immunofluorescent antibody test (IFAT) has been widely used to detect *N. caninum* specific antibody in maternal serum or foetal fluids (Conrad et al., 1993b; Minervino et al., 2008; Benetti et al., 2009; Moore et al., 2009; Moré et al., 2009; Andreotti et al., 2010). In addition to the IFAT, a number of *N. caninum* specific enzyme-linked immunosorbent assays (ELISAs) have been described which utilise either whole, fixed *N. caninum* tachyzoites, aqueous or detergent-soluble tachyzoite extracts, tachyzoite antigens incorporated into immunostimulating complexes (iscoms) or recombinant tachyzoite antigens (Lally et al., 1996; Björkman et al., 1997; Williams et al., 1997; Jenkins et al., 2000; Schares et al., 2000). The *N. caninum* (NC-Liverpool) antibody detection ELISA, which uses whole formalin-fixed tachyzoite-coated plates, has a 96% specificity and 95% sensitivity and showed no cross-reactivity with *T. gondii, Babesia divergens, Cryptosporidium parvum, Sarcocytis cruzi, Eimeria alabamesis* or *E. bovis* (Williams et al., 1997; Williams et al., 1999).

There have been several studies investigating the seroprevalence of *N. caninum* in cattle over time. One study showed that the value of serology can be hampered by

a temporal variation of anti-*N. caninum* antibody levels in adult cattle (Sager et al., 2001). In this study, 543 cattle of 3551 (15%) were found to be seropositive in one serological survey, but a second survey carried out 3-12 months later showed that 39% of the 543 cattle that had tested positive in the first survey were classified as seronegative in the second. The reasons proposed for this were the possibility that the animals may have been misclassified as positive or negative, because the sensitivity and specificity of the ELISA used was not 100%; cattle with borderline antibody reactions above or below the ELISA cut-off value could have been misclassified when tested repeatedly over time; an increase in anti-*N. caninum* antibody in herds in which horizontal transmission of the parasite occurred (Paré et al., 1997; Davison et al., 1999b; Stenlund et al., 1999), or that antibody levels in persistently infected cattle fluctuate over time. Indeed, several studies have shown that antibody levels fluctuate in pregnant cattle that were naturally and persistently infected with *N. caninum* (Guy et al., 2001a; Kyaw et al., 2005). Evidence suggests that in persistently infected cattle, bradyzoites differentiate to tachyzoites during pregnancy and disseminate via the circulation to the placenta leading to foetal infection. Recrudescence of infection leads to an increase in *N. caninum* antibody, typically in the second half of pregnancy (Nogareda et al., 2007; Serrano et al., 2011) Because of these fluctuating antibody levels, some animals test serologically negative as antibody levels decline after pregnancy and because IgG is shunted into the colostrum in the last month of gestation (Nogareda et al., 2007; Dijkstra et al., 2008; Rosbottom et al., 2011).

The discovery of *N. caninum* (Bjerkas et al., 1984), its first description by Dubey et al. (1988) and identification as a cause of bovine abortion are recent events. Neosporosis is ubiquitous and has been reported in all continents outside Antarctica; nevertheless, its significance as a cause of abortion in many countries is still unknown. *Neospora caninum* infection has never been considered as a potential cause of abortion in cattle in Jamaica and no effort has been made to diagnose the disease. The present study investigated the seroprevalence of *N. caninum* infection in cattle in three Jamaican dairy herds with the aim of establishing if *N. caninum* infection was present in cattle in Jamaica.

4.3 MATERIALS AND METHODS

4.3.1 Cattle and sera

Sampling was done on three dairy farms (Farms A, B and C), located in the counties of Middlesex (Farm B and C) and Surrey (Farm A) in Jamaica (Fig. 4.1). These farms were selected for the study because of the large herd sizes and the fact that the farmers agreed to participate. Farm A maintained five small herds, each of which included calves, heifers and adult breeding and milking animals of Holstein-Friesian and Holstein-Friesian crossbreed (crossed with Jamaica Hope, a local breed) animals. Farms B and C comprised smaller herds, mainly with dry cows, also Holstein-Friesian and Holstein-Friesian crossbreds. The farms were isolated in deep rural areas, approximately 10 km from other farms. The majority of the surrounding farms held cattle in single digit numbers and surrounding households sometimes kept one or more cows as part of their livelihood. Cattle on all the farms spent most of their lives at pasture and received feed supplementation during periods of low pasture availability. Milking animals were sometimes housed in open buildings. Calves were kept in housing areas specifically for weaning stocks on the farms and were used for each new young stock.

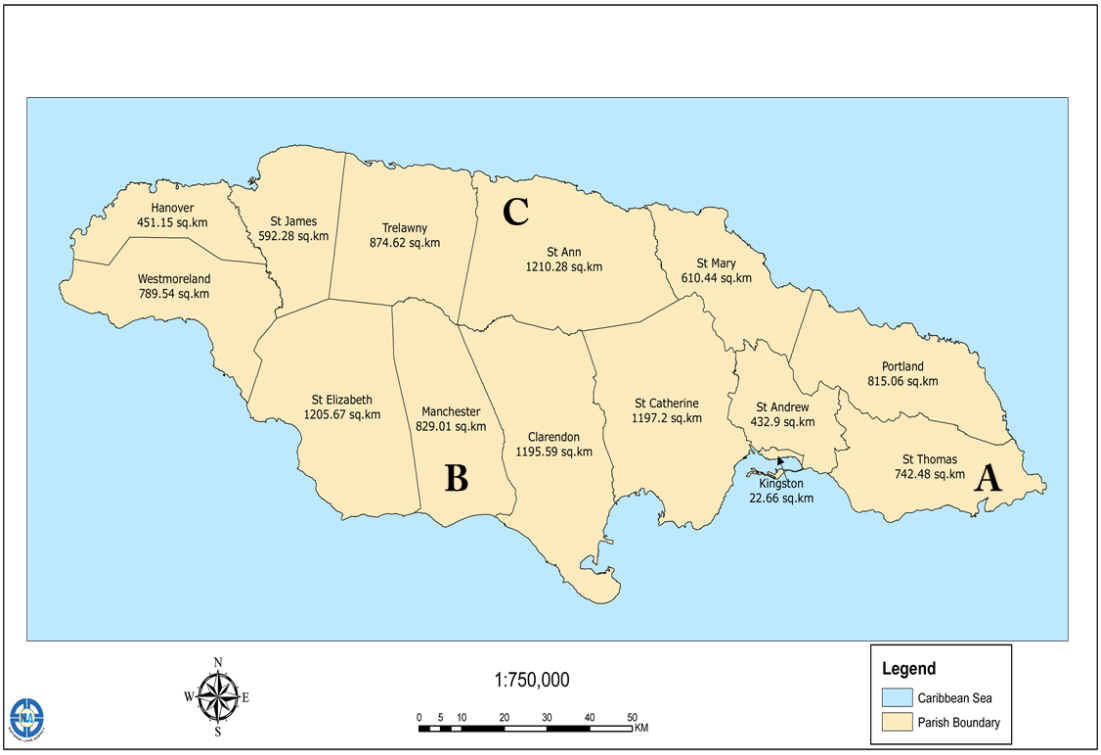

Figure 4.1. Map of Jamaica showing the parishes where the farms are located (A, B and C). Adopted from (www.jis.gov/jm).

4.3.2 Herd management

Dairy cattle on all three farms were reared in a semi-intensive system, kept on pasture. Animals were bred by artificial and natural insemination; cows and heifers calved all year round and were milked twice per day. All animals were routinely screened for bovine tuberculosis and brucellosis and vaccination programmes used for the prevention of brucellosis, leptospirosis, clostridiosis, bovine viral diarrhoea virus and infectious bovine rhinotracheitis (BVDV/IBR). Domestic dogs lived among cattle on some of these farms and were allowed free access to cattle feeding areas and pastures.

4.3.3 Blood sample collection and serology

Blood samples were collected by coccygeal or jugular venipuncture from a total of 499 Holstein-Friesian and Holstein-Friesian crossbreed dairy cattle using a 21 gauge sterile needle and 10 ml vacutainer tubes (BD Ltd, Oxford, UK). The samples were allowed to stand overnight at 4°C before centrifugation at 1,000 g for 10 min, after which the serum was aliquoted in 5 ml-serum tubes (Starlab, Milton Keynes, UK), labelled with all farm and individual identification codes, then heat inactivated at 56°C for 30 min in a water bath before storage at -20°C. Serum samples were later transported on ice packs to the University of Liverpool, UK and stored at -20ºC until tested by ELISA. *N. caninum* specific antibody was measured using an in-house ELISA as detailed below.

4.3.4 Culture and purification of *N. caninum* tachyzoites

Neospora caninum tachyzoites (NC-Liverpool isolate) were maintained in Vero cells grown in RPMI-1640 medium (Lonza, Cambridge, UK) containing 2 % (v/v) horse serum (Invitrogen, Paisley, UK), 100 IU/ml penicillin G and 100 µg/ml streptomycin (Lonza) at 37°C/5% CO_2 in T-75 tissue culture flasks (Nunc, Roskilde, Denmark). Tachyzoites were collected 7 to 10 d after passage when the Vero cell monolayer had been destroyed and there were numerous free tachyzoites in the culture medium. Remaining Vero cells were scraped off the flask using a sterile cell scraper (Fisher Scientific, Loughborough, UK) and the whole suspension of cells and parasites was washed twice in cold sterile phosphate buffered saline (PBS, pH 7.2) by centrifugation at 1,000 x g and 4°C. The final suspension was homogenised by three passages through a 25 gauge needle until all Vero cells had been disrupted and the

intracellular tachyzoites released. The suspension was then applied to a Sephadex G-25M gel filtration column (PD10 column; Pharmacia, Uppsala, Sweden) that was previously equilibrated with PBS as per the manufacturer's instruction. Tachyzoites were then washed in sterile PBS by centrifugation at 700 x g and counted. The tachyzoites were later flash-fixed in 2 % formaldehyde, then washed in PBS.

4.3.5 ELISA technique

To 10 ml of carbonate coating buffer (see Appendix), 100 µl of 1% poly-l-lysine (Sigma-Aldrich, St Louis, Missouri, USA) was added and mixed to give a working strength of 0.01%. To each well of the Immulon ELISA plates, 100 µl of 0.01% poly-L-lysine was added and plates were incubated for 1 h at room temperature (RT), covered. The tachyzoites were diluted in PBS/0.2% azide to $5x10^6$/ml (10ml/96-well plate = $5x10^7$ tachyzoites/plate), then the suspension was swirled and 10 ml removed with 100 µl added to each well using a multichannel pipette. *N. caninum* tachyzoites (diluted in PBS/0.2% azide) (Williams et al., 1997) were then coated onto Immulon I 96-well plates (Nunc, Roskilde, Denmark). Plates were covered and incubated overnight at 4°C. On day two, the fluid in each well was flicked from the plates and 100 µl/well of blocking buffer (see Appendix) was added and incubated for 1 h at RT. After that, the blocking buffer was flicked out and plates were washed 3 times for 1 min each with PBS-Tween (see Appendix). Plates were then dried at 37°C for 30 min. Once dried, they were sealed with a plastic plate sealer, placed in a foil bag with silica crystals and heat sealed. Plates were stored at 4°C until needed.

4.3.6 Measurement of *N. caninum* specific antibody by ELISA

For the assay, ELISA plates, serum samples, 3,3´,5,5´-tetramethylbenzidine (TMB) and PBS-Tween were removed from the fridge and allowed to reach RT. Control sera were diluted by adding 5 µl of each to 2 ml of PBS-Tween (1:400 dilution) and all test samples were diluted in a 1:400 dilution. In a 96-well plate, 5 µl of test serum was added in duplicate to 95 µl of PBS-Tween (1:20). The Immulon plate was removed from the foil wrapper and a multichannel pipette was used to transfer 5 µl of sample from the dilution plate into 95 µl of PBS-Tween on the coated ELISA plate (1:20); the solution was mixed up and down taking care not to scrape the bottom of the plate. For ELISA plate control, a high positive, low positive, negative and a substrate control (blank) were included in quadruplicate on each plate to

assigned wells (100 µl/well). Plates were covered and incubated at 37°C for 30 min after which all wells were washed 3 times for 1 min with PBS-Tween. Plates were tapped on absorbent paper to remove residual fluid. After washing to remove unbound materials, 100 µl of a 1:45,000 dilution of a monoclonal antibody specific for bovine immunoglobulin G conjugated to anti-mouse horseradish peroxidise were added to all wells except for blank wells where only PBS was added. The plates were covered and incubated at 37°C for 30 min. After incubation, plates were washed as previously described. The plates were then incubated with 100µl of TMB solutions (TMB, hydrogen peroxide and proprietary catalysing and stabilising agents; Interchim, Montluçon, France) at RT (18-25°C) in the dark for 10 min. After incubation, the reaction was stopped by adding 100 µl of 0.5M hydrochloric acid (see Appendix) to all wells. The plates were read in a Dynatech MRX ELISA reader (Dynex technologies, Revelation. 3.2) at a wavelength of 450 nm. In order to minimise daily and plate variation, and to allow comparison between tests, the optical density (OD) readings of the test samples were expressed as a percentage of the high positive control (percent positivity-PP) using the following formula:

Percent Positivity (PP) = (Mean OD of test sample/Mean OD of High positive control) x 100. A PP value of ≥20 indicates a positive result (Williams et al., 1999).

4.3.7 Statistical Analysis

The sample size was estimated to give a true seroprevalence of the infection and calculated as described (Humphry et al., 2004). The assumed true prevalence was taken to be 0.5, test sensitivity 95%, specificity 96%, the approximate population size in Jamaica – unknown, confidence level of 95% and desired precision of 5%. For a large population, a sample size of 464 is required. The current study used a sample size of 499 animals. Animal age, pregnancy status, abortion history and parity were obtained from farm records at the time of sampling from November 2011 to January 2012. Association between animal age, pregnancy status, abortion history and parity and PP values were analysed by logistic regression. Both age and PP values were normalised by logarithmic transformation (Log_{10}) prior to analysis and the gestation number of animals was normalised using square root. Normality testing was performed on all variables using the Anderson-Darling test. A backward stepwise regression selection was performed to exclude non-significant factors and the following linear regression equation was used: $y=c+\beta_1x_1+\beta_2x_2+\beta_3x_3$, where y is

the value of the response; c is the value of the response when predictor variables are zero; β_1, β_2 and β_3 represent coefficient variables and x_1, x_2 and x_3 are predictor variables. The response variable in this model was taken to be Log (PP), while the predictor variables were Log age, pregnancy status of animals (+/-) and square root of the number of gestations. Analysis was carried out using Minitab for Windows, version 16 (Minitab Corporation Software, Coventry, UK) and Microsoft Excel (Windows Corporation). A *p* value of ≤ 0.05 is considered significant.

4.4 RESULTS

4.4.1 *Neospora caninum* ELISA results

A total of 499 serum samples collected from Holstein-Friesian and Holstein Friesian crossbreed dairy cattle from three different farms, each located in a separate parish in Jamaica, were tested using the *N. caninum* ELISA and a summary of the results is shown in Table 4.1. Overall, the seroprevalence of *N. caninum* infection was 26% (129/499). Prevalence rates of 24.7%, 26.9% and 27.3% were recorded on Farm A, Farm B and Farm C, respectively (Table 4.1).

Table 4.1: Overall seropositivity to *N. caninum* in cattle from different locations in Jamaica

Farms	Herd size	Number of animals sampled	Number of positive animals	Number of negative animals	Percentage positive
Farm A	5000 [a]	247	61	186	24.7
Farm B	480	197	53	144	26.9
Farm C	600	55	15	40	27.3
Total	NA	499	129	370	25.9

[a] Herd size including calves

The largest group of animals sampled were between 3-5 years of age; however, animals over 12 years of age showed the highest percentage of seropositivity on all three farms (Table 4.2). Animals in the 0-2 and 9-11 year group showed similar seropositivity levels and these groups had the second highest seroprevalence rates within the 3 herds (Table 4.2).

Table 4.2: Seropositivity to *N. caninum* in cattle of different age groups from three different locations in Jamaica

Age groups	Number of animals	Positives (%)	Negatives	Pregnant (%)[a]
0-2	16	5 (31.3)	11	4 (25.0)
3-5	229	53 (23.1)	176	43 (18.8)
6-8	151	33 (21.9)	118	26 (17.2)
9-11	66	22 (33.3)	44	10 (15.1)
>12	30	13 (43.3)	17	4 (13.3)
unknown	7	2 (28.6)	5	0 (0.0)

[a] overall number of pregnant cows sampled

On a per farm basis, the highest seropositivity levels were found in animals 10 years and older compared to all other age groups. Older cows were found to have higher seropositivity values on each individual farm. However, when all data for all

three farms were combined, there was no significant difference between age and *N. caninum* seroprevalence (Table 4.3, $p>0.05$). For all farms, the higher the number of pregnancies an animal had, the lower the PP values. There was a significant negative association between number of pregnancies and PP values in the regression analysis ($p<0.05$).

PP values were affected by the pregnancy status of the animals. An animal that was seropositive to *N. caninum* was more likely to have a higher PP value [an increase in the Log (PP) by 0.033 units] if pregnant ($p<0.05$; Table 4.3). On Farm A, 27.8% of all positive cows were pregnant, 21.9% had recently calved (fresh cows) and 27.2% were non-pregnant cows. Farm B showed similar seropositivity in pregnant cows as Farm A, while all animals from Farm C were non-pregnant (open) cows of which 27.3% were seropositive to *N. caninum*. On all farms, at the time of sampling, only a small number of pregnant animals were sampled (Table 4.4) because the majority of cows on these farms were non-pregnant (open) animals.

Table 4.3: Linear regression model of *N. caninum* seropositivity in Jamaican dairy cattle

Predictors	Coefficient	SE coefficient	P value
Log (age)	0.1789	0.1433	0.213
Pregnancy status	0.03291	0.01616	0.042[a]
SQRT (number of pregnancy)	-0.12099	0.05283	0.022[b]

Abbreviations: SQRT, square root; SE, standard error; [a], significant regression coefficient value for comparison between pregnancy status and seropositivity; [b], significant negative regression coefficient for comparison between number of pregnancy and seropositivity of animals.

Table 4.4: Overall association between the seroprevalence of *N. caninum* infection in pregnant and non-pregnant cattle on three different farms in Jamaica

Category	*N. caninum* positive		Total (%)
	Yes (%)	No (%)	
Pregnant cows	23 (27.7)	60	83 (16.6)
Open cows	92 (26.4)	256	348 (69.7)
Fresh cows	14 (20.6)	54	68 (13.6)
Total	129 (25.9)	370	499

Abortions were recorded on Farm A (7 aborted cases) and Farm B (one animal), representing a total abortion rate of 1.6%; of these, two animals (both on Farm A) were seropositive to *N. caninum*.

4.5 DISCUSSION

This study represents the first serological survey performed to demonstrate the presence of *N. caninum* infection in Jamaica dairy cattle. The overall seroprevalence was 26%. The age of the animals within this study ranged from 2-16 years, with the majority falling between the 3-5 year age group. The estimated prevalence of *N. caninum* infection in cattle varies considerably between herds, regions and countries worldwide (Dubey et al., 2007; Frössling et al., 2008; Dubey and Schares, 2011). The seroprevalence of *N. caninum* have been estimated at approximately 12.9% in the UK (Woodbine et al., 2008), whereas it was as low as 2.8% in Sweden (Loobuyck et al., 2009) and reached 55.9% in Romania (Gavrea and Cozma, 2010), 14-40% in the Americas (Moore, 2005), 6-36% in Asia (Koiwai et al., 2005) and 6-21% in Oceania (Hall et al., 2006); the seroprevalence of 26% in Jamaica reported here is within the range described for other countries. In studies in which large numbers of cattle were sampled, it has been found that seroprevalence increased with age, a trend that would suggest horizontal (postnatal) transmission of the parasite (Romero-Salas et al., 2010; Eiras et al., 2011). However, in the present study there was no significant difference in the seroprevalence between different age groups, suggesting a preponderance of vertical transmission of *N. caninum* infection. The high seroprevalence of *N. caninum* in cows over 12 years was not statistically significant and this category contained only 6% of animals tested ($p>0.05$). Overall, these results suggest that vertical transmission is the most common route of transmission, leading to the persistence of the parasite in a herd by propagating the infection to successive generations.

Dogs are a definitive host for *N. caninum* and often have contact with cows, placentae and foetal remains (Dubey et al., 2007). In some epidemiological studies, the presence of farm dogs was a risk factor for *N. caninum* seropositivity in cattle (Mainar-Jaime et al., 1999; Schares et al., 2004; Corbellini et al., 2006). It was also reported that post-natal transmission was observed on farms where dogs have defecated on stored grass and silage (Dijkstra et al., 2002a). Farm dogs were seen on one of the three farms in Jamaica (Farm B), but were categorically barred from the premises of Farm A. Dogs were not present on Farm C during sampling, but dogs from the nearby communities could easily gain access to the farm. The

seroprevalences on all three farms was similar ($p<0.05$) and although the dogs might not have been present in one area, it is possible that some cows might have acquired the infection in one location and later introduced it to other farms through purchase and movement of these animals. Testing for *N. caninum* is not practiced before acquisition of new arrivals to herds and this might be one important route of introducing infected animals to a once seronegative herd. There has been no history of recent importation of animals from outside the country into these herds. Farms B and C have been in existence for approximately 50 years, while Farm A has been in operation for about 30 years; however, there is no information on the origin of the animals.

Abortion was reported in eight cows of which two were seropositive for *N. caninum*. It is possible that the rate of abortion is much higher than has been recorded in this study as there were reports of cows that had aborted in the field early during gestation before returning to oestrus. This has been observed on some of the farms in Jamaica, but the rate of early abortions is unknown as there is no record documenting these abortion cases. The two seropositive cows from Farm A had aborted in previous gestations, but the cause of abortion was not investigated or recorded. Although there was evidence of *N. caninum* infection serologically, definitive proof of the presence of *N. caninum* in cattle in Jamaica could only be obtained by identification of the parasite, histologically, in aborted foetal material. However obtaining such material is difficult because of practical logistical difficulties in Jamaica.

There was a significant association between pregnancy status of cows and Log PP values; a seropositive pregnant cow was more likely to have higher PP values than a non-pregnant cow ($p<0.05$, Table 3). From the data collected, pregnant cows and those that had calved recently (fresh cows) had higher Log PP values compared to non-pregnant, infected cows. An increase in *N. caninum* specific antibody levels during gestation has been reported in the literature (Dubey et al., 1997; Andrianarivo et al., 2001a; Guy et al., 2001a) and it is known that the enhanced humoral response in *N. caninum*-infected dams reflects reactivation of the parasite and its transplacental transmission to the foetus (Guy et al., 2001a; Williams et al., 2003; Nogareda et al., 2007). A characteristic fluctuation pattern of PP values has been reported in infected cattle. With *N. caninum* infection, some animals may have high antibody levels for their entire life time; some might alternate between seropositive

and seronegative, while others might have detectable levels for only a short time (Weston et al., 2005). Antibody levels of *N. caninum* infected animals may fluctuate as a result of age and stage of gestation (Davison et al., 1999a), which might have been the case in the present study as the exact stage of gestation in infected animals was not ascertained. One infected animal from Farm A showed a PP value, which was much higher than the high positive control (PP-124%, high positive-100%) and this animal might have been pregnant and had experienced parasite recrudescence at the time of testing, or the antibody level had peaked just before the time at which an abortion would have occurred, thus registering the high PP value. The serum sample was tested three times with similar results.

In the present study, gestation number showed a significant negative association with seropositivity. Higher seropositivity levels are more likely in herds with younger animals as older cows that may have aborted have a higher probability of being removed from the herd. This means that with age, the prevalence of *N. caninum* on farms would decrease compared to younger animals. Jensen et al. (1999) observed a different trend with a gradual increase in seropositivity levels in cattle with increased gestation number. He further explained that this could be as a result of the increasing risk of postnatal infection with age or it could be due to the fact that older cows tend to have more stable antibody levels due to prolonged antigenic stimulation after repeated activation of infection.

In conclusion, this study is the first report presenting serological evidence of *N. caninum* infection in dairy cattle in Jamaica. The study shows high serological prevalence among cattle of all age groups, pregnancy status and location. The data provided here is not representative of the entire cattle industry in Jamaica as farms were not randomly selected; therefore, further large scale country-wide investigations are needed to fully evaluate the epidemiology of the parasite and its economic impact on the industry and whether there are any differences in the seroprevalence of the parasites in the local breed compared to the Holstein Friesian, which are more prevalent on dairy farms.

CHAPTER FIVE: General Discussion

The exact cause and mechanisms leading to *N. caninum*-associated abortion is unclear. Once *N. caninum*-infected cows become pregnant, the infection can be efficiently transmitted across the placenta to infect the foetus. The animals either abort throughout gestation, or calves are born alive and clinically healthy or with signs of neuromuscular disorders. Experimental infection of pregnant cows with *N. caninum* tachyzoites in early and late gestation (70 and 210 days gestation age, respectively) resulted in foetal death in all foetuses in early gestation, while those in late gestation were still alive at the time of euthanasia (Gibney, 2008). The aim of our study was to assess the pathological effects of *N. caninum* on bovine foetuses following infection at 70 and 210 days gestation age and to evaluate the immune response towards the parasite. The immunological maturity of the foetus at the time of infection plays an important role and could determine the outcome of the pregnancy (Gibney et al., 2008; Rosbottom et al., 2008). In the current study, the development of the haemolymphatic tissues in infected foetuses was assessed and compared to uninfected controls at the same time points. Foetal immunological development occurs gradually throughout gestation and evidence of low cell turnover in the haemolymphatic tissues of all foetuses in early gestation was shown, compared to the high cell turnover observed in the thymus and spleen of the more mature foetuses in late gestation. The haemolymphatic tissues of foetuses infected in late gestation had no histological changes and there was no difference in the histological composition between infected and control foetuses. The morphological difference in the composition of the haemolymphatic tissues of foetuses in early and late gestation would indicate that the older foetuses are capable of recognising the parasites as non-self and are capable of eliciting an immune response, which probably controlled parasite dissemination. The detection of *N. caninum* parasites in the haemolymphatic tissues of the younger foetuses, and not in the older foetuses, suggests that parasites were able to multiply rapidly in the tissues of the younger foetuses possibly due to the lack of a competent and functional immune response, which was insufficient to control the parasites.

The non-haemolymphatic tissues of foetuses in early gestation showed necrosis and apoptosis in the CNS and liver; and a high parasite burden was detected mainly in the latter organs and heart, but the parasites were not in direct association with inflammatory cells. The importance of the CNS, liver and heart as target organs for *N. caninum* has been reported (Wouda et al., 1997). *Neospora caninum* appeared to

induce hepatocellular necrosis along with apoptosis in the liver, but had no pathological effect in cardiomyocytes. This could be because of the physiology of these cells, hepatocytes have a high cell turnover and high regenerative capacity; whereas cardiomyocytes are non-regenerative and cell turnover is usually not a characteristic feature of this organ after birth. Although high parasite loads were detected in the cardiomyocytes, these were not directly associated with the T cell infiltrates detected; suggesting that lymphocytes recruited into the heart might not be functional and therefore could not respond directly to the presence of the parasites. The CD3-positive T cells detected in the liver and CNS and were also not associated with areas of necrosis or parasites. Macrophages are effective antigen presenting cells and in the spleen and lymph nodes could potentially present *N. caninum* peptides in the context of MHC-II, which could result in activation and proliferation of parasite specific T cells (Dion et al., 2011). The T cells appeared to be recruited in response to the parasites or tissue damage, but they did not appear capable of controlling parasite replication and there was a lack of detectable IFN-γ production. This lends further support to the hypothesis that the T cells present in the infected tissues were immature and non-functional. This is in contrast to what was observed in older foetuses where histological changes were restricted mainly to the CNS (focal necrosis) along with mild to moderate T cell dominated mononuclear infiltrates, which were in direct association with the necrosis and parasites. IFN-γ was also detected in the lung, liver and muscle in the day 210 foetuses, but not in the CNS.

The production of IFN-γ by the spleen and lymph nodes of foetuses in late gestation supports our view that the time when the infection occurs is a deciding factor on whether or not the foetus will live or die. The presence of IFN-γ in the tissues of older foetuses may have served to limit parasite multiplication and dissemination throughout the tissues, hence the low parasite numbers and mild pathological changes. These changes were limited exclusively to the CNS, which is consistent with the predilection site of the parasites in older foetuses especially in the third trimester (Collantes-Fernández et al., 2006a). One of the major roles of the innate immune response in controlling intracellular parasites involves detection of the pathogen and production of cytokines such as IL-12, which are involved in the stimulation of T cells and natural killer cells to produce IFN-γ (Gazzinelli et al., 1993). IFN-γ probably exerts a direct cytotoxic effect on parasite-infected cells, slowing down the growth of the parasites through the induced synthesis of nitric

oxide (NO), which was shown to inhibit *T. gondii* multiplication in infected macrophages (Adams et al., 1990; Chao et al., 1993). The specific mechanism of NO inhibition on parasite replication remains to be determined (Dupont et al., 2012). Another important mechanism of cell killing could involve cytotoxic T cells, which are specialised to recognise and destroy cells infected with pathogens (Gazzinelli et al., 1992). These cells were probably activated by IFN-γ leading to increased killing of *N. caninum*-infected cells (Tanaka et al., 2000). A *N. caninum*-specific cytokine response, elicited by the foetuses around the time of challenge was probably responsible for influencing the disease severity and parasite loads in the older foetuses, unlike those in early gestation where evidence of CMI response was not seen. Others have shown evidence of a cytokine response in studies looking at foetal immune responses in *Neospora*-infected cattle in mid to late gestation (Andrianarivo et al., 2001b; Almeria et al., 2003; Bartley et al., 2004; Bartley et al., 2013a), suggesting that the foetal immune response was sufficiently robust and was able to control the parasite, thus resulting in survival of infected foetuses. An area of further investigation includes the upregulation of the toll-like receptors (TLRs), which are a family of receptors that sense a broad range of microbial and protozoan products (Takeda et al., 2003). TLRs are involved in the innate activation of immune responses (Werling et al., 2006). Upregulation of TLRs was recently reported in the spleen and lymph nodes of *N. caninum*-infected cows and their foetuses following experimental infection at 210 days gestation age (Bartley et al., 2013a).

The immune response in experimentally infected foetuses did not appear to be different to that in the naturally infected foetuses, although pathological changes in the latter were fewer and the parasite burden was lower. The foetuses from naturally infected dams were all alive at the time of euthanasia (Gibney, 2008) and would probably have survived to term. Although foetal infection is common following parasite recrudescence, foetal death usually occurs only in a minority of cases (Davison et al., 1999c). Some of the factors that could contribute to low parasite burden, mild parasite-induced lesions and foetal survival includes the foetal immunocompetence at the time of infection and virulence of the parasites. The majority of *Neospora*-associated abortions are reported to occur between four and seven months gestation age (approximately 120 dg) when the foetal immune system would have started to develop (Barr et al., 1991; Anderson et al., 1995). Since the foetal immunocompetence starts to develop at about 120 days of gestation (Swift and

Kennedy, 1972), it could be argued that the immune response of the naturally infected foetuses, in the current study, played a crucial role in foetal survival. It is important to note that although the immune system starts to develop around the time when abortion cases are reported to occur, it might not provide adequate protection from the the parasites, as this development is a gradual process that continues throughout foetal life until parturition (Swift and Kennedy, 1972). It was shown that the lower virulent strains of *N. caninum* had a low vertical transmission rate in pregnant mice compared to more virulent strains (Rojo-Montejo et al., 2009b; Regidor-Cerrillo et al., 2010). This suggests limited dissemination of the parasites to the placenta and foetus and consequently, reduced parasite-induced lesions as the parasites would probably need more time to multiply in the tissues to produce similar lesions and foetal mortality as with the more virulent strains (Regidor-Cerrillo et al., 2014). In contrast experimental infection early in gestation with the most virulent strains such as Nc-Liverpool resulted in foetal death within 3 weeks post infection in early gestation (Rosbottom et al., 2008).

The findings of high parasite burden in hepatocytes with associated hepatocellular degeneration contrasted with the observation that in cardiomyocytes there were few histological changes associated with parasite infection. These observations were of particular interest and were therefore investigated further. The results presented in Chapter 3 suggest that *N. caninum* is associated with hepatocellular death by apoptosis and is consistent with what has been demonstrated in the livers of foetuses in early gestation where high numbers of apoptotic hepatocytes were detected alongside necrotic cells (Chapter 2). The fact that caspase 3 expression was not detected within infected cells suggests active inhibition of host cell death by the parasites. It is not known how this occurs, but translocation of the p65 subunit of the host cell transcription factor NF-κB to the nucleus was shown to upregulate host anti-apoptotic genes in *T. gondii*-infected cells (Molestina et al., 2003). In contrast nuclear localisation of the p65 subunit in *N. caninum*-infected cells *in vitro* was not observed regardless of the number of parasites within infected cells (Herman et al., 2007). This suggests that both *N. caninum* and *T. gondii* inhibit activation of the effector caspase via different mechanisms even though the parasites are closely related.

Similar results were obtained for cardiomyocytes where no caspase 3 expression was detected in parasite infected cells. In addition, the lack of caspases 8

and 9 activation in the majority of infected hepatocytes and cardiomyocytes supports the findings reported for *T. gondii* where caspase inhibition was evident at the level of both the initiator and effector caspases (Payne et al., 2003). It is likely that the bystander hepatocytes in the livers of *N. caninum* infected foetuses described in Chapter two initially underwent apoptotic cell death, but proceeded to secondary necrosis due to loss of cell integrity from either decreased phagocytosis following massive cell death or following foetal death. The fact that all infected foetuses in early gestation died within 24 hours of euthanasia of the dams, could also serve as a contributing factor to the loss of cell integrity leading to secondary necrosis; however, it is important to note that the cows in the initial experiment were euthanised as soon as foetal death was detected in an effort to minimise post-mortem changes in foetal tissues (Gibney, 2008). The death of the foetuses may have pushed the apoptotic appearance of hepatocytes to one of necrotic cell death, which was observed histologically, though a large quantity of these hepatocytes were expressing cleaved caspase 3. Cells in a living organism would demand energy via adenosine triphosphate production for the initiation of apoptosis; therefore, it is our view that while the foetuses were alive, hepatocellular apoptosis may have been induced by *N. caninum* and/or stress factors during foetal death, but following foetal death hepatocytes gradually lose their integrity and gained equilibrium with the surrounding tissues (secondary necrosis and autolysis). The data presented in Chapter 3 are strongly suggestive of apoptotic cell death in *N. caninum*-infected liver cultures and the mitochondrial organisation in the uninfected bystander cells in the same cultures also strongly supports apoptosis that probably resulted as a direct or indirect effect of the parasites. The data also indicated that cardiomyocyte cell death was not influenced by the presence of *N. caninum*, though similar mitochondrial organisation was observed in uninfected bystander cells in the infected cultures. The latter findings are consistent with the immunohistological findings in Chapter two and the findings of others (Wouda et al., 1997).

Neospora caninum is ubiquitously distributed and is a major cause of reproductive failure in cattle. The seroprevalence of *N. caninum* in cattle has been reported in many different countries and there are considerable differences among countries and regions, and within countries [reviewed in (Dubey and Schares, 2011)]. However, there have been no previous reports of neosporosis within the Caribbean region and therefore it was our aim to investigate its seroprevalence, focusing mainly

on Jamaican dairy herds to understand the epidemiology of the parasite in the region. The *N. caninum* seroprevalence in 499 cows from 3 herds in Jamaica was approximately 26% based on the ELISA results from serum samples collected and this seroprevalence is in line with values published for dairy cattle in the Central American region (Osawa et al., 2002; Romero et al., 2002; Munhoz et al., 2009; Romero-Salas et al., 2010). The three herds we investigated may not have been truly representative of dairy production in Jamaica due to the fact that only three herds were included in the study and a country-wide survey will be needed to give a true representation of the seroprevalence amongst all herds. Nevertheless, given the practical difficulties of sampling cattle over a wide area of the country, investigating seroprevalence within these large commercial herds provides preliminary evidence that the parasite is present within Jamaican cattle.

Abortion was reported in 1.6% of total number of animals on the three farms at least once, but this may not have been a true reflection of the prevalence of *Neospora*-associated abortions, as cases are not always recorded and given the extensive management systems in these herds, abortion in the field could easily be missed. Cows infected with *N. caninum* may abort anywhere from three months gestation age to term, although the majority of abortion cases was reported in cows five to seven months of gestation age (Dubey et al., 2007; Almería and López-Gatius, 2013). Significantly higher numbers of abortion cases were recorded in a retrospective study during the second term of gestation compared to the first and third terms (López-Gatius et al., 2004). Abortions that occurred in the field during early gestation could easily be overlooked, especially if the pregnancy status of the animal was not previously known, as these animals would return to oestrus without any complications. It is therefore possible that the 1.6% presented here in our study is not representative of the true rate of abortion among *N. caninum*-infected cattle in Jamaica. Despite the presence of farm dogs on some farms, the seropositivity in relation to animal age was not significant, indicating that vertical transmission rather than horizontal is the main route of *N. caninum* transmission in Jamaica. An increase in seropositivity with age would suggest horizontal transmission, but it is also likely that vertical transmission could be augmented by horizontal transmission. This would probably occur through contamination of feed and water sources by oocysts from the definitive host (McAllister et al., 1998).

In conclusion, the data provided in this thesis have shed more light on the complex pathogenesis of bovine neosporosis. The results showed widespread pathological changes in foetal tissues with evidence of T cell infiltration, which indicate that foetuses were trying to mount a response but in younger foetuses this was not protective. The placentae from the dams of these foetuses also showed parasite associated damage and inflammation, which may have contributed to foetal death (Gibney, 2008). The results from older foetuses reveal only mild pathological changes mainly in the CNS, which suggest that the immune response elicited in late gestation may have contributed to foetal survival. The high parasite burdens detected in the liver and heart are also consistent with other findings (Wouda et al, 1997). Our data indicate parasite-associated hepatocellular death in uninfected hepatocytes, but not in cardiomyocytes. Why hepatocytes die and not cardiomyocytes is still not clear and needs to be explored further to fully understand how the parasite interact with different cell types.

APPENDIX 1: Detailed histological description of foetal tissues

Table 1: Histological features of infected foetus at 70 days gestation

HO3-2724-98 (I-1)

ORGAN	DESCRIPTION	
Spleen	HE	Red and white pulp were poorly differentiated and exhibited moderate amount of lymphocytes. Numerous apoptotic lymphocytes were present. A large population of haematopoietic precursor cells (myeloid, erythroid and megakaryocyte precursors) was present.
	CD3	Moderate amounts of CD3-positive T cells were detected in the spleen and were not associated with any specific structures.
	MHCII	Low numbers of positive cell were present and randomly scattered.
	PCNA	Low numbers of PCNA-positive proliferating cells were detected and randomly scattered within the spleen.
	Caspase 3	Moderate amounts of caspase 3-positive apoptotic cells were present and randomly scattered.
	Neospora	Low numbers of *N. caninum* tachyzoites were detected within intact cells (mononuclear cells).
Thymus	HE	The thymus was moderately developed. The cortex and medulla were well distinct. The cortex exhibited low numbers of cells, while the medulla contained fewer cells. Apoptotic bodies were present in high numbers in the cortex than the medulla.
	CD3	Moderate amounts of CD3-positive T cells were present within the cortex and fewer positive cells were observed in the medulla.
	PAX5	B lymphocytes were not observed in the thymus.
	MHCII	Low numbers of positive cells were present mainly in the medulla and fewer in the cortex.
	PCNA	Proliferating cells were present in low numbers and mainly in the cortex.
	Caspase 3	High numbers of caspase 3-positive apoptotic cells were present in both cortex and medulla.
	Neospora	*N. caninum* antigen was detected in intact mononuclear cells and cell free in the medulla.
BM	HE	Bone marrow was of low cellularity with precursors of the erythroid and myeloid cell lineages present, but megakaryocytes were not observed. Abundant trabecular bone and cartilage were present.
	CD3	Low numbers of CD3-positive T cells were present in the bone marrow.
	PAX5	B cells were present in low numbers and sparsely scattered.
	MHCII	Low numbers of MHCII-positive cells were present.
	PCNA	Proliferating cells were present in low numbers.
	Casp3	High numbers of caspase 3-positive apoptotic cells were detected.
Kidney	HE	Occasional necrotic tubular epithelial cells were present.
	Neospora	Low numbers of *N. caninum* tachyzoites were detected within intact tubular epithelial cells.
Femoral nerve	HE	NHAIR
	Neospora	*N. caninum* antigen was not detected.
Brain	HE	Multifocal areas of glial cell aggregates were present with few necrotic and apoptotic cells.
	CD3	Low numbers of CD3-positive T cells were present and randomly scattered within the glial cell aggregates and majority of these cells were present within blood vessels.
	MHCII	High numbers of positive cells were present within the glial cell aggregates (activated microglial cells) and endothelial cells were also positive (activated).
	Calprotectin	Low numbers of positive cells were detected within the glial aggregates.
	Caspase 3	High numbers of caspase 3-expressing cells were present within the glial aggregates and also diffusely distributed in the neuropil.
	Neospora	*N. caninum* antigen was detected within intact glial cells.

Spinal cord	HE	Moderate autolysis. Histological abnormalities were not observed.
	Neospora	*N. caninum* antigen was detected in intact glial cells.
Heart	HE	NHAIR
	CD3	Moderate numbers of CD3-positive T cells were present in the epicardium and fewer in the myocardium.
	Caspase 3	Low numbers of caspase 3-positive apoptotic cells were present in the epicardium (leukocytes).
	Neospora	Moderate numbers of *N. caninum* tachyzoites were detected within intact cardiomyocytes.
Skeletal muscle	HE	Moderate numbers of apoptotic cells (myoblasts) were observed.
	CD3	Low numbers of CD3-positive T cells were present in the interstitial areas.
	Caspase 3	High numbers of caspase 3-positive apoptotic cells were observed (foetal myoblast).
	Neospora	*N. caninum* antigen was not detected.
Liver	HE	The hepatic architecture was severely disrupted, hepatic cords and portal areas were inconspicuous. Hepatocytes were hypereosinophlic (necrosis) and moderate amounts of haematopoietic precursor cells were present (all precursors lineages).
	CD3	Moderate numbers of CD3-positive T cells were detected and randomly scattered in the parenchyma.
	Caspase 3	High numbers of caspase 3-positive apoptotic cells (hepatocytes and fewer haematopoietic cells) were present and randomly scattered.
	Neospora	Numerous *N. caninum* tachyzoites were detected within degenerated hepatocytes, a megakaryocyte and cell free.
Lung	HE	Moderate autolysis along with low numbers of apoptotic bronchial epithelial cells.
	CD3	Low numbers of CD3-positive T cells were present in the interstitial areas of the lung and within vessels.
	Caspase 3	High numbers of caspase 3-positive apoptotic cells (pulmonary bronchiolar and bronchial epithelial cells) were observed.
	Neospora	*N. caninum* antigen was detected in moderate amounts within intact interstitial cells and was not associated with any degenerated cells.
kidney	HE	NHAIR
	Neospora	*N. caninum* antigen was detected in low numbers within intact interstitial cells.

HE - Haematoxylin and Eosin

NHAIR - No histological abnormality is recognised

Table 2: Histological features of infected foetus at 70 days gestation

HO5-0562-99 (I-3)

ORGAN	DESCRIPTION	
Spleen	HE	The spleen was moderately developed and contained numerous spindle-shaped cells with low numbers of lymphocytes along with diffuse extramedullary haematopoiesis (all precursor cell lineages). Red and white pulp were poorly differentiated and lymphoid follicles were not formed.
	CD3	Low numbers of CD3-positive T cells were present and not associated with any specific structures.
	PAX5	B cells were present in lower numbers compared to T cells and not associated with any structures.
	MHCII	Low numbers of MHCII-positive cells were present and randomly scattered.
	PCNA	Proliferating cells were present in low numbers and randomly scattered.
	Caspase 3	High numbers of caspase 3-positive apoptotic cells were present and diffusely scattered.
	Neospora	Low numbers of *N. caninum* tachyzoites were detected in intact mononuclear cells and also cell free.
Thymus	HE	The thymus was moderately lobulated with distinct cortex and medulla. The cortex exhibited low numbers of lymphocytes, while medulla contained even fewer, larger cells. High numbers of apoptotic lymphocytes were present within both cortex and medulla.
	CD3	Low numbers of CD3-psitive T cells were present in the cortex and fewer in the medulla.
	PAX5	B cells were not observed in the thymus.
	MHCII	Low numbers of MHCII-positive cells were present in the cortex and higher numbers were observed in the medulla (macrophages and bone marrow derived non-phagocytic dendritic cells).
	PCNA	Proliferating cells were present in low numbers in both cortex and medulla.
	Caspase 3	High numbers of caspase 3-positive apoptotic cells were present in the cortex and fewer in the medulla.
	Neospora	*N. caninum* tachyzoites were detected in low numbers in the medulla within intact mononuclear cells.
BM	HE	Bone marrow was of low cellularity with low numbers of myeloid and erythroid precursor lineages. Megakaryocytes were not observed and low numbers of apoptotic precursor cells were present.
	CD3	Low numbers of CD3-positive T cells were observed.
	PAX5	B cells were not observed in the bone marrow.
	MHCII	Moderate amounts of MHCII-positive cells were present.
	PCNA	Proliferating cells were few and sparsely scattered.
	Caspase 3	High numbers of caspase 3-positive apoptotic cells were detected.
	Neospora	*N. caninum* antigen was not detected in the bone marrow.
Brain	HE	The brain was highly cellular with multifocal aggregates of glial cells. Low numbers of apoptotic cells were present within these aggregates.
	CD3	Low numbers of CD3-positive T cells were present in the aggregates, within blood vessels and individual positives cells were detected in the neuropil.
	MHCII	The majority of cells within the glial cell aggregates were MHCII-positive, consistent with activated microglial cells. MHCII expression was also detected on endothelial within the neuropil.
	Calprotectin	Occasional positive cells were present within the glial cell aggregates.
	Caspase 3	Low numbers of caspase 3-positive glial cells were present within the aggregates and numerous positive cells were also detected randomly scattered in the neuropil.
	Neospora	Small clusters of *N. caninum* tachyzoites were detected within intact glial cells in the glial aggregates and were not associated with inflammation or necrosis.
Spinal cord	HE	There was moderate autolysis. Low numbers of necrotic cells were present in the white matter and not associated with inflammation.
	CD3	Moderate numbers of CD3-positive T cells are detected in the meninges, while fewer are present in the grey and white matter
	Caspase 3	Low numbers of caspase 3-expressing glial cells were detected within grey and white matter
	IFN-γ	IFN-γ-expressing cells were not detected

	Neospora	*N. caninum* antigen was detected within intact glial cells.
Heart	HE	Low numbers of mononuclear cells were present in the epicardium.
	CD3	Moderate amounts of CD3-positive T cells were detected in the epicardium and low numbers were present in the myocardium.
	Caspase 3	The majority of mononuclear cells observed in the epicardium were caspase 3 positive.
	IFN-γ	IFN-γ-expressing cells were not detected
	Neospora	*N. caninum* antigen was not detected.
Lung	HE	Moderate autolysis with numerous sloughed bronchiolar epithelial cells.
	IFN-γ	IFN-γ-expressing cells were not detected
	Neospora	*N. caninum* antigen was not detected.
Liver	HE	Hepatocytes were disorderly arranged and hepatic cords, central veins and portal areas were not discernible. Hepatocytes were hypereosinophilic (extensive hepatocellular necrosis) and low numbers of haematopoietic precursor cells were present.
	IFN-γ	IFN-γ-expressing cells were not detected
	Neospora	*N. caninum* antigen was detected in necrotic hepatocytes and cell free.
Skeletal muscle	HE	Low numbers of apoptotic myoblasts were present and randomly distributed.
	IFN-γ	IFN-γ-expressing cells were not detected
	Neospora	*N. caninum* antigen was not detected.
kidney	HE	Low numbers of epithelial cell necrosis was present in the renal cortex.
	CD3	Occasional T cells were detected within interstitial areas of the kidney
	Neospora	*N. caninum* antigen was detected in intact cells and not associated with necrosis.
Adrenal	HE	NHAIR
	Neospora	*N. caninum* antigen was not detected.
Ileum	HE	NHAIR
	Neospora	*N. caninum* antigen was not detected.
Pancreas	HE	NHAIR
	Neospora	*N. caninum* antigen was not detected.
Femoral nerve	HE	NHAIR
	Neospora	*N. caninum* antigen was not detected.

Table 3: Histological features of infected foetus at 70 days gestation

O5L-0708-118 (I-4)

ORGAN	DESCRIPTION	
Spleen	HE	Spleen is composed of numerous spindle shaped cells with moderate number of lymphocytes not forming any structures. Apoptotic lymphocytes were present in moderate amounts. A large population of extramedullary haematopoietic precursor cells was also present.
	CD3	Moderate amounts of T cells were detected throughout the spleen.
	PAX5	Low numbers of positive cells were present and randomly scattered.
	MHCII	Moderate amounts of positive cells were present.
	PCNA	Low numbers of proliferating cells were present (lymphocytes).
	Caspase 3	High numbers of cells expressing the caspase 3 antibody were present throughout the spleen.
	Neospora	*N. caninum* antigen was detected in intact cells in low numbers.
Thymus	HE	The cortex was moderately cellular and the medulla exhibited fewer cells. Cortex exhibited high numbers of apoptotic lymphocytes and fewer were present in the medullar.
BM	HE	Bone marrow was of low cellularity and contained low numbers of apoptotic lymphocytes.
	CD3	Low numbers of T cells were present throughout the bone marrow.
	PAX5	B cells were not observed.
	MHCII	Low numbers of positive cells were present and randomly scattered throughout.
	PCNA	Proliferating cells were few in the bone marrow.
	Caspase 3	A large proportion of cells were expressing the caspase 3 antibody.
	Neospora	*N. caninum* antigen was not detected.
Brain	HE	Small multifocal aggregates of glial cells were present within the parenchyma.
	CD3	Low numbers of T cells were detected in the brain.
	MHCII	A small population of positive cells were present within the cellular aggregate in the cerebrum and a focal area of positive cells in the granular layer of the cerebellum was also positive.
	Calprotectin	Positive cell were not detected within the brain.
	Caspase 3	High numbers of cells within white and grey matter expressing the caspase 3 antibody. Positive cells were not present within the aggregate of cells described and moderate amounts were detected in the cerebellum.
	Neospora	Small clusters of *N. caninum* tachyzoites were detected and not in association with inflammation.
Spinal cord	HE	Histological changes were not observed. There was moderate autolysis.
	CD3	Low numbers of CD3-positive T cells were detected mainly in the meninges.
	Caspase 3	Low numbers of caspase 3-expressing glial cells were detected
	Neospora	*N. caninum* antigen was detected within a satellite cell in a spinal nerve root.
Heart	HE	NHAIR
	Neospora	Numerous clusters of *N. caninum* antigen were detected within intact cardiomyocytes.
Lung	HE	NHAIR
	Neospora	Low number of parasites were detected in interstitial cells and not associated with degenerated cells.
Liver	HE	The liver was disorderly arranged and hepatic cords were poorly visible. Portal areas and central veins could be seen in some sections. There was moderate multifocal hepatocellular necrosis and low numbers of apoptotic hepatocytes were present alongside necrotic cells. High numbers of haematopoietic precursor cells were present.
	Neospora	High numbers of *N. caninum* parasites were present in degenerated hepatocytes.
Skeletal muscle	HE	NHAIR
	Neospora	*N. caninum* antigen was not detected.
kidney	HE	NHAIR
	Neospora	*N. caninum* antigen was detected in low numbers within intact interstitial cells.
Adrenal	HE	NHAIR

	Neospora	*N. caninum* antigen was not detected.
Ileum	HE	NHAIR
	Neospora	*N. caninum* antigen was not detected.
Pancreas	HE	NHAIR
	Neospora	*N. caninum* antigen was detected in low numbers in acinar cells and was not associated with degenerated cells.
Femoral nerve	HE	NHAIR
	Neospora	*N. caninum* antigen was not detected.

Table 4: Histological features of control foetus at 70 days gestation

HO4-1517-113 (C-3)

ORGAN	DESCRIPTION	
Thymus	HE	Moderately lobulated with high numbers of densely packed lymphocytes in the cortex and fewer larger lymphocytes in the medulla, which contained high numbers of macrophages.
	CD3	CD3+ T cells were present in high numbers in the cortex and fewer larger cells were detected in the medulla.
	PAX5	Low numbers of B cells were present in the medulla only.
	MHCII	Low numbers of MHCII+ cells were present in the cortex and a larger population was present within the medulla (macrophages, dendritic cells and B cells).
	PCNA	Low numbers of proliferating cells were present mainly in the cortex and fewer in the medulla.
	Caspase 3	Low numbers of caspase 3-positive cells were present in the cortex and medulla.
Spleen	HE	Composed of numerous spindle-like cells, low numbers of lymphocytes and diffuse extra-medullary haematopoiesis. Red and white pulp are poorly differentiated. Lymphoid follicles were not identified.
	CD3	Low numbers of T cells were observed and randomly scattered throughout the spleen and was not associated with any structures.
	PAX5	Low numbers of B cells were present and randomly scattered.
	MHCII	Low numbers of positive cells were present in the spleen.
	PCNA	Proliferating cells were present in low numbers (lymphocytes).
	Caspase 3	Caspase 3-positive cells were detected in low numbers and randomly scattered.
Bone marrow	HE	Bone was of low cellularity. Small clusters of the erythroid and myeloid precursor lineages were dispersed throughout the intertrabecular spaces.
	CD3	Low numbers of T cells were randomly scattered throughout the intertrabecular spaces.
	PAX5	Low numbers of B cells were admixed within the T cell population.
	MHCII	A small population of positive cells (monocytes and B cells) were present within the clusters.
	PCNA	Proliferating cells were present in low numbers.
	Caspase 3	Occasional caspase 3-poitive cells were detected.
Heart	HE	NHAIR
Skeletal muscle	HE	NHAIR
Liver	HE	NHAIR
Lung	HE	NHAIR
Brain	HE	NHAIR
	CD3	T cells were not present within the brain parenchyma.
	MHCII	Low numbers of positive cells were detected in a focal area of the white matter.
	Calprotectin	Macrophages were not detected.
Spinal cord	HE	NHAIR
Intestine	HE	NHAIR
Kidney	HE	NHAIR
Femoral nerve	HE	NHAIR

Table 5: Histological features of control foetus at 70 days gestation

HO4-1518-119 (C-4)

ORGAN	DESCRIPTION	
Thymus	HE	Moderately lobulated with high numbers of densely packed lymphocytes in the cortex and fewer larger lymphocytes in the medulla, which contained high numbers of macrophages.
	CD3	Cortex exhibited high numbers of T cells, while medulla had fewer positive cells.
	PAX5	Low numbers of B cells were present in the medulla only.
	MHCII	A small population of positive cells was present in the cortex and higher numbers were observed in the medulla (macrophages, dendritic cells and B cells).
	PCNA	Low numbers of proliferating cells were detected mainly in the cortex.
Spleen	HE	A large population of spindle-shaped cells was present in the spleen. Red and white pulps were poorly differentiated and lymphoid follicles were not observed.
	CD3	Low numbers of T lymphocytes were present in the spleen and were not associated with any structures.
	PAX5	A small population of B cells was randomly scattered throughout the red and white pulp.
	MHCII	Moderate amount of positive cells were present and diffusely scattered in the spleen.
	PCNA	Low numbers of proliferating cells were detected and randomly scattered in red and white pulp.
	Caspase 3	Individual caspase 3-expressing cells were present and randomly scattered.
Bone marrow	HE	Bone was of low cellularity. Small clusters of the erythroid and myeloid precursor lineages were dispersed throughout the intertrabecular spaces.
	CD3	A small population of T lymphocytes was randomly scattered throughout the organ.
	PAX5	Low numbers of B cells were present.
	MHCII	Low numbers of positive cells were detected (monocytes and B cells).
	PCNA	Proliferating cells were present in low numbers.
	Caspase 3	Not detected.
Heart	HE	NHAIR
Skeletal muscle	HE	NHAIR
Liver	HE	NHAIR
Lung	HE	NHAIR
Intestine	HE	NHAIR
Kidney	HE	NHAIR
Femoral nerve	HE	NHAIR
Brain	HE	NHAIR
	CD3	T cells were not present within the brain parenchyma.
	MHCII	Low numbers of positive cells were present within a focal area of the white matter.
	Calprotectin	Possible cells were not detected.
Spinal cord	HE	NHAIR

Table 6: Histological features of infected foetus at 210 days gestation

HO4-986-399G (I-11)

ORGAN	DESCRIPTION	
Thymus	HE	The thymus was highly developed with well differentiated cortex and medulla. The cortex contained numerous small, tightly packed lymphocytes, while the medulla had a smaller population of large lymphocytes with high numbers of reticular medullary epithelial cells, macrophages, dendritic cells and a marked infiltration of polymorphonuclear cells (eosinophils).
	CD3	High numbers of T cells were present in the cortex and a smaller population was observed in the medulla.
	PAX5	Low numbers of B cell were present within the medulla only.
	MHCII	The medulla had high numbers of MHCII-positive cells with few positive cells diffusely scattered in the cortex.
	PCNA	PCNA-positive proliferating cells were present in high numbers in the cortex with fewer in the medulla.
	Caspase 3	Moderate amounts of caspase 3-posiitve cells (lymphocytes) were present in both cortex and medulla.
	IFN-γ	IFN-γ-expressing cells were not detected
	Neospora	*N. caninum* antigen was not detected.
Spleen	HE	The spleen had well differentiated red and white pulp and comprised of high numbers of lymphocytes within the white pulp (PALS and lymphoid follicles) and a fewer were present in the red pulp. Haematopoietic precursor cells were present in low numbers.
	CD3	High numbers of T cells were present in the white pulp. The red pulp contained a smaller population of T cells.
	PAX5	Numerous B cells were present within the lymphoid follicles (not fully formed) and a small population was observed within red pulp areas.
	MHCII	High numbers of MHCII-positive cells were present in the white pulp, mainly in lymphoid follicles (macrophages, follicular dendritic cells, splenic dendritic cells and lymphocytes). The red pulp also contained high numbers of positive cells.
	PCNA	Moderate amounts of PCNA-positive proliferating cells were present in both white and red pulps (lymphocytes and haematopoietic cells).
	Caspase 3	Low numbers of caspase 3-positive apoptotic cells were present and randomly scattered in red and white pulp (mainly in lymphoid follicles).
	IFN-γ	Low numbers of IFN-γ-expressing were detected within the spleen
	Neospora	*N. caninum* antigen was not detected.
Lymph node	HE	Highly developed with distinct superficial cortex, paracortex and medulla. Primary lymphoid follicles were present in the superficial cortex without germinal centres. High numbers of lymphocytes were present in cortex and fewer in the medulla. Low numbers of eosinophils were present in the medulla and occasional neutrophils.
	CD3	High numbers of T cells were present within the paracortex, low numbers scattered in B cell compartments and a smaller population observed in the medulla.
	PAX5	Numerous B cells were present within lymphoid follicles and fewer positive cells were detected in the paracortex and medulla.
	MHCII	A large population of positive MHCII cells were present within the cortex (follicular dendritic cells, dendritic cells, macrophages and B cells) and a smaller population observed in the medulla.
	PCNA	High numbers of proliferating cells were present mainly in the lymphoid follicles.
	Caspase 3	Low numbers of caspase 3-positive apoptotic cells were present and randomly scattered. These were not associated with any specific structures.
	IFN-γ	IFN-γ-expressing cell were detected in moderate numbers mainly in the paracortex
	Neospora	*N. caninum* antigen was not detected.
Bone marrow	HE	The bone marrow was of high cellularity with all haematopoietic precursor cell

		lineages present along with low numbers of adipocytes.
	CD3	Moderate amounts of T cells were present throughout the bone marrow.
	PAX5	High numbers of B cells were present and diffusely scattered throughout the organ.
	MHCII	Moderate amount of positive cells were present in bone marrow (monocyte/macrophages lineage).
	PCNA	High numbers of proliferating cells were observed (haematopoietic precursor cells).
	Caspase 3	Caspase 3-positive cell were not detected.
	IFN-γ	Low numbers of IFN-γ-expressing were present
	Neospora	*N. caninum* antigen was not detected.

ORGAN	**DESCRIPTION**	
Heart	HE	Moderate multifocal to coalescing mononuclear infiltrates were present in the myocardium (non-suppurative myocarditis) and low numbers of eosinophils were observed in the inflammatory infiltrates.
	CD3	T cells were the predominant cell type present within the inflammatory infiltrate.
	PAX5	B cells were not detected in the inflammatory infiltrate.
	MHCII	Low numbers of MHCII-positive cells were present within the inflammatory infiltrate.
	Calprotectin	Low numbers of macrophages were detected within the inflammatory infiltrate.
	Caspase 3	Caspase 3-positive cells were not detected.
		IFN-γ-expressing cells were present in low numbers
	Neospora	*N. caninum* antigen was not detected.
Skeletal muscle	HE	Moderate multifocal mononuclear infiltrates were observed in the interstitial areas of the muscle (non-suppurative myositis).
	CD3	The inflammatory infiltrates were comprised mainly of CC3-positive T cells.
	PAX5	B cells were not present.
	MHCII	MHCII expression was present in the inflammatory foci with mild staining intensity. Endothelial cells were also positive.
	Calprotectin	Low numbers of macrophages were detected in the inflammatory infiltrates.
	Caspase 3	Caspase 3-positive cells were not detected.
	IFN-γ	IFN-γ-expressing were detected in low numbers
	Neospora	*N. caninum* antigen was not detected.
Lung	HE	Mild mononuclear inflammatory infiltrates were present within the alveolar septa and fewer in the interstitial spaces and pleura.
	CD3	Mild T cell infiltrates were detected in the pulmonary interstitium and alveolar septa with low numbers present in the pleura (pleuritis).
	PAX5	B cells were not detected within the infiltrates
	MHCII	High numbers MHCII-positive cells were present in the BALT, interstitial areas, alveolar septa and alveolar sacs. Mild expression was also observed in the pleura.
	Calprotectin	Numerous macrophages were present through the lung parenchyma (alveolar, interstitial and intravascular macrophages) and low numbers were detected in the pleura.
	IFN-γ	Low numbers of IFN-γ-expressing cells were detected mainly in the bronchial epithelium
	Caspase 3	Caspase 3-positive cells were not detected.
	Neospora	*N. caninum* antigen was not detected.
Liver	HE	The architecture of the liver was preserved. Multifocal, mild mononuclear portal infiltrates and low numbers of neutrophils were present. Low numbers of haematopoietic precursor cells were also present.
	CD3	Portal areas contained low numbers of CD3-positive T cells and fewer were detected in the parenchyma.
	PAX5	Low numbers of B cells were present in some portal areas.
	MHCII	High numbers of MHCII-positive cells were detected diffusely in the hepatic parenchyma (macrophages and Kupffer cells) and small clusters were present predominantly in the portal areas (macrophages).
	Calprotectin	Low numbers of macrophages were present in the portal areas and diffuse expression was present in the hepatic parenchyma.
	Caspase 3	Caspase 3-positive cells were not detected.
	IFN-γ	IFN-γ-expressing cells were present in low numbers and randomly scattered in the hepatic parenchyma.
	Neospora	*N. caninum* antigen was not detected.

Brain	HE	Focal area of necrosis with associated mild mononuclear infiltrate was observed in the white matter. In addition, mild perivascular mononuclear inflammatory cells were present. The necrotic foci and perivascular lesions were absent in the consecutive sections and therefore, further immunohistological assessment was done.
	Caspase 3	Caspase 3-positive cells were not detected.
	IFN-γ	IFN-γ-expressing cells were not detected.
	Neospora	*Neospora caninum* tachyzoites were present in low numbers within the focus of necrosis in an intact glial cell in association with the inflammatory infiltrate.
Spinal cord	HE	White and grey matter contained low numbers of mononuclear infiltrates, while meninges were moderately infiltrated with similar cells.
	CD3	Low numbers of CD3-positive T cells were present in the white and grey matter and were randomly scattered. Meninges also exhibited low numbers of T cells.
	PAX5	B cells represented a small proportion of the inflammatory cell in the spinal cord and meninges.
	MHC11	Diffuse MHCII expression was observed in the white and grey matter and meninges, consistent with activated microglial cells.
	Caspase 3	Occasional caspase 3-poisitve apoptotic cells were present in the grey matter (macroglial cells).
	IFN-γ	IFN-γ-expressing cells were not detected.
	Neospora	*N. caninum* antigen was not detected.
Kidney	HE	NHAIR
	Neospora	*N. caninum* antigen was not detected.
Adrenal	HE	NHAIR
	Neospora	*N. caninum* antigen was not detected.
Femoral nerve	HE	NHAIR
	Neospora	*N. caninum* antigen was not detected.

Table 7: Histological features of infected foetus at 210 days gestation

HO4-987-426G (I-12)

ORGAN	DESCRIPTION	
Thymus	HE	Highly developed with well differentiated cortex and medulla. Numerous lymphocytes occupied the cortex and lower numbers of large lymphocytes were present in the medulla along with nigh numbers of macrophages, reticular medullary epithelial cells, dendritic cells and few eosinophils.
	CD3	High numbers of T cells were present in the cortex and a smaller population was detected in the medulla.
	PAX5	Low numbers of B cells were present within the medulla.
	MHCII	A large population of MHCII-positive cells were present in the medulla (macrophages, dendritic cell and lymphocytes) and a smaller population was diffusely scattered in the cortex.
	PCNA	High numbers of proliferating lymphocytes were observed in the cortex and fewer in the medulla.
	IFN-γ	IFN-γ-expressing cells were not detected within the thymus.
	Neospora	*N. caninum* antigen was not detected.
Spleen	HE	The spleen had well differentiated red and white pulp with a large population of lymphocytes in the PALS and primary lymphoid follicles (white pulp) and moderate amounts were observed in the red pulp along with high numbers of macrophages, splenic dendritic cells, and occasional neutrophils and eosinophils. Haematopoietic precursor cells were present in low numbers.
	CD3	The PALS exhibited a high numbers of T cells and fewer were present in and around lymphoid follicles. Moderate amounts were also detected in the red pulp.
	PAX5	B cells were present in high numbers in the lymphoid follicles and low numbers were randomly scattered throughout the red pulp.
	MHCII	A large population of MHCII-positive cells were observed in lymphoid follicles, PALS and red pulp areas (lymphocytes, dendritic cells and splenic macrophages).
	PCNA	High numbers of proliferating cells were present in the white pulp and fewer were present in the red pulp.
	Neospora	*N. caninum* antigen was not detected.
Lymph node	HE	Highly developed with well distinct superficial cortex, paracortex and medulla. Primary follicles were present in the superficial cortex without germinal centres. Paracortex had high numbers of lymphocytes, while low numbers were present in the medulla along with scant polymorphonuclear cells (eosinophils).
	CD3	High numbers of T cells were present in the paracortex with scattered positive cell in the superficial cortex, while a smaller population was detected in the medulla.
	PAX5	Lymphoid follicles contained a high numbers of B cells, low numbers were scattered in the paracortex and moderate numbers were present in the medulla.
	MHCII	Numerous MHCII-positive cells were present in the cortex (dendritic cells, follicular dendritic cells, macrophages and lymphocytes) and a small population was observed in the medulla.
	PCNA	Moderate amounts of proliferating cells were present predominantly in the cortex associated with lymphoid follicles and low numbers were detected in the medulla.
	Caspase 3	Low numbers of caspase 3-positive apoptotic cells were present and randomly scattered in both cortex and medulla (lymphocytes).
	IFN-γ	Low numbers of IFN-γ-expressing cells were detected in the paracortex.
	Neospora	*N. caninum* antigen was not detected.
Bone marrow	HE	Bone marrow was of high cellularity with all haematopoietic precursor cell lines present along with scant adipose tissue.
	CD3	Moderate amounts of T cells were detected within the bone marrow.
	PAX5	High numbers of B cells were detected.
	MHCII	The bone marrow exhibited moderate amount of MHCII-positive cells (cells of the monocyte/macrophage lines and Lymphocytes).

	PCNA	Low numbers of proliferating cells were observed (haematopoietic precursor cells and lymphocytes).
	Caspase 3	Caspase 3-positive apoptotic cells were not observed in the bone marrow.
	Neospora	*N. caninum* antigen was not detected.
Brain	HE	The grey matter exhibited low numbers of mononuclear cells, represented mainly by lymphocytes.
	CD3	Low numbers of CD3-positive T cells were present in the grey matter.
	PAX5	B cells were not detected in the inflammatory infiltrates.
	MHCII	Low numbers of MHCII-positive cells were present in the grey matter (microglial cells).
	PCNA	Low numbers of proliferating cells (glial cells) were present in the grey and white matter.
	Caspase 3	Caspase 3-positive apoptotic cells were not detected.
	Neospora	*N. caninum* antigen was not detected.
Spinal cord	HE	Severe non-suppurative myelitis was observed and represented by multifocal mononuclear infiltrates in the grey and white matter along with perivascular cuffing. The grey matter exhibited numerous mononuclear cells (macrophages and lymphocytes), vessels had activated endothelial cells with evidence of leucocytes adhesion and extravasation. Apoptotic cells were present in low numbers within the inflammatory infiltrates. Severe radiculoneuritis was always present and consisted of similar inflammatory cells.
	CD3	Moderate amounts of T cells were present within the grey matter in the cell rich areas and high numbers were detected in the perivascular cuffing. T cells were more numerous in the spinal nerve roots and fewer were detected in the meninges.
	PAX5	B cells were not detected within the inflammatory infiltrates.
	MHCII	Numerous MHCII-positive cells were observed in the inflammatory infiltrates, consistent with activated microglial cells.
	PCNA	High numbers of positive cells (mononuclear cells) were present in the spinal cord grey matter and fewer were randomly scattered in the white matter.
	Caspase 3	Low numbers of caspase 3-positive apoptotic cells were present in the grey matter and perivascular cuffing in both grey and white matter.
	Neospora	*N. caninum* antigen was detected in low in association with the inflammatory infiltrates.
Heart	HE	Mild non-suppurative myocarditis, represented by multifocal mononuclear infiltrates in the myocardium.
	CD3	Low numbers of T cells were present within the inflammatory infiltrate.
	PAX5	B cells were not detected.
	MHCII	Low numbers of MHCII-positive cells were present within the inflammatory infiltrates.
	PCNA	Low numbers of proliferating cells were detected within the myocardium (cardiomyocytes).
	Caspase 3	Caspase 3-positive apoptotic cells were not detected.
	Neospora	*N. caninum* antigen was not detected.
Lung	HE	Mild multifocal peribronchiolar and peribronchial mononuclear infiltrates were observed.
	CD3	Low numbers of T cells were observed in the peribronchiolar, peribronchial areas and alveolar septa.
	PAX5	B cells were not observed.
	MHCII	High numbers of MHCII-positive cells (alveolar, interstitial, intravascular macrophages and dendritic cells) were detected.
	PCNA	Proliferating cells were not detected.
	Caspase 3	Low numbers of caspase 3-positive cells were present in the peribronchial, peribronchiolar areas and alveolar spaces.
	Neospora	*N. caninum* antigen was detected in high numbers within intact mononuclear cells in alveolar spaces and alveolar septa, consistent with macrophages.
Liver	HE	Moderate multifocal mononuclear portal infiltrates (non-suppurative hepatitis) was observed along with a focal area of necrosis, which was comprised of necrotic debris, surrounding mononuclear infiltrate and low numbers of neutrophils. Haematopoietic cells were present in low numbers.
	CD3	High numbers of T cells were present in the portal areas with fewer scattered positive cells in the hepatic parenchyma.
	PAX5	Low numbers of B cells were present within the inflammatory infiltrates in the portal areas.

	MHCII	There was diffuse staining of the liver (Kupffer cells) and within the inflammatory infiltrates in the portal areas (infiltrating macrophages).
	PCNA	Moderate amounts of proliferating cells were present and randomly scattered (mainly hepatocytes).
	Caspase 3	Low numbers of caspase 3-positive apoptotic hepatocytes and lymphocytes were detected and randomly scattered throughout the hepatic parenchyma.
	Neospora	*N. caninum* antigen was not detected.
Skeletal muscle	HE	Mild non-suppurative myositis was present and consisted of low numbers of mononuclear infiltrates in the interstitial areas.
	CD3	Low numbers of T cells were present within the inflammatory infiltrates.
	PAX5	B cells were not present.
	MHCII	Low numbers of MHCII-positive cells were detected within the inflammatory infiltrates and endothelia cells are also positive.
	PCNA	Proliferating cells were not present.
	Caspase 3	Caspase 3-positive apoptotic cells were not detected.
	Neospora	*N. caninum* antigen was not detected.
kidney	HE	NHAIR
	Neospora	*N. caninum* antigen was not detected.
Adrenal	HE	NHAIR
	Neospora	*N. caninum* antigen was not detected.
Ileum	HE	NHAIR
	Neospora	*N. caninum* antigen was not detected.
Pancreas	HE	NHAIR
	Neospora	*N. caninum* antigen was not detected.
Femoral nerve	HE	NHAIR
	Neospora	*N. caninum* antigen was not detected.

Table 8: Histological features of control foetus at 210 days gestation

HO4-976-382G (C-1)

ORGAN	DESCRIPTION	
Thymus	HE	The thymus exhibited well distinct cortex and medulla. Cortex comprised high numbers of lymphocytes, while the medulla had lower numbers of large lymphocytes and numerous macrophages and reticular medullary epithelial cells. High numbers of eosinophils were also present in the medulla.
	CD3	High numbers of T cells were present in the cortex and a smaller population was detected in the medulla.
	PAX5	B cells were detected in the medulla in moderate amounts.
	MHCII	The medulla exhibited high numbers of MHCII-positive cells (macrophages, dendritic cells and lymphocytes), while lower numbers were present in the cortex and diffusely scattered.
	PCNA	Numerous proliferating cells (lymphocytes) were present in the cortex and lower numbers detected in the medulla.
	Caspase 3	Low numbers of caspase 3-positive apoptotic cells were present and randomly scattered in cortex and medulla.
	Lendrum	The polymorphonuclear cells in the medulla were positive for the Lendrum's stain (eosinophils).
Spleen	HE	The spleen had well differentiated red and white pulp with a large population of lymphocytes in the PALS and primary lymphoid follicles and moderate amounts were observed in the red pulp. Haematopoietic precursor cells were present in low numbers.
	CD3	Numerous T cells were present in the PALS and low numbers in lymphoid follicles. Red pulp exhibited moderate amounts of T cells.
	PAX5	B cells were present in high numbers in the lymphoid follicles and fewer positive cells were detected in the red pulp.
	MHCII	High numbers of MHCII-positive cells (splenic macrophages, dendritic cells and lymphocytes) were detected in the white pulp with intense staining in the lymphoid follicles. The red pulp also exhibited diffuse staining.
	PCNA	High numbers of proliferating cells were present in both red and white pulp.
	Caspase 3	Low numbers of caspase 3-positive apoptotic cells were present in red and white pulp and not associated with any specific structures.
Lymph node	HE	The cortex and medulla were well distinct and well differentiated. High numbers of lymphocytes were present in the superficial and paracortex. Primary follicles were present in the superficial cortex, but without germinal centres. Low numbers of lymphocytes and scant polymorphonuclear cells (eosinophils and few neutrophils) were present in the medulla.
	CD3	High numbers of T cells were present in the cortex within T cell zone and few scattered cells were also present in B cell zones. Low numbers were detected in the medulla.
	PAX5	High numbers of B cells were detected in lymphoid follicles and low numbers were present in the medulla. Occasional B cells were also detected in the paracortex.
	MHCII	High numbers of MHCII-positive cells were present within the superficial cortex (follicular dendritic cell, dendritic cells, macrophages and lymphocytes) and paracortex. Moderate amounts were detected in the medulla.
	PCNA	Proliferating cells were present in low numbers and randomly scattered in the cortex and medulla.
	Caspase 3	Individual caspase 3-positive apoptotic cells were detected and randomly scattered in the cortex and medulla.
Bone marrow	HE	Bone marrow was highly cellular with all haematopoietic precursor cell lines present. Adipose tissue was also present in low numbers.
	CD3	Low numbers of T cells were detected.
	PAX5	Low numbers of B cells were present within the bone marrow.

	MHCII	Low numbers of MHCII-positive cells were detected.
	PCNA	Proliferating cells were present in low numbers.
	Caspase 3	Caspase 3-positive cells were not detected.
Heart	HE	NHAIR
Skeletal muscle	HE	NHAIR
Liver	HE	Occasional mononuclear cells (lymphocytes) were present in the portal areas and low numbers of haematopoietic precursor cells were present in the hepatic parenchyma.
Lung	HE	NHAIR
Intestine	HE	NHAIR
Kidney	HE	NHAIR
Femoral nerve	HE	NHAIR
Brain	HE	NHAIR
Spinal cord	HE	NHAIR

Table 9: Histological features of control foetus at 210 days gestation

HO4-984-411G (C-5)

ORGAN	DESCRIPTION	
Thymus	HE	The thymus exhibited well differentiated cortex and medulla. Cortex contained high numbers of lymphocytes, while the medulla had a smaller population of large lymphocytes, numerous macrophages and reticular medullary epithelial cells. High numbers of eosinophils were also present in the medulla.
	CD3	T cells were present in high numbers in the cortex and a lower numbers were detected in the medulla.
	PAX5	Low numbers of B cells were present in the medulla.
	MHCII	Medulla contained high numbers of MHCII-positive cells and fewer were present in the cortex and diffusely scattered.
	PCNA	High numbers of proliferating lymphocytes were present in the cortex with fewer detected in the medulla.
	Caspase 3	Moderate amounts of caspase 3-positive apoptotic cells were present in both cortex and medulla.
Spleen	HE	The spleen was highly developed with well differentiated red and white pulp. High numbers of lymphocytes were present in the white pulp and fewer were present in the red pulp along with high numbers of macrophages, dendritic cells and fewer neutrophils. Megakaryocytes were the predominant haematopoietic cell type with scant myeloid and erythroid precursors.
	CD3	T cells were present in high numbers in the PALS and few scattered cells were also present in the lymphoid follicles. The red pulp contained moderate amounts of T cells.
	PAX5	Lymphoid follicles exhibited high numbers of B cells and fewer were present in the red pulp.
	MHCII	There was diffuse staining of MHCII-positive cells in the white pulp (dendritic and follicular dendritic cells, macrophages and lymphocytes) and red pulp (macrophages, dendritic cells and lymphocytes).
	PCNA	High numbers of PCNA-positive proliferating cells (haematopoietic cells and lymphocytes) were present. The lymphoid follicles contained the majority of these cells, while lower numbers were present in red pulp.
	Caspase 3	Low numbers of caspase 3-positive cells were present and randomly scattered in red and white pulp.
Lymph node	HE	The cortex and medulla were well differentiated and similar morphologically to other foetuses. Primary follicles were present in the superficial cortex, but without germinal centres. Low numbers of lymphocytes and scant polymorphonuclear cells (eosinophils) were present in the medulla.
	CD3	High numbers of T cells were present in the paracortex and low numbers were detected within lymphoid follicles. Medulla contained a smaller population of T cells.
	PAX5	B cells were predominantly seen in the lymphoid follicles and fewer positive cells were detected in the paracortex and medulla.
	MHCII	Numerous MHCII-positive cells were detected in the cortex (lymphoid follicles) and fewer positive cells were present in the medulla.
	PCNA	Moderate amount of PCNA-positive proliferating cells were present mainly in the lymphoid follicles.
	Caspase 3	Low numbers of caspase 3-positive apoptotic cells were observed mainly in the lymphoid follicles.
Bone marrow	HE	Bone marrow was of high cellularity with all precursor cell lineages were present. Adipocytes were present in low numbers.
	CD3	Low numbers of T cells were detected.
	PAX5	Moderate amounts of B cells were detected.
	MHCII	Diffuse staining of MHCII-positive cells was observed in the bone marrow (monocyte/ macrophage lineage).

	PCNA	Low numbers of proliferating cells were detected.
	Casp3	Caspase 3-positive apoptotic cells were not observed.
Brain	HE	NHAIR
Spinal cord	HE	NHAIR
Heart	HE	NHAIR
Lung	HE	Low numbers of mononuclear cells were present in the BALT.
Liver	HE	Occasional mononuclear cells were present in the portal areas and low numbers of haematopoietic precursor cells were present.
Skeletal muscle	HE	Occasional mononuclear cells and scant polymorphonuclear cells (eosinophils) in interstitial areas.
kidney	HE	NHAIR
Adrenal	HE	NHAIR
Ileum	HE	Low numbers of eosinophils were present in the lamina propria and sub-mucosa.
Pancreas	HE	NHAIR
Femoral nerve	HE	NHAIR

Table 10: Histological features of control foetus at 210 days gestation

HO4-980-398G (C-3)

ORGAN	DESCRIPTION	
Thymus	HE	The thymus had well differentiated cortex and medulla. Cortex contained numerous small lymphocytes, while medulla exhibited lower numbers of large lymphocytes and a high numbers of macrophages, reticular medullary epithelial cells and fewer eosinophils.
Spleen	HE	Spleen exhibited well differentiated red and white pulp. High numbers of lymphocytes were occupied the white pulp (PALS and primary lymphoid follicles), while fewer were present in the red pulp with high numbers of macrophages, splenic dendritic cells and occasional neutrophils. Low numbers of haematopoietic cells were present.
Lymph node	HE	The lymph node exhibited well differentiated cortex and medulla. The superficial cortex contained primary lymphoid follicles without germinal centres, while high numbers of lymphocytes were present in the paracortex. The medulla had low numbers of lymphocytes and scant neutrophils.
BM	HE	Bone marrow was of high cellularity with intense haematopoietic activity. All precursor cell lineages were present and low numbers of adipocytes were observed.
Heart	HE	NHAIR
Lung	HE	NHAIR
Liver	HE	The liver exhibited low numbers of haematopoietic precursor cells and randomly scattered in the hepatic parenchyma. Low numbers of neutrophils were present within hepatic cords.
Skeletal muscle	HE	NHAIR
kidney	HE	NHAIR
Adrenal	HE	NHAIR
Ileum	HE	Mild eosinophilic infiltration was detected in the lamina propria.
Pancreas	HE	NHAIR
Femoral nerve	HE	NHAIR
Brain	HE	NHAIR
Spinal cord	HE	The spinal cord exhibited low numbers of polymorphonuclear cells within the meninges (eosinophils).
	Lendrum	The polymorphonuclear cells were identified as eosinophils.

Table 11: Histological features of naturally infected foetus after parasite recrudescence at 26 weeks gestation (foetal age - 31 weeks gestation age)

05L-2575-438 (R-5)

ORGAN	DESCRIPTION	
Spleen	HE	The spleen was highly developed with well differentiated red and white pulp. Large numbers of lymphocytes occupy the white pulp, which contained prominent primary lymphoid follicles without germinal centres. White pulp contained numerous macrophages, splenic dendritic cells, follicular dendritic cells and fewer lymphocytes. Extramedullary haematopoiesis was present.
	CD3	The white pulp exhibited high numbers of CD3-positive T cells in the PALS and a smaller population was present in the red pulp.
	PAX5	High numbers of B cells were present in the lymphoid follicles and fewer were scattered in the red pulp.
	MHCII	High numbers of MHCII-positive cells were detected in the PALS and large numbers were present and diffusely scattered in the red pulp.
	PCNA	High numbers of proliferating cells were present the white pulp. Mainly in the lymphoid follicles and few were present in red pulp.
	Caspase 3	Low numbers of caspase 3-positive apoptotic cells were present in both red and white pulp.
	IFN-γ	Low numbers of IFN-γ-expressing cells were present.
	Neospora	*N. caninum* antigen was not detected.
Thymus	HE	Highly developed with well differentiated cortex and medulla. Cortex contained high numbers of lymphocytes with fewer present in the medulla. A large population of macrophages, reticular medullary epithelial cells and dendritic cells were present in the medulla along with low numbers of eosinophils.
	CD3	High numbers of CD3-positive T cells were present in the cortex with fewer positive cells in the medulla.
	PAX5	Low numbers of B cells were present within the medulla.
	MHCII	High numbers of MHCII-positive cells were present in the medulla and lower numbers were present in the cortex and diffusely scattered.
	PCNA	PCNA-positive proliferating cells were present in the cortex and medulla in high numbers.
	Caspase 3	Low numbers of caspase 3-positie apoptotic cells were present in both cortex and medulla.
	IFN-γ	IFN-γ-expressing cells were not detected.
	Neospora	*N. caninum* antigen was not detected.
Lymph node	HE	The lymph nodes were highly developed with distinct cortex and medulla. Prominent primary lymphoid follicles were observed in the superficial cortex with numerous lymphocytes; while high numbers of lymphocytes were present in the paracortex and fewer in the medulla (lymphocytes, dendritic cells and macrophages).
	CD3	T cells were present in the paracortex in high numbers and a small population was observed around and within lymphoid follicles. Fewer T cells were present in the medulla.
	PAX5	Numerous B cells were present in lymphoid follicles. Low numbers were scattered in the paracortex and moderate amounts were observed in the medulla.
	MHCII	A large population of MHCII-positive cells were observed in the superficial cortex and paracortex with lower numbers present in the medulla.
	PCNA	Moderate amounts of PCNA-positive proliferating cells were present mainly in the lymphoid follicles.
	Caspase 3	Low numbers of caspase 3-positive apoptotic cells were present and randomly scattered in cortex and medulla.
	IFN-γ	Occasional IFN-γ-expressing cells were present in the paracortex.
	Neospora	*N. caninum* antigen was not detected.
BM	HE	Highly cellular with all precursor cell lines present and low numbers of adipocytes.
	CD3	Moderate amounts of T cells were present in the bone marrow.
	PAX5	High numbers of B cells were observed and diffusely scattered.
	MHCII	High staining intensity was observed and high numbers of positive cells were present.

	PCNA	Low numbers of PCNA-positive proliferating cells were present.
	Caspase 3	Low numbers of caspase 3-positive cells were observed.
	IFN-γ	Low numbers of IFN-γ-expressing cells were detected.
	Neospora	*N. caninum* antigen was not detected.
Spinal cord	HE	The spinal cord exhibited moderate mononuclear infiltrates in the white matter along with moderate perivascular infiltrates. Grey matter had low numbers of mononuclear inflammatory cells. The meninges were infiltrated with high numbers of similar inflammatory cells. Severe non-suppurative radiculoneuritis was also observed.
	CD3	The majority of the infiltrating inflammatory cells in the nerve roots, meninges and spinal cord were CD3-positive T cells.
	PAX5	Low numbers of B cells were present within the meninges and nerve roots of the spinal cord.
	MHCII	The nerve roots and meninges had exhibited high numbers of MHCII-positive cells. Fewer positive cells were present in the perivascular cuffs in the spinal cord.
	Caspase 3	There were low numbers of caspase 3-positve apoptotic cells in the meninges and spinal cord nerve root. Fewer positive cells were present in the inflammatory infiltrates in the spinal cord white matter.
	Calprotectin	Low numbers of macrophages were present in the inflammatory infiltrates of the spinal cord, nerve roots and even fewer detected in the leptomeninges.
	IFN-γ	IFN-γ-expressing cells were not present.
	Neospora	Low numbers of *N. caninum* tachyzoites were detected within intact glial cells in the spinal nerve root.
Brain	HE	The brain exhibited mild multifocal mononuclear perivascular infiltrates in grey and white matter.
	CD3	CD3-positive T cells were present in low numbers within the inflammatory infiltrates.
	PAX5	B cells were not detected within the infiltrates.
	MHCII	Moderate amounts of MHCII-positive cells were present in the inflammatory foci, consistent with activated microglial cells.
	PCNA	Only Ependymal cells showed intense proliferation in the brain.
	Caspase 3	Caspase 3-positive apoptotic cells were not detected in the brain.
	IFN-γ	IFN-γ-expressing cell were not present.
	Neospora	*N. caninum* antigen was not detected.
Heart	HE	The myocardium exhibited low numbers of mononuclear cells (non-suppurative myocarditis).
	CD3	Majority of the cells in the inflammatory infiltrate were CD3-positive T cells.
	PAX5	Low numbers of B cells were present in the inflammatory foci.
	MHCII	Low numbers of MHCII-positive cells were present within the inflammatory foci of the myocardium.
	PCNA	Low numbers of PCNA-positive proliferating cells were observed in the myocardium.
	Caspase 3	Caspase 3-positive cells were not detected.
	IFN-γ	IFN-γ-expressing cells were not detected.
	Neospora	*N. caninum* antigen was not detected.
Skeletal muscle	HE	Mild non-suppurative myositis; the muscle had low numbers of mononuclear multifocally distributed in the interstitial areas and low numbers of neutrophils were found admixed within the inflammatory infiltrate.
	CD3	Low numbers of CD3-positive T cells were present within the inflammatory foci.
	PAX5	B cells were also present, but in lower numbers that B cells.
	MHCII	Low numbers of positive cells observed between within the inflammatory infiltrates and endothelia cells were also positive.
	PCNA	PCNA-positive cells were not present.
	Caspase 3	Caspase 3-positive cells were not detected.
	IFN-γ	IFN-γ-expressing cell were not detected.
	Neospora	*N. caninum* antigen was not detected.
Liver	HE	Mild multifocal mononuclear portal infiltrates were observed.

	CD3	CD3-positive T cells were present in low numbers in the portal areas of the liver.
	PAX5	Low numbers of B cells were admixed with the T cell infiltrates.
	MHCII	High numbers of MHCII-positive cells were present in the parenchyma. Portal areas contained high staining intensity and moderate amounts of positive cells were observed.
	PCNA	High numbers of PCNA-positive cells were present in the parenchyma. These were haematopoietic cells and fewer hepatocytes.
	Caspase 3	Caspase 3-positive cells were not detected.
	IFN-γ	IFN-γ-expressing cells were detected in low numbers.
	Neospora	*N. caninum* antigen was not detected.
Lung	HE	The lung exhibited moderate amounts of mononuclear cells in the BALT and fewer in the alveolar septa.
	CD3	Low numbers of T cells were present in the interstitial areas, BALT and occasional positive cells were observed in the alveolar septa.
	PAX5	B cells were detected in low numbers admixed with T cells in the BALT, alveolar septa and interstitial areas.
	MHCII	High numbers of MHCII-positive cells were present in the BALT and diffuse staining was observed on cells within alveolar spaces and interstitial areas (macrophages).
	PCNA	Proliferating cells were not detected.
	Caspase 3	Low numbers of caspase 3-positive cells were observed within alveolar spaces (macrophages)
	IFN-γ	Moderate amounts of IFN-γ-expressing cells were detected in mainly in the bronchial epithelium.
	Neospora	*N. caninum* antigen was not detected.
Intestine	HE	NHAIR
	CD3	Low numbers of T cells were detected within the lamina propria.
	PCNA	Negative
	Caspase 3	Caspase 3-positive cells were not observed.
	Neospora	*N. caninum* antigen was not detected.
Adrenal	HE	NHAIR
	CD3	T cells were not detected.
	PCNA	Proliferating cells were not present in the adrenals.
	Caspase 3	Caspase 3-positive cells were not observed.
	Neospora	*N. caninum* antigen was not detected.
Pancreas	HE	NHAIR
	CD3	Occasional T cells were present in the interstitial areas.
	MHCII	Mild expression of MHCII was present within interstitial areas. Endothelial cells were positive.
	PCNA	Proliferating cells were not observed.
	Caspase 3	Caspase 3-posiitve cells were not observed.
	Neospora	*N. caninum* antigen was not detected.
Kidney	HE	NHAIR
	CD3	Low numbers of CD3-positive T cells were present within interstitial areas of the cortex and medulla.
	MHCII	Mild expression was observed mainly in the cortex in the areas of T cell infiltrates.
	PCNA	Low numbers of proliferating tubular epithelial cells were observed in the cortex.
	Caspase 3	Caspase 3-positive cells were not observed.
	Neospora	*N. caninum* antigen was not detected.
Femoral nerve	HE	Occasional mononuclear cells were observed (neuritis).
	CD3	Low numbers of T cells were present in nerve fibres.
	MHCII	Mild expression of MHCII was observed in the areas of T cell infiltrates.
	PCNA	Proliferating cells were not present.
	Caspase 3	Caspase 3-positive cells were not observed.
	Neospora	*N. caninum* antigen was not detected.

Table 12: Histological features of the neonatal calf after parasite recrudescence at 40 weeks gestation age

05L-3647-439 (R-10)

ORGAN	DESCRIPTION	
Spleen	HE	The spleen was comprised of well differentiated red and white pulp. White pulp consisted of high numbers of lymphocytes in the PALS and distinct primary lymphoid follicles, which contained prominent germinal centres. The red pulp had high numbers of splenic macrophages, fewer lymphocytes and occasional neutrophils were also present. Haematopoietic precursor cells were present in low numbers.
	CD3	T cells were present in the PALS in high numbers and fewer were present in the red pulp.
	MHCII	Red pulp contained high numbers of positive cells (macrophages, dendritic cells and lymphocytes). The white also had high numbers with high staining intensity and was more prominent in the lymphoid follicles (dendritic cells, follicular dendritic cells, and B cells).
	PCNA	High numbers of proliferating cells were present within the PALS, mainly lymphoid follicles and fewer detected in the red pulp (lymphocytes and fewer haematopoietic cells).
	Caspase 3	Low numbers of caspase 3-positive apoptotic cells were present mainly in the PALS (lymphoid follicles).
	Neospora	*N. caninum* antigen was not detected.
Thymus	HE	Cortex contained high numbers of small compact lymphocytes, while medulla exhibited a small population of larger lymphocytes, high numbers of macrophages, reticular medullary epithelial cell and dendritic cells. Low numbers of eosinophils were present in the medulla.
	CD3	The cortex had high numbers of CD3-positive T cells, while fewer were present in the medulla.
	MHCII	High numbers of MHCII-positive cells were present in the medulla with strong staining intensity, while fewer were detected in the cortex and diffusely distributed.
	PCNA	Numerous PCNA-positive proliferating cells were detected in the cortex and fewer in the medulla.
	Caspase 3	Low numbers of caspase 3-positive apoptotic lymphocytes were present in the cortex and medulla.
	Neospora	*N. caninum* antigen was not detected.
Lymph node	HE	Lymph node had distinct superficial cortex, paracortex cortex and medulla. Prominent primary lymphoid follicles were observed in the superficial cortex without germinal centres, while the T cell compartment contained numerous lymphocytes and fewer were present in the medulla.
	CD3	High numbers of T cells were present in the paracortex with scattered positive cells observed in B cell compartment. Lower numbers of T cells were present in the medulla.
	MHCII	The lymphoid follicles and T cell compartment exhibited high numbers of MHCII-positive cells with high staining intensity. Fewer positive cells were observed in the medulla.
	PCNA	High numbers of proliferating cells were present in the lymphoid follicles mainly and fewer were observed in T cell compartment and medulla.
	Caspase 3	High numbers of caspase 3-positive positive cells were present in the corticomedullary junction and low numbers were detected in the superficial cortex.
	Neospora	*N. caninum* antigen was not detected.
Heart	HE	Occasional mononuclear cells were present in the myocardium.
	CD3	Minimal CD3-positive T cells were detected in the myocardium.
	PAX5	B cells were not detected.
	MHCII	MHCII-positive cells were minimal within the myocardium.
	Calprotectin	Low numbers of macrophages were detected and randomly scattered in the myocardium.
	PCNA	PCNA-positive proliferating cardiomyocytes were present in low numbers.
	Caspase 3	Caspase 3-positive cells were not observed.
	Neospora	*N. caninum* antigen was not detected.

Skeletal muscle	HE	NHAIR
	CD3	T cells were not detected
	PAX5	B cells were not detected.
	MHCII	Minimal numbers of positive cells were present mainly on endothelial cells.
	Calprotectin	Not detected
	PCNA	Not detected
	Caspase 3	Not detected
	Neospora	*N. caninum* antigen was not detected.
Liver	HE	Occasional portal mononuclear inflammatory infiltrates.
	CD3	Occasional CD3-positive T cells were present in portal areas.
	PAX5	B cells were not detected.
	MHCII	Moderate amount of MHCII-positive cells were detected in the portal areas and high numbers were present within the hepatic parenchyma (Kupffer cells).
	Calprotectin	High numbers of macrophages were present with the hepatic parenchyma (Kupffer cells).
	PCNA	Low numbers of PCNA-positive proliferating cells were detected in the parenchyma (hepatocytes).
	Caspase 3	Occasional caspase 3-positive cells were present mainly in the portal areas and few biliary epithelial cells were positive.
	IFN-γ	Low numbers of IFN-γ-expressing cells were detected in the liver.
	Neospora	*N. caninum* antigen was not detected.
Lung	HE	Low numbers of mononuclear cells were present in the BALT and alveolar septa.
	CD3	Occasional CD3 T cells were detected in the BALT and even fewer in the alveolar septa.
	PAX5	B cells were not detected
	MHCII	High numbers of MHCII-positive cells with high staining intensity were observed in interstitial areas, BALT and fewer within alveolar spaces.
	Calprotectin	High numbers of macrophages were present in interstitial areas and fewer in alveolar ducts.
	PCNA	Proliferating cells were not detected.
	Caspase 3	Low numbers of caspase 3-positive apoptotic cells (alveolar epithelial cell) were present.
	IFN-γ	Low numbers of IFN-γ-expressing cells were present mainly within blood vessels
	Neospora	*N. caninum* antigen was not detected.
Brain	HE	Minimal numbers of mononuclear cells were present in the grey matter and multifocally distributed.
	CD3	The mononuclear cells were in the grey matter were CD3-positive T cells.
	PAX5	B cells were not detected in the brain.
	MHCII	Low numbers of MHCII-positive cells were present within the inflammatory infiltrates (activated microglial cells).
	PCNA	Proliferating cells were not observed in the brain.
	Caspase 3	Caspase 3-positive cells were not present.
	Neospora	*N. caninum* antigen was not detected.
Spinal cord	HE	Low numbers of mononuclear inflammatory infiltrates were present in the white matter in the perivascular areas and meninges.
	CD3	The majority of the T cells were detected in the spinal cord meninges with fewer in the spinal cord white matter.
	PAX5	B cells were not detected.
	MHCII	Positive cells were detected in the perivascular areas of the spinal cord white matter and within the meninges in low numbers.
	PCNA	Proliferating cells were not observed.
	Caspase 3	Caspase 3-positive cells were not present.
	Neospora	*N. caninum* antigen was not detected.
Intestine	HE	High numbers of mononuclear cells were present in the intestinal mucosa along with low numbers of polymorphonuclear cells (eosinophils and occasional neutrophils).
	CD3	T cells were the predominant cell type present within the inflammatory infiltrate on the intestinal mucosa.

	PAX5	High numbers of B cells were present in the gastric associated lymphoid tissues (GALT).
	MHCII	High numbers of positive cells were present in the lamina propria and GALT.
	Calprotectin	Moderate amounts of macrophages were present in the mucosa and submucosa of the intestine.
	PCNA	High numbers of proliferating B cells were detected in the GALT.
	Caspase 3	Moderate amounts of caspase 3-positive cells (mainly B cells) were present in the GALT.
	Neospora	*N. caninum* antigen was not detected.
Kidney	HE	NHAIR
	CD3	Minimal T cell infiltrates were randomly scattered in the cortex and medulla.
	PAX5	B cells not detected.
	MHCII	Low numbers of positive cells were present in the both cortex and medulla within the interstitial areas.
	Calprotectin	Low numbers of macrophages were randomly scattered in the interstitial areas of the renal cortex and medulla.
	PCNA	Low numbers of proliferating tubular epithelial cells were present.
	Caspase 3	Caspase 3-positive cells were not detected.
	Neospora	*N. caninum* antigen was not detected.
Adrenal	HE	Focal area of mononuclear inflammatory infiltrate was present in the adrenal cortex (zonae glomerulosa and fasiculata).
	CD3	Minimal T cell infiltrates were randomly scattered in the cortex.
	PAX5	B cells were not detected.
	MHCII	Low numbers of positive cells present and randomly scattered in cortex and medulla.
	Calprotectin	A focal area of mononuclear cell infiltrates was present in the cortex (macrophages) and low numbers were also scattered in the cortex and medulla.
	PCNA	Low numbers of proliferating cells were detected in the adrenal cortex (randomly scattered in all zones).
	Caspase 3	Caspase 3-positive cells were not detected.
	Neospora	*N. caninum* antigen was not detected.
Pancreas	HE	NHAIR
	CD3	T cells were not detected.
	PAX5	B cells were not detected.
	MHCII	Low numbers of MHCII-positive cells were present within pancreatic lobules.
	Calprotectin	Occasional macrophages were also detected within the pancreatic lobules.
	PCNA	Proliferating cells were not detected
	Caspase 3	Caspase 3-positive cells were not detected.
	Neospora	*N. caninum* antigen was not detected.

APPENDIX 2: Reagents and recipes

4% neutral buffered paraformaldehyde

Dissolve 40 g paraformaldehyde into 800 ml PBS at 60°C in a fume hood (adjust pH to 7.24). Adjust concentration to 1 L with PBS (see below).

Mayers Haemalum

Haematoxylin	1 g
Sodium iodate	0.2 g
Potassium alum	50 g
Distilled water	1 L

Dissolve haematoxylin and potassium alum in distilled water using gentle heat and allow to cool. Add sodium iodate and dissolve by shaking. Filter solution and add 20 ml glacial acetic acid.

Eosin working solution

Eosin stock solution	1 g eosin (HD supplies, Aylesbury, UK) in 100 ml distilled water (1% w/v)
Working solution	mix 50 ml of 1% eosin with 390 ml of 95% ethanol and 2 ml glacial acetic acid

Carbol Chromotrope (Lendrum's stain)

Chromotrope 2R	0.5 g
Phenol	1 g
Distilled water	100 ml

Reagents for immunohistology

10x Tris stock	60.57 g	Tris
(Store at 4°C)	610 ml	distilled water
	390 ml	1M HCl
	Adjust pH to 6.0	

1x TBST	100 ml	10x Tris stock
(Store at 4°C)	900 ml	distilled water
	7.2 g	NaCl
	500 µl	Tween 20

Phosphate Buffered Saline (PBS, pH 7.2)

NaCl	42 g
$Na_2HPO_4.2H_2O$	9.26 g
KH_2PO_4	2.15 g

Dissolve in 1 L distilled water for stock solution

Working solution – dilute stock solution 1:5 in distilled water

0.1M Imidazole Stock	6.81 g	Imidazole
(Store at 4°C)	1000 ml	distilled water
Imidazole Buffer	280 ml	0.1M Imidazole Stock
(Make fresh)	120 ml	0.42M HCl
	Adjust pH to 7.18-7.20 using NaOH	

DAB (diaminobenzine) 0.2 g DAB in 280 ml 0.1M Imidazole Buffer and 120 ml 0.42M HCl (Filter). Adjust pH to 7.18-7.20 using 10M NaOH

Activate DAB with 140 µl hydrogen peroxide (H_20_2)

0.42M HCl Add 38.32 ml concentrated HCl to 1 L distilled H_20

Dilute to final volume 2.5 L with distilled H_20

Store at room temperature

Papanicolaou's Solution

Mix Papanicolaou's solution in distilled water (1:20) and filter.

Stock citrate buffers

Stock solution A (0.1M citric acid):

Citric acid ($C_6H_80_7$)	10.505 g
Distilled water	500 ml
	Store at 4°C

Stock solution B (0.1M sodium citrate):

Tri-sodium citrate ($Na_3C_6H_50_7.2H_20$)	14.705 g
Distilled water	500 ml
	Store at 4°C

Citrate 6 buffer (10 mM):

Stock solution A	9 ml
Stock solution B	41 ml
Distilled water	Final volume 500 ml (pH 6.0)
	Store at 4°C

Citrate 4 buffer (10 mM):

Stock solution A	9 ml
Stock solution B	41 ml
Distilled water	Final volume 500 ml (pH 4.0)
	Store at 4°C

Microwave-EDTA (10 mM)

Dissolve 0.93 g EDTA in 2 L distilled H_20 (pH 9.0, NaOH)

Top up with distilled H_20 to final volume of 2.5 L (store at 4°C)

Reagents for Neospora ELISA

Coating buffer	Na_2CO_3 ANHYDROUS	0.159 g
	$NaHCO_3$	0.293 g

Dissolve in 100 ml of distilled water (adjust pH 9.6). Alter with concentrated HCl as required and store at 4°C.

Washing buffer	PBS + 0.05% Tween 20
Blocking buffer	PBS + 0.05% Tween 20 + 2% Marvel – make up fresh
Stopping solution	0.5M HCl

Reagents for SDS-PAGE and western blot [Resolving gel (10 ml)]

30% acrylamide	5 ml
1.5M Tris-HCl pH (8.8)	2.5 ml
dH_2O	2.3 ml
10% (w/v) SDS	100 µl
10% (w/v) APS	100 µl
TEMED	10 µl

Stacking gel (5 ml)

30% acrylamide	830 µl
1M Tris-HCl pH (6.8)	630 µl
dH_2O	3.4 ml
10% (w/v) SDS	50 µl
10% (w/v) APS	50 µl
TEMED	5 µl

10X Phosphate-Buffered Saline (PBS)

NaCl (1.37M)	80 g/L
KCl (27 mM)	2 g/L
$Na_2HPO_42H_2O$ (100 mM)	17.8 g/L
KH_2PO_4 (20 mM)	2.7 g/L

Dissolve the compounds in 800mL of distilled H_2O. Adjust the pH to 7.4 with HCl. Add H_2O to 1L and sterilized by autoclaving and store the buffer at room temperature.

10% Sodium Dodecyl Sulphate (SDS)

Dissolve 20 g in 60 ml of ddH_2O, heat to 68°C and stir with a magnetic stirrer to assist dissolution. If necessary, adjust the pH to 7.2 by adding a few drops of concentrated HCl. Adjust the volume to 200ml with ddH_2O and store at room temperature.

10X Tris-Buffered Saline (TBS)

Tris-base (0.25M)	30 g/L
NaCl (1.5M)	88 g/L

Dissolve the compounds in 800 ml of dH_2O. Adjust to pH 7.4 with HCl. Add dH_2O to 1L and sterilized by autoclaving; store the buffer at room temperature.

1X Towbin buffer (Transfer buffer)

Tris-base (25 mM)	3.03 g/L
Glycine (192 mM)	14.4 g/L
Methanol (20% w/v)	200 ml

Dissolve the compounds in 600 ml of dH_2O and add 200 ml of methanol. Adjust to pH 7.5 with HCl and complete with ddH_2O to 1L; store the buffer at room temperature. The methanol minimizes swelling of the gel and increases the efficiency of binding of proteins too nitrocellulose membrane.

1M Tris-HCl pH 6.8 (1L)

Add 121.14 g of Tris-HCl to 300 ml of ddH_2O, dissolve and adjust to pH 6.8, and then add ddH_2O to adjust volume to 1L.

1M Tris-HCl pH 8.0 (1L)

Adds 121.14 g Tris-HCl to 500 ml of ddH_2O, adjust to pH 8.0, and then add ddH_2O to adjust volume to 1L.

1.5M Tris-HCl pH 8.8 (1L)

Adds 181.7 g Tris-base to 500 ml of ddH_2O, adjust to pH 8.8, and then add ddH_2O to adjust volume to 1L.

APPENDIX 3: Material for culturing HL-1 cardiomyocyte cell line

Chemicals

- Claycomb Medium
- Fetal bovine serum (FBS): current recommended lot number 3J0229.
- Penicillin/Streptomycin (10000 U/ml and 10 mg/ml, respectively)
- Norepinephrine [(±)-Arterenol]
- L-Ascorbic acid, sodium salt
- L-Glutamine, 200 mM, (store at -20°C)
- 95% FBS/5% DMSO (store at 4°C for up to a week)
- Trypsin-EDTA, 1x
- Trypsin inhibitor, soybean
- Dulbecco's phosphate buffered saline (PBS)
- Fibronectin
- Bacto © Gelatin
- Distilled water, cell culture grade

Supplemented Claycomb Medium / Wash Medium

Ingredient	Volume	Final concentration
Claycomb medium	87 ml	87%
Foetal bovine serum	10 ml	10% (5% for wash medium)
Penicillin/Streptomycin	1 ml	100 units/ml Penicillin,100 μg/ml Streptomycin
Norepinephrine (10 mM stock)	1 ml	0.1 mM
L-Glutamine (200 mM stock)	1 ml	2 mM

- Prepare the supplemented medium as listed above.
- Wrap the bottle with the Claycomb medium in aluminium foil, since the medium is extremely light sensitive.
- Use fresh supplemented Claycomb medium (for up to two weeks). In case you want to use leftover medium after two weeks, you have to replenish the L-glutamine, which is chemically unstable.

Norepinephrine Stock Solution

The following instructions are for a 10 mM stock solution of norepinephrine.

Add 1 ml of this stock solution to 100 ml medium for a final concentration of 0.1 mM. The norepinephrine stock solution needs to be freshly prepared monthly.

1. Prepare 100 ml of 30 mM ascorbic acid by adding 0.59 g ascorbic acid to 100 ml of distilled water.
2. Add 80 mg norepinephrine to 25 ml of the 30 mM ascorbic acid.
3. Filter sterilise the solution using a 0.2 μm acrodisc syringe filter.
4. Prepare 1 ml aliquots in sterile microtubes with screw caps.

Soybean Trypsin Inhibitor

1. Dissolve 25 mg of soybean trypsin in 100 ml Dulbecco's phosphate buffered saline (PBS).
2. Filter sterilise (using a 0.2 μm syringe filter) into a 100 ml bottle.
3. Store at 4°C up to a month.

Pre-Coating Culture Flasks

1. Add 0.1 g Bacto-Gelatin to 500 ml distilled water in a glass bottle.
2. Autoclave. The gelatin will dissolve during the autoclavation. The final concentration of gelatin is 0.02%.
3. Fibronectin is provided in 5 ml aliquots. Dilute 1 ml fibronectin in 199 ml of 0.02% gelatin. Mix gently, and immediately aliquot 6 ml per 15 ml centrifuge tube.
4. Store aliquots at -20°C.
5. Before culturing cells, coat the flasks with this coating solution (2 ml/T25 or 6 ml/T75 flask).
6. Close the flasks and incubate at 37°C overnight.
7. Remove the coating solution by aspiration the next day just before adding cells to the flasks.

Culturing and Maintaining Cells

- Cultures are fed with supplemented Claycomb medium (5 ml/T25 flask) every day.
- To avoid feeding the cells on weekends, 10 ml of supplemented Claycomb Medium should be added to each T25 flask on Friday afternoons; this medium is not changed until the following Monday morning.

Digestion with Trypsin

This procedure is necessary for dislodging the cells from the flask bottom before the passaging or freezing.

1. Rinse each T25 flask briefly with 3 ml of 0.05% trypsin/EDTA warmed to 37°C (use 6 ml for T75) by pipetting the trypsin/EDTA onto the bottom of the flask (side opposite the cap), trying not to hit the cells directly with the enzyme.
2. Rinse gently and remove by aspiration.
3. Add another 1.3 ml trypsin/EDTA per T25 flask (3 ml per T75). Incubate at 37°C for 2 min.
4. Remove and add fresh trypsin/EDTA. Incubate for an additional 3–8 min. Examine cells microscopically after 2 min.
5. Examine microscopically and, if cells are still adhered, rap the flask very gently to dislodge remaining cells from the bottom of the flask.
6. To inactivate the enzyme, add an equal amount (1.3 or 3 ml) of soybean trypsin inhibitor directly onto the cells.
7. Rinse the empty flask with 5 ml (8 ml per T75) wash medium, and add this to the cells that are already in the 15 ml centrifuge tube.
8. Centrifuge at 500 g for 5 min.

Passaging the Cells

1. During the digestion or centrifugation steps, remove the coating solution from each T25 flask, and add 4 ml supplemented Claycomb medium per flask. Set aside.
2. Remove the tube containing the harvested HL-cardiomyocytes from the centrifuge. Remove the supernatant by aspiration, and gently resuspend the pellet in 3 ml of supplemented Claycomb medium.
3. Transfer 1 ml into each of three (clearly labelled) coated T25 flasks. Each flask contains 5 ml now.
4. If the cells are passaged on a Friday, use 2x the volume of supplemented Claycomb Medium per flask.

Freezing the Cells

It is useful to freeze the contents of one confluent T75 flask into one cryovial. When cells are needed, this cryovial can be thawed and placed back into one T75 flask.

1. Gently resuspend the cell pellet after the Trypsin digest in 1.5 ml of freezing medium (95% FBS/5% DMSO).
2. Pipette resuspended cells into a cryovial. Place the cryovial containing the cells into a Nalgene freezing jar containing room temperature isopropanol.
3. Immediately place the freezing jar into a -80°C freezer, and freeze cells at a rate of -1°C per min.
4. Six to twelve hours later, transfer the vial to a liquid nitrogen Dewar vessel.

Thawing the Cells

1. Coat a tissue culture flask overnight in a 37°C incubator.
2. Remove the coating solution from the culture flask the next morning, and replace with 10 ml of supplemented Claycomb medium. Place this flask back into the incubator.
3. Transfer 10 ml wash medium into an empty 15 ml centrifuge tube. Incubate tube in a 37°C water bath.

4. Quickly thaw the cells in a 37°C water bath (about 2 min), and transfer them into the 15 ml centrifuge tube containing the wash medium.
5. Centrifuge for 5 min at 500 g.
6. Remove the tube from the centrifuge and remove the wash medium by aspiration.
7. Gently resuspend the cell pellet in 5 ml supplemented Claycomb medium, and add the suspension to the 10 ml medium in the T75 flask.
8. Replace the medium with 15 ml of fresh supplemented Claycomb medium 4 hours later (after cells have attached to the flask bottom).

APPENDIX 4: Quantitative data analysis of cleaved caspase 3-positive lymphocytes (apoptosis) in the haemolymphatic tissues of foetuses from dams infected with *N. caninum* tachyzoites in early gestation

Spleen (70 dg)

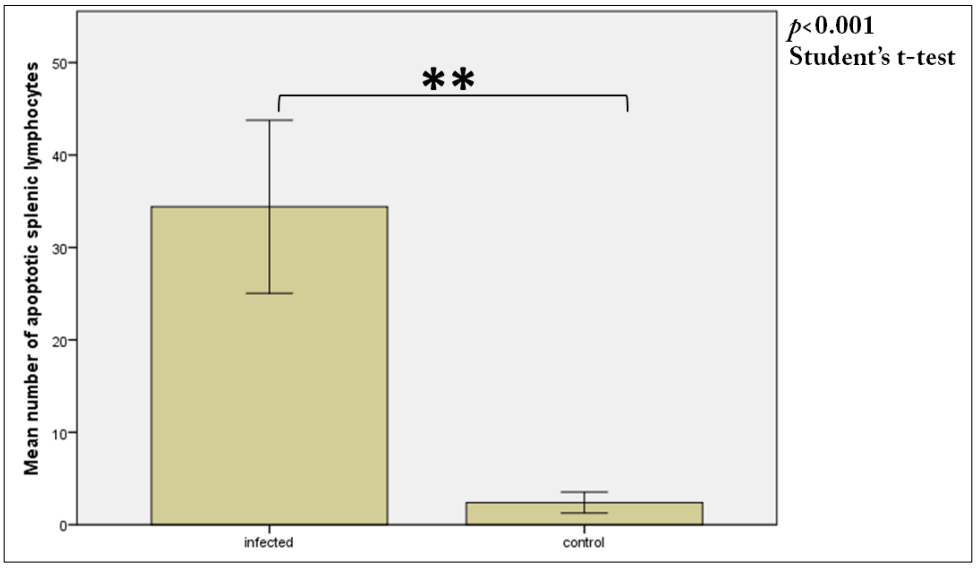

Variables	N	Mean	Std. Deviation	Std. Error Mean
Infected	10	34.40	13.091	4.140
Control	10	2.40	1.578	0.499

Thymus (70 dg)

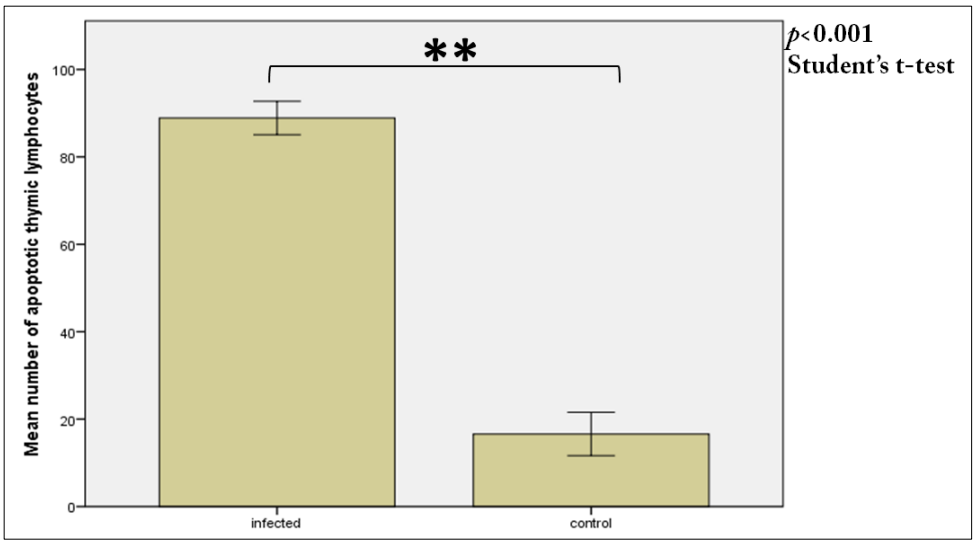

Variables	N	Mean	Std. Deviation	Std. Error Mean
Infected	10	88.90	5.343	1.690
Control	10	16.60	6.947	2.197

Quantitative data analysis of cleaved caspase 3-positive lymphocytes (apoptosis) in the thymus of foetuses from dams infected with *N. caninum* tachyzoites in late gestation

Thymus (210 dg)

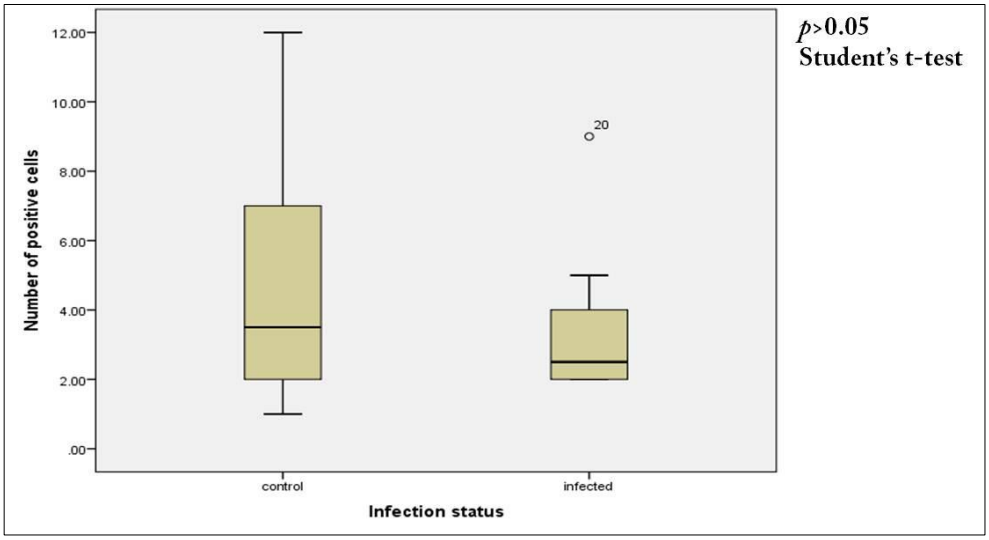

Variables	N	Mean	Std. Deviation	Std. Error Mean
Control	10	4.60	3.836	1.213
Infected	10	3.50	2.224	0.703

APPENDIX 5: Serological survey in Jamaican dairy cattle

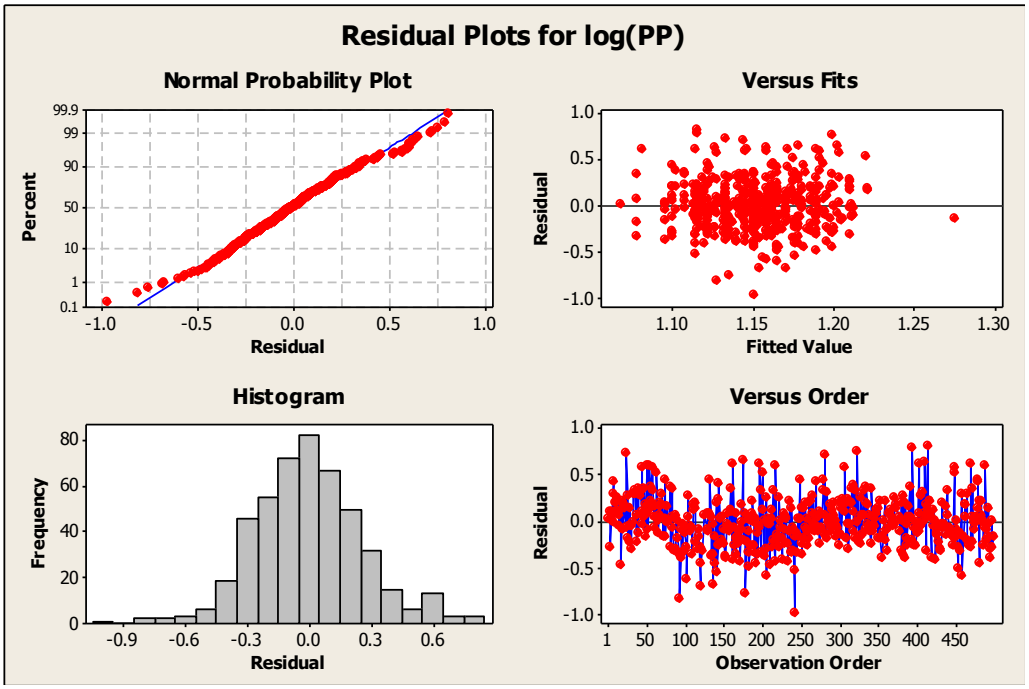

The regression equation describes the relationship between the response and predictor variables.

Response = constant + coefficient (predictor) + ... + coefficient (predictor)

$y = c + \beta_1 x_1 + \beta_2 x_2 + \beta_3 x_3$

where c = constant (y intercept when all variables are zero)

β_1, β_2 and β_3 are coefficients of variables x_1 x_2 and x_3, respectively

x_1, x_2 and x_3 are predictor variables

Log (PP) = 1.11 + 0.179 Log(Age) + 0.0329(preg. status) – 0.121 SQRT(# of preg.)

Predictor	Coefficient	SE coefficient	T	P value
Constant	1.11082	0.07351	15.11	0.000
Log (age)	0.1789	0.1433	1.25	0.213
Pregnancy status	0.03291	0.01616	2.04	0.042
SQRT (# of preg.)	-0.12099	0.05283	-2.29	0.022

S = 0.264440
R^2 = 1.8%
R^2 (adjusted) = 1.2%

Analysis of Variance

Source	Degree of freedom	Sum of squares	Mean squares	F	P value
Regression	3	0.60250	0.20083	2.87	0.036
Residual Error	474	33.14613	0.06993	-	-
Total	477	33.74862	-	-	-

REFERENCES

Abbasi, M., Kowalewska-Grochowska, K., Bahar, M.A., Kilani, R.T., Winkler-Lowen, B., Guilbert, L.J., 2003. Infection of placental trophoblasts by Toxoplasma gondii. Journal of Infectious Diseases 188, 608-616.

Adams, J.M., Cory, S., 1998. The Bcl-2 protein family: Arbiters of cell survival. Science 281, 1322-1326.

Adams, J.M., Cory, S., 2002. Apoptosomes: Engines for caspase activation. Current Opinion in Cell Biology 14, 715-720.

Adams, L.B., Hibbs Jr, J.B., Taintor, R.R., Krahenbuhl, J.L., 1990. Microbiostatic effect of murine-activated macrophages for Toxoplasma gondii. Role for synthesis of inorganic nitrogen oxides from L-arginine. Journal of Immunology 144, 2725-2729.

Agostinelli, C., Sabattini, E., Gjørret, J.O., Righi, S., Rossi, M., Mancini, M., Piccaluga, P.P., Bacci, F., Marafioti, T., Bettini, G., Falini, B., Pileri, S.A., 2010. Characterization of a new monoclonal antibody against PAX5/BASP in 1525 paraffin-embedded human and animal tissue samples. Applied Immunohistochemistry and Molecular Morphology 18, 561-572.

Aguado-Martínez, A., Álvarez-García, G., Fernández-García, A., Risco-Castillo, V., Arnaiz-Seco, I., Rebordosa-Trigueros, X., Navarro-Lozano, V., Ortega-Mora, L.M., 2008. Usefulness of rNcGRA7- and rNcSAG4-based ELISA tests for distinguishing primo-infection, recrudescence, and chronic bovine neosporosis. Veterinary Parasitology 157, 182-195.

Al-Rubeai, M., Singh, R.P., 1998. Apoptosis in cell culture. Current Opinion in Biotechnology 9, 152-156.

Almería, S., Araujo, R., Tuo, W., López-Gatius, F., Dubey, J.P., Gasbarre, L.C., 2010. Fetal death in cows experimentally infected with Neospora caninum at 110 days of gestation. Veterinary Parasitology 169, 304-311.

Almeria, S., Araujo, R.N., Darwich, L., Dubey, J.P., Gasbarre, L.C., 2011. Cytokine gene expression at the materno-foetal interface after experimental Neospora caninum infection of heifers at 110 days of gestation. Parasite Immunology 33, 517-523.

Almeria, S., De Marez, T., Dawson, H., Araujo, R., Dubey, J.P., Gasbarre, L.C., 2003. Cytokine gene expression in dams and foetuses after experimental Neospora caninum infection of heifers at 110 days of gestation. Parasite Immunology 25, 383-392.

Almería, S., López-Gatius, F., 2013. Bovine neosporosis: Clinical and practical aspects. Research in Veterinary Science.

Almería, S., López-Gatius, F., García-Ispierto, I., Nogareda, C., Bech-Sàbat, G., Serrano, B., Santolaria, P., Yániz, J.L., 2009. Effects of crossbreed pregnancies on the abortion risk of Neospora caninum-infected dairy cows. Veterinary Parasitology 163, 323-329.

Almería, S., Serrano, B., Yàniz, J.L., Darwich, L., López-Gatius, F., 2011. Cytokine gene expression profiles in peripheral blood mononuclear cells from Neospora caninum naturally infected dams throughout gestation. Veterinary Parasitology.

Almería, S., Serrano, B., Yàniz, J.L., Darwich, L., López-Gatius, F., 2012. Cytokine gene expression profiles in peripheral blood mononuclear cells from Neospora caninum naturally infected dams throughout gestation. Veterinary Parasitology 183, 237-243.

Aloisi, F., 2001. Immune function of microglia. GLIA 36, 165-179.

Amezcua Vesely, M.C., Bermejo, D.A., Montes, C.L., Acosta-Rodríguez, E.V., Gruppi, A., 2012. B-cell response during protozoan parasite infections. Journal of Parasitology Research 2012.

Anderson, M.L., Andrianarivo, A.G., Conrad, P.A., 2000. Neosporosis in cattle. Animal Reproduction Science 60-61, 417-431.

Anderson, M.L., Blanchard, P.C., Barr, B.C., Dubey, J.P., Hoffman, R.L., Conrad, P.A., 1991. Neospora-like protozoan infection as a major cause of abortion in California dairy cattle. Journal of the American Veterinary Medical Association 198, 241-244.

Anderson, M.L., Palmer, C.W., Thurmond, M.C., Picanso, J.P., Blanchard, P.C., Breitmeyer, R.E., Layton, A.W., McAllister, M., Daft, B., Kinde, H., 1995. Evaluation of abortions in cattle attributable to neosporosis in selected dairy herds in California. Journal of the American Veterinary Medical Association 207, 1206-1210.

Anderson, M.L., Reynolds, J.P., Rowe, J.D., Sverlow, K.W., Packham, A.E., Barr, B.C., Conrad, P.A., 1997. Evidence of vertical transmission of Neospora sp infection in dairy cattle. Journal of the American Veterinary Medical Association 210, 1169-1172.

Andreotti, R., Barros, J.C., Pereira, A.R., Oshiro, L.M., Cunha, R.C., Neto, L.F.F., 2010. Association between seropositivity for Neospora caninum and reproductive performance of beef heifers in the Pantanal of Mato Grosso do Sul, Brazil. Associação entre soropositividade para Neospora caninum e o desempenho reprodutivo de novilhas de corte no Pantanal Sul-Mato-Grossense, Brasil 19, 45-49.

Andrianarivo, A., Barr, B., Anderson, M., Rowe, J., Packham, A., Sverlow, K., Conrad, P., 2001a. Immune responses in pregnant cattle and bovine fetuses following experimental infection with neospora caninum. Parasitology Research 87, 817-825.

Andrianarivo, A.G., Barr, B.C., Anderson, M.L., Rowe, J.D., Packham, A.E., Sverlow, K.W., Conrad, P.A., 2001b. Immune responses in pregnant cattle and bovine fetuses following experimental infection with Neospora caninum. Parasitology Research 87, 817-825.

Andrianarivo, A.G., Rowe, J.D., Barr, B.C., Anderson, M.L., Packham, A.E., Sverlow, K.W., Choromanski, L., Loui, C., Grace, A., Conrad, P.A., 2000. A POLYGEN(TM)-adjuvanted killed Neospora caninum tachyzoite preparation failed to prevent foetal infection in pregnant cattle following i.v./i.m. experimental tachyzoite challenge. International Journal for Parasitology 30, 985-990.

Ashkenazi, A., Dixit, V.M., 1999. Apoptosis control by death and decoy receptors. Current Opinion in Cell Biology 11, 255-260.

Baillargeon, P., Fecteau, G., Paré, J., Lamothe, P., Sauvé, R., 2001. Evaluation of the embryo transfer procedure proposed by the International Embryo Transfer Society as a method of controlling vertical transmission of Neospora caninum in cattle. Journal of the American Veterinary Medical Association 218, 1803-1806.

Ballard, P.L., 1980. Hormonal influences during fetal lung development. Ciba Foundation symposium 78, 251-274.

Bannai, H., Nishikawa, Y., Matsuo, T., Kawase, O., Watanabe, J., Sugimoto, C., Xuan, X., 2008. Programmed Cell Death 5 from Toxoplasma gondii: A secreted molecule that exerts a pro-apoptotic effect on host cells. Molecular and Biochemical Parasitology 159, 112-120.

Barber, J., Trees, A.J., Owen, M., Tennant, B., 1993. Isolation of Neospora caninum from a British dog. Veterinary Record 133, 531-532.

Barber, J.S., Gasser, R.B., Ellis, J., Reichel, M.P., McMillan, D., Trees, A.J., 1997. Prevalence of antibodies to Neospora caninum in different canid populations. Journal of Parasitology 83, 1056-1058.

Barber, J.S., Holmdahl, O.J.M., Owen, M.R., Guy, F., Uggla, A., Trees, A.J., 1995. Characterization of the first European isolate of neospora caninum (Dubey, Carpenter, Speer, Topper and Uggla). Parasitology 111, 563-568.

Barling, K.S., McNeill, J.W., Paschal, J.C., McCollum, F.T., Craig, T.M., Adams, L.G., Thompson, J.A., 2001. Ranch-management factors associated with antibody seropositivity for Neospora caninum in consignments of beef calves in Texas, USA. Preventive Veterinary Medicine 52, 53-61.

Barling, K.S., Sherman, M., Peterson, M.J., Thompson, J.A., McNeill, J.W., Craig, T.M., Adams, L.G., 2000. Spatial associations among density of cattle, abundance of wild canids, and seroprevalence to Neospora caninum in a population of beef calves. Journal of the American Veterinary Medical Association 217, 1361-1365.

Barr, B.C., Anderson, M.L., Blanchard, P.C., Daft, B.M., Kinde, H., Conrad, P.A., 1990. Bovine fetal encephalitis and myocarditis associated with protozoal infections. Veterinary pathology 27, 354-361.

Barr, B.C., Anderson, M.L., Dubey, J.P., Conrad, P.A., 1991. Neospora-like protozoal infections associated with bovine abortions. Veterinary pathology 28, 110-116.

Barr, B.C., Anderson, M.L., Woods, L.W., Dubey, J.P., Conrad, P.A., 1992. Neospora-like protozoal infections associated with abortion in goats. Journal of veterinary diagnostic investigation : official publication of the American Association of Veterinary Laboratory Diagnosticians, Inc 4, 365-367.

Barr, B.C., Rowe, J.D., Sverlow, K.W., BonDurant, R.H., Ardans, A.A., Oliver, M.N., Conrad, P.A., 1994. Experimental reproduction of bovine fetal Neospora infection and death with a bovine Neospora isolate. Journal of veterinary diagnostic investigation : official publication of the American Association of Veterinary Laboratory Diagnosticians, Inc 6, 207-215.

Barrington, G.M., Parish, S.M., 2001. Bovine neonatal immunology. Immunology 17, 463-476.

Barta, O., Barta, V., Ingram, D.G., Hubbert, W.T., 1972. Bactericidal activity of bovine fetal serum against smooth and rough strains of Escherichia coli. American Journal of Veterinary Research 33, 731-740.

Bartley, P.M., Katzer, F., Rocchi, M.S., Maley, S.W., Benavides, J., Nath, M., Pang, Y., Cantón, G., Thomson, J., Chianini, F., Innes, E.A., 2013a. Development of maternal and foetal immune responses in cattle following experimental challenge with Neospora caninum at day 210 of gestation. Veterinary Research, 91.

Bartley, P.M., Kirvar, E., Wright, S., Swales, C., Esteban-Redondo, I., Buxton, D., Maley, S.W., Schock, A., Rae, A.G., Hamilton, C., Innes, E.A., 2004. Maternal and fetal immune responses of cattle inoculated with Neospora caninum at mid-gestation. Journal of Comparative Pathology 130, 81-91.

Bartley, P.M., Wright, S., Sales, J., Chianini, F., Buxton, D., Innes, E.A., 2006. Long-term passage of tachyzoites in tissue culture can attenuate virulence of Neospora caninum in vivo. Parasitology 133, 421-432.

Bartley, P.M., Wright, S.E., Maley, S.W., MacAldowie, C.N., Nath, M., Hamilton, C.M., Katzer, F., Buxton, D., Innes, E.A., 2012. Maternal and foetal immune responses of cattle following an experimental challenge with Neospora caninum at day 70 of gestation. Veterinary Research 43.

Bartley, P.M., Wright, S.E., Zimmer, I.A., Roy, S., Kitchener, A.C., Meredith, A., Innes, E.A., Katzer, F., 2013b. Detection of Neospora caninum in wild carnivorans in Great Britain. Veterinary Parasitology 192, 279-283.

Baszler, T.V., Gay, L.J., Long, M.T., Mathison, B.A., 1999a. Detection by PCR of Neospora caninum in fetal tissues from spontaneous bovine abortions. J Clin Microbiol 37, 4059-4064.

Baszler, T.V., Long, M.T., McElwain, T.F., Mathison, B.A., 1999b. Interferon-γ and interleukin-12 mediate protection to acute Neospora caninum infection in BALB/c mice. International Journal for Parasitology 29, 1635-1646.

Baud, V., Karin, M., 2001. Signal transduction by tumor necrosis factor and its relatives. Trends in Cell Biology 11, 372-377.

Benetti, A.H., Schein, F.B., dos Santos, T.R., Toniollo, G.H., da Costa, A.J., Mineo, J.R., Lobato, J., de Oliveira Silva, D.A., Gennari, S.M., 2009. Inquiry of antibodies anti-Neospora caninum in dairy cattle, dogs and rural workers of the south-west region of mato grosso state. Pesquisa de anticorpos anti-neospora caninum em bovinos leiteiros, cães e trabalhadores rurais da região sudoeste do estado de mato grosso 18, 29-33.

Bergeron, N., Fecteau, G., Paré, J., Martineau, R., Villeneuve, A., 2000. Vertical and horizontal transmission of Neospora caninum in dairy herds in Québec. Canadian Veterinary Journal 41, 464-469.

Bergeron, N., Girard, C., Pare, J., Fecteau, G., Robinson, J., Baillargeon, P., 2001. Rare detection of Neospora caninum in placentas from seropositive dams giving birth to full-term calves. J Vet Diagn Invest 13, 173-175.

Bień, J., Moskwa, B., Cabaj, W., 2010. In vitro isolation and identification of the first Neospora caninum isolate from European bison (Bison bonasus bonasus L.). Veterinary Parasitology 173, 200-205.

Billiards, S.S., Haynes, R.L., Folkerth, R.D., Trachtenberg, F.L., Liu, L.G., Volpe, J.J., Kinney, H.C., 2006. Development of microglia in the cerebral white matter of the human fetus and infant. Journal of Comparative Neurology 497, 199-208.

Bjerkas, I., Mohn, S.F., Presthus, J., 1984. Unidentified cyst-forming Sporozoon causing encephalomyelitis and myositis in dogs. Zeitschrift fur Parasitenkunde 70, 271-274.

Björkman, C., Alenius, S., Emanuellson, U., Uggla, A., 2000. Neospora caninum and Bovine Virus Diarrhoea Virus Infections in Swedish Dairy Cows in Relation to Abortion. Veterinary Journal 159, 201-206.

Björkman, C., Holmdahl, O.J.M., Uggla, A., 1997. An indirect enzyme-linked immunoassay (ELISA) for demonstration of antibodies to Neospora caninum in serum and milk of cattle. Veterinary Parasitology 68, 251-260.

Björkman, C., Johansson, O., Stenlund, S., Holmdahl, O.J.M., Uggla, A., 1996. Neospora species infection in a herd of dairy cattle. Journal of the American Veterinary Medical Association 208, 1441-1444.

Björkman, C., McAllister, M.M., Frössling, J., Näslund, K., Leung, F., Uggla, A., 2003. Application of the Neospora caninum IgG avidity ELISA in assessment of chronic reproductive losses after an outbreak of neosporosis in a herd of beef cattle. Journal of Veterinary Diagnostic Investigation 15, 3-7.

Björkman, C., Näslund, K., Stenlund, S., Maley, S.W., Buxton, D., Uggla, A., 1999. An IgG avidity ELISA to discriminate between recent and chronic Neospora caninum infection. Journal of Veterinary Diagnostic Investigation 11, 41-44.

Black, M.W., Arrizabalaga, G., Boothroyd, J.C., 2000. Ionophore-resistant mutants of Toxoplasma gondii reveal host cell permeabilization as an early event in egress. Molecular and Cellular Biology 20, 9399-9408.

Boger, L.A., Hattel, A.L., 2003. Additional evaluation of undiagnosed bovine abortion cases may reveal fetal neosporosis. Veterinary Parasitology 113, 1-6.

Borsuk, S., Andreotti, R., Leite, F.P.L., da Silva Pinto, L., Simionatto, S., Hartleben, C.P., Goetze, M., Oshiro, L.M., Matos, M.D.F.C., Berne, M.E.A., 2011. Development of an indirect ELISA-NcSRS2 for detection of Neospora caninum antibodies in cattle. Veterinary Parasitology 177, 33-38.

Bouillet, P., Strasser, A., 2002. BH3-only proteins - Evolutionarily conserved pro-apoptotic Bcl-2 family members essential for initiating programmed cell death. Journal of Cell Science 115, 1567-1574.

Boulton, J.G., Gill, P.A., Cook, R.W., Fraser, G.C., Harper, P.A., Dubey, J.P., 1995. Bovine Neospora abortion in north-eastern New South Wales. Australian Veterinary Journal 72, 119-120.

Bruchhaus, I., Roeder, T., Rennenberg, A., Heussler, V.T., 2007. Protozoan parasites: programmed cell death as a mechanism of parasitism. Trends in Parasitology 23, 376-383.

Budzko, D.B., Tyler, L., Armstrong, D., 1989. Fc receptors on the surface of Toxoplasma gondii trophozoites: A confounding factor in testing for anti-Toxoplasma antibodies by indirect immunofluorescence. Journal of Clinical Microbiology 27, 959-961.

Bustin, M., 1999. Regulation of DNA-dependent activities by the functional motifs of the high-mobility-group chromosomal proteins. Molecular and Cellular Biology 19, 5237-5246.

Buxton, D., Maley, S.W., Pastoret, P.P., Brochier, B., Innes, E.A., 1997. Examination of red foxes (Vulpes vulpes) from Belgium for antibody to Neospora caninum and Toxoplasma gondii. Veterinary Record 141, 308-309.

Buxton, D., Maley, S.W., Wright, S., Thomson, K.M., Rae, A.G., Innes, E.A., 1998. The pathogenesis of experimental neosporosis in pregnant sheep. Journal of Comparative Pathology 118, 267-279.

Cain, K., Bratton, S.B., Cohen, G.M., 2002. The Apaf-1 apoptosome: A large caspase-activating complex. Biochimie 84, 203-214.

Caldas, L.A., de Souza, W., Attias, M., 2010. Microscopic analysis of calcium ionophore activated egress of Toxoplasma gondii from the host cell. Veterinary Parasitology 167, 8-18.

Canada, N., Meireles, C.S., Ferreira, P., Correia da Costa, J.M., Rocha, A., 2006. Artificial insemination of cows with semen in vitro contaminated with Neospora caninum tachyzoites failed to induce neosporosis. Veterinary Parasitology 139, 109-114.

Cannas, A., Naguleswaran, A., Müller, N., Eperon, S., Gottstein, B., Hemphill, A., 2003. Vaccination of mice against experimental Neospora caninum infection using NcSAG1 - and NcSRS2-based recombinant antigens and DNA vaccines. Parasitology 126, 303-312.

Carmen, J.C., Hardi, L., Sinai, A.P., 2006. Toxoplasma gondii inhibits ultraviolet light-induced apoptosis through multiple interactions with the mitochondrion-dependent programmed cell death pathway. Cellular Microbiology 8, 301-315.

Caspe, S.G., Moore, D.P., Leunda, M.R., Cano, D.B., Lischinsky, L., Regidor-Cerrillo, J., Álvarez-García, G., Echaide, I.G., Bacigalupe, D., Ortega Mora, L.M., Odeón, A.C., Campero, C.M., 2012. The Neospora caninum-Spain 7 isolate induces placental damage, fetal death and abortion in cattle when inoculated in early gestation. Veterinary Parasitology 189, 171-181.

Chao, C.C., Anderson, W.R., Hu, S., Gekker, G., Martella, A., Peterson, P.K., 1993. Activated microglia inhibit multiplication of Toxoplasma gondii via a nitric oxide mechanism. Clinical Immunology and Immunopathology 67, 178-183.

Chaouat, G., Zourbas, S., Ostojic, S., Lappree-Delage, G., Dubanchet, S., Ledee, N., Martal, J., 2002. A brief review of recent data on some cytokine expressions at the materno-foetal interface which might challenge the classical Th1/Th2 dichotomy. Journal of reproductive immunology 53, 241-256.

Charbord, P., Tavian, M., Humeau, L., Péault, B., 1996. Early ontogeny of the human marrow from long bones: An immunohistochemical study of hematopoiesis and its microenvironment. Blood 87, 4109-4119.

Clark, R.K., Kuhn, R.E., 1999. Trypanosoma cruzi does not induce apoptosis in murine fibroblasts. Parasitology 118, 167-175.

Claycomb, W.C., Lanson Jr, N.A., Stallworth, B.S., Egeland, D.B., Delcarpio, J.B., Bahinski, A., Izzo Jr, N.J., 1998. HL-1 cells: A cardiac muscle cell line that contracts and retains phenotypic characteristics of the adult cardiomyocyte. Proceedings of the National Academy of Sciences of the United States of America 95, 2979-2984.

Clemente, P., Peralta, S., Cruz-Bermudez, A., Echevarría, L., Fontanesi, F., Barrientos, A., Fernandez-Moreno, M.A., Garesse, R., 2013. HCOA3 stabilizes cytochrome c oxidase 1 (COX1) and promotes cytochrome c oxidase assembly in human mitochondria. Journal of Biological Chemistry 288, 8321-8331.

Clouet, A.S., Le Bizec, B., Boerlen, F., Monteau, F., André, F., 1998. Calf primary hepatocyte culture as a tool for anabolic steroid metabolism studies. Analyst 123, 2489-2492.

Cole, R.A., Lindsay, D.S., Dubey, J.P., Blagburn, B.L., 1993. Detection of Neospora caninum in tissue sections using a murine monoclonal antibody. Journal of veterinary diagnostic investigation : official publication of the American Association of Veterinary Laboratory Diagnosticians, Inc 5, 579-584.

Cole, R.A., Lindsay, D.S., Dubey, J.P., Toivio-Kinnucan, M.A., Blagburn, B.L., 1994. Characterization of a murine monoclonal antibody generated against Neospora caninum tachyzoites by use of western blot analysis and immunoelectron microscopy. American Journal of Veterinary Research 55, 1717-1722.

Collantes-Fernández, E., Arnáiz-Seco, I., Burgos, B.M., Rodriguez-Bertos, A., Aduriz, G., Fernández-García, A., Ortega-Mora, L.M., 2006a. Comparison of Neospora caninum distribution, parasite loads and lesions between epidemic and endemic bovine abortion cases. Veterinary Parasitology 142, 187-191.

Collantes-Fernández, E., Rodríguez-Bertos, A., Arnáiz-Seco, I., Moreno, B., Aduriz, G., Ortega-Mora, L.M., 2006b. Influence of the stage of pregnancy on Neospora caninum distribution, parasite loads and lesions in aborted bovine foetuses. Theriogenology 65, 629-641.

Conrad, P.A., Barr, B.C., Sverlow, K.W., Anderson, M., Daft, B., Kinde, H., Dubey, J.P., Munson, L., Ardans, A., 1993a. In vitro isolation and characterization of a Neospora sp. from aborted bovine foetuses. Parasitology 106, 239-249.

Conrad, P.A., Sverlow, K., Anderson, M., Rowe, J., BonDurant, R., Tuter, G., Breitmeyer, R., Palmer, C., Thurmond, M., Ardans, A., 1993b. Detection of serum antibody responses in cattle with natural or experimental Neospora infections. Journal of veterinary diagnostic investigation : official publication of the American Association of Veterinary Laboratory Diagnosticians, Inc 5, 572-578.

Corbellini, L.G., Smith, D.R., Pescador, C.A., Schmitz, M., Correa, A., Steffen, D.J., Driemeier, D., 2006. Herd-level risk factors for Neospora caninum seroprevalence in dairy farms in southern Brazil. Preventive Veterinary Medicine 74, 130-141.

Cortese, J.D., Voglino, A.L., Hackenbrock, C.R., 1998. Multiple conformations of physiological membrane-bound cytochrome c. Biochemistry 37, 6402-6409.

Csak, T., Dolganiuc, A., Kodys, K., Nath, B., Petrasek, J., Bala, S., Lippai, D., Szabo, G., 2011. Mitochondrial antiviral signaling protein defect links impaired antiviral response and liver injury in steatohepatitis in mice. Hepatology 53, 1917-1931.

Czerski, L., Nuñez, G., 2004. Apoptosome formation and caspase activation: Is it different in the heart? Journal of Molecular and Cellular Cardiology 37, 643-652.

Daëron, M. 1997. Fc receptor biology. In Annual Review of Immunology, 203-234.

Darwich, L., Cabezón, O., Echeverria, I., Pabón, M., Marco, I., Molina-López, R., Alarcia-Alejos, O., López-Gatius, F., Lavín, S., Almería, S., 2012. Presence of Toxoplasma gondii and Neospora caninum DNA in the brain of wild birds. Veterinary Parasitology 183, 377-381.

Davison, H.C., French, N.P., Trees, A.J., 1999a. Herd-specific and age-specific seroprevalence of Neospora caninum in 14 British dairy herds. Veterinary Record 144, 547-550.

Davison, H.C., Guy, C.S., McGarry, J.W., Guy, F., Williams, D.J.L., Kelly, D.F., Trees, A.J., 2001. Experimental studies on the transmission of Neospora caninum between cattle. Research in Veterinary Science 70, 163-168.

Davison, H.C., Otter, A., Trees, A.J., 1999b. Estimation of vertical and horizontal transmission parameters of Neospora caninum infections in dairy cattle. International Journal for Parasitology 29, 1683-1689.

Davison, H.C., Otter, A., Trees, A.J., 1999c. Significance of Neospora caninum in British dairy cattle determined by estimation of seroprevalence in normally calving cattle and aborting cattle. International Journal for Parasitology 29, 1189-1194.

De Melo, E.J.T., De Carvalho, T.U., De Souza, W., 1992. Penetration of Toxoplasma gondii into host cells induces changes in the distribution of the mitochondria and the endoplasmic reticulum. Cell Structure and Function 17, 311-317.

De Souza, E.M., Araújo-Jorge, T.C., Bailly, C., Lansiaux, A., Batista, M.M., Oliveira, G.M., Soeiro, M.N.C., 2003. Host and parasite apoptosis following Trypanosoma cruzi infection in in vitro and in vivo models. Cell and Tissue Research 314, 223-235.

Debache, K., Guionaud, C., Kropf, C., Boykin, D., Stephens, C.E., Hemphill, A., 2011. Experimental treatment of Neospora caninum-infected mice with the arylimidamide DB750 and the thiazolide nitazoxanide. Experimental Parasitology 129, 95-100.

Denecker, G., Vercammen, D., Declercq, W., Vandenabeele, P., 2001. Apoptotic and necrotic cell death induced by death domain receptors. Cellular and Molecular Life Sciences 58, 356-370.

Desagher, S., Martinou, J.C., 2000. Mitochondria as the central control point of apoptosis. Trends in Cell Biology 10, 369-377.

Desagher, S., Osen-Sand, A., Nichols, A., Eskes, R., Montessuit, S., Lauper, S., Maundrell, K., Antonsson, B., Martinou, J.C., 1999. Bid-induced conformational change of Bax is responsible for mitochondrial cytochrome c release during apoptosis. Journal of Cell Biology 144, 891-901.

Deveraux, Q.L., Roy, N., Stennicke, H.R., Van Arsdale, T., Zhou, Q., Srinivasula, S.M., Alnemri, E.S., Salvesen, G.S., Reed, J.C., 1998. IAPs block apoptotic

events induced by caspase-8 and cytochrome c by direct inhibition of distinct caspases. EMBO Journal 17, 2215-2223.

Dijkstra, T., Barkema, H.W., Eysker, M., Beiboer, M.L., Wouda, W., 2003. Evaluation of a single serological screening of dairy herds for Neospora caninum antibodies. Veterinary Parasitology 110, 161-169.

Dijkstra, T., Barkema, H.W., Eysker, M., Hesselink, J.W., Wouda, W., 2002a. Natural transmission routes of Neospora caninum between farm dogs and cattle. Veterinary Parasitology 105, 99-104.

Dijkstra, T., Barkema, H.W., Eysker, M., Wouda, W., 2001. Evidence of post-natal transmission of Neospora caninum in Dutch dairy herds. International Journal for Parasitology 31, 209-215.

Dijkstra, T., Barkema, H.W., Hesselink, J.W., Wouda, W., 2002b. Point source exposure of cattle to Neospora caninum consistent with periods of common housing and feeding and related to the introduction of a dog. Veterinary Parasitology 105, 89-98.

Dijkstra, T., Lam, T.J.G.M., Bartels, C.J.M., Eysker, M., Wouda, W., 2008. Natural postnatal Neospora caninum infection in cattle can persist and lead to endogenous transplacental infection. Veterinary Parasitology 152, 220-225.

Dion, S., Germon, S., Guiton, R., Ducournau, C., Dimier-Poisson, I., 2011. Functional activation of T cells by dendritic cells and macrophages exposed to the intracellular parasite Neospora caninum. International Journal for Parasitology 41, 685-695.

Distelhorst, C.W., 2002. Recent insights into the mechanism of glucocorticosteroid-induced apoptosis. Cell Death and Differentiation 9, 6-19.

Dobrowolski, J.M., Carruthers, V.B., Sibley, L.D., 1997a. Participation of myosin in gliding motility and host cell invasion by Toxoplasma gondii. Molecular Microbiology 26, 163-173.

Dobrowolski, J.M., Niesman, I.R., Sibley, L.D., 1997b. Actin in the parasite toxoplasma gondii is encoded by a single copy gene, act1 and exists primarily in a globular form. Cell Motility and the Cytoskeleton 37, 253-262.

Dobrowolski, J.M., Sibley, L.D., 1996. Toxoplasma invasion of mammalian cells is powered by the actin cytoskeleton of the parasite. Cell 84, 933-939.

Dockrell, D.H., 2003. The multiple roles of Fas ligand in the pathogenesis of infectious diseases. Clinical Microbiology and Infection 9, 766-779.

Dorn, G.W., 2013. Molecular mechanisms that differentiate apoptosis from programmed necrosis. Toxicologic Pathology 41, 227-234.

Dubey, J.P., 1999. Recent advances in Neospora and neosporosis. Veterinary Parasitology 84, 349-367.

Dubey, J.P., 2003. Review of Neospora caninum and neosporosis in animals. The Korean journal of parasitology 41, 1-16.

Dubey, J.P., Abbitt, B., Topper, M.J., Edwards, J.F., 1998. Hydrocephalus associated with Neospora caninum infection in an aborted bovine fetus. Journal of Comparative Pathology 118, 169-173.

Dubey, J.P., Barr, B.C., Barta, J.R., Bjerkås, I., Björkman, C., Blagburn, B.L., Bowman, D.D., Buxton, D., Ellis, J.T., Gottstein, B., Hemphill, A., Hill, D.E., Howe, D.K., Jenkins, M.C., Kobayashi, Y., Koudela, B., Marsh, A.E., Mattsson, J.G., McAllister, M.M., Modrý, D., Omata, Y., Sibley, L.D., Speer, C.A., Trees, A.J., Uggla, A., Upton, S.J., Williams, D.J.L., Lindsay, D.S., 2002. Redescription of Neospora caninum and its differentiation from related coccidia. International Journal for Parasitology 32, 929-946.

Dubey, J.P., Buxton, D., Wouda, W., 2006. Pathogenesis of Bovine Neosporosis. Journal of Comparative Pathology 134, 267-289.

Dubey, J.P., Carpenter, J.L., Speer, C.A., Topper, M.J., Uggla, A., 1988a. Newly recognized fatal protozoan disease of dogs. Journal of the American Veterinary Medical Association 192, 1269-1285.

Dubey, J.P., Hartley, W.J., Lindsay, D.S., Topper, M.J., 1990a. Fatal congenital Neospora caninum infection in a lamb. Journal of Parasitology 76, 127-130.

Dubey, J.P., Hattel, A.L., Lindsay, D.S., Topper, M.J., 1988b. Neonatal Neospora caninum infection in dogs: isolation of the causative agent and experimental transmission. Journal of the American Veterinary Medical Association 193, 1259-1263.

Dubey, J.P., Jenkins, M.C., Adams, D.S., McAllister, M.M., Anderson-Sprecher, R., Baszler, T.V., Kwok, O.C.H., Lally, N.C., Björkman, C., Uggla, A., 1997. Antibody responses of cows during an outbreak of neospo evaluated by indirect fluorescent antibody test and different enzyme-linked immunosorbent assays. Journal of Parasitology 83, 1063-1069.

Dubey, J.P., Jenkins, M.C., Rajendran, C., Miska, K., Ferreira, L.R., Martins, J., Kwok, O.C.H., Choudhary, S., 2011. Gray wolf (Canis lupus) is a natural definitive host for Neospora caninum. Veterinary Parasitology 181, 382-387.

Dubey, J.P., Leathers, C.W., Lindsay, D.S., 1989. Neospora caninum-like protozoon associated with fatal myelitis in newborn calves. Journal of Parasitology 75, 146-148.

Dubey, J.P., Lindsay, D.S., 1996. A review of Neospora caninum and neosporosis. Veterinary Parasitology 67, 1-59.

Dubey, J.P., Miller, S., Lindsay, D.S., Topper, M.J., 1990b. Neospora caninum-associated myocarditis and encephalitis in an aborted calf. Journal of veterinary diagnostic investigation : official publication of the American Association of Veterinary Laboratory Diagnosticians, Inc 2, 66-69.

Dubey, J.P., Porterfield, M.L., 1990. Neospora caninum (Apicomplexa) in an aborted equine fetus. Journal of Parasitology 76, 732-734.

Dubey, J.P., Schares, G., 2006. Diagnosis of bovine neosporosis. Veterinary Parasitology 140, 1-34.

Dubey, J.P., Schares, G., 2011. Neosporosis in animals-The last five years. Veterinary Parasitology 180, 90-108.

Dubey, J.P., Schares, G., Ortega-Mora, L.M., 2007. Epidemiology and control of neosporosis and Neospora caninum. Clinical Microbiology Reviews 20, 323-367.

Dubey, J.P., Sreekumar, C., Knickman, E., Miska, K.B., Vianna, M.C.B., Kwok, O.C.H., Hill, D.E., Jenkins, M.C., Lindsay, D.S., Greene, C.E., 2004. Biologic, morphologic, and molecular characterisation of Neospora caninum isolates from littermate dogs. International Journal for Parasitology 34, 1157-1167.

Duong, M.C., Alenius, S., Huong, L.T.T., Björkman, C., 2008. Prevalence of Neospora caninum and bovine viral diarrhoea virus in dairy cows in Southern Vietnam. Veterinary Journal 175, 390-394.

Dupont, C.D., Christian, D.A., Hunter, C.A., 2012. Immune response and immunopathology during toxoplasmosis. Seminars in Immunopathology 34, 793-813.

Dyer, R.M., Jenkins, M.C., Kwok, O.C.H., Douglas, L.W., Dubey, J.P., 2000. Serologic survey of Neospora caninum infection in a closed dairy cattle herd in Maryland: Risk of serologic reactivity by production groups. Veterinary Parasitology 90, 171-181.

Eckle, V.S., Buchmann, A., Bursch, W., Schulte-Hermann, R., Schwarz, M., 2004. Immunohistochemical Detection of Activated Caspases in Apoptotic Hepatocytes in Rat Liver. Toxicologic Pathology 32, 9-15.

Eguchi, Y., Srinivasan, A., Tomaselli, K.J., Shimizu, S., Tsujimoto, Y., 1999. ATP-dependent steps in apoptotic signal transduction. Cancer Research 59, 2174-2181.

Eiras, C., Arnaiz, I., Álvarez-García, G., Ortega-Mora, L.M., Sanjuánl, M.L., Yus, E., Diéguez, F.J., 2011. Neospora caninum seroprevalence in dairy and beef cattle from the northwest region of Spain, Galicia. Preventive Veterinary Medicine 98, 128-132.

Ekman, A., Pessa-Morikawa, T., Liljavirta, J., Niku, M., Iivanainen, A., 2010. B-cell development in bovine fetuses proceeds via a pre-B like cell in bone marrow and lymph nodes. Developmental and Comparative Immunology 34, 896-903.

Ellis, J.T., Amoyal, G., Ryce, C., Harper, P.A.W., Clough, K.A., Homan, W.L., Brindley, P.J., 1998. Comparison of the large subunit ribosomal DNA of

Neospora and Toxoplasma and development of a new genetic marker for their differentiation based on the D2 domain. Molecular and Cellular Probes 12, 1-13.

Ellis, J.T., McMillan, D., Ryce, C., Payne, S., Atkinson, R., Harper, P.A.W., 1999. Development of a single tube nested polymerase chain reaction assay for the detection of Neospora caninum DNA. International Journal for Parasitology 29, 1589-1596.

Elmore, S., 2007. Apoptosis: A Review of Programmed Cell Death. Toxicologic Pathology 35, 495-516.

Entrican, G., 2002. Immune regulation during pregnancy and host-pathogen interactions in infectious abortion. Journal of Comparative Pathology 126, 79-94.

Eskes, R., Antonsson, B., Osen-Sand, A., Montessuit, S., Richter, C., Sadoul, R., Mazzei, G., Nichols, A., Martinou, J.C., 1998. Bax-induced cytochrome C release from mitochondria is independent of the permeability transition pore but highly dependent on Mg2+ ions. Journal of Cell Biology 143, 217-224.

Farr, A.G., Dooley, J.L., Erickson, M., 2002. Organization of thymic medullary epithelial heterogeneity: Implications for mechanisms of epithelial differentiation. Immunological Reviews 189, 20-27.

Ferreira De Miranda-Santos, I.K., Campos-Neto, A., 1981. Receptor for immunoglobulin Fc on pathogenic but not on nonpathogenic protozoa of the Trypanosomatidae. Journal of Experimental Medicine 154, 1732-1742.

Fink, S.L., Cookson, B.T., 2005. Apoptosis, pyroptosis, and necrosis: Mechanistic description of dead and dying eukaryotic cells. Infection and Immunity 73, 1907-1916.

Flores, K.G., Li, J., Hale, L.P., 2001. B cells in epithelial and perivascular compartments of human adult thymus. Human Pathology 32, 926-934.

Forestier, F., Daffos, F., Catherine, N., Renard, M., Andreux, J.P., 1991. Developmental hematopoiesis in normal human fetal blood. Blood 77, 2360-2363.

Forsell, J.H., Jesse, B.W., Shull, L.R., 1985. A technique for isolation of bovine hepatocytes. Journal of animal science 60, 1597-1609.

French, N.P., Clancy, D., Davison, H.C., Trees, A.J., 1999. Mathematical models of Neospora caninum infection in dairy cattle: Transmission and options for control. International Journal for Parasitology 29, 1691-1704.

Frenkel, J.K., Dubey, J.P., Miller, N.L., 1970. Toxoplasma gondii in cats: Fecal stages identified as coccidian oocysts. Science 167, 893-896.

Frössling, J., Nødtvedt, A., Lindberg, A., Björkman, C., 2008. Spatial analysis of Neospora caninum distribution in dairy cattle from Sweden. Geospat Health 3, 39-45.

Fruth, I.A., Arrizabalaga, G., 2007. Toxoplasma gondii: Induction of egress by the potassium ionophore nigericin. International Journal for Parasitology 37, 1559-1567.

Fuchs, N., Sonda, S., Gottstein, B., Hemphill, A., 1998. Differential expression of cell surface- and dense granule-associated Neospora caninum proteins in tachyzoites and bradyzoites. Journal of Parasitology 84, 753-758.

Gavrea, R.R., Cozma, V., 2010. Seroprevalence of Neospora caninum in cows with reproductive failure in center and northwest of Romania. Sci. Parasitol. 11, 67-70.

Gazzinelli, R., Xu, Y., Hieny, S., Cheever, A., Sher, A., 1992. Simultaneous depletion of CD4+ and CD8+ T lymphocytes is required to reactivate chronic infection with Toxoplasma gondii. Journal of Immunology 149, 175-180.

Gazzinelli, R.T., Hieny, S., Wynn, T.A., Wolf, S., Sher, A., 1993. Interleukin 12 is required for the T-lymphocyte-independent induction of interferon γ by an intracellular parasite and induces resistance in T-cell- deficient hosts. Proceedings of the National Academy of Sciences of the United States of America 90, 6115-6119.

Gazzinelli, R.T., Wysocka, M., Hayashi, S., Denkers, E.Y., Hieny, S., Caspar, P., Trinchieri, G., Sher, A., 1994. Parasite-induced IL-12 stimulates early IFN-γ synthesis and resistance during acute infection with Toxoplasma gondii. Journal of Immunology 153, 2533-2543.

Ghosh, S., 1999. Regulation of inducible gene expression by the transcription factor NF-κB. Immunologic Research 19, 183-190.

Gibney, E.H., 2008. Does *Neospora caninum* cause death by multiplying uncontrollably in an immunologically immature fetus? Ph.D. University of Liverpool, Liverpool.

Gibney, E.H., Kipar, A., Rosbottom, A., Guy, C.S., Smith, R.F., Hetzel, U., Trees, A.J., Williams, D.J.L., 2008. The extent of parasite-associated necrosis in the placenta and foetal tissues of cattle following Neospora caninum infection in early and late gestation correlates with foetal death. International Journal for Parasitology 38, 579-588.

Gjørret, J.O., Fabian, D., Avery, B., Maddox-Hyttel, P., 2007. Active caspase-3 and ultrastructural evidence of apoptosis in spontaneous and induced cell death in bovine in vitro produced pre-implantation embryos. Molecular Reproduction and Development 74, 961-971.

Goebel, S., Gross, U., Lüder, C.G.K., 2001. Inhibition of host cell apoptosis by Toxoplasma gondii is accompanied by reduced activation of the caspase

cascade and alterations of poly(ADP-ribose) polymerase expression. Journal of Cell Science 114, 3495-3505.

Goebel, S., Lüder, C.G.K., Lugert, R., Bohne, W., Gross, U., 1998. Toxoplasma gondii inhibits the in vitro induced apoptosis of HL-60 Cells. Tokai Journal of Experimental and Clinical Medicine 23, 351-356.

Goldstein, J.C., Waterhouse, N.J., Juin, P., Evan, G.I., Green, D.R., 2000. The coordinate release of cytochrome c during apoptosis is rapid, complete and kinetically invariant. Nature Cell Biology 2, 156-162.

Gondim, L.F.P., Gao, L., McAllister, M.M., 2002. Improved production of Neospora caninum oocysts, cyclical oral transmission between dogs and cattle, and in vitro isolation from oocysts. Journal of Parasitology 88, 1159-1163.

Gondim, L.F.P., Lindsay, D.S., McAllister, M.M., 2009. Canine and bovine neospora caninum control sera examined for cross-reactivity using neospora caninum and neospora hughesi indirect fluorescent antibody tests. Journal of Parasitology 95, 86-88.

Gondim, L.F.P., McAllister, M.M., Anderson-Sprecher, R.C., Björkman, C., Lock, T.F., Firkins, L.D., Gao, L., Fischer, W.R., 2004a. Transplacental transmission and abortion in cows administered Neospora caninum oocysts. Journal of Parasitology 90, 1394-1400.

Gondim, L.F.P., McAllister, M.M., Pitt, W.C., Zemlicka, D.E., 2004b. Coyotes (Canis latrans) are definitive hosts of Neospora caninum. International Journal for Parasitology 34, 159-161.

Gondim, L.F.P., Pinheiro, A.M., Santos, P.O.M., Jesus, E.E.V., Ribeiro, M.B., Fernandes, H.S., Almeida, M.A.O., Freire, S.M., Meyer, R., McAllister, M.M., 2001. Isolation of Neospora caninum from the brain of a naturally infected dog, and production of encysted bradyzoites in gerbils. Veterinary Parasitology 101, 1-7.

Goodswen, S.J., Kennedy, P.J., Ellis, J.T., 2013. A review of the infection, genetics, and evolution of Neospora caninum: From the past to the present. Infection, Genetics and Evolution 13, 133-150.

Gottstein, B., Hentrich, B., Wyss, R., Thür, B., Busato, A., Stärk, K.D.C., Müller, N., 1998. Molecular and immunodiagnostic investigations on bovine neosporosis in Switzerland. International Journal for Parasitology 28, 679-691.

Graewe, S., Stanway, R.R., Rennenberg, A., Heussler, V.T., 2012. Chronicle of a death foretold: Plasmodium liver stage parasites decide on the fate of the host cell. FEMS Microbiology Reviews 36, 111-130.

Grasl-Kraupp, B., Ruttkay-Nedecky, B., Koudelka, H., Bukowska, K., Bursch, W., Schulte-Hermann, R., 1995. In among apoptosis, necrosis, and autolytic cell death: A cautionary note. Hepatology 21, 1465-1468.

Graumann, K., Hippe, D., Groß, U., Lüder, C.G.K., 2009. Mammalian apoptotic signalling pathways: multiple targets of protozoan parasites to activate or deactivate host cell death. Microbes and Infection 11, 1079-1087.

Green, D.R., Reed, J.C., 1998. Mitochondria and apoptosis. Science 281, 1309-1312.

Guy, C.S., Williams, D.J.L., Kelly, D.F., McGarry, J.W., Guy, F., Björkman, C., Smith, R.F., Trees, A.J., 2001a. Neospora caninum in persistently infected, pregnant cows: Spontaneous transplacental infection is associated with an acute increase in maternal antibody. Veterinary Record 149, 443-449.

Guy, C.S., Williams, D.J.L., Kelly, D.F., McGarry, J.W., Guy, F., Björkman, C., Smith, R.F., Trees, A.J., 2001b. Neospora caninum in persistently infected, pregnant cows: Spontaneous transplacental infection is associated with an acute increase in maternal antibody. Veterinary Record 149, 443-449.

Haddad, J.P.A., Dohoo, I.R., VanLeewen, J.A., 2005. A review of Neospora caninum in dairy and beef cattle - A Canadian perspective. Canadian Veterinary Journal 46, 230-243.

Haga, N., Fujita, N., Tsuruo, T., 2003. Mitochondrial aggregation precedes cytochrome c release from mitochondria during apoptosis. Oncogene 22, 5579-5585.

Hall, C.A., Reichel, M.P., Ellis, J.T., 2005. Neospora abortions in dairy cattle: Diagnosis, mode of transmission and control. Veterinary Parasitology 128, 231-241.

Hall, C.A., Reichel, M.P., Ellis, J.T., 2006. Prevalence of Neospora caninum infection in Australian (NSW) dairy cattle estimated by a newly validated ELISA for milk. Veterinary Parasitology 142, 173-178.

Harris, H.E., Andersson, U., Pisetsky, D.S., 2012. HMGB1: A multifunctional alarmin driving autoimmune and inflammatory disease. Nature Reviews Rheumatology 8, 195-202.

Hartley, W.J., Bridge, P.S., 1975. A case of suspected congenital Toxoplasma encephalomyelitis in a lamb associated with a spinal cord anomaly. British Veterinary Journal 131, 380-384.

Haynes, B.F., Hale, L.P., 1998. The human thymus. A chimeric organ comprised of central and peripheral lymphoid components. Immunologic Research 18, 61-78.

Hemphill, A. 1999. The host-parasite relationship in neosporosis, 47-104.

Hemphill, A., Fuchs, N., Sonda, S., Gottstein, B., Hentrich, B., 1997. Identification and partial characterization of a 36 kDa surface protein on Neospora caninum tachyzoites. Parasitology 115, 371-380.

Hemphill, A., Fuchs, N., Sonda, S., Hehl, A., 1999. The antigenic composition of Neospora caninum. International Journal for Parasitology 29, 1175-1188.

Hemphill, A., Gottstein, B., 1996. Identification of a major surface protein on Neospora caninum tachyzoites. Parasitology Research 82, 497-504.

Hemphill, A., Gottstein, B., 2006. Neospora caninum and neosporosis - Recent achievements in host and parasite cell biology and treatment. Acta Parasitologica 51, 15-25.

Hemphill, A., Gottstein, B., Kaufmann, H., 1996. Adhesion and invasion of bovine endothelial cells by Neospora caninum. Parasitology 112, 183-197.

Hemphill, A., Vonlaufen, N., Naguleswaran, A., 2006. Cellular and immunological basis of the host-parasite relationship during infection with Neospora caninum. Parasitology 133, 261-278.

Hemphill, A., Vonlaufen, N., Naguleswaran, A., Keller, N., Riesen, M., Guetg, N., Srinivasan, S., Alaeddine, F., 2004. Tissue culture and explant approaches to studying and visualizing Neospora caninum and its interactions with the host cell. Microscopy and Microanalysis 10, 602-620.

Herman, R.K., Molestina, R.E., Sinai, A.P., Howe, D.K., 2007. The apicomplexan pathogen Neospora caninum inhibits host cell apoptosis in the absence of discernible NF-κB activation. Infection and Immunity 75, 4255-4262.

Heussler, V., Rennenberg, A., Stanway, R., 2010. Host cell death induced by the egress of intracellular Plasmodium parasites. Apoptosis 15, 376-385.

Heussler, V.T., Küenzi, P., Rottenberg, S., 2001. Inhibition of apoptosis by intracellular protozoan parasites. International Journal for Parasitology 31, 1166-1176.

Hiasa, J., Kohara, J., Nishimura, M., Xuan, X., Tokimitsu, H., Nishikawa, Y., 2012. ELISAs based on rNcGRA7 and rNcSAG1 antigens as an indicator of Neospora caninum activation. Veterinary Parasitology 187, 379-385.

Hietala, S.K., Thurmond, M.C., 1999. Postnatal Neospora caninum transmission and transient serologic responses in two dairies. International Journal for Parasitology 29, 1669-1676.

Ho, M.S., Barr, B.C., Marsh, A.E., Anderson, M.L., Rowe, J.D., Tarantal, A.F., Hendrickx, A.G., Sverlow, K., Dubey, J.P., Conrad, P.A., 1996. Identification of bovine Neospora parasites by PCR amplification and specific small-subunit rRNA sequence probe hybridization. J Clin Microbiol 34, 1203-1208.

Ho, M.S.Y., Barr, B.C., Rowe, J.D., Anderson, M.L., Sverlow, K.W., Packham, A., Marsh, A.E., Conrad, P.A., 1997. Detection of Neospora sp. from infected bovine tissues by PCR and probe hybridization. Journal of Parasitology 83, 508-514.

Holling, T.M., Schooten, E., Van Den Elsen, P.J., 2004. Function and regulation of MHC class II molecules in T-lymphocytes: Of mice and men. Human Immunology 65, 282-290.

Holmdahl, O.J.M., Mattsson, J.G., 1996. Rapid and sensitive identification of Neospora caninum by in vitro amplification of the internal transcribed spacer 1. Parasitology 112, 177-182.

Hsu, S.M., Raine, L., Fanger, H., 1981. The use of antiavidin antibody and avidin-biotin-peroxidase complex in immunoperoxidase technics. American Journal of Clinical Pathology 75, 816-821.

Hughes, C.C.W., Savage, C.O.S., Pober, J.S., 1990. The endothelial cell as a regulator of T-cell function. Immunological Reviews, 85-102.

Hulbert, L.E., Carroll, J.A., Burdick, N.C., Randel, R.D., Brown, M.S., Ballou, M.A., 2011. Innate immune responses of temperamental and calm cattle after transportation. Veterinary Immunology and Immunopathology 143, 66-74.

Humphry, R.W., Cameron, A., Gunn, G.J., 2004. A practical approach to calculate sample size for herd prevalence surveys. Preventive Veterinary Medicine 65, 173-188.

Ichikawa, D., Funakoshi-Tago, M., Aizu-Yokota, E., Sonoda, Y., Inoue, J.i., Kasahara, T., 2006. TNF-receptor associated factor 6-deficient fibroblast is sensitive to the TNF-α-induced cell death: Involvement of reactive oxygen species. Biochemical and Biophysical Research Communications 351, 93-98.

Innes, E.A., Andrianarivo, A.G., Björkman, C., Williams, D.J.L., Conrad, P.A., 2002. Immune responses to Neospora caninum and prospects for vaccination. Trends in Parasitology 18, 497-504.

Innes, E.A., Panton, W.R.M., Marks, J., Trees, A.J., Holmdahl, J., Buxton, D., 1995. Interferon gamma inhibits the intracellular multiplication of Neospora caninum, as shown by incorporation of 3H uracil. Journal of Comparative Pathology 113, 95-100.

Innes, E.A., Wright, S., Bartley, P., Maley, S., Macaldowie, C., Esteban-Redondo, I., Buxton, D., 2005. The host-parasite relationship in bovine neosporosis. Veterinary Immunology and Immunopathology 108, 29-36.

Innes, E.A., Wright, S.E., Maley, S., Rae, A., Schock, A., Kirvar, E., Bartley, P., Hamilton, C., Carey, I.M., Buxton, D., 2001. Protection against vertical transmission in bovine neosporosis. International Journal for Parasitology 31, 1523-1534.

Ishino, S., Kadota, K., Matsubara, Y., Agawa, H., Matsui, N., 1991. Immunohistochemical studies on ontogeny of bovine lymphoid tissues. The Journal of veterinary medical science / the Japanese Society of Veterinary Science 53, 877-882.

Jenkins, M., Baszler, T., Björkman, C., Schares, G., Williams, D., 2002. Diagnosis and seroepidemiology of Neospora caninum-associated bovine abortion. International Journal for Parasitology 32, 631-636.

Jenkins, M.C., Caver, J.A., Björkman, C., Anderson, T.C., Romand, S., Vinyard, B., Uggla, A., Thulliez, P., Dubey, J.P., 2000. Serological investigation of an outbreak of Neospora caninum-associated abortion in a dairy herd in southeastern United States. Veterinary Parasitology 94, 17-26.

Jensen, A.M., Björkman, C., Kjeldsen, A.M., Wedderkopp, A., Willadsen, C., Uggla, A., Lind, P., 1999. Associations of Neospora caninum seropositivity with gestation number and pregnancy outcome in Danish dairy herds. Preventive Veterinary Medicine 40, 151-163.

Johns, J.L., Christopher, M.M., 2012. Extramedullary Hematopoiesis: A New Look at the Underlying Stem Cell Niche, Theories of Development, and Occurrence in Animals. Veterinary Pathology 49, 508-523.

Jones, T.C., Hirsch, J.G., 1972. The interaction between Toxoplasma gondii and mammalian cells. II. The absence of lysosomal fusion with phagocytic vacuoles containing living parasites. Journal of Experimental Medicine 136, 1173-1194.

Jozani, R.J., Asadpour, R., Nematolahi, A., Hosseininejad, M., 2012. Detection of non-spermatozoal cells of Neospora caninum in fresh semen of naturally infected bulls. Acta Scientiae Veterinariae 40.

Kafsack, B.F.C., Pena, J.D.O., Coppens, I., Ravindran, S., Boothroyd, J.C., Carruthers, V.B., 2009. Rapid membrane disruption by a perforin-like protein facilitates parasite exit from host cells. Science 323, 530-533.

Kaliński, P., Hilkens, C.M.U., Snijders, A., Snijdewint, F.G.M., Kapsenberg, M.L., 1997. IL-12-Deficient Dendritic Cells, Generated in the Presence of Prostaglandin E2, Promote Type 2 Cytokine Production in Maturing Human Naive T Helper Cells. Journal of Immunology 159, 28-35.

Kaufmann, S.H.E., 2008. Immunology's foundation: The 100-year anniversary of the Nobel Prize to Paul Ehrlich and Elie Metchnikoff. Nature Immunology 9, 705-712.

Keller, N., Naguleswaran, A., Cannas, A., Vonlaufen, N., Bienz, M., Björkman, C., Bohne, W., Hemphill, A., 2002. Identification of a Neospora caninum microneme protein (NcMIC1) which interacts with sulfated host cell surface glycosaminoglycans. Infection and Immunity 70, 3187-3198.

Khan, I.A., Schwartzman, J.D., Fonseka, S., Kasper, L.H., 1997. Neospora caninum: Role for immune cytokines in host immunity. Experimental Parasitology 85, 24-34.

King, A., Jokhi, P.P., Smith, S.K., Sharkey, A.M., Loke, Y.W., 1995. Screening for cytokine mRNA in human villous and extravillous trophoblasts using the reverse-transcriptase polymerase chain reaction (RT-PCR). Cytokine 7, 364-371.

King, J.S., Jenkins, D.J., Ellis, J.T., Fleming, P., Windsor, P.A., Šlapeta, J., 2011. Implications of wild dog ecology on the sylvatic and domestic life cycle of Neospora caninum in Australia. Veterinary Journal 188, 24-33.

King, J.S., Šlapeta, J., Jenkins, D.J., Al-Qassab, S.E., Ellis, J.T., Windsor, P.A., 2010. Australian dingoes are definitive hosts of Neospora caninum. International Journal for Parasitology 40, 945-950.

Kipar, A., Bellmann, S., Kremendahl, J., Köhler, K., Reinacher, M., 1998. Cellular composition, coronavirus antigen expression and production of specific antibodies in lesions in feline infectious peritonitis. Veterinary Immunology and Immunopathology 65, 243-257.

Koiwai, M., Hamaoka, T., Haritani, M., Shimizu, S., Kimura, K., Yamane, I., 2005. Proportion of abortions due to neosporosis among dairy cattle in Japan. Journal of Veterinary Medical Science 67, 1173-1175.

Koyama, T., Kobayashi, Y., Omata, Y., Yamada, M., Furuoka, H., Maeda, R., Matsui, T., Saito, A., Mikami, T., 2001. Isolation of Neospora caninum from the brain of a pregnant sheep. Journal of Parasitology 87, 1486-1488.

Kritzner, S., Sager, H., Blum, J., Krebber, R., Greif, G., Gottstein, B., 2002. An explorative study to assess the efficacy of Toltrazuril-sulfone (Ponazuril) in calves experimentally infected with Neospora caninum. Annals of Clinical Microbiology and Antimicrobials 1.

Kubben, F.J.G.M., Peeters-Haesevoets, A., Engels, L.G.J.B., Baeten, C.G.M.I., Schutte, B., Arends, J.W., Stockbrügger, R.W., Blijham, G.H., 1994. Proliferating cell nuclear antigen (PCNA): A new marker to study human colonic cell proliferation. Gut 35, 530-535.

Kumar, K.A., Garcia, C.R.S., Chandran, V.R., Van Rooijen, N., Zhou, Y., Winzeler, E., Nussenzweig, V., 2007. Exposure of Plasmodium sporozoites to the intracellular concentration of potassium enhances infectivity and reduces cell passage activity. Molecular and Biochemical Parasitology 156, 32-40.

Kyaw, T., Suwimonteerabutr, J., Virakul, P., Lohachit, C., Kalpravidh, W., 2005. Seronegative conversion in four Neospora caninum-infected cows, with a low rate of transplacental transmission. Veterinary Parasitology 131, 145-150.

Lally, N.C., Jenkins, M.C., Dubey, J.P., 1996. Evaluation of two Neospora caninum recombinant antigens for use in an enzyme-linked immunosorbent assay for the diagnosis of bovine neosporosis. Clinical and Diagnostic Laboratory Immunology 3, 275-279.

Larson, R.L., Hardin, D.K., Pierce, V.L., 2004. Economic considerations for diagnostic and control options for Neospora caninum-induced abortions in endemically infected herds of beef cattle. Journal of the American Veterinary Medical Association 224, 1597-1604.

Lee, Y., Gustafsson, Å.B., 2009. Role of apoptosis in cardiovascular disease. Apoptosis 14, 536-548.

Leirião, P., Rodrigues, C.D., Albuquerque, S.S., Mota, M.M., 2004. Survival of protozoan intracellular parasites in host cells. EMBO Reports 5, 1142-1147.

Leist, M., Single, B., Castoldi, A.F., Kühnle, S., Nicotera, P., 1997. Intracellular adenosine triphosphate (ATP) concentration: A switch in the decision between apoptosis and necrosis. Journal of Experimental Medicine 185, 1481-1486.

Lemasters, J.J., Qian, T., Bradham, C.A., Brenner, D.A., Cascio, W.E., Trost, L.C., Nishimura, Y., Nieminen, A.L., Herman, B., 1999. Mitochondrial dysfunction in the pathogenesis of necrotic and apoptotic cell death. Journal of Bioenergetics and Biomembranes 31, 305-319.

Lemos, M.P., Esquivel, F., Scott, P., Laufer, T.M., 2004. MHC Class II Expression Restricted to CD8α+ and CD11b + Dendritic Cells Is Sufficient for Control of Leishmania major. Journal of Experimental Medicine 199, 725-730.

Lieberman, J., 2003. The ABCs of granule-mediated cytotoxicity: New weapons in the arsenal. Nature Reviews Immunology 3, 361-370.

Lindsay, D.S., Dubey, J.P., 1989a. Immunohistochemical diagnosis of Neospora caninum in tissue sections. American Journal of Veterinary Research 50, 1981-1983.

Lindsay, D.S., Dubey, J.P., 1989b. In vitro development of Neospora caninum (Protozoa: Apicomplexa) from dogs. Journal of Parasitology 75, 163-165.

Lindsay, D.S., Kelly, E.J., McKown, R.D., Stein, F.J., Plozer, J., Herman, J., Blagburn, B.L., Dubey, J.P., 1996. Prevalence of Neospora caninum and Toxoplasma gondii antibodies in coyotes (Canis latrans) and experimental infections of coyotes with Neospora caninum. Journal of Parasitology 82, 657-659.

Lindsay, D.S., Upton, S.J., Dubey, J.P., 1999. A structural study of the Neospora caninum oocyst. International Journal for Parasitology 29, 1521-1523.

Linton, P.J., Dorshkind, K., 2004. Age-related changes in lymphocyte development and function. Nature Immunology 5, 133-139.

Liu, X., Van Vleet, T., Schnellmann, R.G. 2004. The Role of Calpain in Oncotic Cell Death. In Annual Review of Pharmacology and Toxicology, 349-370.

Lobach, D.F., Haynes, B.F., 1987. Ontogeny of the human thymus during fetal development. Journal of Clinical Immunology 7, 81-97.

Long, M.T., Baszler, T.V., 2000. Neturalization of maternal IL-4 modulates congenital protozoal transmission: Comparison of innate versus acquired immune responses. Journal of Immunology 164, 4768-4774.

Loobuyck, M., Frössling, J., Lindberg, A., Björkman, C., 2009. Seroprevalence and spatial distribution of Neospora caninum in a population of beef cattle. Preventive Veterinary Medicine 92, 116-122.

López-Gatius, F., Almería, S., Donofrio, G., Nogareda, C., García-Ispierto, I., Bech-Sàbat, G., Santolaria, P., Yániz, J.L., Pabón, M., de Sousa, N.M., Beckers, J.F., 2007. Protection against abortion linked to gamma interferon production in pregnant dairy cows naturally infected with Neospora caninum. Theriogenology 68, 1067-1073.

López-Gatius, F., López-Béjar, M., Murugavel, K., Pabón, M., Ferrer, D., Almería, S., 2004. Neospora-associated abortion episode over a 1-year period in a dairy herd in north-east Spain. Journal of Veterinary Medicine Series B: Infectious Diseases and Veterinary Public Health 51, 348-352.

López-Gatius, F., Santolaria, P., Yániz, J.L., Garbayo, J.M., Almería, S., 2005. The use of beef bull semen reduced the risk of abortion in Neospora-seropositive dairy cows. Journal of Veterinary Medicine Series B: Infectious Diseases and Veterinary Public Health 52, 88-92.

Löschenberger, K., Szölgyényi, W., Peschke, R., Prosl, H., 2004. Detection of the protozoan Neospora caninum using in situ polymerase chain reaction. Biotechnic and Histochemistry 79, 101-105.

Lüder, C.G.K., Stanway, R.R., Chaussepied, M., Langsley, G., Heussler, V.T., 2009. Intracellular survival of apicomplexan parasites and host cell modification. International Journal for Parasitology 39, 163-173.

Lukovic, D., Komoriya, A., Packard, B.Z., Ucker, D.S., 2003. Caspase activity is not sufficient to execute cell death. Experimental Cell Research 289, 384-395.

Lund, J., Faucher, D.J., Ford, S.P., Porter, J.C., Waterman, M.R., Mason, J.I., 1988. Developmental expression of bovine adrenocortical steroid hydroxylases. Regulation of P-450(17α) expression leads to episodic fetal cortisol production. Journal of Biological Chemistry 263, 16195-16201.

Lv, Q., Li, J., Gong, P., Xing, S., Zhang, X., 2010. Neospora caninum: In vitro culture of tachyzoites in MCF-7 human breast carcinoma cells. Experimental Parasitology 126, 536-539.

Macaldowie, C., Maley, S.W., Wright, S., Bartley, P., Esteban-Redondo, I., Buxton, D., Innes, E.A., 2004. Placental pathology associated with fetal death in cattle inoculated with Neospora caninum by two different routes in early pregnancy. Journal of Comparative Pathology 131, 142-156.

Maddox, J.F., Mackay, C.R., Brandon, M.R., 1987. Ontogeny of ovine lymphocytes. III. an immunohistological study on the development of T lymphocytes in sheep fetal lymph nodes. Immunology 62, 113-118.

Magno, R.C., Straker, L.C., De Souza, W., Attias, M., 2005. Interrelations between the parasitophorous vacuole of Toxoplasma gondii and host cell organelles. Microscopy and Microanalysis 11, 166-174.

Mainar-Jaime, R.C., Thurmond, M.C., Berzal-Herranz, B., Hietala, S.K., 1999. Seroprevalence of Neospora caninum and abortion in dairy cows in northern Spain. Veterinary Record 145, 72-75.

Majno, G., Joris, I., 1995. Apoptosis, oncosis, and necrosis: An overview of cell death. American Journal of Pathology 146, 3-15.

Maley, S.W., Buxton, D., Macaldowie, C.N., Anderson, I.E., Wright, S.E., Bartley, P.M., Esteban-Redondo, I., Hamilton, C.M., Storset, A.K., Innes, E.A., 2006. Characterization of the Immune Response in the Placenta of Cattle Experimentally Infected with Neospora caninum in Early Gestation. Journal of Comparative Pathology 135, 130-141.

Maley, S.W., Buxton, D., Rae, A.G., Wright, S.E., Schock, A., Bartley, P.M., Esteban-Redondo, I., Swales, C., Hamilton, C.M., Sales, J., Innes, E.A., 2003. The pathogenesis of neosporosis in pregnant cattle: Inoculation at mid-gestation. Journal of Comparative Pathology 129, 186-195.

Marks, J., Lundén, A., Harkins, D., Innes, E., 1998. Identification of Neospora antigens recognized by CD4+ T cells and immune sera from experimentally infected cattle. Parasite Immunology 20, 303-309.

Marsh, A.E., Barr, B.C., Madigan, J.E., Conrad, P.A., 1996. In vitro cultivation and characterization of a Neospora isolate obtained from a horse with protozoal myeloencephalitis. Proc. Am. Soc. Parasitol. and the Society of Protozoologists, 114.

Marsh, A.E., Barr, B.C., Packham, A.E., Conrad, P.A., 1998. Description of a new Neospora species (Protozoa: Apicomplexa: Sarcocystidae). Journal of Parasitology 84, 983-991.

Matsumoto, A., Bessho, H., Uehira, K., Suda, T., 1991. Morphological studies of the association of mitochondria with chlamydial inclusions and the fusion of chlamydial inclusions. Journal of Electron Microscopy 40, 356-363.

Matsumura, G., Sasaki, K., 1989. Megakaryocytes in the yolk sac, liver and bone marrow of the mouse: A cytometrical analysis by semithin light microscopy. J Anat 167, 181-187.

McAllister, M.M., 1999. Uncovering the biology and epidemiology of Neosporo caninum. Parasitology Today 15, 216-217.

McAllister, M.M., Björkman, C., Anderson-Sprecher, R., Rogers, D.G., 2000. Evidence of point-source exposure to Neospora caninum and protective immunity in a herd of beef cows. Journal of the American Veterinary Medical Association 217, 881-887.

McAllister, M.M., Dubey, J.P., Lindsay, D.S., Jolley, W.R., Wills, R.A., McGuire, A.M., 1998. Dogs are definitive hosts of Neospora caninum. International Journal for Parasitology 28, 1473-1478.

McAllister, M.M., Huffman, E.M., Hietala, S.K., Conrad, P.A., Anderson, M.L., Salman, M.D., 1996. Evidence suggesting a point source exposure in an outbreak of bovine abortion due to neosporosis. Journal of Veterinary Diagnostic Investigation 8, 355-357.

McCann, C.M., McAllister, M.M., Gondim, L.F.P., Smith, R.F., Cripps, P.J., Kipar, A., Williams, D.J.L., Trees, A.J., 2007. Neospora caninum in cattle: Experimental infection with oocysts can result in exogenous transplacental infection, but not endogenous transplacental infection in the subsequent pregnancy. International Journal for Parasitology 37, 1631-1639.

McIlwain, D.R., Berger, T., Mak, T.W., 2013. Caspase functions in cell death and disease. Cold Spring Harbor Perspectives in Biology 5, 1-28.

Medvinsky, A., Rybtsov, S., Taoudi, S., 2011. Embryonic origin of the adult hematopoietic system: Advances and questions. Development 138, 1017-1031.

Meissner, M., Schlüter, D., Soldati, D., 2002. Role of Toxoplasma gondii myosin a in powering parasite gliding and host cell invasion. Science 298, 837-840.

Mel'nikova, V.I., Afanas'eva, M.A., Sapozhnikov, A.M., Zakharova, L.A., 2006. Dynamics of apoptosis and proliferation in the rat thymus and spleen during perinatal development. Ontogenez 37, 286-291.

Mele, R., Gomez Morales, M.A., Tosini, F., Pozio, E., 2004. Cryptosporidium parvum at different developmental stages modulates host cell apoptosis in vitro. Infection and Immunity 72, 6061-6067.

Minervino, A.H.H., Ragozo, A.M.A., Monteiro, R.M., Ortolani, E.L., Gennari, S.M., 2008. Prevalence of Neospora caninum antibodies in cattle from Santarém, Pará, Brazil. Research in Veterinary Science 84, 254-256.

Moen, A.R., Wouda, W., Mul, M.F., Graat, E.A.M., Van Werven, T., 1998. Increased risk of abortion following Neospora caninure abortion outbreaks: A retrospective and prospective cohort study in four dairy herds. Theriogenology 49, 1301-1309.

Molestina, R.E., Payne, T.M., Coppens, I., Sinai, A.P., 2003. Activation of NF-KB by Toxoplasma gondii correlates with increased expression of antiapoptotic genes and localization of phosphorylated IKB to the parasitophorous vacuole membrane. Journal of Cell Science 116, 4359-4371.

Molestina, R.E., Sinai, A.P., 2005. Detection of a novel parasite kinase activity at the Toxoplasma gondii parasitophorous vacuole membrane capable of phosphorylating host lκBα. Cellular Microbiology 7, 351-362.

Molina-López, R., Cabezón, O., Pabón, M., Darwich, L., Obón, E., Lopez-Gatius, F., Dubey, J.P., Almería, S., 2012. High seroprevalence of Toxoplasma gondii and Neospora caninum in the Common raven (Corvus corax) in the Northeast of Spain. Research in Veterinary Science 93, 300-302.

Moore, D.P., 2005. Neosporosis in South America. Veterinary Parasitology 127, 87-97.

Moore, D.P., Pérez, A., Agliano, S., Brace, M., Cantón, G., Cano, D., Leunda, M.R., Odeón, A.C., Odriozola, E., Campero, C.M., 2009. Risk factors associated

with Neospora caninum infections in cattle in Argentina. Veterinary Parasitology 161, 122-125.

Mordue, D.G., Monroy, F., La Regina, M., Dinarello, C.A., Sibley, L.D., 2001. Acute toxoplasmosis leads to lethal overproduction of Th1 cytokines. Journal of Immunology 167, 4574-4584.

Moré, G., Bacigalupe, D., Basso, W., Rambeaud, M., Beltrame, F., Ramirez, B., Venturini, M.C., Venturini, L., 2009. Frequency of horizontal and vertical transmission for Sarcocystis cruzi and Neospora caninum in dairy cattle. Veterinary Parasitology 160, 51-54.

Moskwa, B., Goździk, K., Bień, J., Cabaj, W., 2008. Studies on Neospora caninum DNA detection in the oocytes and embryos collected from infected cows. Veterinary Parasitology 158, 370-375.

Moudy, R., Manning, T.J., Beckers, C.J., 2001. The Loss of Cytoplasmic Potassium upon Host Cell Breakdown Triggers Egress of Toxoplasma gondii. Journal of Biological Chemistry 276, 41492-41501.

Munhoz, A.D., Pereira, M.J.S., Flausino, W., Lopes, C.W.G., 2009. Neospora caninum seropositivity in cattle breeds in the South Fluminense Paraíba Valley, state of Rio de Janeiro. Soropositividade para Neospora caninum e raças bovinas no vale do Paraíba sulfluminense, estado do Rio de Janeiro 29, 29-32.

Naguleswaran, A., Cannas, A., Keller, N., Vonlaufen, N., Schares, G., Conraths, F.J., Björkman, C., Hemphill, A., 2001. Neospora caninum microneme protein NcMIC3: Secretion, subcellular localization, and functional involvement in host cell interaction. Infection and Immunity 69, 6483-6494.

Naguleswaran, A., Müller, N., Hemphill, A., 2003. Neospora caninum and Toxoplasma gondii: A novel adhesion/invasion assay reveals distinct differences in tachyzoite-host cell interactions. Experimental Parasitology 104, 149-158.

Namikawa, R., Mizuno, T., Matsuoka, H., 1986. Ontogenic development of T and B cells and non-lymphoid cells in the white pulp of human spleen. Immunology 57, 61-69.

Nash, P.B., Purner, M.B., Leon, R.P., Clarke, P., Duke, R.C., Curiel, T.J., 1998. Toxoplasma gondii-infected cells are resistant to multiple inducers of apoptosis. Journal of Immunology 160, 1824-1830.

Nettleton, P.F., Entrican, G., 1995. Ruminant pestiviruses. British Veterinary Journal 151, 615-642.

Nicotera, P., Leist, M., Ferrando-May, E., 1998. Intracellular ATP, a switch in the decision between apoptosis and necrosis. Toxicology Letters 102-103, 139-142.

Niknafs, B., Taki, T.M., Rezazadeh, M., Alimohammadian, M.H., 1998. Morphological study of mouse (BALB/c) thymus after high and low dose dexamethasone treatment. Medical Journal of the Islamic Republic of Iran 12, 65-69.

Nishikawa, Y., Mishima, M., Nagasawa, H., Igarashi, I., Fujisaki, K., Otsuka, H., Mikami, T., 2001. Interferon-gamma-induced apoptosis in host cells infected with Neospora caninum. Parasitology 123, 25-31.

Nishimura, M., Kohara, J., Hiasa, J., Muroi, Y., Yokoyama, N., Kida, K., Xuan, X., Furuoka, H., Nishikawa, Y., 2013. Tissue distribution of neospora caninum in experimentally infected cattle. Clinical and Vaccine Immunology 20, 309-312.

Nogareda, C., López-Gatius, F., Santolaria, P., García-Ispierto, I., Bech-Sàbat, G., Pabón, M., Mezo, M., Gonzalez-Warleta, M., Castro-Hermida, J.A., Yániz, J., Almeria, S., 2007. Dynamics of anti-Neospora caninum antibodies during gestation in chronically infected dairy cows. Veterinary Parasitology 148, 193-199.

O'Toole, D., Jeffrey, M., 1987. Congenital sporozoan encephalomyelitis in a calf. Veterinary Record 121, 563-566.

Okeoma, C.M., Williamson, N.B., Pomroy, W.E., Stowell, K.M., Gillespie, L., 2004. The use of PCR to detect Neospora caninum DNA in the blood of naturally infected cows. Veterinary Parasitology 122, 307-315.

Ortega-Mora, L.M., Fernández-García, A., Gómez-Bautista, M., 2006. Diagnosis of bovine neosporosis: Recent advances and perspectives. Acta Parasitologica 51, 1-14.

Ortega-Mora, L.M., Ferre, I., Del-Pozo, I., Caetano-Da-Silva, A., Collantes-Fernández, E., Regidor-Cerrillo, J., Ugarte-Garagalza, C., Aduriz, G., 2003. Detection of Neospora caninum in semen of bulls. Veterinary Parasitology 117, 301-308.

Osawa, T., Wastling, J., Acosta, L., Ortellado, C., Ibarra, J., Innes, E.A., 2002. Seroprevalence of Neospora caninum infection in dairy and beef cattle in Paraguay. Veterinary Parasitology 110, 17-23.

Osburn, B.I., 1986. Ontogeny of immune responses in cattle. The Ruminant Immune System in Health and Disease, 252-260.

Osburn, B.I., MacLachlan, N.J., Terrell, T.G., 1982. Ontogeny of the immune system. Journal of the American Veterinary Medical Association 181, 1049-1052.

Osburn, B.I., Schultz, R.D., 1973. Immune responsiveness of the fetus and neonate. Journal of the American Veterinary Medical Association 163, 801-806.

Pan, Y., Jansen, G.B., Duffield, T.F., Hietala, S., Kelton, D., Lin, C.Y., Peregrine, A.S., 2004. Genetic susceptibility to Neospora caninum infection in Holstein cattle in Ontario. Journal of dairy science 87, 3967-3975.

Paré, J., Thurmond, M.C., Hietala, S.K., 1996. Congenital Neospora caninum infection in dairy cattle and associated calfhood mortality. Canadian Journal of Veterinary Research 60, 133-139.

Paré, J., Thurmond, M.C., Hietala, S.K., 1997. Neospora caninum antibodies in cows during pregnancy as a predictor of congenital infection and abortion. Journal of Parasitology 83, 82-87.

Parish, S.M., Maag-Miller, L., Besser, T.E., Weidner, J.P., McElwain, T., Knowles, D.P., Leathers, C.W., 1987. Myelitis associated with protozoal infection in newborn calves. Journal of the American Veterinary Medical Association 191, 1599-1600.

Payne, S., Ellis, J., 1996. Detection of Neospora caninum DNA by the polymerase chain reaction. International Journal for Parasitology 26, 347-351.

Payne, T.M., Molestina, R.E., Sinai, A.P., 2003. Inhibition of caspase activation and a requirement for NF=KB function in the Toxoplasma gondii-mediated blockade of host apoptosis. Journal of Cell Science 116, 4345-4358.

Pearse, G., 2006. Normal structure, function and histology of the thymus. Toxicologic Pathology 34, 504-514.

Pescador, C.A., Corbellini, L.G., Oliveira, E.C., Raymundo, D.L., Driemeier, D., 2007. Histopathological and immunohistochemical aspects of Neospora caninum diagnosis in bovine aborted fetuses. Veterinary Parasitology 150, 159-163.

Peters, M., Lütkefels, E., Heckeroth, A.R., Schares, G., 2001. Immunohistochemical and ultrastructural evidence for Neospora caninum tissue cysts in skeletal muscles of naturally infected dogs and cattle. International Journal for Parasitology 31, 1144-1148.

Peters, M., Wagner, F., Schares, G., 2000. Canine neosporosis: Clinical and pathological findings and first isolation of Neospora caninum in Germany. Parasitology Research 86, 1-7.

Piccinni, M.P., Giudizi, M.G., Biagiotti, R., Beloni, L., Giannarini, L., Sampognaro, S., Parronchi, P., Manetti, R., Annunziato, F., Livi, C., Romagnani, S., Maggi, E., 1995. Progesterone favors the development of human T helper cells producing Th2- type cytokines and promotes both IL-4 production and membrane CD30 expression in established Th1 cell clones. Journal of Immunology 155, 128-133.

Piergili Fioretti, D., Pasquali, P., Diaferia, M., Mangili, V., Rosignoli, L., 2003. Neospora caninum Infection and Congenital Transmission: Serological and Parasitological Study of Cows up to the Fourth Gestation. Journal of

Veterinary Medicine Series B: Infectious Diseases and Veterinary Public Health 50, 399-404.

Pusterla, N., Conrad, P.A., Packham, A.E., Mapes, S.M., Finno, C.J., Gardner, I.A., Barr, B.C., Ferraro, G.L., Wilson, W.D., 2011. Endogenous transplacental transmission of neospora hughesi in naturally infected horses. Journal of Parasitology 97, 281-285.

R.L. Larson, Hardin, D.K., 2003. Review: Neospora caninum-induced Abortion in Cattle. The Bovine Practitioner 37, 121-126.

Raghupathy, R., 2001. Pregnancy: Success and failure within the Th1/Th2/Th3 paradigm. Seminars in Immunology 13, 219-227.

Regidor-Cerrillo, J., Arranz-Solís, D., Benavides, J., Gómez-Bautista, M., Castro-Hermida, J.A., Mezo, M., Pérez, V., Ortega-Mora, L.M., González-Warleta, M., 2014. Neospora caninum infection during early pregnancy in cattle: How the isolate influences infection dynamics, clinical outcome and peripheral and local immune responses. Veterinary Research 45.

Regidor-Cerrillo, J., Gómez-Bautista, M., Del Pozo, I., Jiménez-Ruiz, E., Aduriz, G., Ortega-Mora, L.M., 2010. Influence of Neospora caninum intra-specific variability in the outcome of infection in a pregnant BALB/c mouse model. Vet Res 41.

Reichel, M.P., Alejandra Ayanegui-Alcérreca, M., Gondim, L.F.P., Ellis, J.T., 2013. What is the global economic impact of Neospora caninum in cattle - The billion dollar question. International Journal for Parasitology 43, 133-142.

Reichel, M.P., Ellis, J.T., 2002. Control options for Neospora caninum infections in cattle - Current state of knowledge. New Zealand Veterinary Journal 50, 86-92.

Reichel, M.P., Ellis, J.T., 2009. Neospora caninum - How close are we to development of an efficacious vaccine that prevents abortion in cattle? International Journal for Parasitology 39, 1173-1187.

Reid, A.J., Vermont, S.J., Cotton, J.A., Harris, D., Hill-Cawthorne, G.A., Könen-Waisman, S., Latham, S.M., Mourier, T., Norton, R., Quail, M.A., Sanders, M., Shanmugam, D., Sohal, A., Wasmuth, J.D., Brunk, B., Grigg, M.E., Howard, J.C., Parkinson, J., Roos, D.S., Trees, A.J., Berriman, M., Pain, A., Wastling, J.M., 2012. Comparative genomics of the apicomplexan parasites Toxoplasma gondii and neospora caninum: Coccidia differing in host range and transmission strategy. PLoS Pathogens 8.

Reiterová, K., Spilovska, S., Cobadiova, A., Mucha, R., 2011. First in vitro isolation of Neospora caninum from a naturally infected adult dairy cow in Slovakia. Acta Parasitologica 56, 111-115.

Ressel, L., Poli, A., 2010. Simultaneous double labelling of routinely processed paraffin tissue sections using combined immunoperoxidase,

immunofluorescence, and digital image editing. Research in Veterinary Science 88, 122-126.

Rinaldi, L., Fusco, G., Musella, V., Veneziano, V., Guarino, A., Taddei, R., Cringoli, G., 2005. Neospora caninum in pastured cattle: Determination of climatic, environmental, farm management and individual animal risk factors using remote sensing and geographical information systems. Veterinary Parasitology 128, 219-230.

Risal, P., Cho, B.H., Sylvester, K.G., Kim, J.C., Kim, H.T., Jeong, Y.J., 2011. The establishment and characterization of immortal hepatocyte cell lines from a mouse liver injury model. In Vitro Cellular and Developmental Biology - Animal 47, 526-534.

Ritter, P.M., Marti, A., Blanc, C., Baltzer, A., Krajewski, S., Reed, J.C., Jaggi, R., 2000. Nuclear localization of procaspase-9 and processing by a caspase-3-like activity in mammary epithelial cells. European Journal of Cell Biology 79, 358-364.

Rock, K.L., Lai, J.J., Kono, H., 2011. Innate and adaptive immune responses to cell death. Immunological Reviews 243, 191-205.

Rodrigues, A.A.R., Gennari, S.M., Aguiar, D.M., Sreekumar, C., Hill, D.E., Miska, K.B., Vianna, M.C.B., Dubey, J.P., 2004. Shedding of Neospora caninum oocysts by dogs fed tissues from naturally infected water buffaloes (Bubalus bubalis) from Brazil. Veterinary Parasitology 124, 139-150.

Roiko, M.S., Carruthers, V.B., 2009. New roles for perforins and proteases in apicomplexan egress. Cellular Microbiology 11, 1444-1452.

Rojo-Montejo, S., Collantes-Fernández, E., Blanco-Murcia, J., Rodríguez-Bertos, A., Risco-Castillo, V., Ortega-Mora, L.M., 2009a. Experimental infection with a low virulence isolate of Neospora caninum at 70 days gestation in cattle did not result in foetopathy. Veterinary Research 40.

Rojo-Montejo, S., Collantes-Fernández, E., Regidor-Cerrillo, J., Álvarez-García, G., Marugan-Hernández, V., Pedraza-Díaz, S., Blanco-Murcia, J., Prenafeta, A., Ortega-Mora, L.M., 2009b. Isolation and characterization of a bovine isolate of Neospora caninum with low virulence. Veterinary Parasitology 159, 7-16.

Rojo-Montejo, S., Collantes-Fernández, E., Regidor-Cerrillo, J., Rodríguez-Bertos, A., Prenafeta, A., Gomez-Bautista, M., Ortega-Mora, L.M., 2011. Influence of adjuvant and antigen dose on protection induced by an inactivated whole vaccine against Neospora caninum infection in mice. Veterinary Parasitology 175, 220-229.

Romero-Salas, D., García-Vázquez, Z., Montiel-Palacios, F., Montiel-Peña, T., Aguilar-Domínguez, M., Medina-Esparza, L., Cruz-Vázquez, C., 2010. Seroprevalence of Neospora caninum antibodies in cattle in veracruz, Mexico. Journal of Animal and Veterinary Advances 9, 1445-1451.

Romero, J.J., Frankena, K., 2003. The effect of the dam-calf relationship on serostatus to Neospora caninum on 20 Costa Rican dairy farms. Veterinary Parasitology 114, 159-171.

Romero, J.J., Perez, E., Dolz, G., Frankena, K., 2002. Factors associated with Neospora caninum serostatus in cattle of 20 specialised Costa Rican dairy herds. Preventive Veterinary Medicine 53, 263-273.

Romero, J.J., Pérez, E., Frankena, K., 2004. Effect of a killed whole Neospora caninum tachyzoite vaccine on the crude abortion rate of Costa Rican dairy cows under field conditions. Veterinary Parasitology 123, 149-159.

Rosbottom, A., Gibney, E.H., Guy, C.S., Kipar, A., Smith, R.F., Kaiser, P., Trees, A.J., Williams, D.J.L., 2008. Upregulation of cytokines is detected in the placentas of cattle infected with Neospora caninum and is more marked early in gestation when fetal death is observed. Infection and Immunity 76, 2352-2361.

Rosbottom, A., Gibney, H., Kaiser, P., Hartley, C., Smith, R.F., Robinson, R., Kipar, A., Williams, D.J.L., 2011. Up regulation of the maternal immune response in the placenta of cattle naturally infected with Neospora caninum. PLoS ONE 6.

Rosbottom, A., Guy, C.S., Gibney, E.H., Smith, R.F., Valarcher, J.F., Taylor, G., Williams, D.J.L., 2007. Peripheral immune responses in pregnant cattle following Neospora caninum infection. Parasite Immunology 29, 219-228.

Rovere-Querini, P., Capobianco, A., Scaffidi, P., Valentinis, B., Catalanotti, F., Giazzon, M., Dumitriu, I.E., Müller, S., Iannacone, M., Traversari, C., Bianchi, M.E., Manfredi, A.A., 2004. HMGB1 is an endogenous immune adjuvant released by necrotic cells. EMBO Reports 5, 825-830.

Sager, H., Fischer, I., Furrer, K., Strasser, M., Waldvogel, A., Boerlin, P., Audigé, L., Gottstein, B., 2001. A Swiss case-control study to assess Neospora caninum-associated bovine abortions by PCR, histopathology and serology. Veterinary Parasitology 102, 1-15.

Saliba, K.J., Kirk, K., 2001. Nutrient acquisition by intracellular apicomplexan parasites: Staying in for dinner. International Journal for Parasitology 31, 1321-1330.

Samraj, A.K., Keil, E., Ueffing, N., Schulze-Osthoff, K., Schmitz, I., 2006. Loss of caspase-9 provides genetic evidence for the type I/II concept of CD95-mediated apoptosis. Journal of Biological Chemistry 281, 29652-29659.

Sanderson, M.W., Gay, J.M., Baszler, T.V., 2000. Neospora caninum seroprevalence and associated risk factors in beef cattle in the northwestern United States. Veterinary Parasitology 90, 15-24.

Scaffidi, P., Misteli, T., Bianchi, M.E., 2002. Release of chromatin protein HMGB1 by necrotic cells triggers inflammation. Nature 418, 191-195.

Schares, G., Bärwald, A., Staubach, C., Söndgen, P., Rauser, M., Schröder, R., Peters, M., Wurm, R., Selhorst, T., Conraths, F.J., 2002. p38-avidity-ELISA: Examination of herds experiencing epidemic or endemic Neospora caninum-associated bovine abortion. Veterinary Parasitology 106, 293-305.

Schares, G., Bärwald, A., Staubach, C., Ziller, M., Klöss, D., Schröder, R., Labohm, R., Dräger, K., Fasen, W., Hess, R.G., Conraths, F.J., 2004. Potential risk factors for bovine Neospora caninum infection in Germany are not under the control of the farmers. Parasitology 129, 301-309.

Schares, G., Pantchev, N., Barutzki, D., Heydorn, A.O., Bauer, C., Conraths, F.J., 2005. Oocysts of Neospora caninum, Hammondia heydorni, Toxoplasma gondii and Hammondia hammondi in faeces collected from dogs in Germany. International Journal for Parasitology 35, 1525-1537.

Schares, G., Peters, M., Wurm, R., Bärwald, A., J. Conraths, F., 1998. The efficiency of vertical transmission of Neospora caninum in dairy cattle analysed by serological techniques. Veterinary Parasitology 80, 87-98.

Schares, G., Rauser, M., Söndgen, P., Rehberg, P., Bärwald, A., Dubey, J.P., Edelhofer, R., Conraths, F.J., 2000. Use of purified tachyzoite surface antigen p38 in an ELISA to diagnose bovine neosporosis. International Journal for Parasitology 30, 1123-1130.

Schares, G., Wilking, H., Bolln, M., Conraths, F.J., Bauer, C., 2009. Neospora caninum in dairy herds in Schleswig-Holstein, Germany. Berliner und Munchener Tierarztliche Wochenschrift 122, 47-50.

Schatzberg, S.J., Haley, N.J., Barr, S.C., deLahunta, A., Olby, N., Munana, K., Sharp, N.J.H., 2003. Use of a multiplex polymerase chain reaction assay in the antemortem diagnosis of toxoplasmosis and neosporosis in the central nervous system of cats and dogs. American Journal of Veterinary Research 64, 1507-1513.

Schaumburg, F., Hippe, D., Vutova, P., Lüder, C.G.K., 2006. Pro- and anti-apoptotic activities of protozoan parasites. Parasitology 132, S69-S85.

Schultz, R.D., 1973. Developmental aspects of the fetal bovine immune response: a review. CORNELL VET. 63, 507-535.

Schultz, R.D., Confer, F., Dunne, H.W., 1971a. Occurrence of blood cells and serum proteins in bovine fetuses and calves. Canadian Journal of Comparative Medicine 35, 93-98.

Schultz, R.D., Dunne, H.W., Heist, C.E., 1971b. Transport, distribution and synthesis of bovine immunoglobulins. Ontogeny of the bovine immune response. Journal of dairy science 54, 1321-1322.

Schultz, R.D., Dunne, H.W., Heist, C.E., 1973. Ontogeny of the bovine immune response. Infection and Immunity 7, 981-991.

Senogles, D.R., Paul, P.S., Johnson, D.W., Muscoplat, C.C., 1979. Ontogeny of T cells, B cells and monocytes in the bovine foetus. Clinical and Experimental Immunology 36, 299-303.

Serrano-Martínez, E., Ferre, I., Martínez, A., Osoro, K., Mateos-Sanz, A., del-Pozo, I., Aduriz, G., Tamargo, C., Hidalgo, C.O., Ortega-Mora, L.M., 2007. Experimental neosporosis in bulls: Parasite detection in semen and blood and specific antibody and interferon-gamma responses. Theriogenology 67, 1175-1184.

Serrano, B., Almería, S., García-Ispierto, I., Yániz, J.L., Abdelfattah-Hassan, A., López-Gatius, F., 2011. Peripheral white blood cell counts throughout pregnancy in non-aborting Neospora caninum-seronegative and seropositive high-producing dairy cows in a Holstein Friesian herd. Research in Veterinary Science 90, 457-462.

Silva, K.L.O., Melo, L.M., Perosso, J., Oliveira, B.B., Santos, P.S.P.D., Eugênio, F.D.R., Lima, V.M.F.D., 2013. CD95 (FAS) and CD178 (FASL) induce the apoptosis of CD4+ and CD8+ cells isolated from the peripheral blood and spleen of dogs naturally infected with Leishmania spp. Veterinary Parasitology 197, 470-476.

Silva, M.T., 2010. When two is better than one: Macrophages and neutrophils work in concert in innate immunity as complementary and cooperative partners of a myeloid phagocyte system. Journal of leukocyte biology 87, 93-106.

Sinai, A.P., Joiner, K.A. 1997. Safe haven: The cell biology of nonfusogenic pathogen vacuoles, 415-462.

Sinai, A.P., Payne, T.M., Carmen, J.C., Hardi, L., Watson, S.J., Molestina, R.E., 2004. Mechanisms underlying the manipulation of host apoptotic pathways by Toxoplasma gondii. International Journal for Parasitology 34, 381-391.

Sinai, A.P., Webster, P., Joiner, K.A., 1997. Association of host cell endoplasmic reticulum and mitochondria with the Toxoplasma grondii parasitophorous vacuole membrane: A high affinity interaction. Journal of Cell Science 110, 2117-2128.

Singh, R.P., al-Rubeai, M., 1998. Apoptosis and bioprocess technology. Advances in biochemical engineering/biotechnology 62, 167-184.

Singh, R.P., Finka, G., Emery, A.N., Al-Rubeai, M., 1997. Apoptosis and its control in cell culture systems. Cytotechnology 23, 87-93.

Slee, E.A., Harte, M.T., Kluck, R.M., Wolf, B.B., Casiano, C.A., Newmeyer, D.D., Wang, H.G., Reed, J.C., Nicholson, D.W., Alnemri, E.S., Green, D.R., Martin, S.J., 1999. Ordering the cytochrome c-initiated caspase cascade: Hierarchical activation of caspases-2,-3,-6,-7,-8, and -10 in a caspase-9-dependent manner. Journal of Cell Biology 144, 281-292.

Speer, C.A., Dubey, J.P., McAllister, M.M., Blixt, J.A., 1999. Comparative ultrastructure of tachyzoites, bradyzoites, and tissue cysts of Neospora

caninum and Toxoplasma gondii. International Journal for Parasitology 29, 1509-1519.

Spencer, J., Choy, M., Hussell, T., Papadaki, L., Kington, J.P., Isaacson, P.G., 1992. Properties of human thymic B cells. Immunology 75, 596-600.

Stenlund, S., Björkman, C., Holmdahl, O.J.M., Kindahl, H., Uggla, A., 1997. Characterization of a Swedish bovine isolate of Neospora caninum. Parasitology Research 83, 214-219.

Stenlund, S., Kindahl, H., Magnusson, U., Uggla, A., Björkman, C., 1999. Serum antibody profile and reproductive performance during two consecutive pregnancies of cows naturally infected with Neospora caninum. Veterinary Parasitology 85, 227-234.

Stoppini, L., Buchs, P.A., Muller, D., 1991. A simple method for organotypic cultures of nervous tissue. Journal of Neuroscience Methods 37, 173-182.

Strohbusch, M., Müller, N., Hemphill, A., Krebber, R., Greif, G., Gottstein, B., 2009. Toltrazuril treatment of congenitally acquired Neospora caninum infection in newborn mice. Parasitology Research 104, 1335-1343.

Suen, D.F., Norris, K.L., Youle, R.J., 2008. Mitochondrial dynamics and apoptosis. Genes and Development 22, 1577-1590.

Swift, B.L., Kennedy, P.C., 1972. Experimentally induced infection of in utero bovine fetuses with bovine parainfluenza 3 virus. American Journal of Veterinary Research 33, 57-63.

Szépfalusi, Z., 2008. The maturation of the fetal and neonatal immune system. Journal of Nutrition 138, 1773S-1781S.

Takeda, K., Kaisho, T., Akira, S. 2003. Toll-like receptors, 335-376.

Tanaka, T., Hamada, T., Inoue, N., Nagasawa, H., Fujisaki, K., Suzuki, N., Mikami, T., 2000. The role of CD4+ or CD8+ T cells in the protective immune response of BALB/c mice to Neospora caninum infection. Veterinary Parasitology 90, 183-191.

Thurmond, M.C., Hietala, S.K., 1997a. Effect of congenitally acquired Neospora caninum infection on risk of abortion and subsequent abortions in dairy cattle. American Journal of Veterinary Research 58, 1381-1385.

Thurmond, M.C., Hietala, S.K., 1997b. Effect of Neospora caninum infection on milk production in first-lactation dairy cows. Journal of the American Veterinary Medical Association 210, 672-674.

Thurmond, M.C., Hietala, S.K., Blanchard, P.C., 1997. Herd-based diagnosis of Neospora caninum-induced endemic and epidemic abortion in cows and evidence for congenital and postnatal transmission. Journal of Veterinary Diagnostic Investigation 9, 44-49.

Thurmond, M.C., Hietala, S.K., Blanchard, P.C., 1999. Predictive values of fetal histopathology and immunoperoxidase staining in diagnosing bovine abortion caused by Neospora caninum in a dairy herd. Journal of Veterinary Diagnostic Investigation 11, 90-94.

Torres, M.P., Ortega, Y.R., 2006. Neospora caninum antibodies in commercial fetal bovine serum. Veterinary Parasitology 140, 352-355.

Trees, A.J., Davison, H.C., Innes, E.A., Wastling, J.M., 1999. Towards evaluating the economic impact of bovine neosporosis. International Journal for Parasitology 29, 1195-1200.

Trees, A.J., McAllister, M.M., Guy, C.S., McGarry, J.W., Smith, R.F., Williams, D.J.L., 2002. Neospora caninum: Oocyst challenge of pregnant cows. Veterinary Parasitology 109, 147-154.

Trees, A.J., Williams, D.J.L., 2005. Endogenous and exogenous transplacental infection in Neospora caninum and Toxoplasma gondii. Trends in Parasitology 21, 558-561.

Ueda, T., Yoshida, M., 2010. HMGB proteins and transcriptional regulation. Biochimica et Biophysica Acta - Gene Regulatory Mechanisms 1799, 114-118.

Uggla, A., Stenlund, S., Holmdahl, O.J.M., Jakubek, E.B., Thebo, P., Kindahl, H., Björkman, C., 1998. Oral Neospora caninum inoculation of neonatal calves. International Journal for Parasitology 28, 1467-1472.

Uzêda, R.S., Schares, G., Ortega-Mora, L.M., Madruga, C.R., Aguado-Martinez, A., Corbellini, L.G., Driemeier, D., Gondim, L.F.P., 2013. Combination of monoclonal antibodies improves immunohistochemical diagnosis of Neospora caninum. Veterinary Parasitology.

Van Maanen, C., Wouda, W., Schares, G., Von Blumröder, D., Conraths, F.J., Norton, R., Williams, D.J.L., Esteban-Redondo, I., Innes, E.A., Mattsson, J.G., Björkman, C., Fernández-García, A., Ortega-Mora, L.M., Müller, N., Sager, H., Hemphill, A., 2004. An interlaboratory comparison of immunohistochemistry and PCR methods for detection of Neospora caninum in bovine foetal tissues. Veterinary Parasitology 126, 351-364.

VanLeeuwen, J.A., Greenwood, S., Clark, F., Acorn, A., Markham, F., McCarron, J., O'Handley, R., 2011. Monensin use against Neospora caninum challenge in dairy cattle. Veterinary Parasitology 175, 372-376.

Veis, D.J., Sorenson, C.M., Shutter, J.R., Korsmeyer, S.J., 1993. Bcl-2-deficient mice demonstrate fulminant lymphoid apoptosis, polycystic kidneys, and hypopigmented hair. Cell 75, 229-240.

Veras, P.S.T., De Chastellier, C., Moreau, M.F., Villiers, V., Thibon, M., Mattei, D., Rabinovitch, M., 1994. Fusion between large phagocytic vesicles: Targeting of yeast and other particulates to phagolysosomes that shelter the bacterium

Coxiella burnetii or the protozoan Leishmania amazonensis in Chinese hamster ovary cells. Journal of Cell Science 107, 3065-3076.

Vercammen, D., Beyaert, R., Denecker, G., Goossens, V., Van Loo, G., Declercq, W., Grooten, J., Fiers, W., Vandenabeele, P., 1998a. Inhibition of caspases increases the sensitivity of L929 cells to necrosis mediated by tumor necrosis factor. Journal of Experimental Medicine 187, 1477-1485.

Vercammen, M., El Bouhdidi, A., Ben Messaoud, A., De Meuter, F., Bazin, H., Dubremetz, J.F., Carlier, Y., 1998b. Identification and characterization of a Fc receptor activity on the Toxoplasma gondii tachyzoite. Parasite Immunology 20, 37-47.

Von Blumröder, D., Stambusch, R., Labohm, R., Klawonn, W., Dräger, K., Fasen, W., Conraths, F.J., Schares, G., 2006. Potential risk factors for the serological detection of Neospora caninum-infections in cattle herds in Rhineland-Palatinate (Germany). Potenzielle risikofaktoren für den serologischen nachweis von Neospora-caninum-infektionen in rinderherden in Rheinland-Pfalz 34, 141-147.

Vonlaufen, N., Gianinazzi, C., Müller, N., Simon, F., Björkman, C., Jungi, T.W., Leib, S.L., Hemphill, A., 2002. Infection of organotypic slice cultures from rat central nervous tissue with Neospora caninum: An alternative approach to study host-parasite interactions. International Journal for Parasitology 32, 533-542.

Vonlaufen, N., Guetg, N., Naguleswaran, A., Müller, N., Björkman, C., Schares, G., Von Blumroeder, D., Ellis, J., Hemphill, A., 2004. In Vitro Induction of Neospora caninum Bradyzoites in Vero Cells Reveals Differential Antigen Expression, Localization, and Host-Cell Recognition of Tachyzoites and Bradyzoites. Infection and Immunity 72, 576-583.

Waldner, C.L., Janzen, E.D., Henderson, J., Haines, D.M., 1999. Outbreak of abortion associated with Neospora caninum infection in a beef herd. Journal of the American Veterinary Medical Association 215, 1485-1490.

Wapenaar, W., Barkema, H.W., VanLeeuwen, J.A., McClure, J.T., O'Handley, R.M., Kwok, O.C.H., Thulliez, P., Dubey, J.P., Jenkins, M.C., 2007. Comparison of serological methods for the diagnosis of Neospora caninum infection in cattle. Veterinary Parasitology 143, 166-173.

Watanabe, N., Wang, Y.H., Lee, H.K., Ito, T., Cao, W., Liu, Y.J., 2005. Hassall's corpuscles instruct dendritic cells to induce CD4 +CD25 + regulatory T cells in human thymus. Nature 436, 1181-1185.

Watkin, K.L., Gallagher, T.M., Logemann, J.A., Rademaker, A.W., 2001. Apoptosis and its clinical impact. Head and Neck 23, 409-425.

Weber, F.H., Jackson, J.A., Sobecki, B., Choromanski, L., Olsen, M., Meinert, T., Frank, R., Reichel, M.P., Ellis, J.T., 2013. On the efficacy and safety of vaccination with live tachyzoites of Neospora caninum for prevention of

Neospora-associated fetal loss in cattle. Clinical and Vaccine Immunology 20, 99-105.

Wegmann, T.G., Lin, H., Guilbert, L., Mosmann, T.R., 1993. Bidirectional cytokine interactions in the maternal-fetal relationship: Is successful pregnancy a TH2 phenomenon? Immunology Today 14, 353-356.

Weiss, L.M., Kim, K., 2000. The development and biology of bradyzoites of Toxoplasma gondii. Front Biosci 5, D391-405.

Weiss, L.M., Ma, Y.F., Halonen, S., McAllister, M.M., Zhang, Y.W., 1999. The in vitro development of Neospora caninum bradyzoites. International Journal for Parasitology 29, 1713-1723.

Werling, D., Piercy, J., Coffey, T.J., 2006. Expression of TOLL-like receptors (TLR) by bovine antigen-presenting cells-Potential role in pathogen discrimination? Veterinary Immunology and Immunopathology 112, 2-11.

Weston, J.F., Heuer, C., Williamson, N.B., 2012. Efficacy of a Neospora caninum killed tachyzoite vaccine in preventing abortion and vertical transmission in dairy cattle. Preventive Veterinary Medicine 103, 136-144.

Weston, J.F., Williamson, N.B., Pomroy, W.E., 2005. Associations between pregnancy outcome and serological response to Neospora caninum among a group of dairy heifers. New Zealand Veterinary Journal 53, 142-148.

Williams, D.J.L., Davison, H.C., Helmick, B., McGarry, J., Guy, F., Otter, A., Trees, A.J., 1999. Evaluation of a commercial ELlSA for detecting serum antibody to Neospora caninum in cattle. Veterinary Record 145, 571-575.

Williams, D.J.L., Guy, C.S., McGarry, J.W., Guy, F., Tasker, L., Smith, R.F., MacEachern, K., Cripps, P.J., Kelly, D.F., Trees, A.J., 2000. Neospora caninum-associated abortion in cattle: The time of experimentally-induced parasitaemia during gestation determines foetal survival. Parasitology 121, 347-358.

Williams, D.J.L., Guy, C.S., Smith, R.F., Ellis, J., Björkman, C., Reichel, M.P., Trees, A.J., 2007a. Immunization of cattle with live tachyzoites of Neospora caninum confers protection against fetal death. Infection and Immunity 75, 1343-1348.

Williams, D.J.L., Guy, C.S., Smith, R.F., Ellis, J., Björkman, C., Reichel, M.P., Trees, A.J., 2007b. Immunization of cattle with live tachyzoites of Neospora caninum confers protection against fetal death. Infection and Immunity 75, 1343-1348.

Williams, D.J.L., Guy, C.S., Smith, R.F., Guy, F., McGarry, J.W., McKay, J.S., Trees, A.J., 2003. First demonstration of protective immunity against foetopathy in cattle with latent Neospora caninum infection. International Journal for Parasitology 33, 1059-1065.

Williams, D.J.L., Hartley, C.S., Björkman, C., Trees, A.J., 2009. Endogenous and exogenous transplacental transmission of Neospora caninum - How the route of transmission impacts on epidemiology and control of disease. Parasitology 136, 1895-1900.

Williams, D.J.L., McGarry, J., Guy, F., Barber, J., Trees, A.J., 1997. Novel ELIS A for detection of Neospora-specific antibodies in cattle. Veterinary Record 140, 328-331.

Williams, D.J.L., Trees, A.J., 2006. Protecting babies: Vaccine strategies to prevent foetopathy in Neospora caninum-infected cattle. Parasite Immunology 28, 61-67.

Williams, G.T., 1994. Programmed cell death: A fundamental protective response to pathogens. Trends in Microbiology 2, 463-464.

Woodbine, K.A., Medley, G.F., Moore, S.J., Ramirez-Villaescusa, A., Mason, S., Green, L.E., 2008. A four year longitudinal sero-epidemiology study of Neospora caninum in adult cattle from 114 cattle herds in south west England: Associations with age, herd and dam-offspring Pairs. BMC Vet Res 4.

Woods, L.W., Anderson, M.L., Swift, P.K., Sverlow, K.W., 1994. Systemic neosporosis in a California black-tailed deer (Odocoileus hemionus columbianus). Journal of veterinary diagnostic investigation : official publication of the American Association of Veterinary Laboratory Diagnosticians, Inc 6, 508-510.

Wouda, W., Moen, A.R., Schukken, Y.H., 1998. Abortion risk in progeny of cows after a Neospora caninum epidemic. Theriogenology 49, 1311-1316.

Wouda, W., Moen, A.R., Visser, I.J.R., Van Knapen, F., 1997. Bovine fetal neosporosis: A comparison of epizootic and sporadic abortion cases and different age classes with regard to lesion severity and immunohistochemical identification of organisms in brain, heart, and liver. Journal of Veterinary Diagnostic Investigation 9, 180-185.

Yaeger, M.J., Shawd-Wessels, S., Leslie-Steen, P., 1994. Neospora abortion storm in a midwestern dairy. Journal of veterinary diagnostic investigation : official publication of the American Association of Veterinary Laboratory Diagnosticians, Inc 6, 506-508.

Yagoob, G., 2012. Seroepidemiology of Neospora sp. in Horses in East-Azerbaijan province of Iran. Journal of Animal and Veterinary Advances 11, 480-482.

Yamane, I., Shibahara, T., Kokuho, T., Shimura, K., Hamaoka, T., Haritani, M., Conrad, P.A., Park, C.H., Sawada, M., Umemura, T., 1998. An improved isolation technique for bovine Neospora species. Journal of Veterinary Diagnostic Investigation 10, 364-368.

Yan, W., 2012. Impact of prenatal stress and adulthood srtress on immune system: A review. Biomedical Research 3, 315-320.

Yániz, J.L., López-Gatius, F., García-Ispierto, I., Bech-Sàbat, G., Serrano, B., Nogareda, C., Sanchez-Nadal, J.A., Almeria, S., Santolaria, P., 2010. Some factors affecting the abortion rate in dairy herds with high incidence of neospora-associated abortions are different in cows and heifers. Reproduction in Domestic Animals 45, 699-705.

Zeh Iii, H.J., Lotze, M.T., 2005. Addicted to death: Invasive cancer and the immune response to unscheduled cell death. Journal of Immunotherapy 28, 1-9.

Zeiss, C.J., 2003. The apoptosis-necrosis continuum: Insights from genetically altered mice. Veterinary Pathology 40, 481-495.

Zhang, J., Andrade, Z.A., Yu, Z.X., Andrade, S.G., Takeda, K., Sadirgursky, M., Ferrans, V.J., 1999. Apoptosis in a canine model of acute chagasic myocarditis. Journal of Molecular and Cellular Cardiology 31, 581-596.

Zhang, Z.G., Li, X.B., Gao, L., Liu, G.W., Kong, T., Li, Y.F., Wang, H.B., Zhang, C., Wang, Z., Zhang, R.H., 2011. An updated method for the isolation and culture of primary calf hepatocytes. Veterinary Journal.

Zhao, Y.O., Khaminets, A., Hunn, J.P., Howard, J.C., 2009. Disruption of the Toxoplasma gondii parasitophorous vacuole by IFNγ-inducible immunity-related GTPases (IRG proteins) triggers necrotic cell death. PLoS Pathogens 5.

Zhivotovsky, B., 2004. Apoptosis, necrosis and between. Cell Cycle 3, 64-66.

Zhou, R.R., Zhao, S.S., Zou, M.X., Zhang, P., Zhang, B.X., Dai, X.H., Li, N., Liu, H.B., Wang, H., Fan, X.G., 2011. HMGB1 cytoplasmic translocation in patients with acute liver failure. BMC Gastroenterology 11.

Zong, W.X., Thompson, C.B., 2006. Necrotic death as a cell fate. Genes and Development 20, 1-15.